

**International
Progress Report**

IPR-01-65

Äspö Hard Rock Laboratory

Prototype Repository

Hydrogeology

Summary report of investigations before the operation phase

Ingvar Rhén
Torbjörn Forsmark
VBB VIAK

October 2001

Svensk Kärnbränslehantering AB

Swedish Nuclear Fuel
and Waste Management Co
Box 5864
SE-102 40 Stockholm Sweden
Tel +46 8 459 84 00
Fax +46 8 661 57 19



**Äspö Hard Rock
Laboratory**

Report no.	No.
IPR-01-65	F63K
Author	Date
Rhén, Forsmark	01-10-30
Checked by	Date
Lars-Olof Dahlström	01-10-30
Approved	Date
Christer Svemar	02-04-11

Äspö Hard Rock Laboratory

Prototype Repository

Hydrogeology

Summary report of investigations before the operation phase

Ingvar Rhén
Torbjörn Forsmark
VBB VIAK

October 2001

Keywords: Äspö Hard Rock Laboratory, Prototype Repository, characterization, hydrogeology, hydraulic tests, groundwater flow modelling

This report concerns a study which was conducted for SKB. The conclusions and viewpoints presented in the report are those of the author(s) and do not necessarily coincide with those of the client.



PROTOTYPE REPOSITORY

Deliverable D 27

Hydrogeology
Summary Report of investigations
before the operation phase

Ingvar Rhén
Torbjörn Forsmark
VBB VIAK

October 2001

EC Contract FIKW-2000-00055

EC-5th EURATOM Framework programme 1998-2002
Key Action: Nuclear Fission

Abstract

The Prototype Repository is an international, EC-supported activity with the objective to investigate, on a full-scale, the integrated performance of engineered barriers and near-field rock of a simulated deep repository. This is done in crystalline rock with respect to heat evolution, mechanics, water flow, water chemistry, gas evolution and microbial processes under natural and realistic conditions at approximately 450 m depth below the ground surface. The test site is a 65 m long TBM-bored drift from which six 1.75m diameter deposition holes are extended downwards to about 8 m depth in accordance with the KBS-3 concept. The test site is divided in two parts; an inner 40 m long section (Section I) with 4 deposition holes and an outer section (Section II) with two deposition holes. Stiff and tight plugs will separate the sections and Section II from the rest of the Äspö Hard Rock Laboratory.

A large number of boreholes have been drilled to characterize the rock mass. These boreholes will be used for the long-time monitoring of the Prototype Repository. The report summarizes the hydrogeological investigations.

Hydraulic tests performed are e.g. measurements of pressure responses in nearby borehole sections during drilling, flow logging with packer spacing of 1 or 3 meter, flow logging with the UCM-tool, pressure build-up tests of the entire borehole and some pressure build-up tests of the 1 or 3 meter test sections, hydro chemical sampling of several 1 or 3 meter test sections and 14 “Long-time” interference tests with around 60 pressure observation sections. Inflow measurements to tunnel sections in the Prototype Repository tunnel and to each deposition hole have been made as well as detailed inflow measurements to two of the deposition holes.

Sammanfattning

Prototypförvaret är ett internationellt, EC-stött projekt med syfte att i full skala undersöka den integrerade funktionen hos ingenjör-barriärer och närfältsberg i ett simulerat slutförvar i kristallint berg med hänsyn till värmeutveckling, mekanik, vattengenomströmning, vattenkemi, gasbildning och mikrobiologi under naturliga och realistiska förhållanden på ca 450m djup. Försöksplatsen är en 65 m lång TBM-borrade ort från vilken sex vertikala deponeringshål med 1.75m diameter och 8m djup borrar i enlighet med KBS-3 konceptet. Testplatsen är delad i två delar; en inre 40m lång sektion (sektion I) med 4 deponeringshål och en yttre del (sektion II) med två deponeringshål. Stela och täta pluggar separerar sektionerna och sektion II från resten av Äspölaboratoriet.

Ett stort antal borrhål har borrar för att karakterisera berget. Dessa borrhål kommer att användas för långtidsobservationerna av Prototypförvaret. Denna rapport sammanfattar de hydrogeologiska undersökningarna.

Hydrauliska tester som utförts omfattar tex mätningar av tryckresponser i närliggande borrhål under borrhållning, flödesloggning med dubbelmanschett med testsektionslängd 1 eller 3m, flödesloggning med UCM-logg, tryckuppbyggnadstest av hela borrhålet och några 1 eller 3 meters testsektioner, vattenprovtagning för hydrokemisk analys i några 1 eller 3 meters testsektioner och 14 ”långtids” interferenstester med ca 60 observations sektioner för tryckresponser. Mätningar av inflöde till tunnelsektioner och varje depositionshål samt detaljerade inflödes mätningar till två depositionshål har utförts.

Executive Summary

The Prototype Repository is an international, EC-supported activity with the objective to investigate, on a full-scale, the integrated performance of engineered barriers and near-field rock of a simulated deep repository. This is done in crystalline rock with respect to heat evolution, mechanics, water flow, water chemistry, gas evolution and microbial processes under natural and realistic conditions at approximately 450 m depth below the ground surface. The test site is a 65 m long TBM-bored drift from which six 1.75m diameter deposition holes are extended downwards to about 8 m depth in accordance with the KBS-3 concept. The test site is divided in two parts, an inner 40 m long section (Section I) with 4 deposition holes and an outer section (Section II) with two deposition holes. Stiff and tight plugs will separate the sections and Section II from the rest of the Äspö Hard Rock Laboratory.

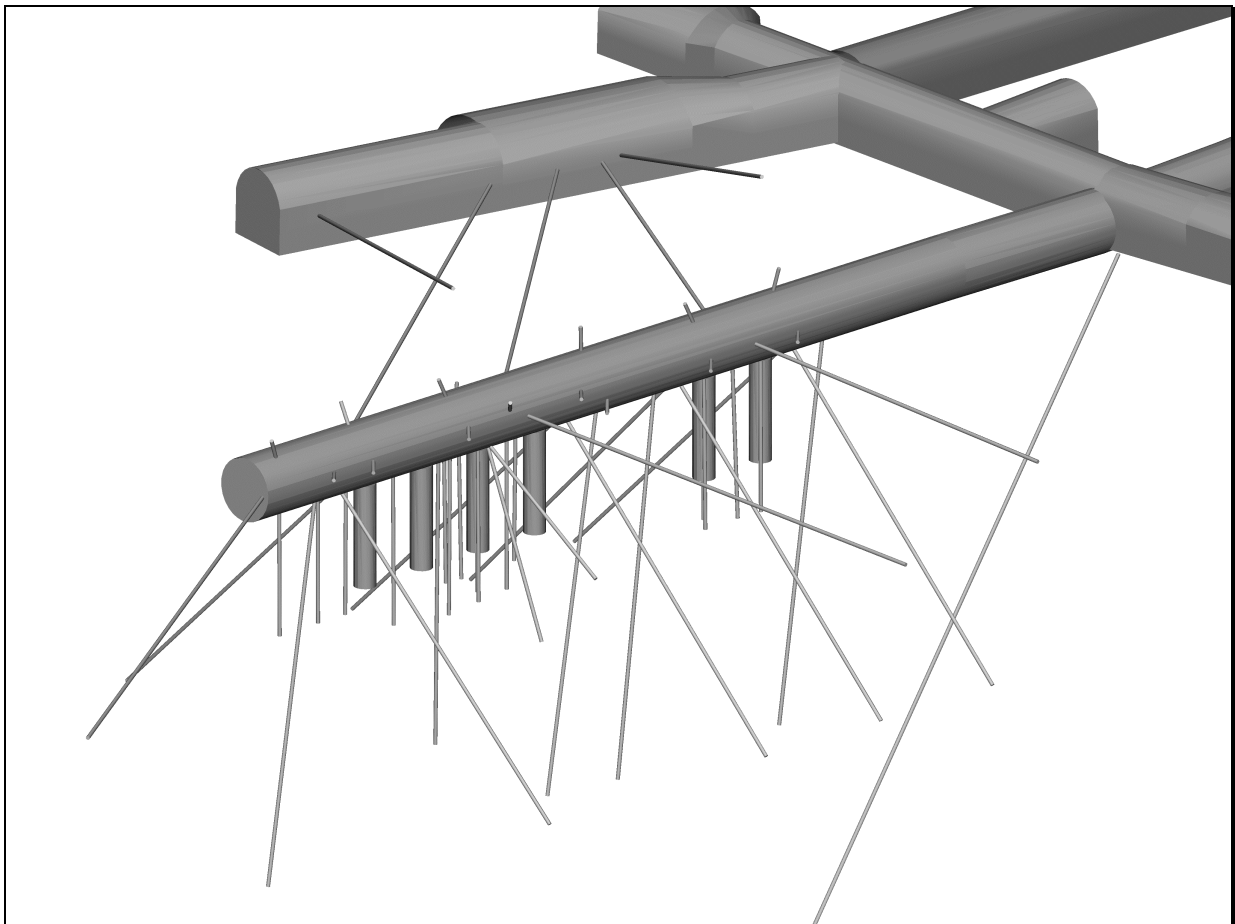


Figure 1. Boreholes used for characterization of the rock mass.

Investigations

A large number of boreholes have been drilled to characterize the rock mass. These boreholes will be used for the long-time monitoring of the Prototype Repository. The objectives of the pilot and the exploratory holes was to obtain data for prediction of the characteristics in the depositions holes, data for modelling and to quantify the criteria needed for validation of the suitability of the position for canister deposition.

39 core holes around the Prototype tunnel have been available for the characterization. In 33 of these core holes a large number of hydraulic tests have been performed. In 6 of the core holes a limited amount of hydraulic tests was performed (3 core holes drilled before the Prototype Repository project started and in 3 of the core holes drilled by the Prototype Repository project). The systematic tests, which have been made in most of the 33 boreholes, consist of the following:

- Measurements of pressure responses in nearby borehole sections during drilling.
- Measurements of flow rates from the entire bore hole.
- Flow logging with packer spacing of 1 or 3 meter.
- Flow logging with the UCM-tool (some boreholes).
- Pressure build-up tests of the entire borehole.
- Pressure build-up test of 1 or 3 meter test section if the flow rate out of that particular test section exceeded 10 mL/min.
- Interference tests, with up to 11 observation bore hole sections, were made if the flow rate out of the bore hole exceeded 10 mL/min.
- Measurements of the undisturbed pressure in the entire bore hole.
- Hydro chemical sampling of 1 or 3 meter test section if the flow rate out of a particular test section exceeds 10 mL/min.
- 14 “Long-time” interference tests with around 60 pressure observation sections. 10 of these tests are judged to be useful for calibrating numerical models.

The deposition holes and the tunnel have also been hydraulically characterized:

- Inflow measurements to tunnel sections in the Prototype tunnel.
- Inflow measurements to each deposition hole.
- Detailed inflow measurements to two of the deposition holes.

From previous projects tunnel mapping of the Prototype Repository tunnel was available, and as mentioned above, a few hydraulic tests in 3 core holes.

Characterization

Based on the results from the flow logging with packer spacing of 1 and 3 meter the distance between conductive features was analysed. The result is presented in Figure 2.

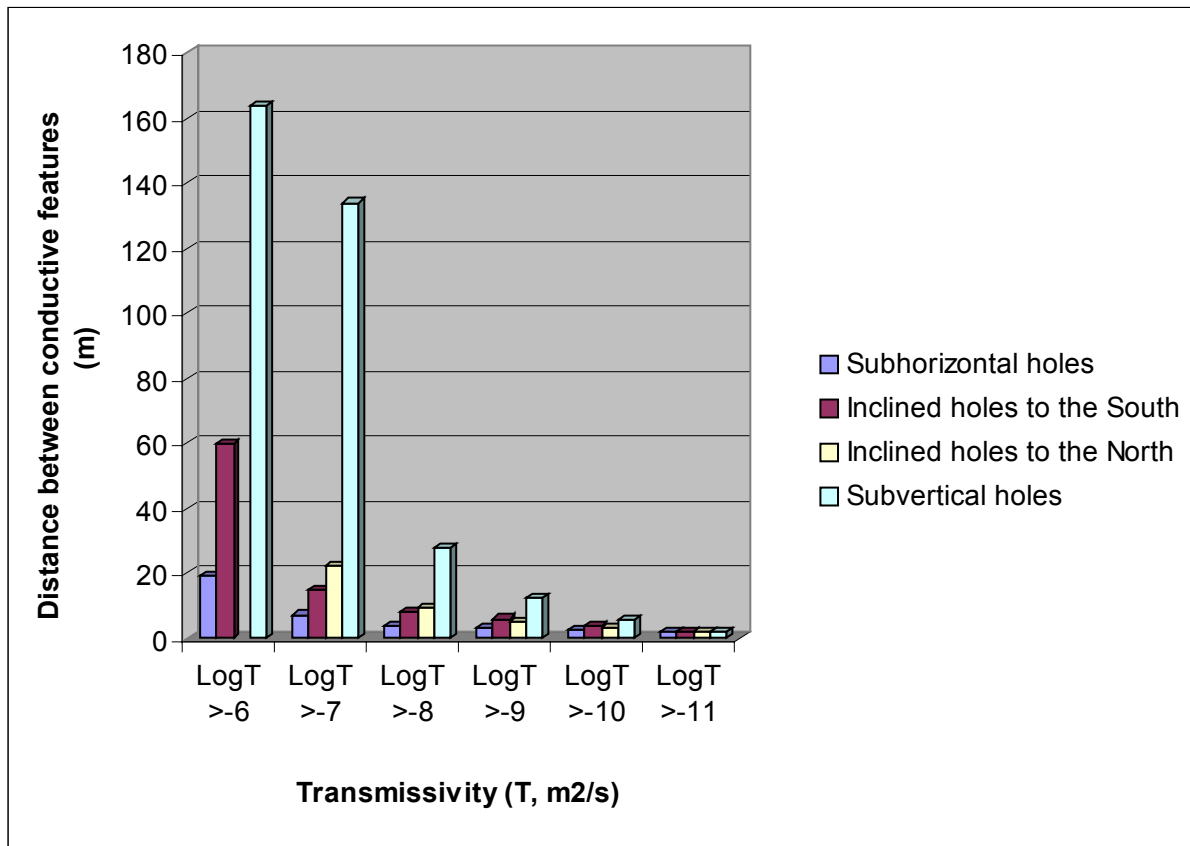


Figure 2. Distances between conductive features.

When the core is mapped, open fractures are reported as “Natural”. In the text below “All fractures” includes “Natural fractures” and “Sealed fractures”. Part of the analysis of the fracture network for the DFN (Discrete Fracture Network) is made in the ISIS software of the FracMan package. The assumed cut-off in the DFN model for T of “natural” fractures is $3 \cdot 10^{-11} \text{ m}^2/\text{s}$. Fractures with a lower transmissivity are assumed to be “sealed”. The “natural” fractures still contain fractures that have little impact for the flow solution. The highest truncation value that was possible to use without losing accuracy for the flow was $5 \cdot 10^{-10} \text{ m}^2/\text{s}$. Conductive fractures in the DFN model have therefore been defined as fractures with a transmissivity larger than or equal to $5 \cdot 10^{-10} \text{ m}^2/\text{s}$.

The fracture frequency along boreholes or a line (P_{10}) does not by itself explain how fractured the rock mass is as boreholes are only line samples. Maps of outcrops and tunnel walls show two-dimensional intersections with fractures in the network and are also subject of sampling bias. On a surface the fracture trace length per area (P_{21}) can be defined. From a DFN point of view, intensity is best described by a three-dimensional measure, fracture area per unit volume (m^2/m^3), P_{32} . The fracture intensity measure, P_{32} , cannot be measured directly in the field. However, it has been shown that P_{21} and P_{10} is linearly correlated to P_{32} and can thus be estimated by simulations.

Table 1 shows the fracture intensity, P_{32} , for all, natural- and conductive fractures. The measured and simulated fracture frequency for different transmissivity cut-off is shown in Figure 3. One can see a good match for measured and simulated frequencies for the sub-vertical holes, sub-horizontal holes and holes inclined towards north, but the southerly inclined holes is intersected by approximately 30% too few fractures.

Table 1. P_{32} for the three different fracture sets with different truncation level.

	<i>Set 1</i>	<i>Set 2</i>	<i>Set 3</i>	Σ
$P_{32, all}$	0.85	1.59	0.97	3.41
$P_{32, natural}$	0.26	0.85	0.18	1.25
$P_{32, conductive}$	0.15	0.51	0.06	0.71

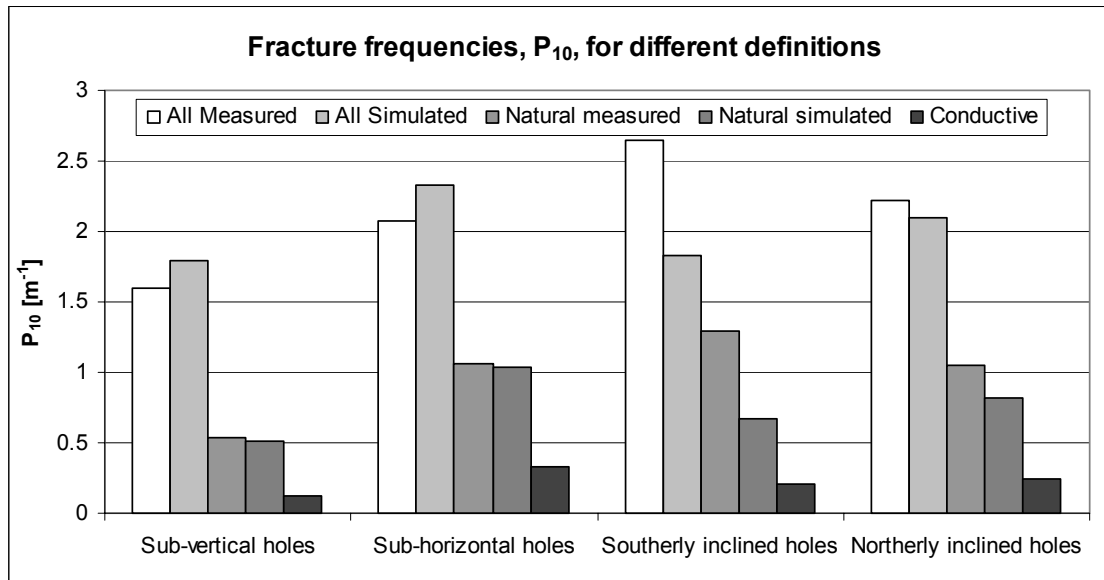


Figure 3. The fracture frequency in different borehole directions for different transmissivity cut-off.

An important base for the DFN model is the results from the flow logging with packer spacing of 1 and 3 meter. The results from these tests have also been the base to estimate the statistical distributions of the evaluated transmissivities, which have been converted to a hydraulic conductivity by dividing with the test section length. The result is presented in Table 2.

As can be noted the horizontal bore holes show considerably higher values of hydraulic conductivity than vertical bore holes. Observe that the tested sections for the 1 m and 3 m tests are not in the same part of the boreholes. To a minor extent probably the data is biased as the same feature (fracture or fracture system) and may have been tested in an adjacent test section due to a local hydraulically well - interconnected fracture network or long intersections between a conductive fracture and the bore hole.

Table 2. Statistical analysis of Log₁₀ K. Scale 1 m and 3 m.

Subclass	Geometric mean (m/s) 1 m	Standard deviation (Log10 K) 1 m	Geometric mean (m/s) 3 m	Standard deviation (Log10 K) 3 m	Geometric mean (m/s) 1*3 + 3 m	Standard deviation (Log10 K) 1*3 + 3 m
All test sections	$8.5 \cdot 10^{-11}$	1.48	$4.1 \cdot 10^{-10}$	1.83	$3.2 \cdot 10^{-10}$	1.76
Sub vertical holes	$2.6 \cdot 10^{-11}$	1.09	$2.5 \cdot 10^{-11}$	1.71	$3.7 \cdot 10^{-11}$	1.47
Subhorizontal holes	$2.6 \cdot 10^{-9}$	1.91	$2.5 \cdot 10^{-9}$	1.98	$8.7 \cdot 10^{-9}$	1.70
Inclined holes, South	$9.0 \cdot 10^{-11}$	1.08	$9.4 \cdot 10^{-10}$	1.83	$6.2 \cdot 10^{-10}$	1.62
Inclined holes, North	$1.9 \cdot 10^{-10}$	1.26	$9.1 \cdot 10^{-10}$	1.19	$8.1 \cdot 10^{-10}$	1.28

The storativity is not always received from a hydraulic test. In order to estimate an approximate value of the parameter a relationship between the evaluated transmissivity (T_{EVAL}) and the evaluated storativity (S) is established from the fourteen evaluated interference tests. The results are shown in Figure 4.

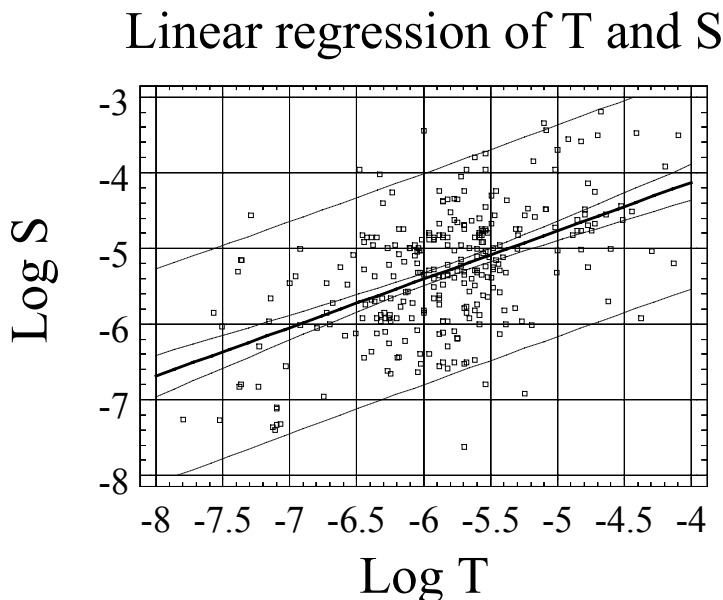


Figure 4. Linear regression of T_{EVAL} and S .

The hydraulic connectivity of the rock around the Prototype Repository was analysed based on the responses from the 14 interference tests. The flow period was about 6 to 7 h for most of the tests and about 1 h for two tests and 10 minutes for one test. Most monitoring sections were located within 50 m from the flowing section. It could be shown that about 25 % of the test sections show no responses and about 33 % of the test sections only show small responses ($0.1 \text{ m} < dP < 1 \text{ m}$) after flow time of the test. The rest or 42 % percent of the responses are larger than 1 meter and show good response.

Thirty-nine injection tests were made twice, before and after the deposition holes were drilled. The first test was performed with the UHT (Underground Hydraulic Test system) and the second with a more simple system. The upper part (0.25-1.75m) of boreholes close to the deposition holes was tested with test section length 0.5m. In order to study any link between the positions of the holes in relation to the deposition holes the tested boreholes were divided into three categories:

Category 1 (holes close to a deposition hole):

Category 2 (holes more distant to a deposition hole):

Category 3 (inclined holes; most distant to deposition hole):

There are only a few test sections that indicate more reliable changes of the transmissivity due to drilling of the deposition holes. No category 2 holes show reliable changes. All other sections indicate transmissivities below $2 \cdot 10^{-10} \text{ m}^2/\text{s}$ (i.e. $K = 4 \cdot 10^{-10} \text{ m/s}$), which was the approximate measurement limit. If there are changes in these sections, they are at least small. As noticed in Figure 5 a few of the sections show a significant transmissivity increase between the tests in 1999 and the tests in 2001.

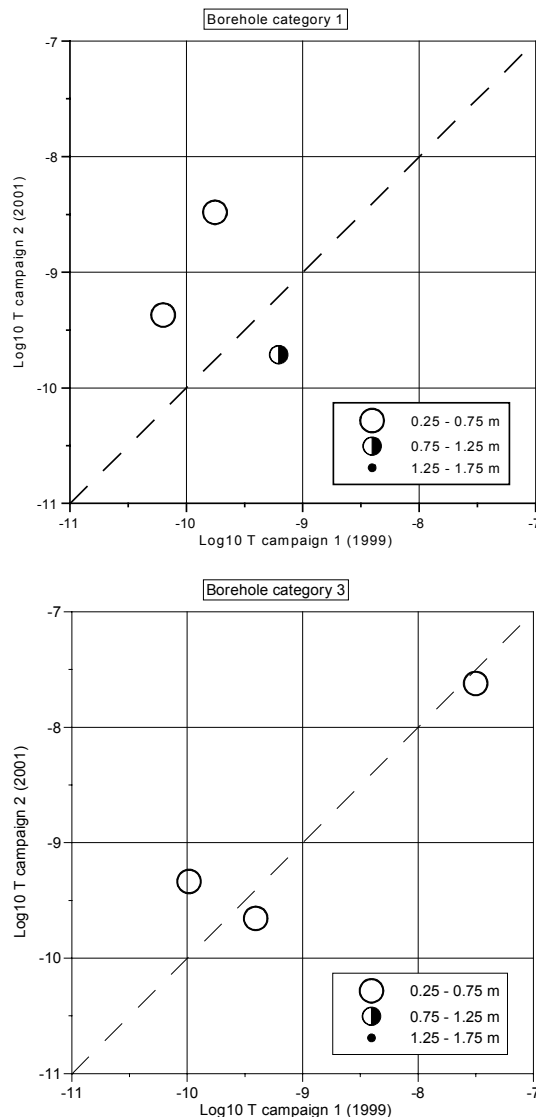


Figure 5. Relative overall change of transmissivities. Campaign 1: tests before the deposition holes were drilled. Campaign 2: tests after the deposition holes were drilled.

The pressure in a large number of borehole sections has been monitored for long time periods. These measurements have been the base to estimate the “undisturbed pressures” before and after the deposition holes were drilled. In Figure 6 the “undisturbed pressures” before the deposition holes were drilled is shown. The pressure after the deposition holes were drilled is more or less the same, due to the small inflow rates to the deposition holes.

The mean salinity of the water in the boreholes is 6.8 mg/L with max and min values of 8.7 mg/L and 5.5 mg/L respectively.

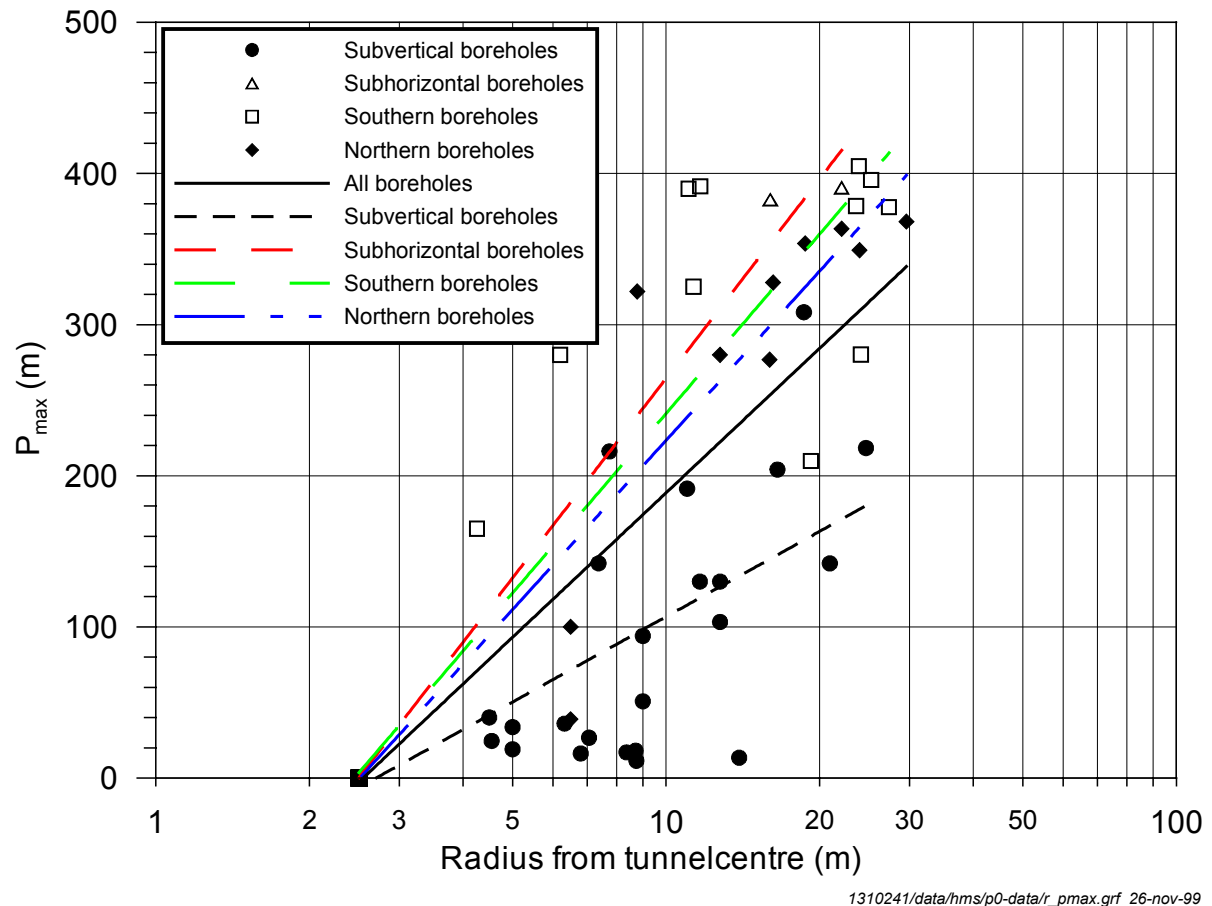


Figure 6. Maximum pressures plotted as function of the distance to the tunnel centre.

In Figure 7 an overview is given of the estimated inflow to different tunnels near the Prototype Repository. In Table 3, the result of the inflow measurements in the deposition holes is shown.

There is probably some minor leakage from the tunnel floor included in the figures in Table 3 in all boreholes except to DA3575G01. The last two measurements in DA3551G01 are considered representative as leaking water from the tunnel floor was sealed off. Sealing was also made in DA3545G01 after the first measurement and the measurement done in March 2000 is considered the most representative. Possibly, there are new leakages from the tunnel floor during the measurement in June/July 2000.

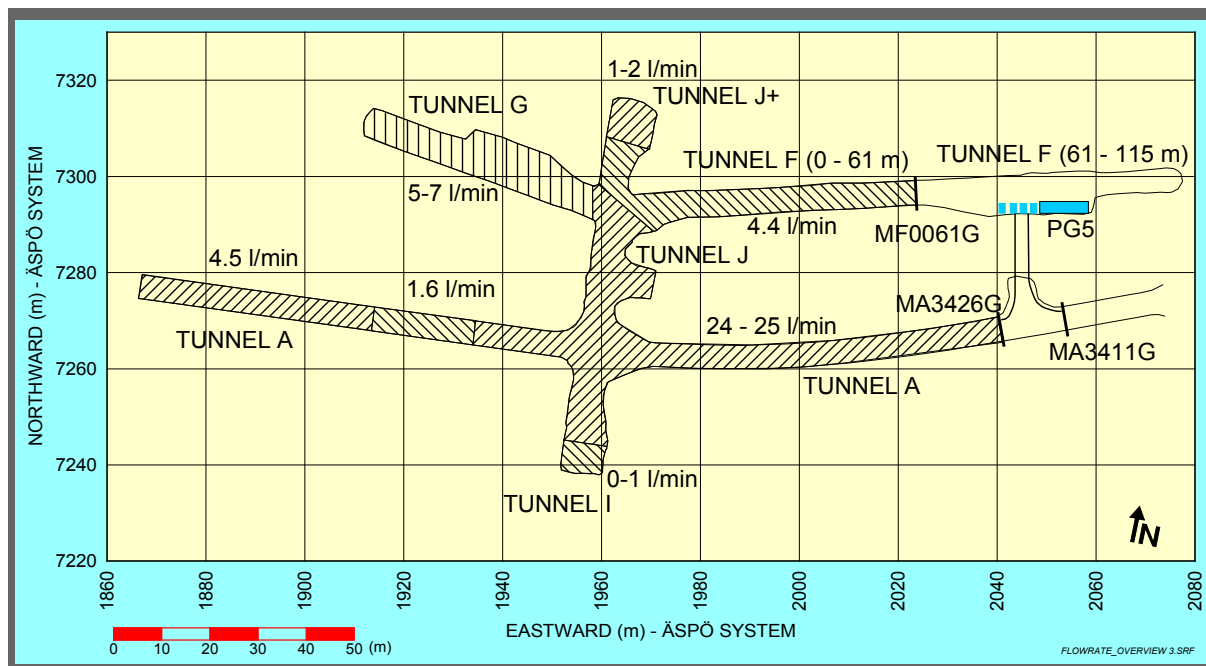


Figure 7. Estimated flowrates of tunnel segments.

Table 3. Result of inflow measurements to deposition boreholes. (Figures in bold are considered as the most representative flowrates.)

Borehole	Q 1999-12-08 – 1999-12-13 (L/min)	Q 2000-03-28 – 2000-03-31 (L/min)	Q June / July 2000 (L/min)
DA3587G01	0.08000	0.07870	N/A
DA3581G01	0.00160	0.00220	0.00220*
DA3575G01	0.00280	0.00310	0.00410**
DA3569G01	0.00072	0	0.00472**
DA3551G01	0.00270	0.00155	0.00160***
DA3545G01	0.00610	0.00270	0.00740***
SUM	0.09392	0.08825	N/A

*Estimated from diaper measurements

**Measurements made 2000-06-21 to 2000-06-24

***Measurements made 2000-07-13 to 2000-07-26

Modelling

Two numerical modelling exercises have been performed to estimate DFN (Discrete Fracture Network) properties and to test the predictive capacity. A simple prediction based on analytical equations has also been performed. A continuum model has also been used to estimate the pressure and salinity conditions around the Prototype Repository tunnel during the operation phase with the buffer and backfill emplaced.

The first DFN model was based on a limited data set but succeeded to predict the fracture orientations and fracture frequencies fairly well. The inflow prediction was less good. The predicted inflows were greater than the measured. All available data were not used and possibly the predictions could have improved to some extent if all data had been used.

The second DFN model was based on a large data set but not all now available data. The predictions of fracture frequencies and fracture trace statistics were fairly good but the inflows to the deposition holes were much greater than measured. The predicted pressures were also a bit too high and showed less variability than the measured pressures.

The results indicate that the DFN model can be improved and probably the hydraulic tests can be most useful when testing new modelling ideas. The reason for this is that these test are probably less affected of two phase flow and rock stress conditions that may play a significant role when modelling the inflow to the tunnels and deposition holes. New data that can be useful are the mapping of the deposition holes and a large number of interference tests. Inflow to the deposition holes and the pressure responses during the drilling of the deposition holes is also a data set not used for setting up the present DFN model.

The simple analytical predictions of the mean inflow rate into the deposition holes, based on measured flow rates and pressures from pilot bore holes drilled within the circumference of the deposition holes and boreholes a few decimetre from the circumference of the deposition holes, were within 10 to 0.1 of the measured flow rate. Predictions based on just the pilot bore holes drilled within the circumference of the deposition holes (one bore hole per deposition hole) were less good but still in several cases within or near the limits mention above. Predictions based on all boreholes showed a rather large variation, mainly depending on results from the inclined boreholes that indicated high transmissivities. In a case with vertical deposition holes and if the most conductive fracture sets are subvertical, subvertical boreholes give the most reliable predictions.

The continuum model was based on a fracture network with given transmissivity distribution that was converted to a conductivity field in a continuum model with cell size of 1 m close to the tunnel. Boundary conditions for the model were generated with larger scale models and variable density flow was included in the modelling.

The realisations with different fracture networks showed rather different pressure fields when the tunnel was open. When the tunnel was closed the differences between the realisations were less compared to the open conditions but were anyhow present.

With the backfill and buffer in the tunnel the cases with no skin (hydraulic resistance around the tunnel) and skin as for open conditions were tested. The hydraulic conductivity of the backfill was also varied with two limiting cases: maximum ($= 10^{-9}$ m/s) conductivity in backfill and no skin (hydraulic resistance around the tunnel) and minimum ($= 10^{-11}$ m/s) conductivity and skin as for open conditions. The result was that the pressure distribution in the rock was very similar between the cases.

Contents

1	BACKGROUND	31
1.1	Äspö Hard Rock Laboratory	31
1.2	Prototype repository	32
1.2.1	General objectives	33
1.2.2	Objectives – hydrogeology investigations	34
1.3	This report	36
2	DESCRIPTION OF TEST SITE	37
2.1	Introduction	37
2.1.1	General layout	37
2.2	Characterization and monitoring of existing boreholes	38
3	OVERVIEW OF GEOLOGY	41
3.1	Prototype Repositoryarea	41
3.2	Documentation	46
4	OVERVIEW OF TESTS AND INVESTIGATIONS	49
4.1	Hydraulic tests prior to prototype pre-investigation tests	49
4.2	Drilling campaign 1	49
4.3	Drilling campaign 2	50
4.4	Drilling campaign 3	51
4.5	Interference test campaign 1 after drilling campaign 3	52
4.6	Interference test campaign 2 after drilling campaign 3	53
4.7	Injection test campaign 1 and 2	53
4.8	Lead-through holes	54
4.9	Water inflow measurements to the tunnel and deposition holes	54
4.10	Documentation	54
5	DRILLING	57
5.1	Drilling campaign 1	57
5.1.1	Pressure responses during drilling	57

5.2	Drilling campaign 2	57
5.2.1	Pressure responses during drilling	57
5.3	Drilling campaign 3	58
5.3.1	Pressure responses during drilling	58
5.4	Interference test campaign 1 after drilling campaign 3	60
5.5	Interference test campaign 2 after drilling campaign 3	60
5.6	Lead-through holes from G-tunnel to A-tunnel	60
5.6.1	Pressure responses during drilling	60
5.7	Deposition holes	62
6	FLOW MEASUREMENTS	67
6.1	Drilling campaign 1	67
6.2	Drilling campaign 2	70
6.3	Drilling campaign 3	73
6.4	Interference test campaign 1 after drilling campaign 3	78
6.5	Interference test campaign 2 after drilling campaign 3	78
6.6	Lead-through holes from G-tunnel to A-tunnel	78
6.7	Flow logging with UCM tool	79
6.8	Tunnel measurements	80
6.9	Deposition boreholes	82
6.9.1	Mapping and feature leakage measurements	82
6.9.2	Total inflow to deposition holes	90
6.9.3	Diaper measurements	91
6.10	Groundwater leakage into G-, I- and J-tunnel	97
7	HYDRAULIC TESTS OF BORE HOLE SECTIONS	99
7.1	Drilling campaign 1	99
7.2	Drilling campaign 2	101
7.3	Drilling campaign 3	102
7.4	Interference test campaign 1 after drilling campaign 3	105
7.5	Interference test campaign 2 after drilling campaign 3	106
7.6	Injection tests	106
7.7	Lead-through holes	110

8	HYDRAULIC INTERFERENCE TESTS	113
8.1	Drilling campaign 1	113
8.2	Drilling campaign 2	113
8.3	Drilling campaign 3	116
8.4	Interference test campaign 1 after drilling campaign 3	120
8.4.1	Interference test 1:1	120
8.4.2	Interference test 1:2	123
8.4.3	Interference test 1:3	126
8.4.4	Interference test 1:4	129
8.4.5	Interference test 1:5	132
8.4.6	Interference test 1:6	135
8.5	Interference test campaign 2 after drilling campaign 3	138
8.5.1	Interference test 2:7	138
8.5.2	Interference test 2:8	141
8.5.3	Interference test 2:9	144
8.5.4	Interference test 2:10	147
8.5.5	Interference test 2:11	150
8.5.6	Interference test 2:12	153
8.5.7	Interference test 2:13	156
8.5.8	Interference test 2:14	159
9	BLASTING	163
10	LABORATORY MEASUREMENTS OF POROSITY IN THE DEPOSITION HOLES	165
11	HYDRAULIC PROPERTIES OF ROCK MASS	167
11.1	Transmissivity	167
11.1.1	Distance between features	167
11.1.2	Measurement limit of transmissivity	173
11.1.3	DFN properties	173
11.2	Hydraulic conductivity	177
11.2.1	Undisturbed rock mass	177
11.3	Hydraulic diffusivity	179
11.4	Storativity	179
11.5	Connectivity	181
11.6	Preliminary model of deterministic features	186
12	UNDISTURBED HYDRAULIC PRESSURE	189
12.1	Before the deposition holes were drilled	189
12.2	After the deposition holes were drilled	194

13	GROUNDWATER SALINITY AND CHEMICAL COMPOSITION	197
13.1	Sampling procedure	197
13.2	Salinity estimations	197
14	CALIBRATION CASES FOR NUMERICAL MODELLING	203
15	PREDICTIONS WITH NUMERICAL AND ANALYTICAL MODELS	205
15.1	DFN predictions	205
15.1.1	DFN model 1	206
15.1.2	DFN model 2. Inner boundaries: tunnels, pilot holes and deposition holes	209
15.1.3	DFN model 2. Calibration	211
15.1.4	DFN model 2. Transient simulation	211
15.1.5	DFN model 2. Predictions of fracture traces in the deposition holes	212
15.1.6	DFN model 2. Predicted inflow to the deposition holes	217
15.1.7	DFN model 2. Predicted heads	217
15.1.8	DFN model 2. Improvements suggested by the modelling team	219
15.2	Simple prediction of the inflow to the deposition holes	220
15.2.1	Method	220
15.2.2	Predicted flow rates	222
15.2.3	Predicted properties	229
15.3	Continuum model	232
15.4	Conclusions	238
15.4.1	DFN model	238
15.4.2	Simple inflow prediction	238
16	REFERENCES	239

APPENDIX

Summary of hydrogeology in WellCad sheets

List of Figures

Figure 1-1	Äspö Hard Rock Laboratory.	31
Figure 1-2	Tunnel systems at Äspö.	32
Figure 2-1	Tunnel systems close to the Prototype Repository.	37
Figure 2-2	Schematic view of the layout of the Prototype Repository and deposition hole in the A-tunnel (not to scale).	38
Figure 2-3	Boreholes used for characterization of the rock mass.	39
Figure 2-4	Existing boreholes to be used as monitoring holes.	40
Figure 2-5	Existing boreholes to be used as monitoring holes.	40
Figure 3-1	Mapping of the TBM tunnel (from Markström and Erlström, 1996).	41
Figure 3-2	Lower hemisphere projection of poles to fracture planes in the 36 bore- and exploratory holes.	42
Figure 3-3	Lower hemisphere projection of poles to fracture planes for “natural” fractures in the 36 exploratory holes.	43
Figure 3-4	Trace map over the last 120 m of the TBM tunnel after Follin and Hermanson (1996).	45
Figure 3-5	The orientation of the principal stresses compared to the prototype tunnel.	46
Figure 3-6	Example 1 of geological documentation of drilled core holes (Fracture directions in columns Natural mineral to Sealed mineral are as seen in the borehole wall).	47
Figure 3-7	Example 2 of geological documentation of drilled core holes (Fracture directions in columns Natural mineral to Sealed mineral are as seen as they would appear in a vertical borehole).	47
Figure 4-1	Example of hydrogeological documentation of drilled core holes.	55
Figure 4-2	Example of hydrochemistry documentation of drilled core holes.	55
Figure 5-1	Pressure responses during drilling of KG0023A01 (14.38 - 15.77 m).	62
Figure 5-2	Pressure increase/decrease during drilling of deposition boreholes (+ = increase, - = decrease of pressure).(11: deposition bore hole No 1, 21: deposition bore hole No 2 etc, according to Table 5-5.)	64
Figure 5-3	Borehole subclass orientation(S=South, N=North).	66
Figure 6-1	The results from flowlogging in KA3539G, KA3545G, KA3551G and KA3557G. The red bars in the transmissivity diagrams indicate single section PBTs.	68
Figure 6-2	The results from flowlogging in KA3563G, KA3695G, KA3575G and KA3581G. The red bars in the transmissivity diagrams indicate single section PBTs.	69

Figure 6-3	The results from flowlogging in KA3587G, KA3935G. The red bars in the transmissivity diagrams indicate single section PBTs.	70
Figure 6-4	The results from flowlogging in KA3544G01, KA3546G01, KA3548G01 and KA3550G01. The red bars in the transmissivity diagrams indicate single section PBTs.	71
Figure 6-5	The results from flowlogging in KA3552G01, KA3572G01, KA3578G01 and KA3584G01. The red bars in the transmissivity diagrams indicate single section PBTs.	72
Figure 6-6	The results from flowlogging in KA3586G01, KA3588G01. The red bars in the transmissivity diagrams indicate single section PBTs.	73
Figure 6-7	The results from flowlogging in KA3539G (extended), KA3542G01, KA3542G02 and KA3548A01. The red bars in the transmissivity diagrams indicate single section PBTs.	74
Figure 6-8	The results from flowlogging in KA3554G01, KA3554G02, KA3557G (extended) and KA3563G (extended). The red bars in the transmissivity diagrams indicate single section PBTs.	75
Figure 6-9	The results from flowlogging in KA3566G01, KA3566G02, KA3574G01 and KA3576G01. The red bars in the transmissivity diagrams indicate single section PBTs.	76
Figure 6-10	The results from flowlogging in KA3579G, KA3590G01, KA3590G02 and KA3593G (extended). The red bars in the transmissivity diagrams indicate single section PBTs.	77
Figure 6-11	The results from flowlogging in KG0021A01 and KG0048A01. The red bars in the transmissivity diagrams indicate single section PBTs.	78
Figure 6-12	Weir measurements 1997, 1999 and 2000.	81
Figure 6-13	Deposition hole mapping in DA3587G01. Mapped water bearing features are marked with shaded areas.	84
Figure 6-14	Deposition hole mapping in DA3581G01. Mapped water bearing features are marked with shaded areas.	85
Figure 6-15	Deposition hole mapping in DA3575G01. No water bearing features was observed.	86
Figure 6-16	Deposition hole mapping in DA3569G01. Water bearing features are marked with shaded areas.	87
Figure 6-17	Deposition hole mapping in DA3551G01. Water bearing features are marked with shaded areas.	88
Figure 6-18	Deposition hole mapping in DA3545G01. Water bearing features are marked with shaded areas.	89
Figure 6-19	Diaper measurement arrangement in DA3581G01.	91
Figure 6-20	Diaper measurement arrangement in DA3581G01 (left) and DA3575G01 (right).	92
Figure 6-21	Inflow measurements in DA3581G01 using diapers. Flowing fracture shown as thick line in the upper right part of the figure.	93
Figure 6-22	Hydraulic conductivity of DA3581G01 as estimated from diaper measurements	94

Figure 6-23	Inflow measurements in DA3575G01 using diapers. Flowing fracture shown as thick line in the upper right part of the figure.	95
Figure 6-24	Hydraulic conductivity of DA3575G01 as estimated from diaper measurements	96
Figure 6-25	Estimated flowrates of tunnel segments	97
Figure 7-1	Relative overall change of transmissivities. Campaign 1: tests before the deposition holes were drilled. Campaign 2: tests after the deposition holes were drilled.	109
Figure 7-2	The transmissivity changes of the test section plotted against the squared distance.	110
Figure 8-1	Drawdown during flowing of KA3566G01:2 (Interference test 1:1) - plan view.	120
Figure 8-2	Drawdown during flowing of KA3566G01:2 (Interference test 1:1) - vertical view.	121
Figure 8-3	Drawdown during flowing of KA3566G02:2 (Interference test 1:2) - plan view.	123
Figure 8-4	Drawdown during flowing of KA3566G02:2 (Interference test 1:2) - vertical view.	124
Figure 8-5	Drawdown during flowing of KA3590G01:3 (Interference test 1:3) - plan view.	126
Figure 8-6	Drawdown during flowing of KA3590G01:3 (Interference test 1:3) - vertical view.	127
Figure 8-7	Drawdown during flowing of KA3590G01:2 (Interference test 1:4) - plan view.	129
Figure 8-8	Drawdown during flowing of KA3590G01:2 (Interference test 1:4) - vertical view.	130
Figure 8-9	Drawdown during flowing of KA3590G02:1 (Interference test 1:5) - plan view.	132
Figure 8-10	Drawdown during flowing of KA3590G02:1 (Interference test 1:5) - vertical view.	133
Figure 8-11	Drawdown during flowing of KA3590G01:3 (Interference test 1:6) - plan view.	135
Figure 8-12	Drawdown during flowing of KA3590G01:3 (Interference test 1:6) - vertical view.	136
Figure 8-13	Drawdown during flowing of KG0048A01:1 (Interference test 2:7) - plan view.	138
Figure 8-14	Drawdown during flowing of KG0048A01:1 (Interference test 2:7) - vertical view.	139
Figure 8-15	Drawdown during flowing of KA3554G01:1 (Interference test 2:8) - plan view.	141
Figure 8-16	Drawdown during flowing of KA3554G01:1 (Interference test 2:8) - vertical view.	142
Figure 8-17	Drawdown during flowing of KA3554G02:2 (Interference test 2:9) - plan view.	144
Figure 8-18	Drawdown during flowing of KA3554G02:2 (Interference test 2:9) - vertical view.	145
Figure 8-19	Drawdown during flowing of KA3542G01:2 (Interference test 2:10) - plan view.	147
Figure 8-20	Drawdown during flowing of KA3542G01:2 (Interference test 2:10) - vertical view.	148
Figure 8-21	Drawdown during flowing of KA3542G02:4 (Interference test 2:11) - plan view.	150
Figure 8-22	Drawdown during flowing of KA3542G02:4 (Interference test 2:11) - vertical view.	151
Figure 8-23	Drawdown during flowing of KA3539G:2 (Interference test 2:12) - plan view.	153
Figure 8-24	Drawdown during flowing of KA3539G:2 (Interference test 2:12) - vertical view.	154
Figure 8-25	Drawdown during flowing of KG0021A01:1 (Interference test 2:13) - plan view.	156
Figure 8-26	Drawdown during flowing of KG0021A01:1 (Interference test 2:13) - vertical view.	157

Figure 8-27	Drawdown during flowing of KG0021A01:3 (Interference test 2:14) - plan view.	159
Figure 8-28	Drawdown during flowing of KG0021A01:3 (Interference test 2:14) - vertical view.	160
Figure 9-1	Example of pressure response due to blasting.	163
Figure 10-1	Porosity of rock determined by using ¹⁴ C-PMMA-method with respect to the distance from the surface of the experimental deposition holes 3 and 4 in the Prototype Repository tunnel at Äspö Hard Rock Laboratory.	165
Figure 11-1	Methods for calculation of distance between features in several boreholes.	167
Figure 11-2	Log normal probability plot for distances between features with a transmissivity greater than $1 \cdot 10^{-9} \text{ m}^2/\text{s}$ for data set 1.	168
Figure 11-3	Distances between features. Summary of data set 1- 5 for subclass 1 (all boreholes).	170
Figure 11-4	Distances between features. Summary of data set 1- 5 for subclass 2 and 3 (vertical and horizontal boreholes).	171
Figure 11-5	Distances between features. Summary of data set 1- 5 for subclass 2 and 3 (southerly and northerly inclined boreholes).	172
Figure 11-6	Probability distribution of Log ₁₀ T.	173
Figure 11-7.	The fracture frequency in different borehole directions for different transmissivity cut-off.	174
Figure 11-8.	Estimated conductive fracture frequencies by Forsmark and Rhén (1999) and simulated frequency.	175
Figure 11-9.	Fracture frequency in the 36 pilot and exploratory holes in the vicinity of the Prototype Repository of the TBM tunnel.	175
Figure 11-10	Statistical analysis of Log ₁₀ K (1*3 + 3 m), geometric mean and standard deviation.	178
Figure 11-11	Linear regression plots of timelag, t_L (min) and diffusivity versus distance, r, (m).	179
Figure 11-12	Linear regression of T_{EVAL} and S.	180
Figure 11-13	Linear regressions of T_{EVAL} and S*.	180
Figure 11-14	Distribution of responses versus distance to test section. White: No responses, Line screen: Some response (0.1-1.0m), Black: god response(>1.0m)	185
Figure 11-15	Major hydraulic features located during interference tests 1:1 - 1:6.	186
Figure 11-16	Minor identified features in the close vicinity of the deposition bore holes labelled with feature name and strike/dip.	187
Figure 12-1	Pressures based on different times and methods of selection	190
Figure 12-2	Maximum pressures plotted as function of the distance to the tunnel centre.	192
Figure 12-3	Difference between the maximum registered pressures and start and stop values of the studied period, 1999-03-01 and 1999-06-19.	193
Figure 12-4	Pressures 1999-12-01 plotted as function of the distance to the tunnel centre.	196

Figure 13-1	Distribution of salinity (g/l) – horizontal view of prototype repository.	198
Figure 13-2	Distribution of salinity (g/l) - vertical view of prototype repository.	199
Figure 13-3	Normal probability plot salinity analysis.	200
Figure 13-4	Diagrams of salinity distribution over a 2-year period in four hole sections. The six deposition holes were all drilled within the period between the fourth and fifth value above. Deposition holes were drilled from mid-June 1999 to mid-september 1999.	201
Figure 15-1	Left: Lower hemisphere projection of the predicted poles of the conductive fractures that intersects the boreholes in drill campaign 2. Right: Lower hemisphere projection of the measured poles of the intersecting fractures in the boreholes from drill campaign 2.	207
Figure 15-2	Simulated and measured inflow to the ten exploratory holes in drill campaign 2. Unfortunately the simulated and measured inflow tests are made under different circumstances.	209
Figure 15-3	Model domain showing sub-horizontal and inclined boreholes together with the included A-, G-, I-, and J-tunnels. The shaded F-tunnel is excluded.	210
Figure 15-4	The position and numbering of the 6 deposition holes in the Prototype Repository tunnel.	210
Figure 15-5	Illustration of groupflux boundaries.	211
Figure 15-6	Fracture traces on the wall of the deposition holes in realisation 1. Upper row from left: all fractures, “natural” fractures ($T > 5 \cdot 10^{-11} \text{ m}^2/\text{s}$) and conductive fractures ($T > 5 \cdot 10^{-10} \text{ m}^2/\text{s}$) for deposition hole 1. Lower: “natural” fractures in deposition hole 2, 3 and 4.	212
Figure 15-7	Number of “natural” fracture traces per deposition hole. Summary statistics based on 20 realisations of the calibrated DFN model.	214
Figure 15-8	Trace length of individual “natural” fractures per deposition hole. Summary statistics based on 20 realisations of the calibrated DFN model.	214
Figure 15-9	Fracture intensity, P_{21} (m/m^2), for “natural” fractures on the deposition hole walls. Summary statistics based on 20 realisations of the calibrated DFN model.	215
Figure 15-10	Transmissivity of individual conductive fractures intersecting the deposition holes. Summary statistics based on 20 realisations of the calibrated DFN model.	215
Figure 15-11	Example of modelled (left) and measured (right) trace maps. The modelled traces are fewer but longer compared to the measured.	216
Figure 15-12	Simulated heads versus measured heads.	218
Figure 15-13	Schematic layout of deposition bore hole and exploratory borehole.	221
Figure 15-14	Estimated mean flow rates (Q_{d1} and Q_{d2}) and measure flow rates according to Table 15-5 and Forsmark and Rhen (1999b).	223
Figure 15-15	Estimated mean flow rates (Q_{d1} and Q_{d2} , based on boreholes drilled close or within the circumference of the deposition holes) and measure flow rates according to Forsmark and Rhen (1999b).	224

Figure 15-16	Estimated flow rates(Qd1) according to Table 7-1 to 7-3 in (Forsmark, Rhén, 1999b) and measured flow rates according to Table 8-2 in (Forsmark et al, 2001a). X_m = mean at $\text{Log}_{10}(X)$, S = standard deviation of $\text{Log}_{10}(X)$. 1: drill batch 1, 2: drill batch 2 and 3:drill batch 3.	225
Figure 15-17	Estimated flow rates (Qd1) according to Table 7-4 to 7-6 in (Forsmark, Rhén, 1999b) and measured flow rates according to Table 8-2 in (Forsmark et al, 2001a). X_m = mean at $\text{Log}_{10}(X)$, S = standard deviation of $\text{Log}_{10}(X)$. 1: drill batch 1, 2: drill batch 2 and 3: drill batch 3.	226
Figure 15-18	Estimated flow rates (Qd2) according to Table 7-1 to 7-3 in (Forsmark, Rhén, 1999b) and measured flow rates according to Table 8-2 in (Forsmark et al, 2001a). X_m = mean at $\text{Log}_{10}(X)$, S = standard deviation of $\text{Log}_{10}(X)$. 1: drill batch 1, 2: drill batch 2 and 3: drill batch 3.	227
Figure 15-19	Estimated flow rates (Qd2) according to Table 7-4 to 7-6 in (Forsmark, Rhén, 1999b) and measured flow rates according to Table 8-2 in (Forsmark et al, 2001a). X_m = mean at $\text{Log}_{10}(X)$, S = standard deviation of $\text{Log}_{10}(X)$. 1: drill batch 1, 2: drill batch 2 and 3: drill batch 3.	228
Figure 15-20	Predicted geometric mean hydraulic conductivity for each deposition hole based on boreholes located within a few meters from the deposition hole. (db: drill batch).	231
Figure 15-21	Predicted geometric mean hydraulic conductivity for each deposition hole based on boreholes located within the deposition hole (db1) or a few decimetres from the outer radius of the deposition hole. (db: drill batch).	231
Figure 15-22	Hydraulic conductivity field at a depth of 447 metres below ground level.	233
Figure 15-23	Pressure head (in metres) (top) and salinity (in %) distributions at a depth of 447 metres below ground level. Realisation 2.	234
Figure 15-24	Pressure head (in metres) (top) and salinity (in %) distributions at a depth of 447 metres below ground level. Realisation 5.	235
Figure 15-25	Pressure head (in metres) (top) and salinity (in %) distributions at a depth of 447 metres below ground level. Saturated conditions in section I and II. Skin as for open conditions. Hydraulic conductivity for backfill 10^{-10} m/s. Realisation 2.	236
Figure 15-26	Pressure head (in metres) (top) and salinity (in %) distributions at a depth of 447 metres below ground level. Saturated conditions in section I and II.	237

List of Tables

Table 3-1	Statistical separation of fracture sets of the 36 pilot and exploratory holes. The Fisher distribution is used for all fracture sets.	44
Table 3-2	The principal stresses at the depth of the prototype repository. The strikes refers to the local north of the Äspö local coordinate system (local north is 12° west of magnetic north).	45
Table 4-1	Interference tests carried out during February and April 1999.	52
Table 4-2	Interference tests carried out during June and August 1999.	53
Table 5-1	Pressure responses during drilling of exploratory boreholes. (X= drilled borehole, 0 = NO response, 1 = response, blank= no observations made).	58
Table 5-2	Pressure responses during drilling of exploratory boreholes (X= drilled borehole, 0 = NO response, 1 = response, blank= no observations made).	59
Table 5-3	Registered pressure changes in observation sections during drilling of observed water-bearing section in drilled borehole [0=no response (<0.1 m), 1= some response (> 0.1 m & < 1.0 m), 2= good response (> 1.0 m)].	61
Table 5-4	Pressure responses during drilling of deposition boreholes (0=NO response, 1=response).	63
Table 5-5	Statistics of pressure increase/decrease during drilling of deposition boreholes.	65
Table 5-6	Pressure increase or decrease around prototype tunnel during drilling of deposition boreholes.	66
Table 6-1	Uptake with increasing inflow during drilling of the lead-through boreholes.	79
Table 6-2	Result of inflow measurements to Prototype Repositorytunnel.	80
Table 6-3	Inleakage measurements of features in deposition holes, see Figures 6-13 to 6-18.	82
Table 6-4	Result of inflow measurements to deposition boreholes. (Figures in bold are considered as the most representative flowrates).	90
Table 6-5	Summary of flows into different tunnel sections.	98
Table 7-1	Evaluated and estimated hydrogeological parameters (s = pressure change, Q = flow rate, Spec_cap = Specific capacity, T(Spec_cap) = transmissivity calculated from eq. 7-1, T_eval = evaluated transmissivity where possible).	99
Table 7-2	Result from the part of bore hole pressure build-up tests (s = pressure change, Q = flow rate, Spec_cap = Specific capacity, T(Spec_cap) = transmissivity calculated from eq. 7-1, T_eval = evaluated transmissivity where possible). Shaded values : values are considered uncertain.	100

Table 7-3	Evaluated and estimated hydrogeological parameters (s = pressure change, Q = flow rate, Spec_cap = Specific capacity, $T(\text{Spec_cap})$ = transmissivity calculated from eq. 5-1, T_{eval} = evaluated transmissivity where possible).	101
Table 7-4	Result from the part of bore hole pressure build-up tests (s = pressure change, Q = flow rate, Spec_cap = Specific capacity, $T(\text{Spec_cap})$ = transmissivity calculated from eq. 7-1, T_{eval} = evaluated transmissivity where possible).	101
Table 7-5	Evaluated and estimated hydrogeological parameters (s = pressure change, Q = flow rate, Spec_cap = Specific capacity, $T(\text{Spec_cap})$ = transmissivity calculated from equations 7-1 or 7-2 T_{eval} = evaluated transmissivity where possible).	102
Table 7-6	Result from the part of bore hole pressure build-up tests (s = pressure change, Q = flow rate, Spec_cap = Specific capacity, $T(\text{Spec_cap})$ = transmissivity calculated from eq. 7-1, T_{eval} = evaluated transmissivity where possible).	103
Table 7-7	Result from the part of bore hole pressure build-up tests (s = pressure change, Q = flow rate, Spec_cap = Specific capacity, $T(\text{Spec_cap})$ = transmissivity calculated from eq. 7-1, T_{eval} = evaluated transmissivity where possible).	104
Table 7-8	Results from evaluation of test sections during interference test campaign 1 after drilling campaign 3.	105
Table 7-9	Results from evaluation of test sections during interference test campaign 2 after drilling campaign 3.	106
Table 7-10	Comparison of the two test campaigns. Sections with measurement limits in italics and sections with measured value in bold. Fracture location within brackets is located outside the test section but close by.	107
Table 7-11	Evaluated and estimated hydrogeological parameters (s = pressure change, Q = flow rate, Spec. cap = specific capacity, $T(\text{Spec. cap})$ = transmissivity calculated from equation 6-1, T_{eval} = evaluated transmissivity where radial flow occurs).	111
Table 8-1	Interference test results for KA3544G, KA3546G, KA3548G, KA3550G and KA3552G. (r = aprox. distance from flowing bore hole section to observation bore hole section, t_L = time lag for a pressure response of 0.1 m to be registered in an observation section, T = transmissivity, S = storage coefficient, S^* = storage coefficient from diffusivity, η .)	114
Table 8-2	Interference test results for KA3588G. (r = aprox. distance from flowing bore hole section to observation bore hole section, t_L = time lag for a pressure response to reach an observation section, T = transmissivity, S = storage coefficient, S^* = storage coefficient from diffusivity, η .)	115

Table 8-3	Interference test results for KA3539G, KA3542G01 and KA3542G02. (r = aprox. distance from flowing bore hole section to observation bore hole section, t_L = time lag for a pressure response of 0.1 m to be registered in an observation section, T = transmissivity, S = storage coefficient, S^* = storage coefficient from diffusivity, η .)	116
Table 8-4	Interference test results for KA3548A01, KA3554G01, KA3554G02 and KA3566G01.	117
Table 8-5	Interference test results for KA3566G02, KA3590G01, KA3590G02 and KA3593G.	118
Table 8-6	Interference test results for KG0021A01 and KG0048A01.	119
Table 8-7	Interference test results for KA3566G01, 12.30 - 19.80 m. (r = aprox. distance from flowing bore hole section to observation bore hole section, t_L = time lag for a pressure response of 0.1 m to be registered in an observation section, T = transmissivity, S = storage coefficient, S^* = storage coefficient from diffusivity, η .) The response is classified as 1 = no response (< 0.1 m), 2 = some response (0.1 m - 1.0 m) and 3 = good response (> 1.0 m). P_0 = Initial pressure before opening of the valve, P_p = Pressure just before closing the valve, P_f = Pressure at the end of the pressure build-up period.	122
Table 8-8	Interference test results for KA3566G02, 12.30 - 18.30 m. (r = aprox. distance from flowing bore hole section to observation bore hole section, t_L = time lag for a pressure response of 0.1 m to be registered in an observation section, T = transmissivity, S = storage coefficient, S^* = storage coefficient from diffusivity, η .) The response is classified as 1 = no response (< 0.1 m), 2 = some response (0.1 m - 1.0 m) and 3 = good response (> 1.0 m). P_0 = Initial pressure before opening of the valve, P_p = Pressure just before closing the valve, P_f = Pressure at the end of the pressure build-up period.	125
Table 8-9	Interference test results for KA3590G01, 1.30 - 6.80 m. (r = aprox. distance from flowing bore hole section to observation bore hole section, t_L = time lag for a pressure response of 0.1 m to be registered in an observation section, T = transmissivity, S = storage coefficient, S^* = storage coefficient from diffusivity, η .) The response is classified as 1 = no response (< 0.1 m), 2 = some response (0.1 m - 1.0 m) and 3 = good response (> 1.0 m). P_0 = Initial pressure before opening of the valve, P_p = Pressure just before closing the valve, P_f = Pressure at the end of the pressure build-up period.	128
Table 8-10	Interference test results for KA3590G01, 7.80 - 16.30 m. (r = aprox. distance from flowing bore hole section to observation bore hole section, t_L = time lag for a pressure response of 0.1 m to be registered in an observation section, T = transmissivity, S = storage coefficient, S^* = storage coefficient from diffusivity, η .) The response is classified as 1 = no response (< 0.1 m), 2 = some response (0.1 m - 1.0 m) and 3 = good response (> 1.0 m). P_0 = Initial pressure before opening of the valve, P_p = Pressure just before closing the valve, P_f = Pressure at the end of the pressure build-up period.	131

- Table 8-11** Interference test results for KA3590G02, 23.30 - 30.05 m. (r = aprox. distance from flowing bore hole section to observation bore hole section, t_L = time lag for a pressure response of 0.1 m to be registered in an observation section, T = transmissivity, S = storage coefficient, S^* = storage coefficient from diffusivity, η .) The response is classified as 1 = no response (< 0.1 m), 2 = some response (0.1 m - 1.0 m) and 3 = good response (> 1.0 m). P_0 = Initial pressure before opening of the valve, P_p = Pressure just before closing the valve, P_f = Pressure at the end of the pressure build-up period. 134
- Table 8-12** Interference test results for KA3590G01, 1.30 - 6.80 m. (r = aprox. distance from flowing bore hole section to observation bore hole section, t_L = time lag for a pressure response of 0.1 m to be registered in an observation section, T = transmissivity, S = storage coefficient, S^* = storage coefficient from diffusivity, η .) The response is classified as 1 = no response (< 0.1 m), 2 = some response (0.1 m - 1.0 m) and 3 = good response (> 1.0 m). P_0 = Initial pressure before opening of the valve, P_p = Pressure just before closing the valve, P_f = Pressure at the end of the pressure build-up period. 137
- Table 8-13** Interference test results for KG0048A01, 49.00 - 54.69 m. (r = aprox. distance from flowing bore hole section to observation bore hole section, t_L = time lag for a pressure response of 0.1 m to be registered in an observation section, T = transmissivity, S = storage coefficient, S^* = storage coefficient from diffusivity, η .) The response is classified as 1 = no response (< 0.1 m), 2 = some response (0.1 m - 1.0 m) and 3 = good response (> 1.0 m). P_0 = Initial pressure before opening of the valve, P_p = Pressure just before closing the valve, P_f = Pressure at the end of the pressure build-up period. 140
- Table 8-14** Interference test results for KA3554G01, 22.30 - 30.01 m. (r = aprox. distance from flowing bore hole section to observation bore hole section, t_L = time lag for a pressure response of 0.1 m to be registered in an observation section, T = transmissivity, S = storage coefficient, S^* = storage coefficient from diffusivity, η .) The response is classified as 1 = no response (< 0.1 m), 2 = some response (0.1 m - 1.0 m) and 3 = good response (> 1.0 m). P_0 = Initial pressure before opening of the valve, P_p = Pressure just before closing the valve, P_f = Pressure at the end of the pressure build-up period. 143
- Table 8-15** Interference test results for KA3554G02, 10.30 - 21.80 m. (r = aprox. distance from flowing bore hole section to observation bore hole section, t_L = time lag for a pressure response of 0.1 m to be registered in an observation section, T = transmissivity, S = storage coefficient, S^* = storage coefficient from diffusivity, η .) The response is classified as 1 = no response (< 0.1 m), 2 = some response (0.1 m - 1.0 m) and 3 = good response (> 1.0 m). P_0 = Initial pressure before opening of the valve, P_p = Pressure just before closing the valve, P_f = Pressure at the end of the pressure build-up period. 146

- Table 8-16** Interference test results for KA3542G01, 8.80 - 24.80 m. . (r = aprox. distance from flowing bore hole section to observation bore hole section, t_L = time lag for a pressure response of 0.1 m to be registered in an observation section, T = transmissivity, S = storage coefficient, S^* = storage coefficient from diffusivity, η .) The response is classified as 1 = no response (< 0.1 m), 2 = some response (0.1 m - 1.0 m) and 3 = good response (> 1.0 m). P_0 = Initial pressure before opening of the valve, P_p = Pressure just before closing the valve, P_f = Pressure at the end of the pressure build-up period. 149
- Table 8-17** §Interference test results for KA3542G02, 1.30 – 7.80 m. . (r = aprox. distance from flowing bore hole section to observation bore hole section, t_L = time lag for a pressure response of 0.1 m to be registered in an observation section, T = transmissivity, S = storage coefficient, S^* = storage coefficient from diffusivity, η .) The response is classified as 1 = no response (< 0.1 m), 2 = some response (0.1 m - 1.0 m) and 3 = good response (> 1.0 m). P_0 = Initial pressure before opening of the valve, P_p = Pressure just before closing the valve, P_f = Pressure at the end of the pressure build-up period. 152
- Table 8-18** Interference test results for KA3539G, 9.80 - 18.30 m. . (r = aprox. distance from flowing bore hole section to observation bore hole section, t_L = time lag for a pressure response of 0.1 m to be registered in an observation section, T = transmissivity, S = storage coefficient, S^* = storage coefficient from diffusivity, η .) The response is classified as 1 = no response (< 0.1 m), 2 = some response (0.1 m - 1.0 m) and 3 = good response (> 1.0 m). P_0 = Initial pressure before opening of the valve, P_p = Pressure just before closing the valve, P_f = Pressure at the end of the pressure build-up period. 155
- Table 8-19** Interference test results for KG0021A01:1, 42.50 – 48.82 m. . (r = aprox. distance from flowing bore hole section to observation bore hole section, t_L = time lag for a pressure response of 0.1 m to be registered in an observation section, T = transmissivity, S = storage coefficient, S^* = storage coefficient from diffusivity, η .) The response is classified as 1 = no response (< 0.1 m), 2 = some response (0.1 m - 1.0 m) and 3 = good response (> 1.0 m). P_0 = Initial pressure before opening of the valve, P_p = Pressure just before closing the valve, P_f = Pressure at the end of the pressure build-up period. 158
- Table 8-20** Interference test results for KG0021A01:1, 42.50 – 48.82 m. (r = aprox. distance from flowing bore hole section to observation bore hole section, t_L = time lag for a pressure response of 0.1 m to be registered in an observation section, T = transmissivity, S = storage coefficient, S^* = storage coefficient from diffusivity, η .) The response is classified as 1 = no response (< 0.1 m), 2 = some response (0.1 m - 1.0 m) and 3 = good response (> 1.0 m). P_0 = Initial pressure before opening of the valve, P_p = Pressure just before closing the valve, P_f = Pressure at the end of the pressure build-up period. 161
- Table 9-1** Total increase of the pressure in available observation sections after the blasting of the two niches. 164

Table 11-1	Distance between hydraulic features with $T > 10^{-6}$, $T > 10^{-7}$, $T > 10^{-8}$, $T > 10^{-9}$, $T > 10^{-10}$ and $T > 10^{-11}$ m ² /s respectively. Summary of data set 1 - 5. (n = sample size, D_a = arithmetic mean, D_{median} = median, D_g = geometric mean, $S(\text{Log}_{10} D)$ = standard deviation.	169
Table 11-2	P_{32} for the three different fracture sets with different truncation level.	174
Table 11-3	Summary of used parameters for the DFN model (mean = arithmetic mean of the distribution).	176
Table 11-4	Statistical analysis of $\text{Log}_{10} K$. Scale 1 m and 3 m.	177
Table 11-5	Summary of responses in 14 interference tests. The response is classified as 0 = no response (< 0.1 m), 1 = some response (0.1 – 1.0 m) and 2 = good response (> 1.0 m).	181
Table 11-6	Data of minor features. The co-ordinates indicate the centre of the feature plane.	188
Table 12-1	Undisturbed pressure. Estimated high pressures are marked with grey boxes and uncertain values are italicised.	191
Table 12-2	Pressures 1999-12-01 after deposition holes were drilled. CLASS: refers to main borehole direction, see below in text and Figure 11-3.	194
Table 13-1	Results of statistical analysis of chemical components.	202
Table 15-1	Used and measured for fracture orientation of Drill campaign 2. For more details see Hermanson et al (1999).	207
Table 15-2	Statistics (predictions) of the “natural” fracture traces around the perimeter of deposition holes 1 to 6 based on 20 realisations of the calibrated DFN model. The min and maximum values for trace length and transmissivity is for a single trace in the deposition hole, other values are calculated for a whole hole.	213
Table 15-3	Comparison of measured and modelled fracture trace length statistics for all fractures.	216
Table 15-4	Comparison of measured and calculated inflow to deposition holes.	217
Table 15-5	Maximum and mean values for calculated flow rate (based on drill batch 1-3) and measured flow rate for each deposition bore hole. Measured is according to Table 6-3. Q_{d1} is based on measured flow rate and pressure in pilot bore holes. Q_{d2} is based on evaluated transmissivity and pressure in pilot bore holes.	222
Table 15-6	Transmissivity estimation for each deposition hole position after drill campaign 2 and after campaign 3 respectively. T_A : Arithmetic mean transmissivity. T_G : Geometric mean transmissivity (T), $\text{Std}(\log_{10}(T))$: Standard deviation of $\text{Log}_{10}(T)$. 1+2+3(close): Only borehole drilled within deposition hole or a few decimetres outside the deposition hole included.	230

1 BACKGROUND

1.1 Äspö Hard Rock Laboratory

In order to prepare for the localisation and licensing of a spent fuel repository SKB has constructed an underground research laboratory.

In the autumn of 1990, SKB began the construction of Äspö Hard Rock Laboratory (Äspö HRL), see Figure 1-1 and 1-2, near Oskarshamn in the south-eastern part of Sweden. A 3.6 km long tunnel was excavated in crystalline rock down to a depth of approximately 460 m.

The laboratory was completed in 1995 and research concerning the disposal of nuclear waste in crystalline rock has since been carried out.

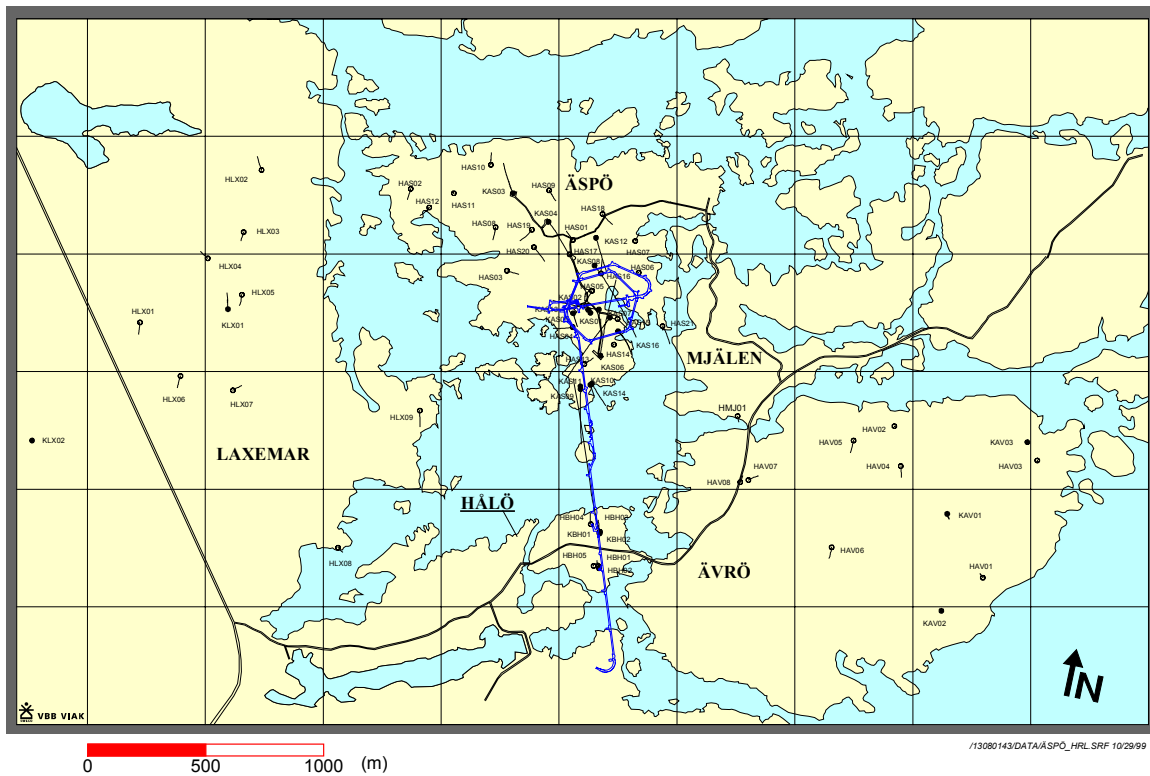


Figure 1-1 Äspö Hard Rock Laboratory.

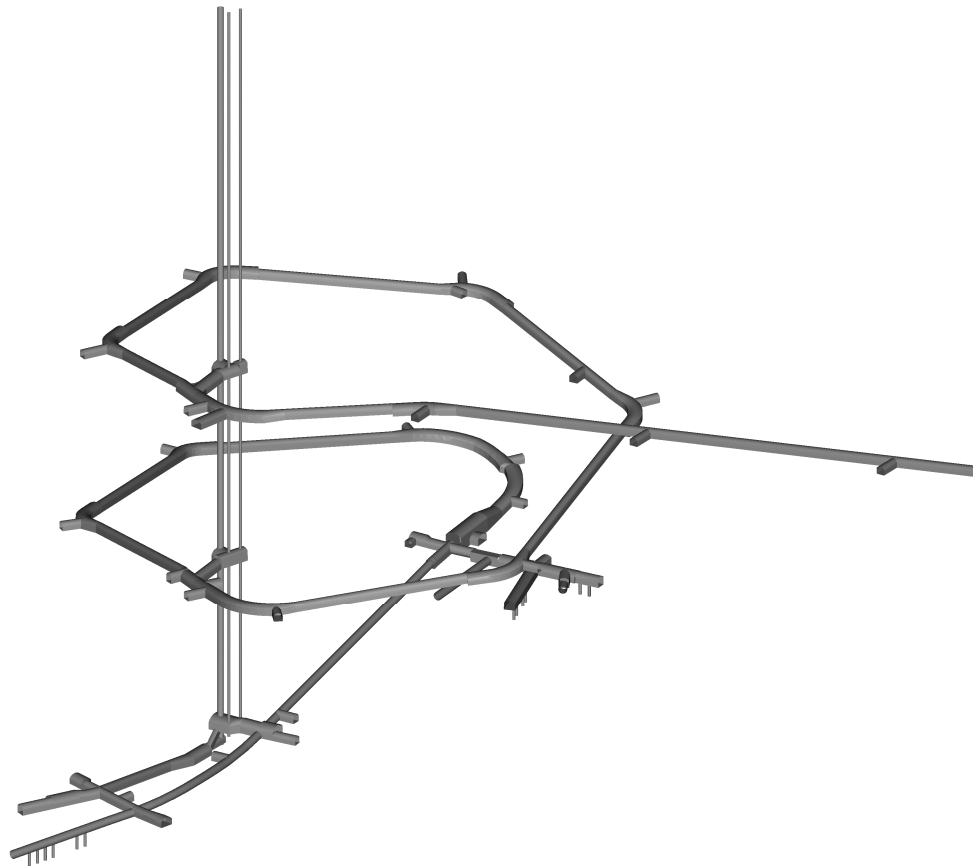


Figure 1-2 Tunnel systems at Äspö.

1.2 Prototype repository

The Äspö Hard Rock Laboratory is an essential part of the research, development, and demonstration work performed by SKB in preparation for construction and operation of the deep repository for spent fuel. Within the scope of the SKB program for R&D 1995, SKB has decided to carry out a project with the designation “Prototype Repository Project“. The aim of the project is to test important components in the SKB deep repository system in full scale and in a realistic environment.

The Prototype Repository project is expected to show the technical feasibility of geological disposal of highly radioactive waste and to provide an improved scientific basis for the safety assessment of such disposal. It involves key experts from several EU countries that make use of nuclear energy, including also Japan, which will optimise scientific networking and improve modelling results. In addition to the scientific merits, it has a great practical value by demonstrating, on a full scale, the construction of a repository at depth and simulating the handling of radioactive waste packages.

SKB has selected the so-called KBS-3 system as reference concept for deep disposal of spent nuclear fuel, on which comprehensive research, development and demonstration work has been performed. Conceptual and mathematical models have been developed that describe the function of the system.

In the Äspö Hard Rock Laboratory (ÄHRL) SKB has initiated several full-scale demonstration projects in the underground laboratory comprising full-scale canister deposition and retrieval techniques, backfill and plug construction, and long-term physic/chemical testing of buffer, backfills and plugs. The Prototype Repository is an application of several of the techniques and activities that have been investigated individually in these tests and constitutes as complete as possible a test of the main repository issues.

- Design and excavation of deposition holes and drifts.
- Characterisation of near-field rock (geologic structure, heat transport potential, hydraulic regime, state of stress, strain and flow in the near-field rock including the excavation-disturbed zone (EDZ).
- Design of engineered barrier systems (EBS).
- Preparation and application of clay-based buffer and backfill (selection and preparation of materials, quality designation, compaction, transport and storage).
- Handling and deposition of canisters.
- Performance of buffer and backfill (determination and modelling of thermal and wetting/drying processes, gas evolution and migration, stress and strain, and chemical processes including microbial activities, and longevity).

Project plan and project description for the Prototype Repository is described in Svemar and Pusch (2000) and Persson and Broman (2000).

1.2.1 General objectives

The Prototype Repository should simulate, in as many aspects as possible, a real repository, regarding for example geometry, materials, and rock environment. The Prototype Repository is a demonstration of the integrated function of the repository components. Results will be compared with conceptual and numerical models and assumptions to their validity.

The major objectives for the Prototype Repository are:

- To simulate part of future KBS-3 deep repository to the extent possible with respect to geometry, design, materials, construction and rock environment except that radioactive waste is simulated by electrical heaters.
- To test and demonstrate the integrated function of the repository components under realistic conditions in full scale.

- To develop, test and demonstrate appropriate engineering standards and quality assurance methods.
- To accomplish confidence building as the capability of modelling EBS performance.

The objectives for the characterisation program are:

- To provide a basis for determination of localisation of the deposition holes.
- To provide data on boundary and rock conditions to enable interpretation of the experimental data

1.2.2 Objectives – hydrogeology investigations

The objectives of the pilot and the exploratory holes was to obtain data for prediction of the characteristics in the depositions holes, data for modelling and to quantify the criteria needed for validation of the suitability of the position for canister deposition. Acceptance of a canister position is based on scrutinization of characterisation data such as fracturing, permeability and stability of the borehole wall.

The objectives for the hydraulic tests in the pilot holes (Drilling campaign 1):

- The hydraulic tests the pilot holes should be fairly simple in order to test a methodology that possibly can be useful as a robust engineering process in the deep repository when investigating each canister position.
- The tests shall provide hydraulic data useful for a first judgement of if the position can be used for deposition of a canister.

The objectives for the hydraulic tests in the short exploratory holes (Drilling campaign 2):

- The hydraulic tests the exploratory holes should be simple in order to test a methodology that possibly can be useful as a robust engineering process in the deep repository when investigating each canister position.
- The tests shall provide hydraulic data useful for a first judgement of if the position can be used for deposition of a canister.
- The tests shall provide hydraulic data useful for the geohydrological model of the rock mass around the TBM tunnel where the Prototype Repository is situated.

The objectives for the hydraulic tests in the long exploratory holes (Drilling campaign 3):

- The hydraulic tests of the long exploratory holes shall provide hydrogeological data. These data will be useful for setting up a hydrogeological model of the rock volume around the TBM tunnel, up to a distance of approximately 30 m from the tunnel.

- Data shall together with the geological interpretation form a base for designing specific interference tests with several packed off sections in a number of bore holes and to choose sections for flow measurements during natural conditions and during interference tests.
- The tests shall partly be of similar character as for drill campaign 1 and 2 in order to provide data for statistical treatment of the data.

The objectives for the interference tests in the long exploratory holes (Interference test campaigns 1 and 2):

- The hydraulic tests the exploratory holes shall provide hydrogeological data useful for setting up a hydrogeological model of the rock volume around the TBM tunnel.
- Identification of the position and properties of larger conductive features and possible minor features intersecting the planned deposition bore holes.

The objectives for the injection tests in the exploratory boreholes:

- The hydraulic tests in the exploratory holes shall provide hydrogeological data useful for setting up a hydrogeological model, of the rock volume around the TBM tunnel.
- Data shall constitute together with the geological and other investigations a basis for interpretation of changes, of the rock characteristics, around the upper part of the rock volume due to drilling of the deposition holes.

The objectives for the pressure response observations during the drilling of the deposition boreholes and the inleakage measurements in the tunnel and into the deposition boreholes:

- To provide data for the estimation of the wetting process of the bentonite clay surrounding the canisters.
- To provide data for the structure model of the rock volume around the prototype repository.
- To provide data for the numerical groundwater flow modeling.

The objectives of the pressure response observations during the drilling of the lead-through boreholes and of the hydraulic tests in the holes:

- To detect any hydraulic connections with already existing boreholes and thus provide additional data to the structure model.
- To hydraulically characterise the boreholes before the planned grouting.

The objectives, of the pressure response observations during the blasting of the niches for the plugs in the Prototype tunnel:

- To provide data to evaluate possible pressure changes and their cause in monitored sections around the Prototype tunnel.

1.3 This report

Chapter 2 gives an overview of the test site and Chapter 3 summarises some important aspects of geology. An overview of the performed hydrogeological investigation is presented in Chapter 4 and a detailed presentation of these investigations is reported in Chapters 5 to 10. In Chapters 11 to 13 properties of the rock mass and the groundwater as well as pressure distribution around the tunnel is presented. In Chapter 14 suitable calibration cases are suggested. Chapter 15 summarises the predictions and numerical simulations made.

2 DESCRIPTION OF TEST SITE

2.1 Introduction

A full-scale replica of the deep repository planned for disposal of spent nuclear fuel in Sweden will be constructed and tested at about 450 m depth in the Äspö HRL, see Figure 2-1 and 2-2. This KBS3-type “Prototype Repository” consists of a 5 m diameter TBM-drilled drift with about 65 m length with six vertical deposition holes, 8.37 m deep and 1.75 m in diameter, in which electrically heated canisters surrounded by compacted blocks and pellets of MX-80 bentonite will be placed. The drift from which the holes extend downwards will be backfilled with 30% MX-80 bentonite and 70% crushed TBM muck.

2.1.1 General layout

The six deposition holes form two groups, one with four holes that are 6 m apart in the inner section (Section I), and the other consisting of two holes, 6 m apart, in the outer section (Section II). Canisters with a design, shape and weight according to the KBS3 concept and with heaters for simulating the thermal energy produced by the waste, will be placed in the holes in which bentonite buffer has been applied in a preceding operation. The prototype drift will be backfilled with MX-80 bentonite and crushed TBM muck. A tight plug will separate the inner and outer parts of the test drift and a second plug will separate the test area from the open part of the drift. The plugs are designed and constructed as the already prepared plug in the ZEDEX drift, omitting the bentonite O-ring seal.

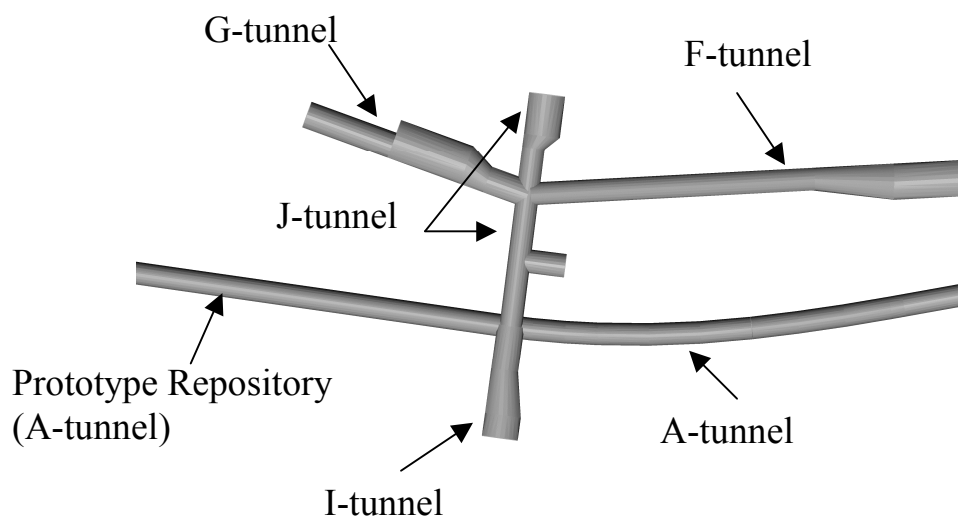


Figure 2-1 Tunnel systems close to the Prototype Repository.

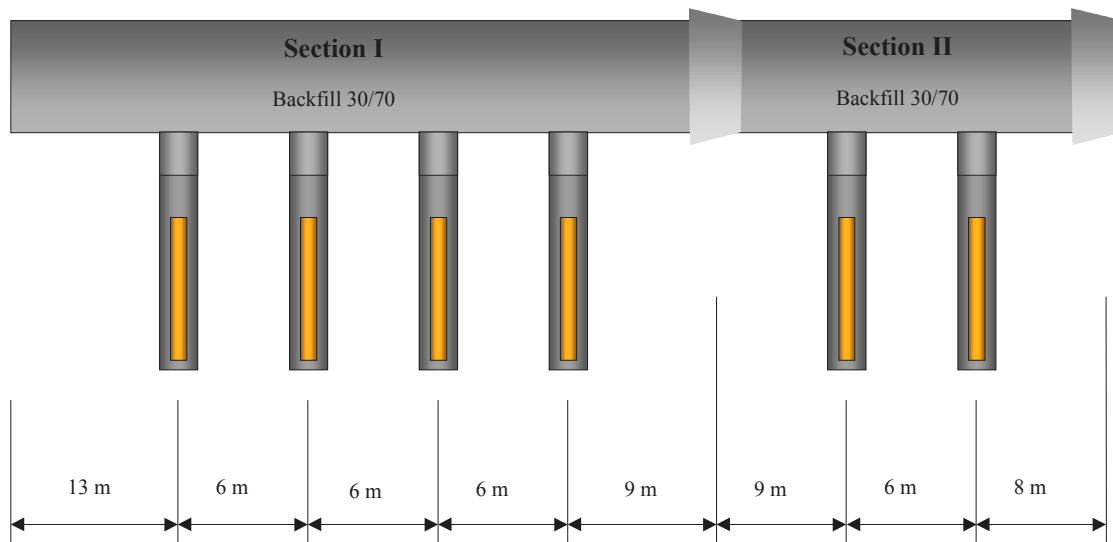


Figure 2-2 Schematic view of the layout of the Prototype Repository and deposition hole in the A-tunnel (not to scale).

2.2 Characterization and monitoring of existing boreholes

A number of boreholes have been drilled during the pre-investigation phase of the repository. In Figure 2-3, the core drilled holes are shown. Within the diameter of each deposition hole a core hole was drilled before the deposition holes were drilled, which cannot be seen in Figure 2-3. These core holes are the basis, together with the mapping of the TBM-tunnel and the deposition holes, for the geological and hydrogeological characterization. These core holes have been used for pressure observations during interference tests and for water sampling during the characterisation phase.

A number of percussion-drilled boreholes between the G-tunnel and A-tunnel (Lead-through holes for the instrumentation) were only to a minor extent characterized. A short flow measurement was made at one occasion and the holes were video filmed with the BIPS system.

For the operation phase, several of these holes will be equipped with different kinds of packer systems allowing for:

- pressure measurements
- water sampling
- dilution measurements
- interference tests
- hydromechanical measurements and tests

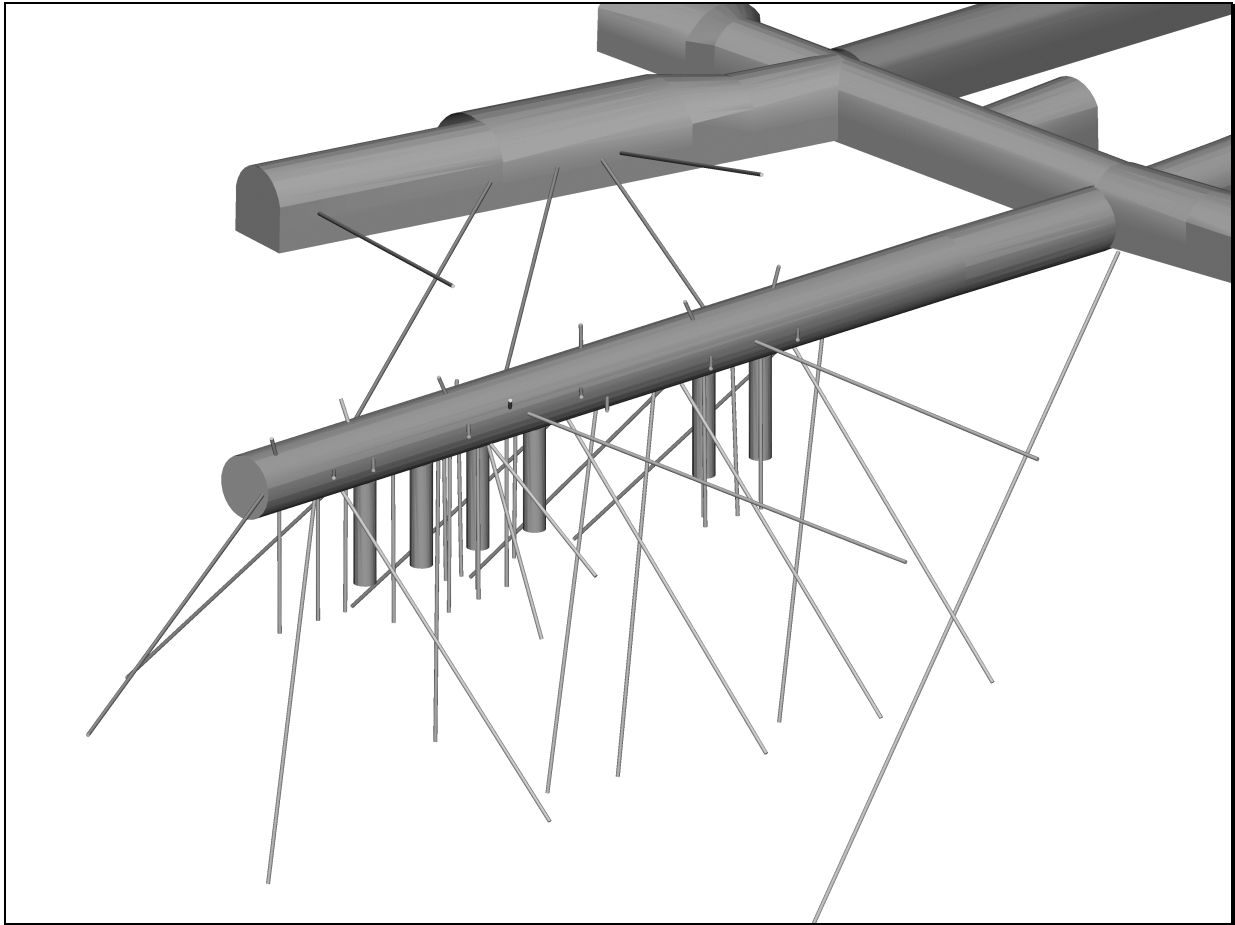
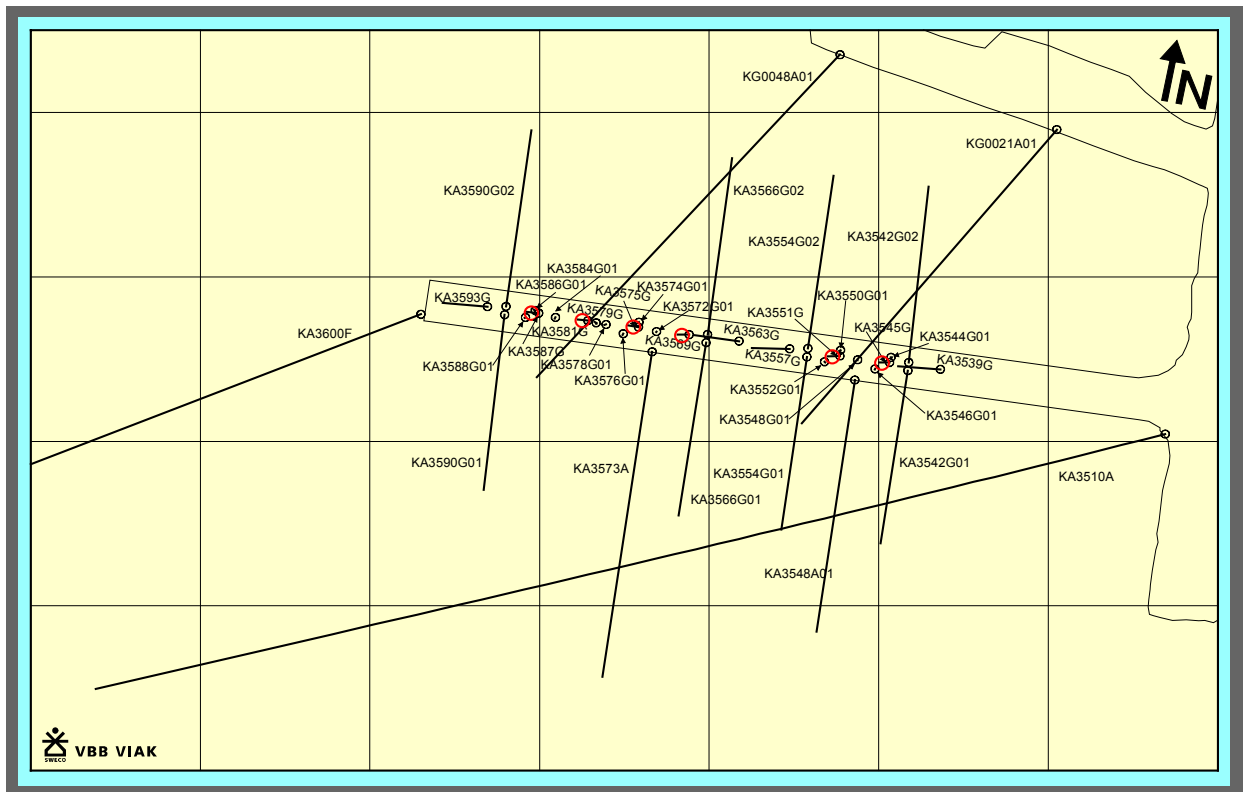


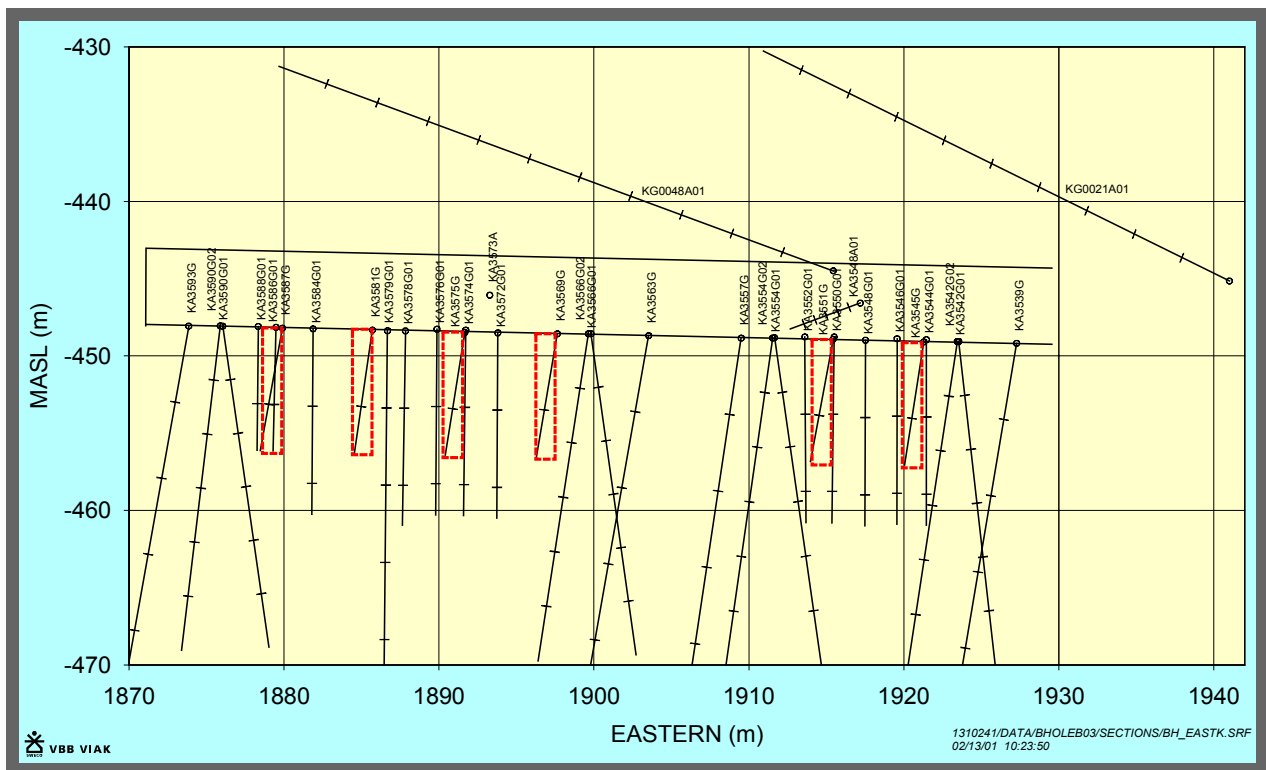
Figure 2-3 Boreholes used for characterization of the rock mass.

In Figures 2-4 and 2-5, the most important characterisation holes are shown in more detail.



1310241/DATA/BHOLEB03/SECTIONS/BH_PLANG.SRF

Figure 2-4 Existing boreholes to be used as monitoring holes.



1310241/DATA/BHOLEB03/SECTIONS/BH_EASTK.SRF
02/13/01 10:23:50

Figure 2-5 Existing boreholes to be used as monitoring holes.

3 OVERVIEW OF GEOLOGY

The detailed mapping of the Prototype tunnel was first presented in Patel et al (1997) and later updated in Patel and Dahlström (2001). The fracture network for DFN modelling was analysed in Hermansson et al (1999) and later updated in Stigsson et al (2001). In Alm and Rhén (2001) and Rhén et al (1997) the rock stress situation is described. Below is a brief description of the geology in the Prototype Repository area.

3.1 Prototype Repository area

Rock types

The mapping of the TBM tunnel between chainage 3500 and 3600 meter shows that the main rock type is Äspö diorite with veins and inclusions of fine-grained granite and greenstone, see Figure 3-1. The mapping shown in Figure 3-1 was made during the drilling of the TBM tunnel.

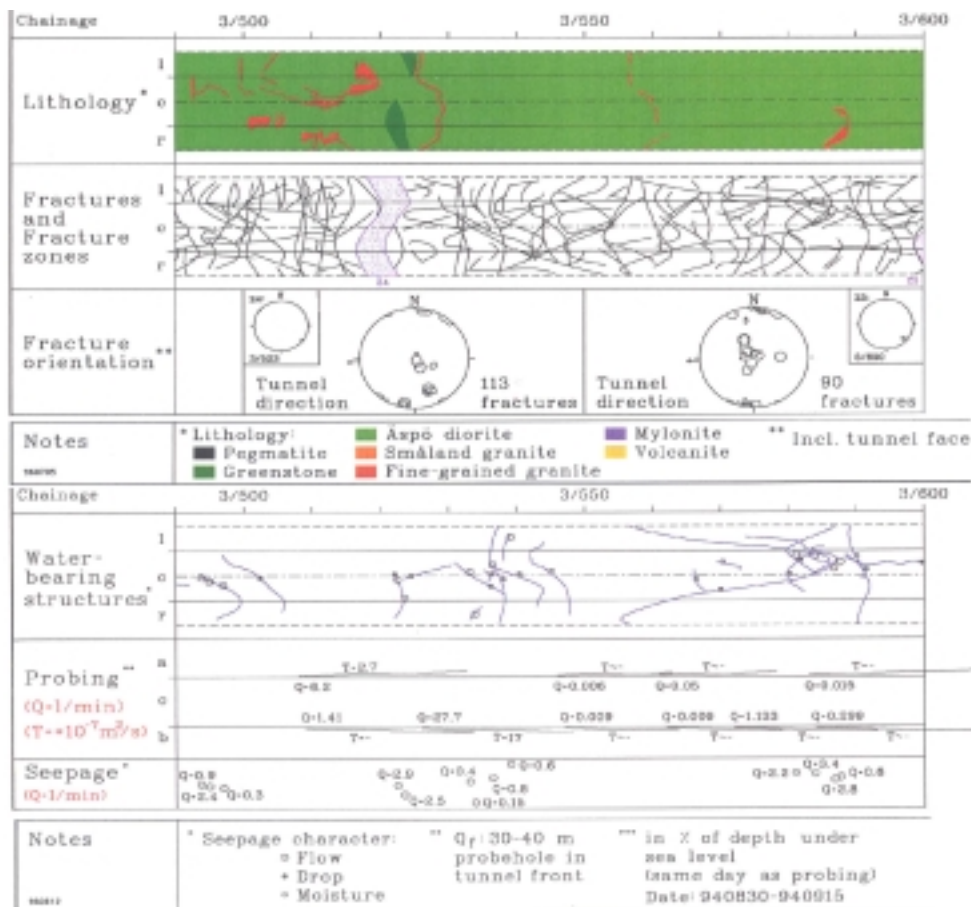


Figure 3-1. Mapping of the TBM tunnel (from Markström and Erlström, 1996).

Fractures

The mapped fractures was analysed in Stigsson et al (2001) and some results are presented below. The projections of the poles of all the fractures of all exploratory boreholes are plotted on an equal area lower hemisphere projection in Figure 3-2. The plot shows at least two fracture sets, one that is sub-horizontal and one that is a steep north-west set. There are also indications of a third set with steep fractures in the north-east direction. The latter fracture set is diffuse, but this may be a visual bias because most of the boreholes are in the same plane. The bias can be corrected using the Terzaghi correction method (Terzaghi, 1965), which compensates for fractures that are sub-parallel to the borehole axis. In this study a maximum correction factor of five is used based on previous experience, see Stigsson et al (2001).

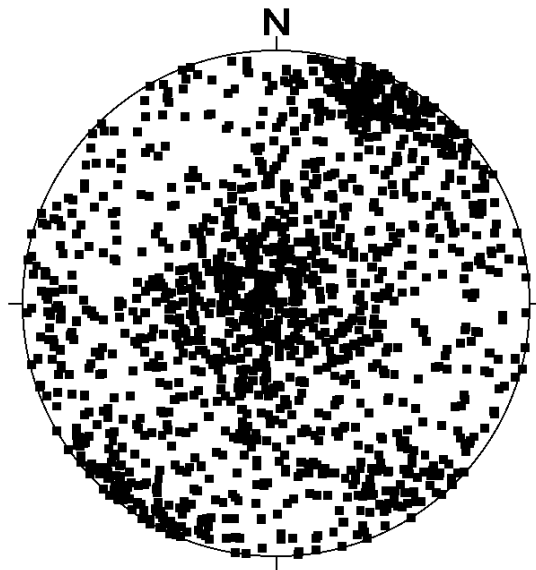


Figure 3-2. Lower hemisphere projection of poles to fracture planes in the 36 bore- and exploratory holes.

Fractures intersecting boreholes are defined as either “sealed” or “natural” in the SKB data base SICADA. Based on this the analysis of the fracture orientation can be refined using the information if the intersecting fracture is “sealed” or “natural”. The general assumption is that “sealed” fractures cannot be water bearing, at least not in the intersection with the borehole. “Natural” fractures are possibly water bearing but does not necessarily take part in the conductive network. Figure 3-3 shows the poles of the “natural” fracture planes.

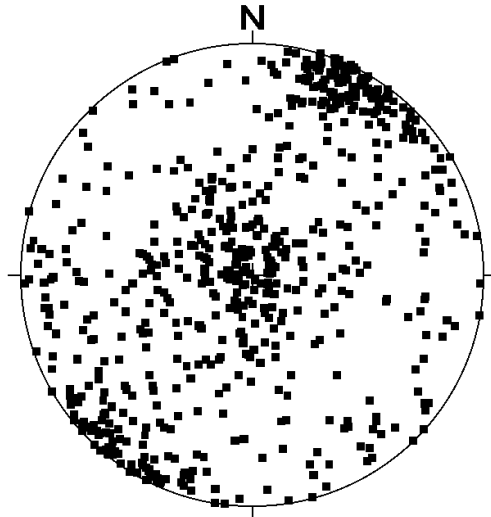


Figure 3-3. Lower hemisphere projection of poles to fracture planes for “natural” fractures in the 36 exploratory holes.

At least two different fracture sets can be visually discerned from the “natural” fractures group. As a complement to the visual observations, a set identification algorithm can be used to fit a statistical distribution to each fracture set. This is attractive as the knowledge of the distribution of each set makes it possible to simulate orientations according to a statistical model. In this case, the ISIS software of the FracMan package is used for the set identification. Based on the visual investigation it is assumed that the fractures shall be divided into three sets. The ISIS algorithm then tries to fit statistical distributions to the data.

Several statistical distributions have been tested for the three fracture set assumptions. The Fisher distribution was the most successful in all tests and is used as statistical model in all fracture sets both in this model and in the previously analysed data from Hermanson et al. (1999). The results from the ISIS analysis are shown in Table 3-1. It is clear that the statistics shows similar results for both “all” fractures as for “natural” fractures respectively. The major difference is that set 2 has a larger proportion of “natural” fractures than the other two sets.

This indicates that we have fractures in the north-west direction that have gone through a more recent brittle deformation phase and are thus more likely to conduct water than the other two fracture sets. This is also the dominating direction of fracturing at Äspö.

The orientation analysis based on the data from drill campaigns 2 and 3 show that the assumption of three fracture sets is nicely approximated by Fisher statistical distributions.

Several studies have tried to statistically separate fractures into sets based on fracture mineralogy, orientation, trace length, termination mode, surface roughness, kinematical evidence etc. The main conclusion from these studies, according to Stigsson et al (2001), is that the geological fracture properties are weakly correlated to the fracture orientation. The only significant coupling is the increase in trace length for water bearing fractures mapped in the tunnel drift.

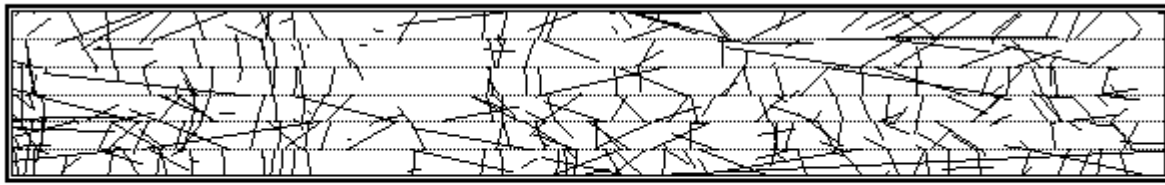
Table 3-1. Statistical separation of fracture sets of the 36 pilot and exploratory holes. The Fisher distribution is used for all fracture sets.

SET 1	Prototype DFN 2		Prototype DFN 1
	All	Natural	True BS
Strike	219	212.8	207.9
Dip	83.7	83.7	77.1
K	4.84	3.96	5.64
%-fractures	26.50%	23.20%	12%
KS-%	0.050;15.7%	0.075;26.6%	0.16;38.5%

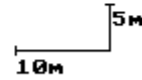
SET 2	Prototype DFN 2		Prototype DFN 1
	All	Natural	True BS
Strike	127	126.9	290.4
Dip	84.2	86.8	88
K	8.35	10.53	15.75
%-fractures	35.60%	43.30%	46%
KS-%	0.040;23.4%	0.069;8.3%	0.163;4.6%

SET 3	Prototype DFN 2		Prototype DFN 1
	All	Natural	True BS
Strike	20.6	17.9	276.5
Dip	6	7.5	8.9
K	8.33	9.32	13.6
%-fractures	37.90%	33.50%	42%
KS-%	0.043;14.4%	0.068;19.2%	0.095;79.7%

A spatial analysis of the trace maps from the TBM tunnel has been done by Follin and Hermanson (1996). The spatial model is estimated by analysing the pattern of fracturing along an outcrop such as the end of the TBM tunnel, c.f. Figure 3-4. In Chapter 11 and Stigsson et al (2001) more details are found concerning the DFN modelling.



Version: Fracsys 2.512
 Date: 14:13 May 31 1996
 File: seg3.f2d



Centre line characteristics: L = 122.03 m, Trend = 277.16, Plunge = -0.94
 x = 1,984.84, y = 7,262.33, z = -447.768
 $P_{21} = 0.656 \text{ m/m}^2$

Figure 3-4. Trace map over the last 120 m of the TBM tunnel after Follin and Hermanson (1996).

Larger structures

The dominant ones are steep and oriented NW/SE and several of them are the most hydraulically active fractures in the test drift. A few steep NE/SW-oriented fractures are present in the test area, they are somewhat inclined, and flat lying ones, striking more or less W/E., where the latter appear in the roof, walls and floor.

Rock stress conditions

After excavation of the prototype tunnel, stress measurements (overcoring) were done in a vertical borehole (KA3579 G) drilled from tunnel floor. Measurements were done at 11 points along the borehole down to a depth of 22.31 metres (Klasson et al, 2001). The four deepest measurements (from 20.06-22.31) were assumed to be unaffected of disturbance caused by the tunnel itself and therefore the average stresses were evaluated from these four measurements (see Table 3-2 and Figure 3-5).

Table 3-2 The principal stresses at the depth of the prototype repository. The strikes refers to the local north of the Äspö local coordinate system (local north is 12° west of magnetic north).

Principal stress	Magnitude [MPa]	Strike [°]	Dip [°]
σ_1	34.2	141	3
σ_2	17.7	245	80
σ_3	13.1	50	10

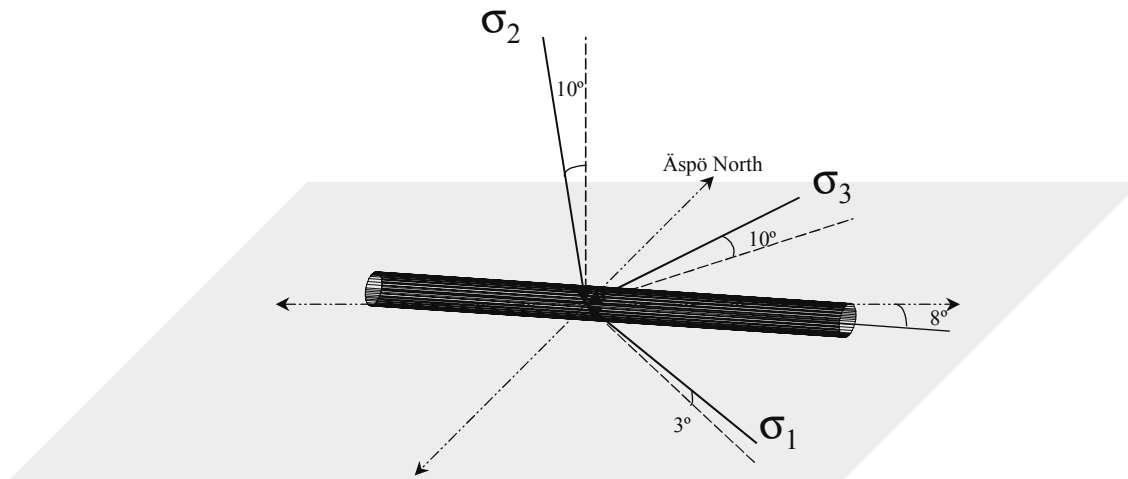


Figure 3-5 The orientation of the principal stresses compared to the prototype tunnel.

Since the stress at the junction of the tunnel and the deposition holes will be in the order of 100-130 MPa after excavation of tunnel and deposition holes, i.e. slightly lower than the unconfined compressive strength, the holes are expected to be stable in principle but local stress concentrations and creep may induce delayed failure. After 10 years of heating the stress is estimated to be in the range of 150-200 MPa. Local breakage at the upper end of the holes is in fact expected due to overloading and spalling during the heating period when the stresses are expected to exceed the unconfined compressive strength. At the drilling of the holes some block-fall took place lower down in the holes and correlation of these spots with the rock structure models and stress calculations will be made for examination of the stability conditions and for preparation of the buffer application phase.

3.2 Documentation

The information from the mapping of the tunnel, deposition holes and core holes is stored in the SICADA database. The result from the core mapping has also been compiled in data sheets and examples are shown in Figures 3-6 to 3-7.

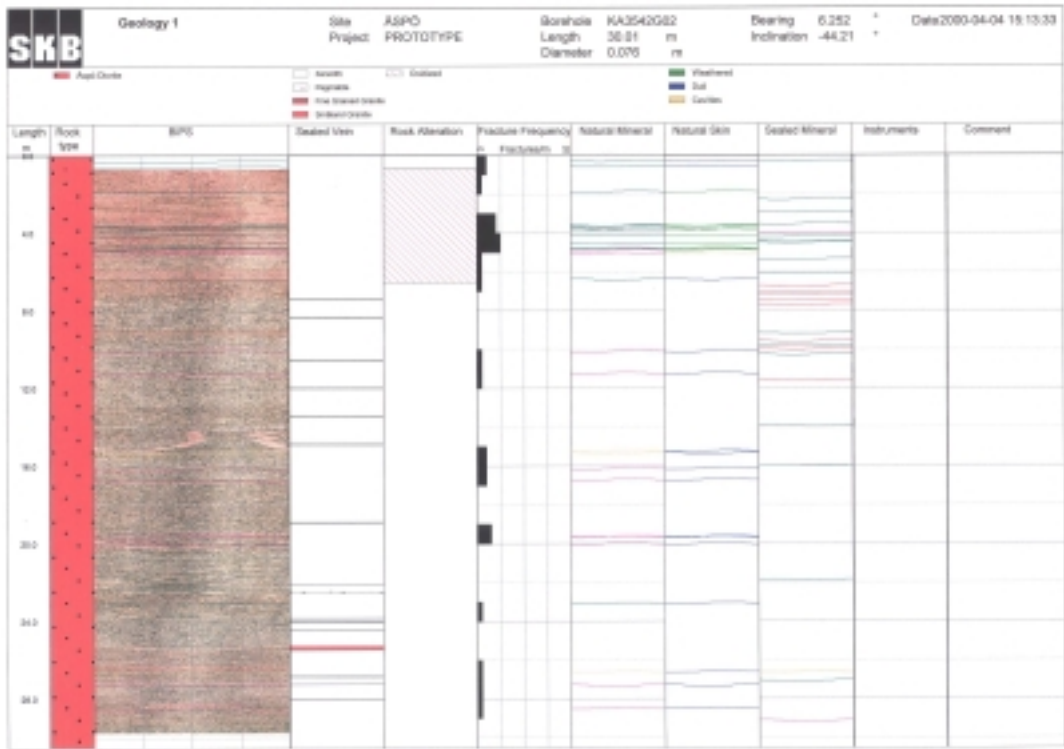


Figure 3-6 Example 1 of geological documentation of drilled core holes (Fracture directions in columns Natural mineral to Sealed mineral are as seen in the borehole wall).

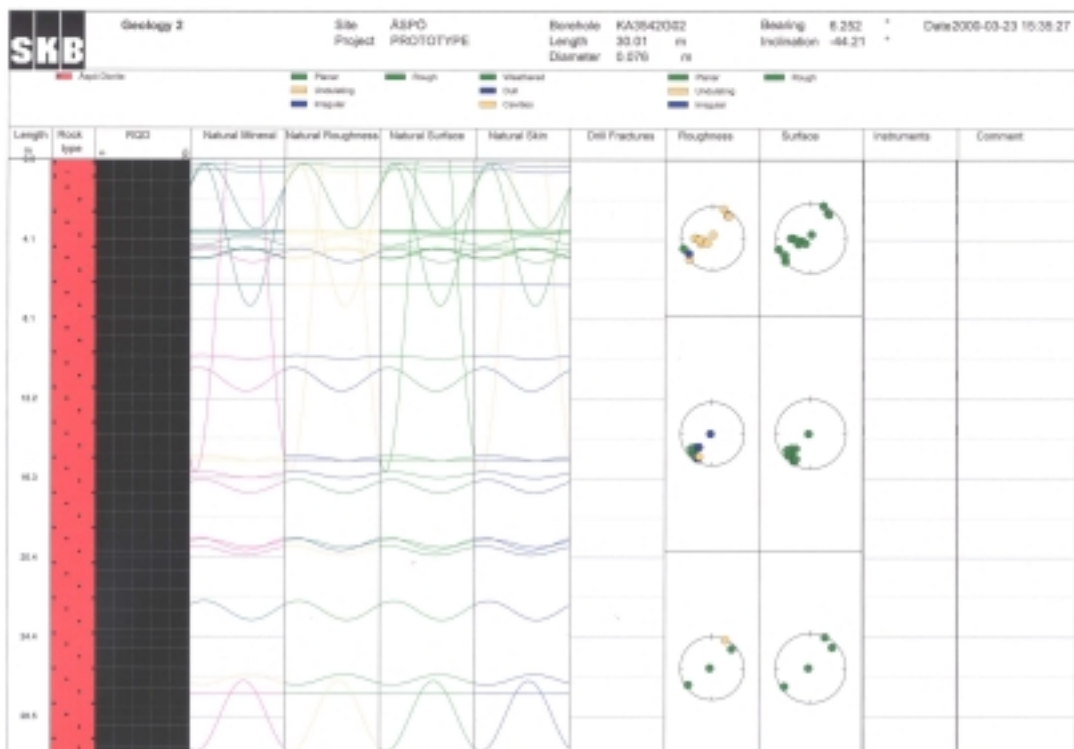


Figure 3-7 Example 2 of geological documentation of drilled core holes (Fracture directions in columns Natural mineral to Sealed mineral are as seen as they would appear in a vertical borehole).

4 OVERVIEW OF TESTS AND INVESTIGATIONS

The hydraulic testing of the rock, close to the repository test site, was divided into several different stages. The detailed field reports of the tests for the Prototype Repository is found in Gentzschein (1997b to 2001) and the detailed description of the analysis is found in Rhén and Forsmark (1998a,b), Forsmark and Rhén (1999a to 2000b) and Forsmark et al (2001a,b).

4.1 Hydraulic tests prior to prototype pre-investigation tests

Three of the boreholes mentioned, in this document, in conjunction with the Prototype Repository were completed earlier. The boreholes are KA3510A, KA3573A and KA3600F. They were drilled and used for different purposes before the pre-investigations of the Prototype Repository. They were later included in the project and have been used as observation holes and will be used as monitoring holes during the operation phase of the Repository.

Due to different reasons they have, however, not been hydraulically tested to the same extension as the other holes of the repository. They have been tested in the following manner:

- flow logging using UCM-tool, see Forsmark and Rhén (1999b).
- KA3510 have been flow logged using Posiva Difference Flow Meter (Rouhiainen, Heikkinen, 1998).
- KA3510A, 50 – 150 m, have been tested using pressure build-up tests in 5 meter sections, see Hermansson and Stigsson (1999) (*Original data was presented in Gentzschein (1997a).*) The transmissivity data from this investigation has been used in the analysis and modelling.

4.2 Drilling campaign 1

Pressure build-up tests, interference tests and flow logging was performed in the following pilot holes located at the end of the TBM tunnel:

KA3593G, KA3587G, KA3581G, KA3575G, KA3569G, KA3563G, KA3557G, KA3551G
KA3545G and KA3539G.

The boreholes were subvertical, 8 m long and with a diameter of 76 mm. The scope was to evaluate hydraulic tests done in the above-mentioned boreholes.

The hydraulic investigations were:

- measurements of flow rates from the entire bore hole (see Section 6.1)
- flow logging with packer spacing of 1 meter (see Section 6.1)
- pressure build-up testing the entire bore hole (see Section 7.1)
- pressure build-up test of 1 meter test section if the flow rate out of that particular test section exceeded 10 mL/min (see Section 7.1)
- interference testing, with up to 4 observation bore holes, if the flow rate out of the bore hole exceeded 10 mL/min (see Section 8.1)
- measurements of the undisturbed pressure in the entire bore hole (see Chapter 11 interpreted pressure distribution)

4.3 Drilling campaign 2

Pressure observations were made during drilling of the exploratory boreholes. Pressure build-up tests, interference tests and flow logging was performed in the following bore holes located at the end of the TBM tunnel:

KA3588G01, KA3586G01, KA3584G01, KA3578G01, KA3572G01, KA3552G01, KA3550G01, KA3548G01, KA3546G01 and KA3544G01.

Two of the bore holes were vertical, 8 m long and with a diameter of 76 mm while eight of them were 12 m long but with the same diameter and drilled vertical as well. The scope was to evaluate hydraulic tests done in the above-mentioned boreholes.

The hydraulic investigations were:

- pressure measurements were made during the drilling of the boreholes (see Section 5.2)
- measurements of flow rates from the entire bore hole (see Section 6.2)
- flow logging with packer spacing of 1 meter (see Section 6.2)
- pressure build-up testing the entire bore hole (see Section 7.2)
- pressure build-up test of 1 meter test section if the flow rate out of that particular test section exceeded 10 mL/min (see Section 7.2)
- interference testing, with up to 11 observation bore hole sections, if the flow rate out of the bore hole exceeded 10 mL/min (see Section 8.2)
- measurements of the undisturbed pressure in the entire bore hole (see Chapter 11)

4.4 Drilling campaign 3

Pressure observations were made during drilling of the long exploratory boreholes. Pressure build-up tests, interference tests and flow logging were performed in the following boreholes located at the end of the TBM tunnel:

Extended pilot holes: KA3539G, KA3557G, KA3563G and KA3593G

New boreholes: KA3542G01, KA3542G02, KA3554G01, KA3554G02, KA3566G01, KA3566G02, KA3590G01, KA3590G01 and KA3548A01.

Boreholes drilled from the G-tunnel : KG0021A01 and KG0048A01.

The extended and the new boreholes are approximately 30 m long, while the G-holes are approximately 50 meters long. An additional bore hole, KA3579G, in the TBM tunnel was also utilised during some of the test series. All boreholes have a diameter of 76 mm and are drilled sub-vertically. The exceptions to this are KA3548A01 and the two KG-holes, which are drilled sub-horizontally.

The scope was to evaluate hydraulic tests done in the above-mentioned boreholes.

The hydraulic investigations were:

- pressure measurements were made during the drilling of the boreholes (see Section 5.3)
- measurements of flow rates from the entire bore hole (see Section 6.3)
- flow logging with packer spacing of 1 or 3 meter (see Section 6.3)
- pressure build-up tests of the entire bore hole (see Section 7.3)
- pressure build-up test of 1 or 3 meter test section if the flow rate out of that particular test section exceeded 10 mL/min (see Section 7.3)
- interference tests, with up to 11 observation bore hole sections, were made if the flow rate out of the bore hole exceeded 10 mL/min (see Section 8.3)
- measurements of the undisturbed pressure in the entire bore hole (see Chapter 11)
- hydro chemical sampling of 1 or 3 meter test section if the flow rate out of a particular test section exceeds 10 mL/min. These results are only briefly reported in this report (see Chapter 12)

4.5 Interference test campaign 1 after drilling campaign 3

Interference tests were performed in five borehole sections in four of the long exploratory holes of the Prototype Repository tunnel. The tested intervals and basic test data are listed in Table 4-1. Six tests were done. Test number 1:3 was repeated as test number 1:6, while test number 1:4 was merely a function test. The first figure in the test number indicates the first Interference test campaign number, while the second number indicate the chronological order of the interference tests. The results are detailed in Section 7.4 and Section 8.4.

Observations were carried out in 56 observations borehole sections located around the flow section of each test. All test sections were connected to the Hydro Monitoring System (HMS) at Äspö Hard Rock Laboratory.

Table 4-1 Interference tests carried out during February and April 1999.

Bore hole	Section	Date of test	Test no.	Start of test	Valve opened	Valve closed	End of test
KA3566G01:2	12.30-19.80	1999-02-20	1:1	00:00	14:01	20:05	08:00 (1999-02-24)
KA3566G02:2	12.30-18.30	1999-02-24	1:2	07:00	08:26	14:43	08:00 (1999-02-25)
KA3590G01:3	1.30-6.80	1999-02-25	1:3	07:30	08:20	14:23	07:30 (1999-02-26)
KA3590G01:2	7.80-16.30	1999-02-26	1:4	07:30	07:53	08:03	08:33 (1999-02-26)
KA3590G02:1	23.30-30.05	1999-02-26	1:5	07:30	08:35	16:05	08:00 (1999-03-01)
KA3590G01:3	1.30-6.80	1999-04-06	1:6	09:00	09:59	16:01	06:30 (1999-04-07)

4.6 Interference test campaign 2 after drilling campaign 3

Interference tests were performed in eight borehole sections in seven of the long exploratory holes of the Prototype Repository tunnel. The tested intervals and basic test data are listed in Table 4-2.

During interference test 2:7 observations were carried out in 60 observations bore hole sections located around the flow section of each test, while during test 2:8 - 2:14 observations were carried out in 65 observations bore hole sections located around the flow section of each test. The results are detailed in Section 7.5 and Section 8.5

Table 4-2 Interference tests carried out during June and August 1999.

Bore hole	Section	Date of test	Test no.	Start of test	Valve opened	Valve closed	End of test
KG0048A01:1	49.00-54.69	1999-06-17	2:7	00:00	08:00.00	09:25.00	14:20 (1999-06-17)
KA3554G01:1	22.30-30.01	1999-08-18	2:8	08:00	10:00.03	16:04.05	08:55 (1999-08-19)
KA3554G02:2	10.30-21.30	1999-08-16	2:9	09:00	11:02.07	17:06.05	09:20 (1999-08-17)
KA3542G01:2	8.80-24.80	1999-08-17	2:10	09:00	11:00.03	17:05.03	09:55 (1999-08-18)
KA3542G02:3	1.30-7.80	1999-08-19	2:11	07:00	09:00.01	15:01.01	07:55 (1999-08-20)
KA3539G:2	9.80-18.30	1999-08-22	2:12	07:00	08:00.07	09:11.05	18:00 (1999-08-22)
KG0021A01:1	42.50-48.82	1999-08-21	2:13	07:00	09:00.05	15:02.10	07:55 (1999-08-22)
KG0021A01:3	25.00-34.00	1999-08-20	2:14	06:00	08:00.05	14:00.07	08:55 (1999-08-21)

4.7 Injection test campaign 1 and 2

Two injection test campaigns were done, before and after the drilling of the deposition holes.

The main objectives for the injection tests were

- The hydraulic tests in the exploratory holes should provide hydrogeological data useful for setting up a hydrogeological model, of the rock volume around the TBM tunnel.
- Data should constitute together with the geological and other investigations a basis for interpretation of changes, of the rock characteristics, around the upper part of the rock volume due to drilling of the deposition holes.

The tests were performed in 13 holes located in the prototype tunnel between section 3542 m and section 3578 m (Forsmark and Rhén, 2000a, 2001b). The first campaign was in January 1999 while the second one was in February 2001.

4.8 Lead-through holes

In total 27 lead-through holes have been drilled and tested hydraulically. They are drilled between the prototype tunnel and tunnel G. Monitoring cables and cables for the heaters in the canisters are run in them from the monitoring boreholes, buffer and backfill to the measurement panels in tunnel G.

Three of the holes have been tested hydraulically. During the drilling of the three tested holes the inflow rates were registered and four pressure build-up tests were done in the most conductive sections (Forsmark and Rhén, 2001a).

4.9 Water inflow measurements to the tunnel and deposition holes

Measurements of the inflow to the prototype tunnel were done in two campaigns (Forsmark and Rhén, 2001a).

The inflow rate to each of the six deposition holes was estimated during measurement campaigns. During these campaigns (Forsmark and Rhén, 2001a, 2001b), the total inflow rate to the whole hole was made. In two of the holes a detailed measurement was done, using diapers mounted at the walls for a period and then weighted.

4.10 Documentation

Hydrogeological and hydro chemical data have been compiled and presented in a number of sheets (WellCad format). In Figure 4-1 and Figure 4-2, examples of these presentations are shown.

In these datasheets results from for example geological mapping, flow estimation during drilling, packer flow measurements, UCM flow measurement, hydraulic tests are seen.

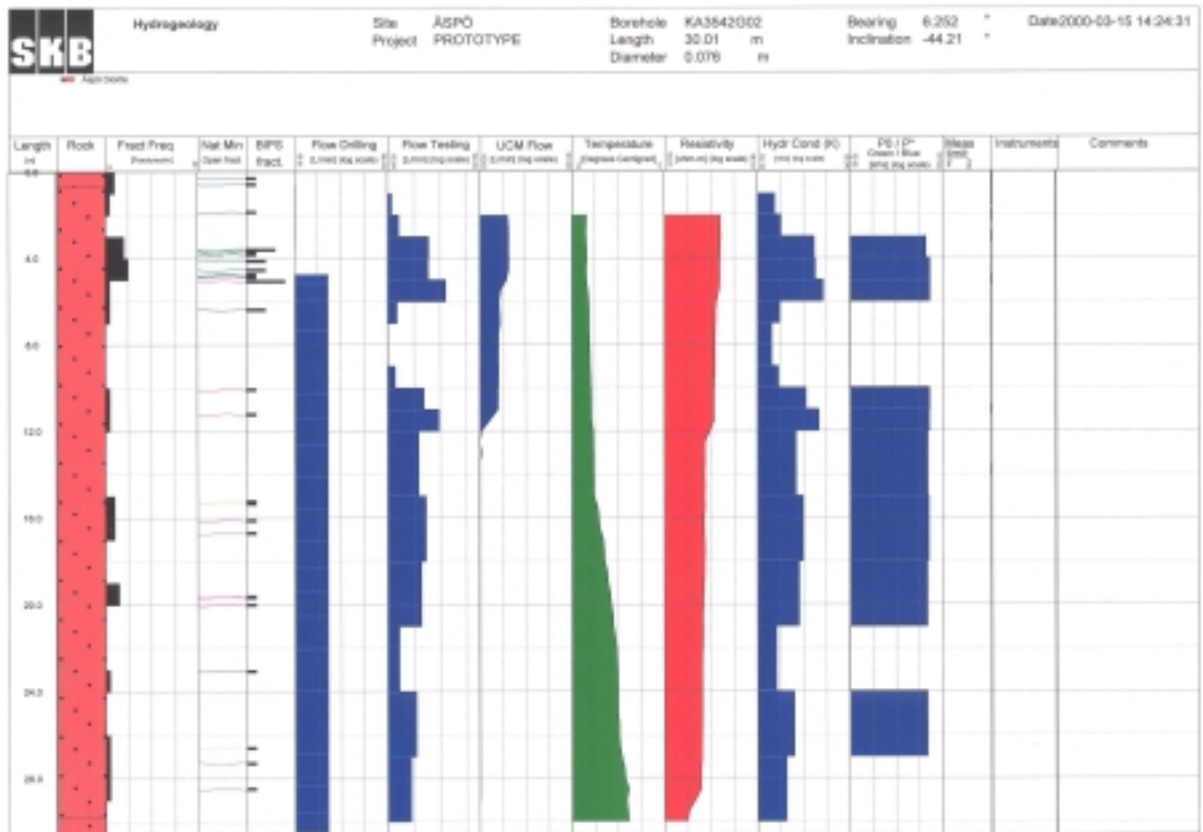


Figure 4-1 Example of hydrogeological documentation of drilled core holes.

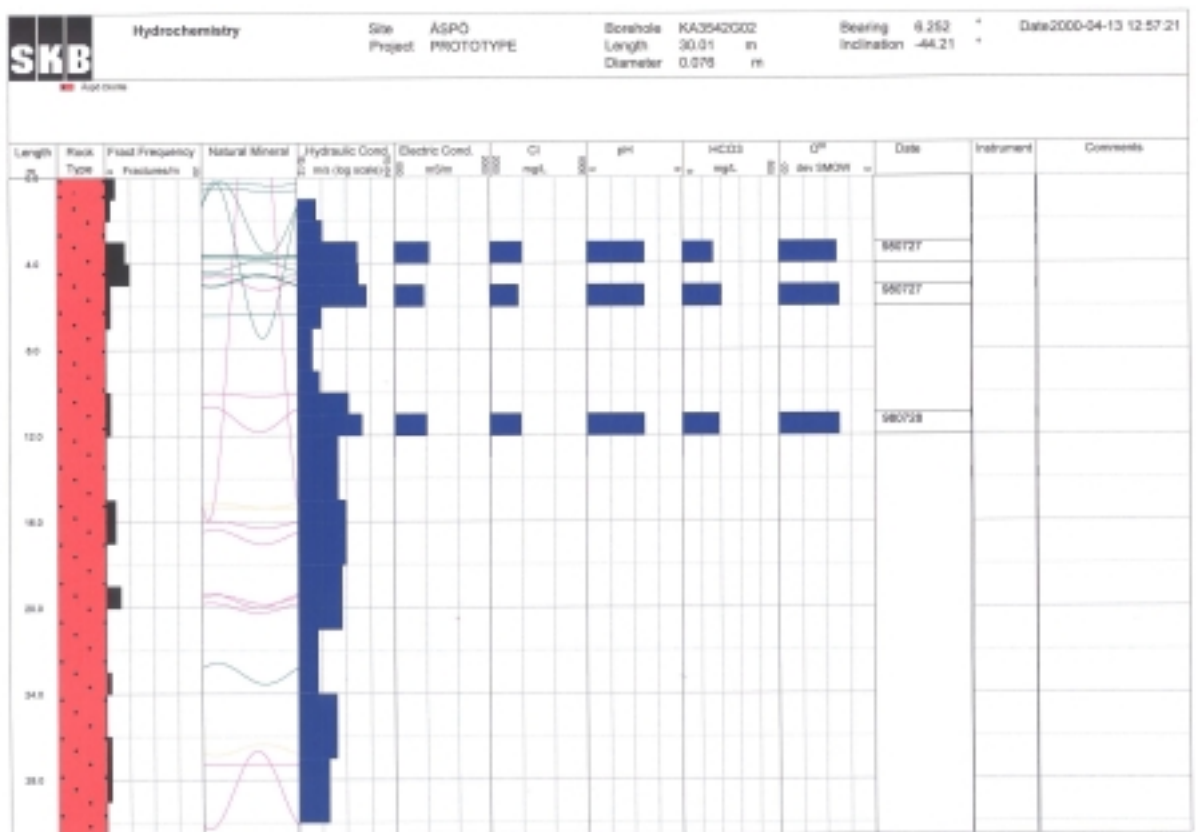


Figure 4-2 Example of hydrochemistry documentation of drilled core holes.

5 DRILLING

5.1 Drilling campaign 1

During the first drilling campaign, 10 pilot holes were drilled. Six of them were drilled at the location of future deposition holes to be used during the long-term experiment of a repository. The ten pilot boreholes were drilled with a downward inclination of 81° towards SW. The length of each borehole is 8.04 m and the nominal diameter is 76 mm. The pilot holes are KA3593G, KA3587G, KA3581G, KA3575G, KA3569G, KA3563G, KA3557G, KA3551G, KA3545G and KA3539G.

5.1.1 Pressure responses during drilling

No pressure recordings were done during these drillings.

5.2 Drilling campaign 2

During this campaign, the short exploratory holes were drilled. In total ten new boreholes were drilled during drill campaign 2. Eight of them are approximately 12 meters long and two are 8 meters long. They are drilled almost vertical. The short exploratory holes are KA3588G, KA3586G, KA3584G, KA3578G, KA3572G, KA3552G, KA3550G, KA3548G, KA3546G and KA3544G.

5.2.1 Pressure responses during drilling

During drilling of each of the exploratory boreholes, 2 - 4 other boreholes were used as observation holes. In the Table 5-1, the observation boreholes are presented together with the major pressure responses noticed during the drilling. As can be seen in Table 5-1 only a few pressure responses were seen.

Table 5-1 Pressure responses during drilling of exploratory boreholes. (X= drilled borehole, 0 = NO response, 1 = response, blank= no observations made).

Observation borehole			Drilled borehole										
Bh name	Secup	Seclow	Bhname:	KA3544G01	KA3546G01	KA3548G01	KA3550G01	KA3552G01	KA3572G01	KA3578G01	KA3584G01	KA3586G01	KA3588G01
			Section:	10.3	7.1	6.8	6.5						4.8
KA3539G	0.39	8.04											
KA3544G01	0.39	12.00		X									
KA3545G	0.39	8.04											
KA3546G01	0.39	12.00		1	X								
KA3548G01	0.25	12.01		1	1	X							
KA3550G01	0.25	12.03		1	1	1	X						
KA3551G	0.39	8.04		0	0	0	0						
KA3552G01	0.39	12.01			1	1	1	X					
KA3557G	0.39	8.04				0	0	0					
KA3563G	0.39	8.04						0					
KA3569G	0.39	8.04						0					
KA3572G01	0.39	12.00							X				
KA3575G	0.39	8.04							0				
KA3578G01	0.39	12.58							0	X			
KA3579G01	0.00	22.65							0	0			0
KA3581G	0.39	8.04							0	0			0
KA3584G01	0.39	12.00								0	X		
KA3586G01	0.39	8.00									0	X	
KA3587G	0.39	8.04								0	0		
KA3588G01	0.39	8.00									0	0	X
KA3593G	0.39	8.04									0	0	1

5.3 Drilling campaign 3

During this campaign, the long exploratory holes were drilled. Thirteen new boreholes were drilled during drill campaign 3 and four pilot holes were extended. Nine of the new holes are approximately 30 meters long, two are 12 meters long, while the last two are approximately 50 meters long. The long exploratory holes are:

Extended pilot boreholes: KA3539G, KA3557G, KA3563G and KA3593G

New boreholes: KA3542G01, KA3542G02, KA3554G01, KA3554G02, KA3566G01, KA3566G02, KA3590G01, KA3590G01 and KA3548A01.

Boreholes drilled from the G-tunnel: KG0021A01 and KG0048A01.

5.3.1 Pressure responses during drilling

During drilling of each of the exploratory boreholes, 5 - 12 other bore hole sections were used as observation sections. In Table 5-1, the observation boreholes are presented together with the major pressure responses noticed during the drilling. In Forsmark, Rhén, 1999b, all registered pressure levels are presented for all observation bore holes together with the drilling record of each exploratory borehole.

Only a few certain pressure responses were observed during the drilling. These responses were seen in nearby boreholes for boreholes drilled in the TBM tunnel. The drilling of KG0021A01 and KG0048A01 show influenced observation sections further away than for other drillings.

Table 5-2 Pressure responses during drilling of exploratory boreholes (X= drilled borehole, 0 = NO response, 1 = response, blank= no observations made).

Observation borehole			Drilled borehole										
Bh name	Secup	Seclow	Bhname:	KA3539G	KA3542G01	KA3542G02	KA3542G02	KA3548A01	KA3554G01	KA3554G02	KA3557G	KA3563G	KA3566G01
			Section:	18	19	4.35	12	7	24				
KA3539G	0.39	30.01		X	1	1	1						
KA3542G01	0.39	30.06			X			1					
KA3542G02	0.39	30.05				X	X	1					
KA3544G01	0.39	12.00		1	1	1	1	0			0		
KA3545G	0.39	8.04		1	1	1	1				0		
KA3546G01	0.39	12.00		1	1	1	1		0	0			
KA3548A01	0.25	30.00						X					
KA3548G01	0.25	12.01		1	1	1	1		0	0			
KA3550G01	0.25	12.03		1	1	1	1	0	0	0		0	
KA3551G	0.39	8.04		1	0	0	0		0	0		0	
KA3552G01	0.39	12.01		1				0	0	0	0		
KA3554G01	0.39	30.06						1	X				
KA3554G02	0.39	30.05						1		X			
KA3557G	0.39	30.04								0	0	X	0
KA3563G	0.39	30.00							0	0		0	0
KA3566G01	0.39	30.06										X	0
KA3566G02	0.39	30.05											X
KA3569G	0.39	8.04									0	0	0
KA3572G01	0.39	12.00										0	0
KA3574G01	0.39	12.00										0	0
KA3575G	0.39	8.04										0	0
KA3576G01	0.39	12.00										0	0
KA3578G01	0.39	12.58										0	0
KA3579G01	0.00	22.65											
KA3581G	0.39	8.04											
KA3584G01	0.39	12.00											
KA3586G01	0.39	8.00											
KA3587G	0.39	8.04											
KA3588G01	0.39	8.00											
KA3590G01	0.39	30.06											
KA3590G02	0.39	30.05											
KA3593G	0.39	30.02											
KA3510A	0.00	150.00		0	0	0	0	0	0	0	0	0	0
KA3573A:1	18.00	40.00		1	1	0	0	1	1	0	0	0	0
KA3573A:2	4.50	17.00		1	1	0	0	1	1	0	0	0	0
KA3600A:1	22.00	50.10		0	0	0	0	0	0	0	0	0	0
KA3600A:2	4.50	21.00		0	0	0	0	0	0	0	0	0	0

Observation borehole			Drilled borehole										
Bh name	Secup	Seclow	Bhname:	KA3566G02	KA3574G01	KA3576G01	KA3590G01	KA3590G02	KA3593G01	KG0021A01	KG0021A01	KG0048A01	KG0048A01
			Section:			6.8	1.5			25	29	49	54
KA3539G	0.39	30.01											
KA3542G01	0.39	30.06											
KA3542G02	0.39	30.05											
KA3544G01	0.39	12.00											
KA3545G	0.39	8.04											
KA3546G01	0.39	12.00											
KA3548A01	0.25	30.00											
KA3548G01	0.25	12.01											
KA3550G01	0.25	12.03											
KA3551G	0.39	8.04											
KA3552G01	0.39	12.01											
KA3554G01	0.39	30.06											
KA3554G02	0.39	30.05											
KA3557G	0.39	30.04		0									
KA3563G	0.39	30.00		0	0	0							
KA3566G01	0.39	30.06											
KA3566G02	0.39	30.05		X									
KA3569G	0.39	8.04		0	0	0							
KA3572G01	0.39	12.00		0									
KA3574G01	0.39	12.00		0	X								
KA3575G	0.39	8.04		0									
KA3576G01	0.39	12.00		0	0	X							
KA3578G01	0.39	12.58			0	1							
KA3579G01	0.00	22.65			0	0	0	0	0				
KA3581G	0.39	8.04			0	0	0	0	0				
KA3584G01	0.39	12.00			0	0	0	0	0				
KA3586G01	0.39	8.00				0	0	0	0				
KA3587G	0.39	8.04				0	1	0	0				
KA3588G01	0.39	8.00					1	0	0				
KA3590G01	0.39	30.06					X						
KA3590G02	0.39	30.05						X					
KA3593G	0.39	30.02					1	0	X				
KA3510A	0.00	150.00		0	0	0	0	0	0	1	0	1	1
KA3573A:1	18.00	40.00		0	0	0	0	0	0	1	0	1	0
KA3573A:2	4.50	17.00		0	0	0	0	0	0	1	0	1	0
KA3600A:1	22.00	50.10		0	0	0	0	0	0	0	1	1	1
KA3600A:2	4.50	21.00		0	0	0	0	0	0	0	1	1	1

5.4 Interference test campaign 1 after drilling campaign 3

No drilling was done during this campaign.

5.5 Interference test campaign 2 after drilling campaign 3

No drilling was done during this campaign.

5.6 Lead-through holes from G-tunnel to A-tunnel

Three boreholes, among several, were drilled from the G-tunnel to the prototype tunnel (A-tunnel). They are inclined 2 degrees downward as seen from G-tunnel. The diameter of the holes is 76 mm. The boreholes are KG0023A01, KG0027A01 and KG0033A01.

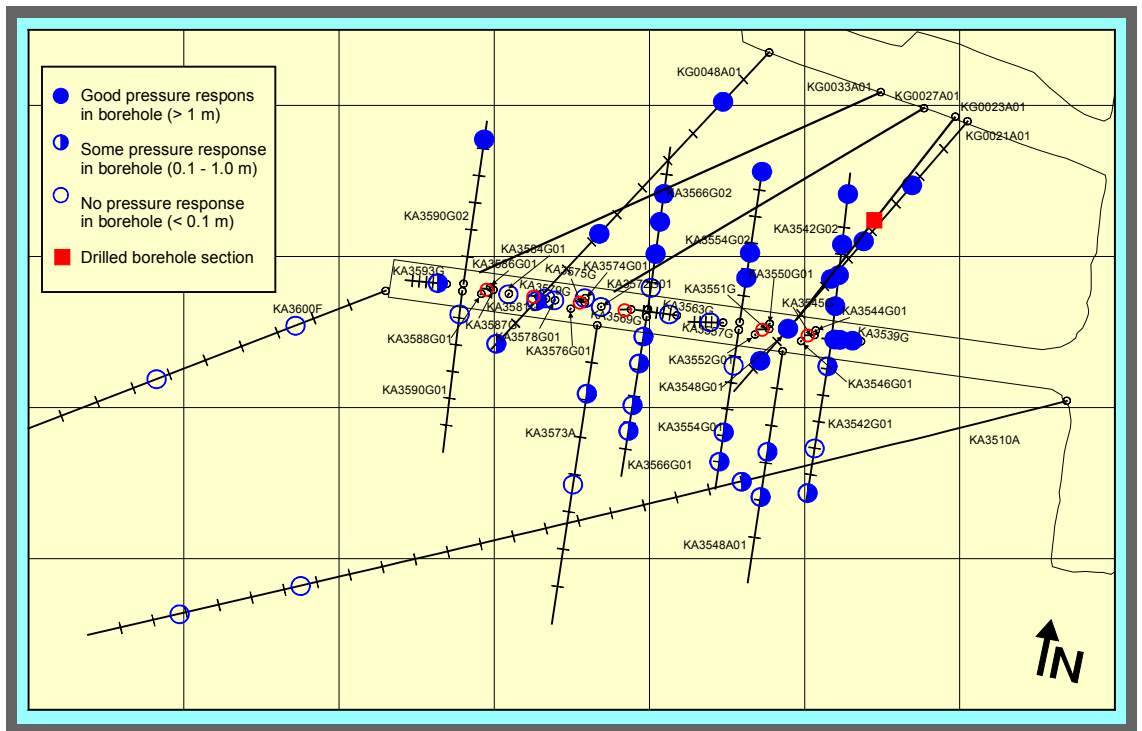
5.6.1 Pressure responses during drilling

With the observed water-bearing sections as a basis, for each drilled borehole, an attempt to correlate these sections to registered pressure changes in the observation sections were made. In Table 5-3 observed responses have been indicated. In Forsmark et al (2001a), plots of pressure responses are presented.

Table 5-3 Registered pressure changes in observation sections during drilling of observed water-bearing section in drilled borehole [0=no response (<0.1 m), 1= some response (> 0.1 m & < 1.0 m), 2= good response (> 1.0 m)].

Observation section	Observation secup	Observation seclow	Observation hydraulic centre	KG0023A01 14.38 - 15.77 m	KG0023A01 24.42 - 27.78 m	KG0027A01 8.05 - 9.92 m	KG0027A01 41.57 - 44.52 m	KG0033A01 7.93 - 10.73 m	KG0033A01 34.65 - 39.53 m	KG0033A01 42.65 - 43.62 m
KA3510A:1	122.02	150.00	136.00	0	0	1	0	0	0	0
KA3510A:2	114.02	121.02	117.50	0	0	1	0	0	0	0
KA3510A:3	4.52	113.02	50.00	0	1	2	0	1	1	0
KA3539G:1	19.30	30.01	20.56	0	2	2	0	2	2	0
KA3539G:2	9.80	18.30	16.37	0	2	2	0	2	2	0
KA3539G:3	1.30	8.80	6.59	0	2	2	0	0	0	0
KA3542G01:1	25.80	30.04	28.50	0	1	2	0	1	1	0
KA3542G01:2	8.80	24.80	20.06	0	0	2	0	1	1	0
KA3542G01:3	1.30	7.80	4.50	0	1	2	0	1	1	0
KA3542G02:1	22.30	30.01	26.21	0	2	2	0	2	0	0
KA3542G02:2	13.80	21.30	16.83	0	2	2	0	2	2	0
KA3542G02:3	8.80	12.80	11.13	0	2	2	0	2	2	0
KA3542G02:4	1.30	7.80	5.36	0	2	2	0	2	2	0
KA3548A01:1	15.00	30.00	19.56	0	1	2	0	1	1	0
KA3548A01:2	10.00	14.00	13.49	0	1	2	0	1	1	0
KA3554G01:1	22.30	30.01	24.95	0	1	2	0	0	2	0
KA3554G01:2	12.30	21.30	19.39	0	1	2	0	1	1	0
KA3554G01:3	1.30	11.30	6.78	0	0	1	0	1	1	0
KA3554G02:1	22.30	30.01	28.47	0	2	2	0	2	2	0
KA3554G02:2	10.30	21.01	13.13	0	2	2	0	2	2	0
KA3554G02:3	1.30	9.30	8.39	0	2	2	0	2	2	0
KA3557G:1	0.30	30.04	11.40	0	0	0	0	0	1	0
KA3563G01:1	0.30	30.00	5.60	0	0	0	0	0	0	0
KA3566G01:1	20.80	30.01	21.57	0	1	1	0	1	1	0
KA3566G01:2	12.30	19.80	16.71	0	1	1	0	1	1	0
KA3566G01:3	7.30	11.30	8.81	0	1	1	0	1	1	0
KA3566G01:4	1.30	6.30	3.70	0	1	1	0	1	1	0
KA3566G02:1	19.30	30.01	21.41	0	2	2	0	2	2	0
KA3566G02:2	12.30	18.30	16.23	0	2	2	0	2	2	0
KA3566G02:3	7.80	11.30	10.25	0	2	1	0	1	2	0
KA3566G02:4	1.30	6.80	3.99	0	0	0	0	1	2	0
KA3572G01:1	0.30	12.00	7.67	0	0	1	0	0	1	0
KA3573A:1	18.00	40.07	21.34	0	0	1	0	1	1	0
KA3573A:2	4.50	17.00	9.16	0	1	2	0	1	1	0
KA3574G01:1	0.30	12.00	4.93	0	0	0	0	0	0	0
KA3578G01:1	0.30	12.58	7.03	0	0	0	0	0	0	0
KA3579G01:1	0.30	22.65	7.62	0	0	0	0	0	0	0
KA3584G01:1	0.30	12.00	6.24	0	0	0	0	0	0	0
KA3590G01:1	0.30	30.06	4.33	0	0	1	0	0	0	0
KA3590G02:1	0.30	30.05	26.73	0	2	2	0	2	2	0
KA3593G01:1	0.30	30.02	6.45	0	1	1	0	0	2	0
KA3600F:1	22.00	50.10	31.78	0	0	1	0	0	0	0
KA3600F:2	4.50	21.00	12.51	0	0	1	0	0	0	0
KG0021A01:1	42.50	48.82	43.53	0	2	2	0	2	1	0
KG0021A01:2	35.00	41.50	37.70	0	2	2	0	2	1	0
KG0021A01:3	25.00	34.00	28.64	0	2	2	0	2	1	0
KG0021A01:4	17.00	24.00	21.80	0	2	2	0	2	1	0
KG0021A01:5	4.00	16.00	11.64	0	2	2	0	2	0	0
KG0048A01:1	49.00	54.69	53.81	0	1	2	0	1	1	0
KG0048A01:2	41.00	48.00	45.90	0	1	2	0	1	1	0
KG0048A01:3	30.00	40.00	33.50	0	2	2	0	2	2	0
KG0048A01:4	4.00	29.00	9.12	0	2	2	0	2	0	0

The drilling of lead-through boreholes from tunnel G to tunnel A confirms the, during earlier investigations, indicated pattern of a hydraulically dominant response direction running WNW. All three drillings documented in this report show the same pattern, see for example Figure 5-1.



/1311/1310241/DATA/Boreholes between A and G tunnels/Response/KG0023A01/Resp_1_0023.SRF
02/07/01 08:56:48

Figure 5-1 Pressure responses during drilling of KG0023A01 (14.38 - 15.77 m).

5.7 Deposition holes

Six deposition boreholes in the prototype repository were drilled during the period June-September 1999. The drillings were not done as continuous drillings, but in several stages. In Forsmark et al (2001a), all times for each sub-drilling is detailed.

Sudden pressure responses that in a certain manner can be assigned to the drilling activities are shown in Table 5-4. Only a few certain responses could be observed. It is however to be noted that the inleakage rates are low in the deposition boreholes. In Forsmark et al (2001a), the pressure changes during all drilling period are presented. Of all the observation sections used during the drillings 66 % show a decrease while 34 % show an increase.

Table 5-4 Pressure responses during drilling of deposition boreholes (0=NO response, 1=response).

OBSERVATION SECTIONS			DRILLED BOREHOLE			
Bh name	Secup	Seclow	Bhname:	DA3545G01	DA3551G01	DA3587G01
			Section:	3.7	2	6.5
KA3510A:1	122.02	150.00		0	0	0
KA3510A:2	114.02	121.02		0	0	0
KA3510A:3	4.52	113.02		0	0	0
KA3539G:1	19.30	30.01		1	0	0
KA3539G:2	9.80	18.30		1	0	0
KA3539G:3	1.30	8.80		0	0	0
KA3542G01:1	25.80	30.04		0	0	0
KA3542G01:2	8.80	24.80		0	0	0
KA3542G01:3	1.30	7.80		0	0	0
KA3542G02:1	22.30	30.01		0	0	0
KA3542G02:2	13.80	21.30		0	0	0
KA3542G02:3	8.80	12.80		0	0	0
KA3542G02:4	1.30	7.80		1	0	0
KA3544G01:1	6.30	12.00		1	0	0
KA3544G01:2	1.30	5.30		1	0	0
KA3546G01:1	6.80	12.00		1	0	0
KA3546G01:2	1.30	5.80		1	0	0
KA3548A01:1	15.00	30.00		0	0	0
KA3548A01:2	10.00	14.00		0	0	0
KA3548G01:1	0.30	12.01		0	0	0
KA3550G01:1	6.30	12.03		0	0	0
KA3550G01:2	1.30	5.30		0	0	0
KA3552G01:1	8.80	12.01		0	0	0
KA3552G01:2	4.05	7.80		0	1	0
KA3552G01:3	1.30	3.05		0	0	0
KA3554G01:1	22.30	30.01		0	0	0
KA3554G01:2	12.30	21.30		0	0	0
KA3554G01:3	1.30	11.30		0	0	0
KA3554G02:1	22.30	30.01		0	0	0
KA3554G02:2	10.30	21.01		0	0	0
KA3554G02:3	1.30	9.30		0	0	0
KA3557G:1	0.30	30.04		0	0	0
KA3563G01:1	9.30	30.00		0	0	0
KA3563G01:2	3.80	8.30		0	0	0
KA3563G01:3	1.30	2.80		0	0	0
KA3566G01:1	20.80	30.01		0	0	0
KA3566G01:2	12.30	19.80		0	0	0
KA3566G01:3	7.30	11.30		0	0	0
KA3566G01:4	1.30	6.30		0	0	0
KA3566G02:1	19.30	30.01		0	0	0
KA3566G02:2	12.30	18.30		0	0	0
KA3566G02:3	7.80	11.30		0	0	0
KA3566G02:4	1.30	6.80		0	0	0
KA3572G01:1	6.30	12.00		0	0	0
KA3572G01:2	1.30	5.30		0	0	0
KA3573A:1	18.00	40.07		0	0	0
KA3573A:2	4.50	17.00		0	0	0
KA3574G01:1	8.80	12.00		0	0	0
KA3574G01:2	5.30	7.80		0	0	0
KA3574G01:3	1.30	4.30		0	0	0
KA3576G01:1	8.80	12.01		0	0	0
KA3576G01:2	3.80	7.80		0	0	0
KA3576G01:3	1.30	2.80		0	0	0
KA3578G01:1	6.80	12.58		0	0	0
KA3578G01:2	1.30	5.80		0	0	0
KA3579G01:1	9.30	22.65		0	0	0
KA3579G01:2	5.30	8.30		0	0	0
KA3579G01:3	1.30	4.30		0	0	0
KA3584G01:1	0.30	12.00		0	0	0
KA3590G01:1	17.30	30.06		0	0	0
KA3590G01:2	7.80	16.30		0	0	1
KA3590G01:3	1.30	6.80		0	0	1
KA3590G02:1	23.30	30.05		0	0	0
KA3590G02:2	17.30	22.30		0	0	0
KA3590G02:3	8.30	16.30		0	0	0
KA3590G02:4	1.20	7.20		0	0	0
KA3593G01:1	8.30	30.02		0	0	1
KA3593G01:2	1.3	7.3		0	0	1
KA3600F:1	22	50.1		0	0	0
KA3600F:2	4.5	21		0	0	0
KG0021A01:1	42.5	48.82		0	0	0
KG0021A01:2	35	41.5		0	0	0
KG0021A01:3	25	34		0	0	0
KG0021A01:4	17	24		0	0	0
KG0021A01:5	4	16		0	0	0
KG0048A01:1	49	54.69		0	0	0
KG0048A01:2	41	48		0	0	0
KG0048A01:3	30	40		0	0	0
KG0048A01:4	4	29		0	0	0

In order to study the overall influence, to the surrounding rock mass, due to the drilling of deposition boreholes a study of pressure differences was made. When drilling the boreholes of the inner section 63 observation sections were available and during the drilling of the boreholes in the outer section 62 sections were used. The pressure in an observation section at the start of a drilling of a deposition borehole was compared with the pressure at the end of the drilling period and a pressure difference was calculated, see Figure 5-2. If the pressure increased that resulted in a positive number, while if the pressure decreased then that resulted in a negative number. Plots and data of all observation sections are detailed in Forsmark et al (2001a).

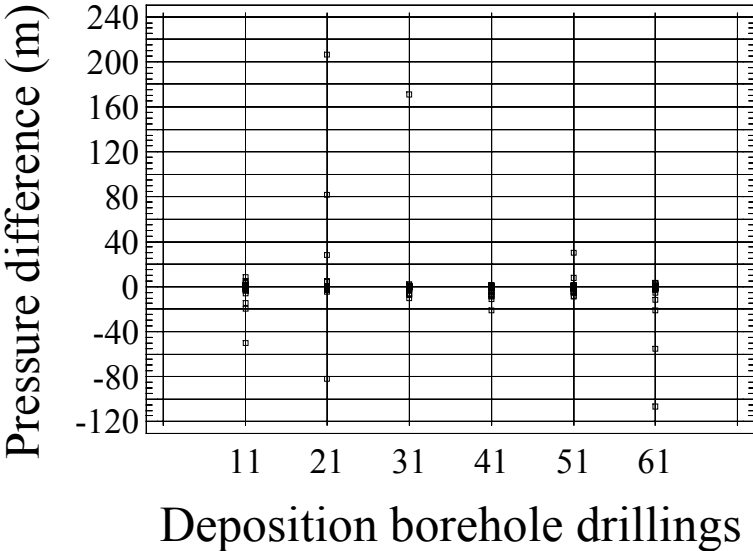


Figure 5-2 Pressure increase/decrease during drilling of deposition boreholes (+ = increase, - = decrease of pressure). (11: deposition bore hole No 1, 21: deposition bore hole No 2 etc, according to Table 5-5.)

In Table 5-5, the result of the analysis of pressure increase/decrease is shown. The major responses in the figure above are identified in the table.

Table 5-5 Statistics of pressure increase/decrease during drilling of deposition boreholes.

Borehole	Bh nr	Median (m)	Stand. dev	n (Pressure increase, +)	n (Pressure decrease, -)	Major pressure differences in observation sections
DA3587G01	1	0.04	7.21	40	23	KA3590G02:3 (-20.00 m);KA3590G02:4 (-14.32 m); KA3593G01:2 (-50.12 m)
DA3581G01	2	-0.33	30.06	14	49	KA3574G01:1 (28.04 m);KA3574G01:2 (-81.76 m) KA3576G01:1 (81.69 m);KA3576G01:3 (206.17 m)
DA3575G01	3	0.08	21.70	37	26	KA3576G01:3 (170.84 m)
DA3569G01	4	-0.16	3.44	10	53	KA3576G01:3 (-21.12 m)
DA3551G01	5	-0.59	4.51	16	46	KA3552G01:3 (29.95 m)
DA3545G01	6	-0.37	15.39	12	50	KA3539G:3 (-55.50 m); KA3544G01:1 (-21.45 m); KA3544G01:2 (-106.84 m)

As can be seen in the table above, during the drilling of two, out of the total of six, deposition boreholes, and more pressure increases than pressure decreases occurs. This indicates different influence of those deposition boreholes, DA3587G01 and DA3575G01, to the surrounding rock mass than for the four other deposition boreholes, where the majority of the pressure registrations are decreasing during the drilling period of these boreholes. Explanations to this could be stress re-distributions in the rock mass due to the drillings causing decrease in pressure, but also increase in pressure. Minor decreasing pressures can also be explained as natural long-term trends in the hydraulic head pressure around the Prototype Repository Tunnel. Another possibility for pressure changes during drilling periods is clogging of fractures due to vibration from the drilling process. This in turn could create a local pressure increase.

The available boreholes during the drilling period were divided into 5 subclasses, see Figure 5-3 in order to see the importance of the borehole inclination:

- All boreholes (Subclass 1)
- Sub-vertical bore holes (Subclass 2)
- Sub-horizontal boreholes (KG0021A01, KG0048A01, KA3548A01, KA3510A, KA3573A and KA3600F) (Subclass 3)
- Southerly inclined boreholes (KA3542G01, KA3554G01, KA3566G01 and KA3590G01) (Subclass 4)
- Northerly inclined boreholes (KA3542G02, KA3554G02, KA3566G02 and KA3590G02) (Subclass 5)

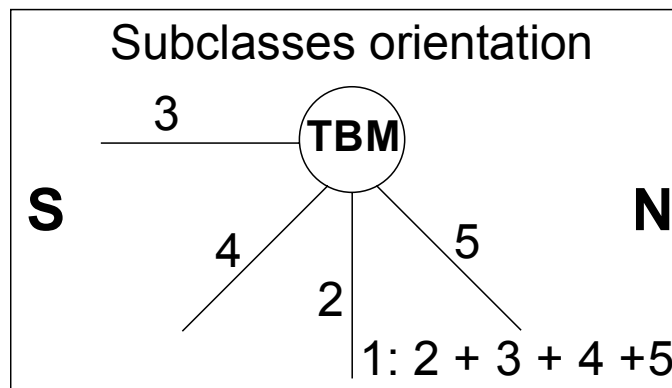


Figure 5-3 Borehole subclass orientation (S=South, N=North).

An attempt to observe any systematic pressure change tendency around the tunnel is shown in Table 5-6.

Table 5-6 Pressure increase or decrease around prototype tunnel during drilling of deposition boreholes.

Subclass	n	n increase	% increase	n decrease	% decrease
1	376	129	34	247	66
2	146	58	40	88	60
3	108	37	34	71	66
4	58	18	31	40	69
5	64	16	25	48	75

The results were similar all around the tunnel, with about one-third of the changes being increasing pressures and two-thirds of the values showing decreasing pressures.

During the drilling period some of the recently drilled deposition boreholes became filled with water (no pumping was made) (Forsmark et al, 2001a). No immediate influence to surrounding boreholes was however discerned.

6 FLOW MEASUREMENTS

6.1 Drilling campaign 1

In all bore holes flow logging was made using a double packer system. The packer inflation can influence the accuracy of the flow measurements in low conductive sections. The generated flow in a double packer section caused by the packers used in the exploratory borehole tests has been tested in the laboratory. These laboratory tests indicate that the packers themselves generate a flow rate which decrease by time and the flow rate is about 0.5 mL/min after 30 minutes expansion. According to the test results, it is believed that the generated flow from packer expansion must be lower, at least in some cases. The results indicate that a flow measurement less than $1 \cdot 10^{-4}$ L/min can possibly be considered as a packer generated flow. In those cases the flow of the section is set to, $Q_m = 1 \cdot 10^{-4}$ L/min.

The measured flow then used to estimate the transmissivity of the 1-meter section,

$$T_{\text{sect}} = (Q_{\text{sect}} \cdot T_{\text{TOT}}) / Q_{\text{secttot}} \quad \text{where}$$

Q_{sect} is the measured flow from the section, or if less than $1 \cdot 10^{-4}$ L/min, then it is set to $1 \cdot 10^{-4}$ L/min

Q_{secttot} is the accumulated flow for the entire bore hole from the flow logging

T_{TOT} is the estimated transmissivity valid for the entire bore hole, estimated from the borehole pressure build-up test described in Chapter 7. If the flow rate of the measurement section exceeded 10 mL/min a Pressure Build-up Test (PBT) of the section was done.

In Figures 6-1 to 6-3 an overview of the flow logging results of boreholes investigated during drill campaign 1 are shown. Q_{TOT} in the figures is the measured flow during the hydraulic test where T_{TOT} was estimated. In Rhén and Forsmark (1998a) the results are detailed.

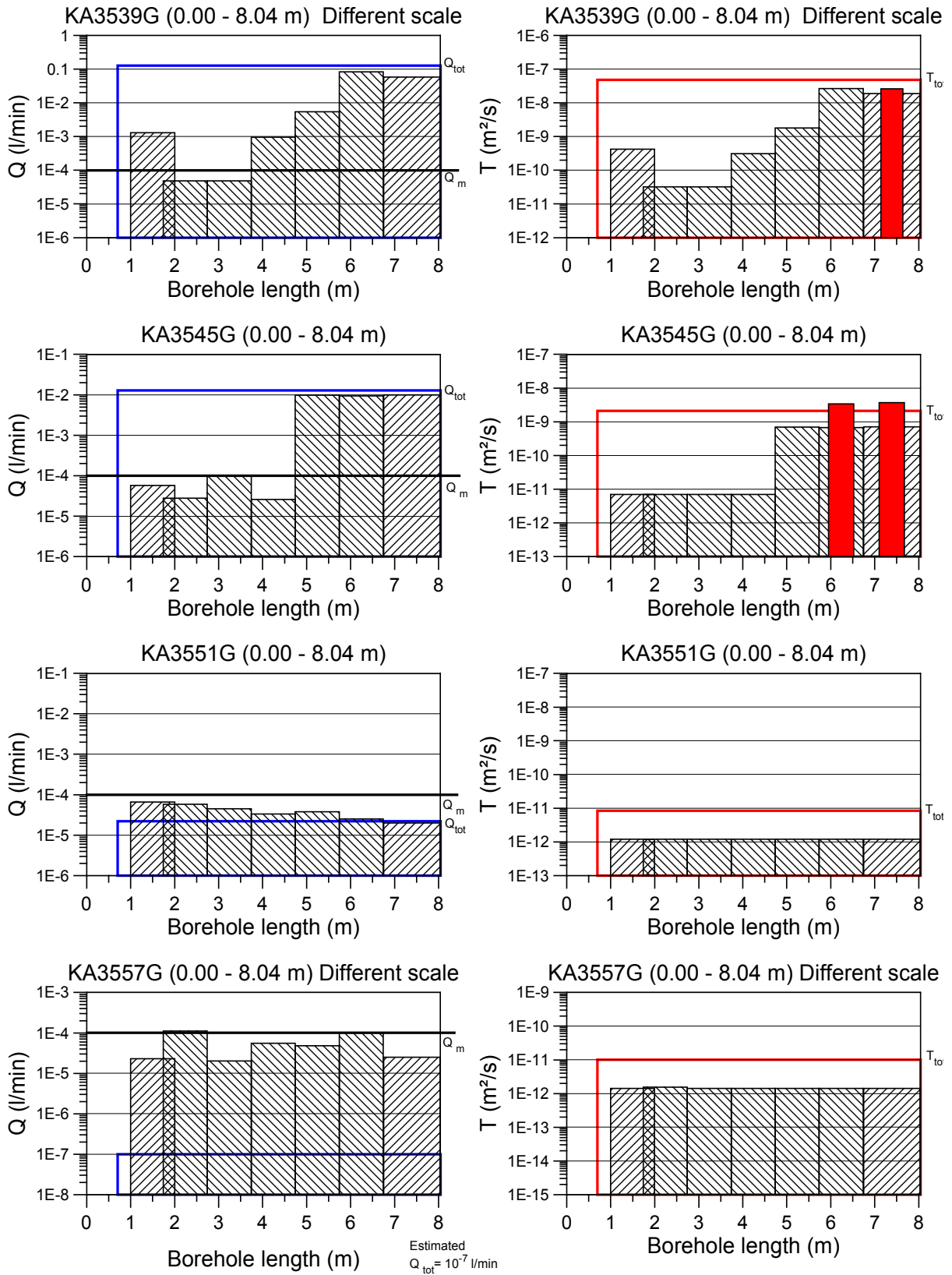


Figure 6-1 The results from flowlogging in KA3539G, KA3545G, KA3551G and KA3557G. The red bars in the transmissivity diagrams indicate single section PBTs.

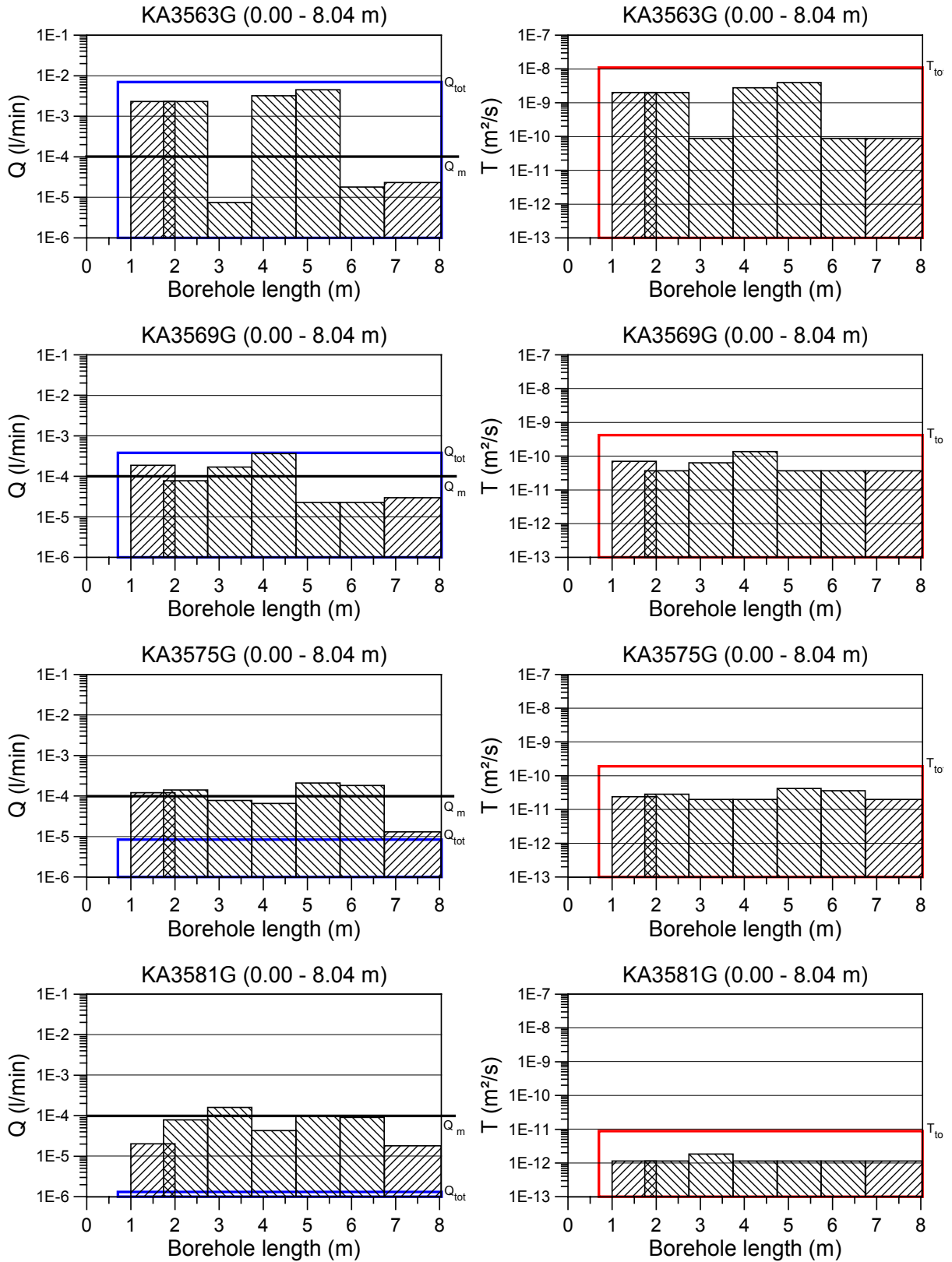


Figure 6-2 The results from flowlogging in KA3563G, KA3695G, KA3575G and KA3581G. The red bars in the transmissivity diagrams indicate single section PBTs.

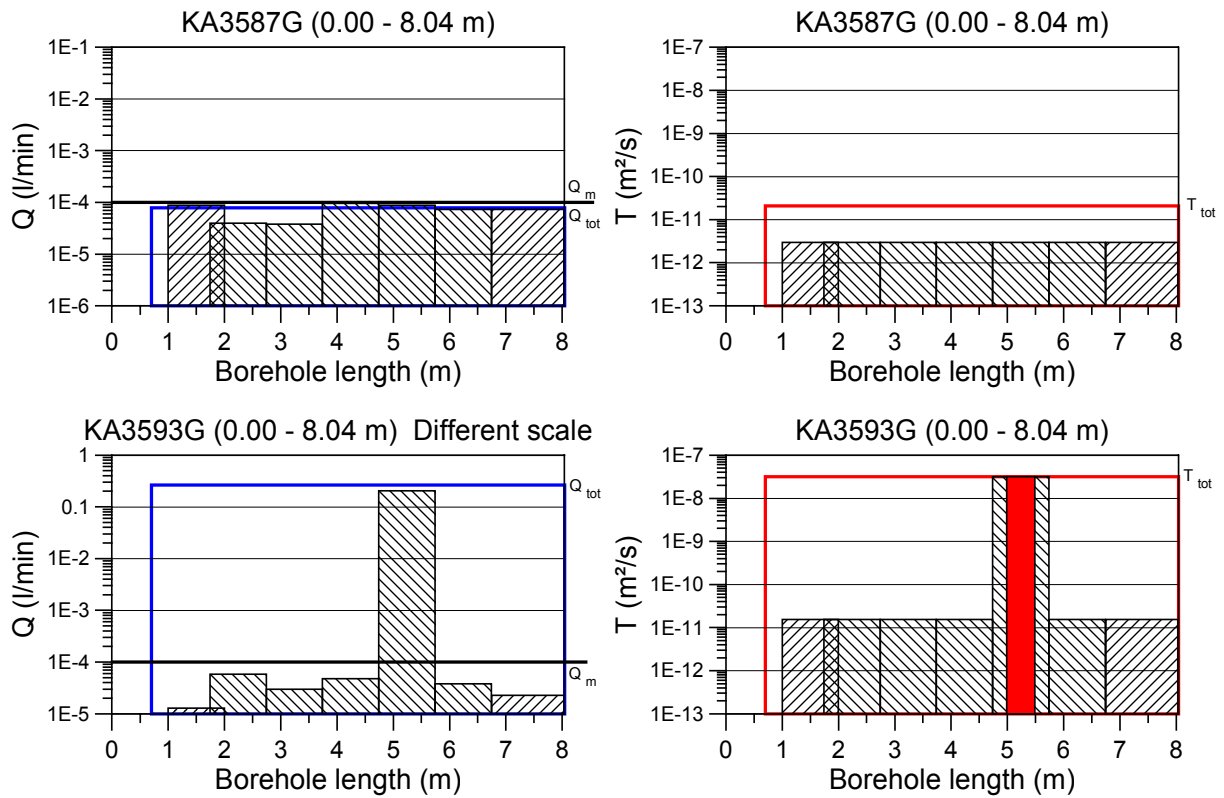


Figure 6-3 The results from flowlogging in KA3587G, KA3935G. The red bars in the transmissivity diagrams indicate single section PBTs.

The flow logging produced five sections to be tested as a pressure build-up test, see figures above and Section 7.1.

6.2 Drilling campaign 2

The same flow logging procedures applied during drilling campaign 1 was used for the flow logging of the holes drilled during campaign 2. In Figure 6-4 to 6-6 an overview of the flow logging results of boreholes investigated during drill campaign 2 are shown. The results are detailed in Rhén and Forsmark (1998b).

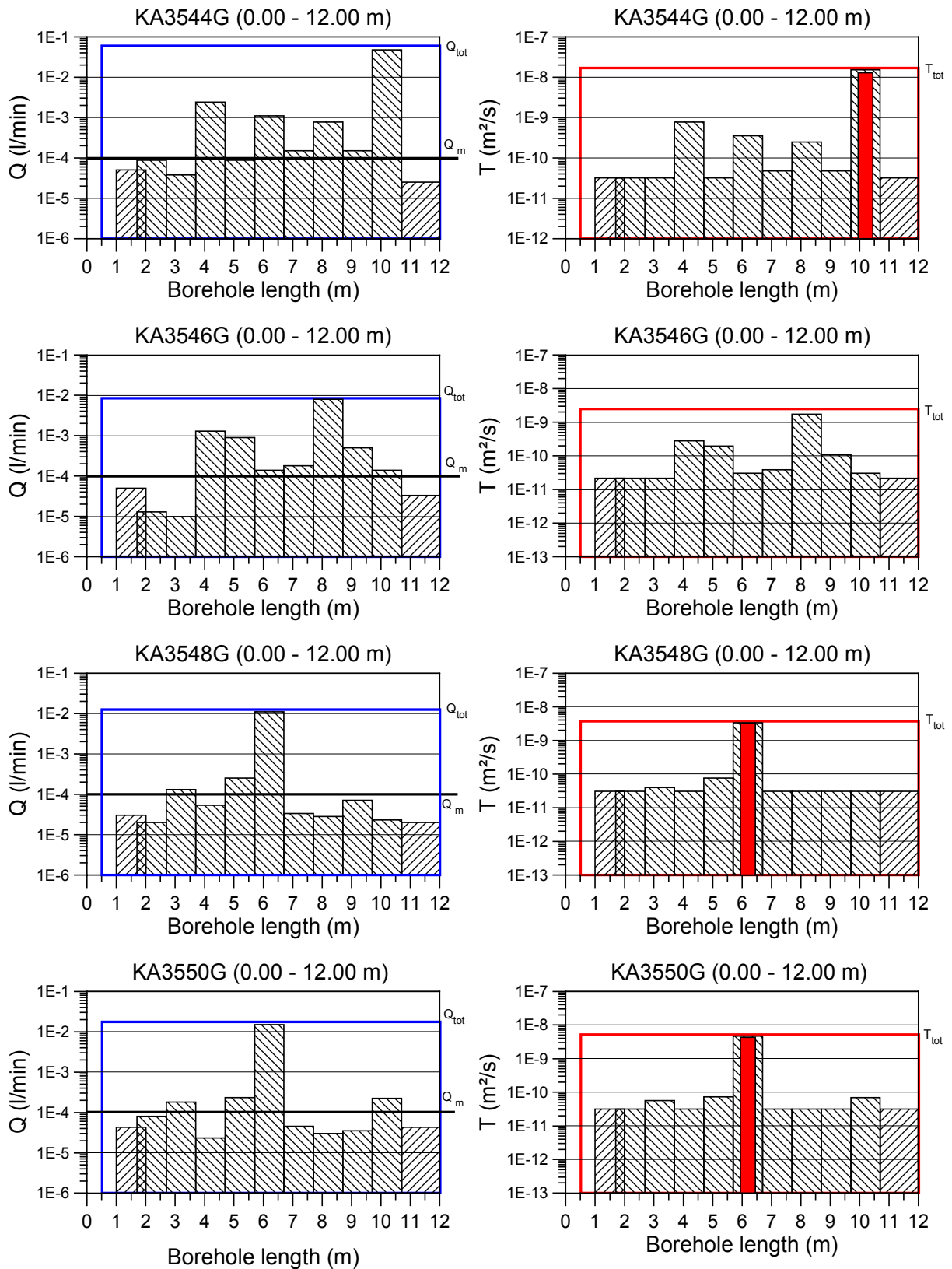


Figure 6-4 The results from flowlogging in KA3544G01, KA3546G01, KA3548G01 and KA3550G01. The red bars in the transmissivity diagrams indicate single section PBTs.

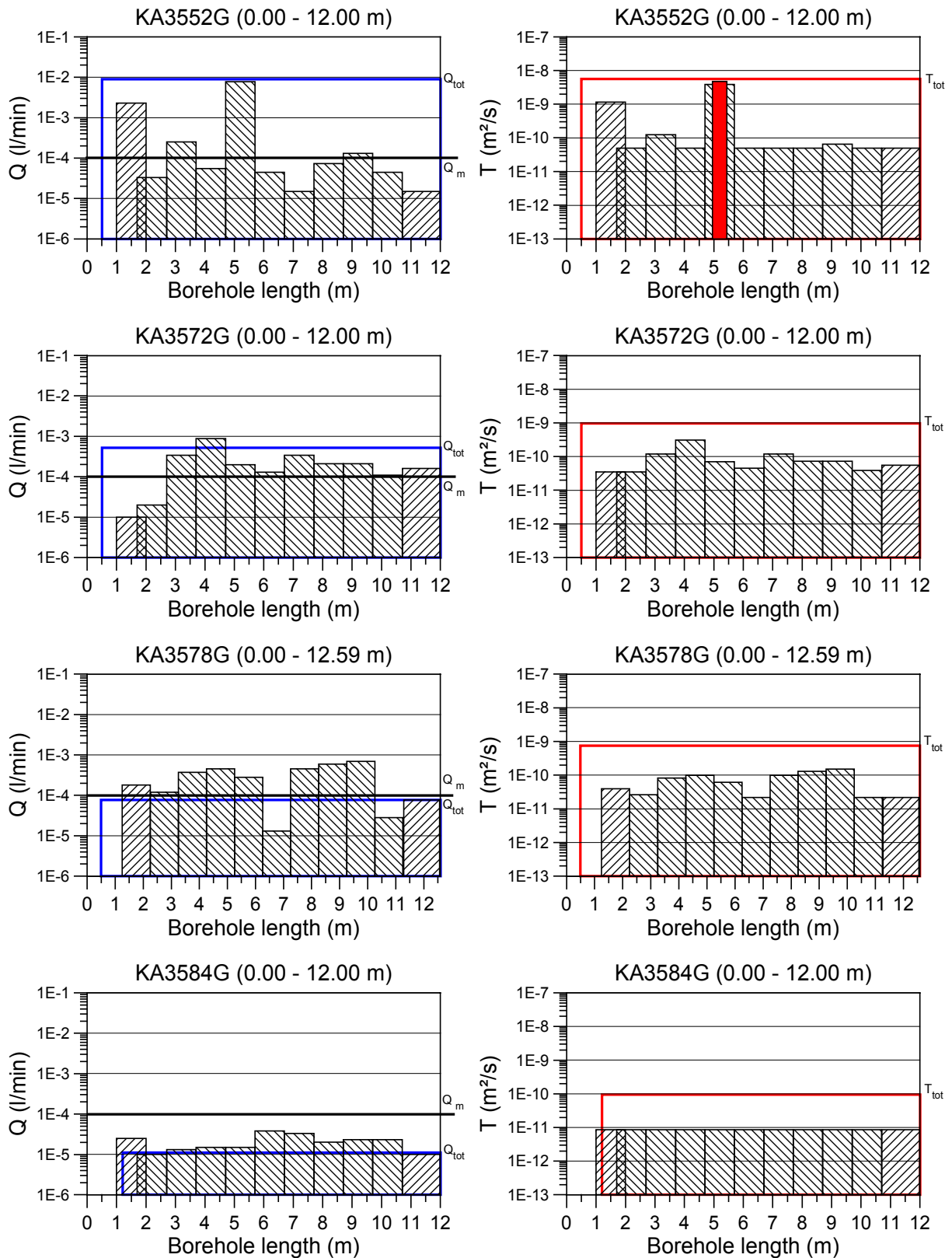


Figure 6-5 The results from flowlogging in KA3552G01, KA3572G01, KA3578G01 and KA3584G01. The red bars in the transmissivity diagrams indicate single section PBTs.

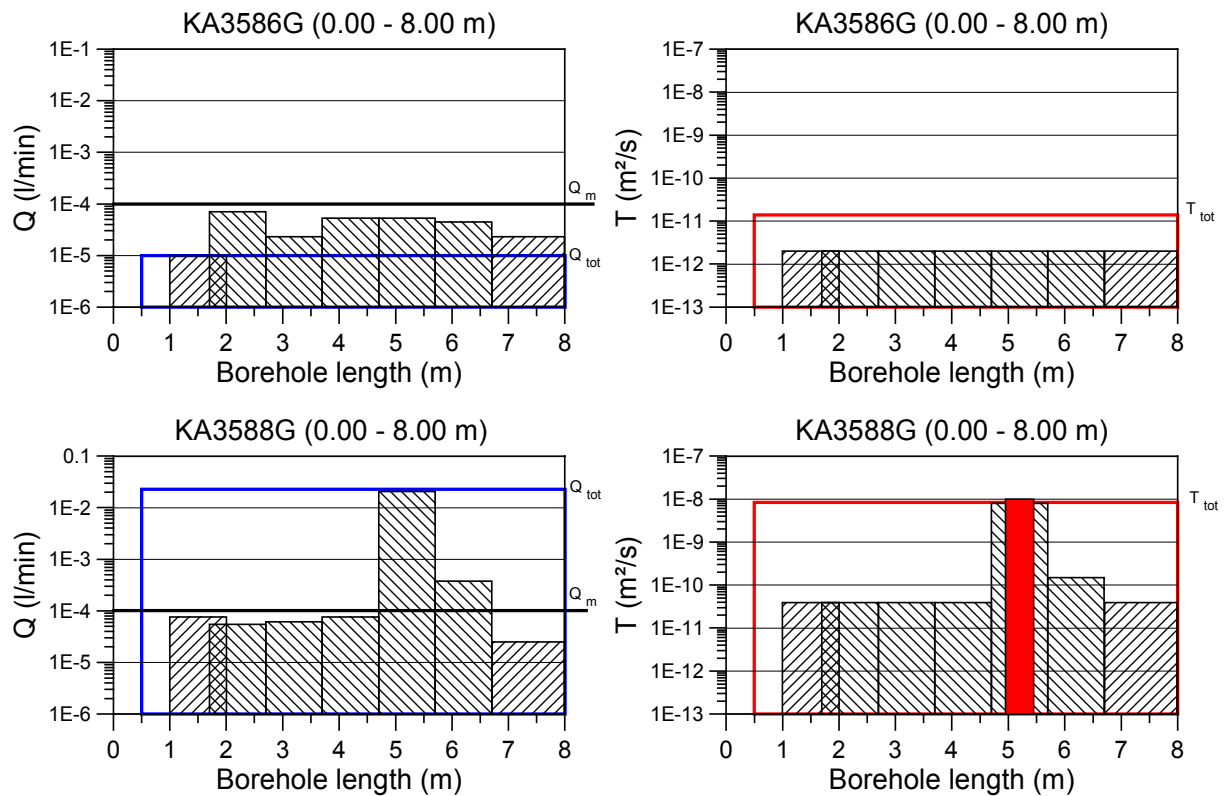


Figure 6-6 The results from flowlogging in KA3586G01, KA3588G01. The red bars in the transmissivity diagrams indicate single section PBTs.

The flow logging produced six sections to be tested as a pressure build-up test. These tests are indicated in the figures above and described in Section 7.2.

6.3 Drilling campaign 3

The same flow logging procedures applied during drilling campaign 1 was used for the flow logging of the holes drilled during campaign 2. In Figure 6-4 to 6-6 an overview of the flow logging results of boreholes investigated during drill campaign 2 are shown. The results are detailed in Forsmark and Rhén (1999b).

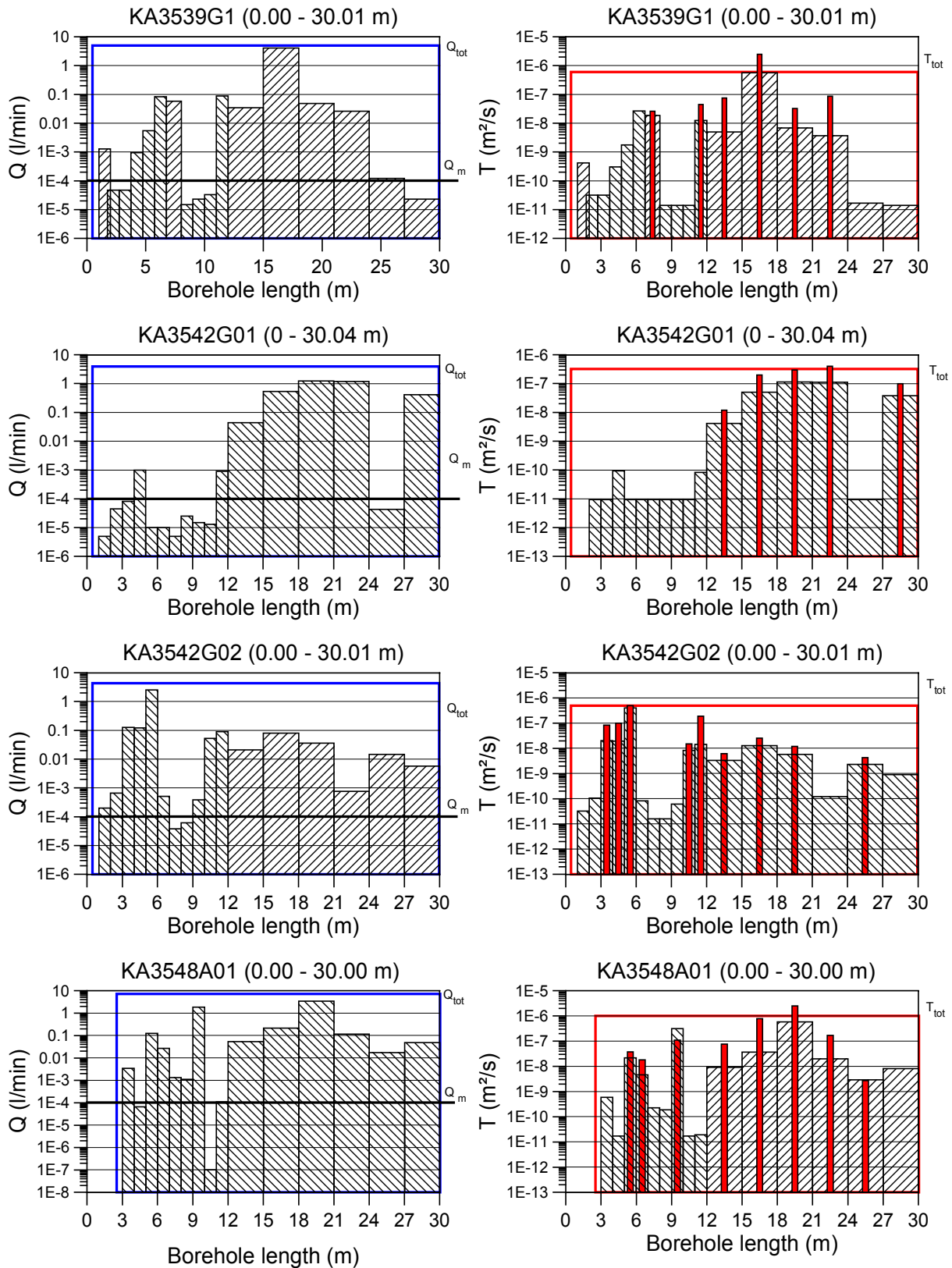


Figure 6-7 The results from flowlogging in KA3539G (extended), KA3542G01, KA3542G02 and KA3548A01. The red bars in the transmissivity diagrams indicate single section PBTs.

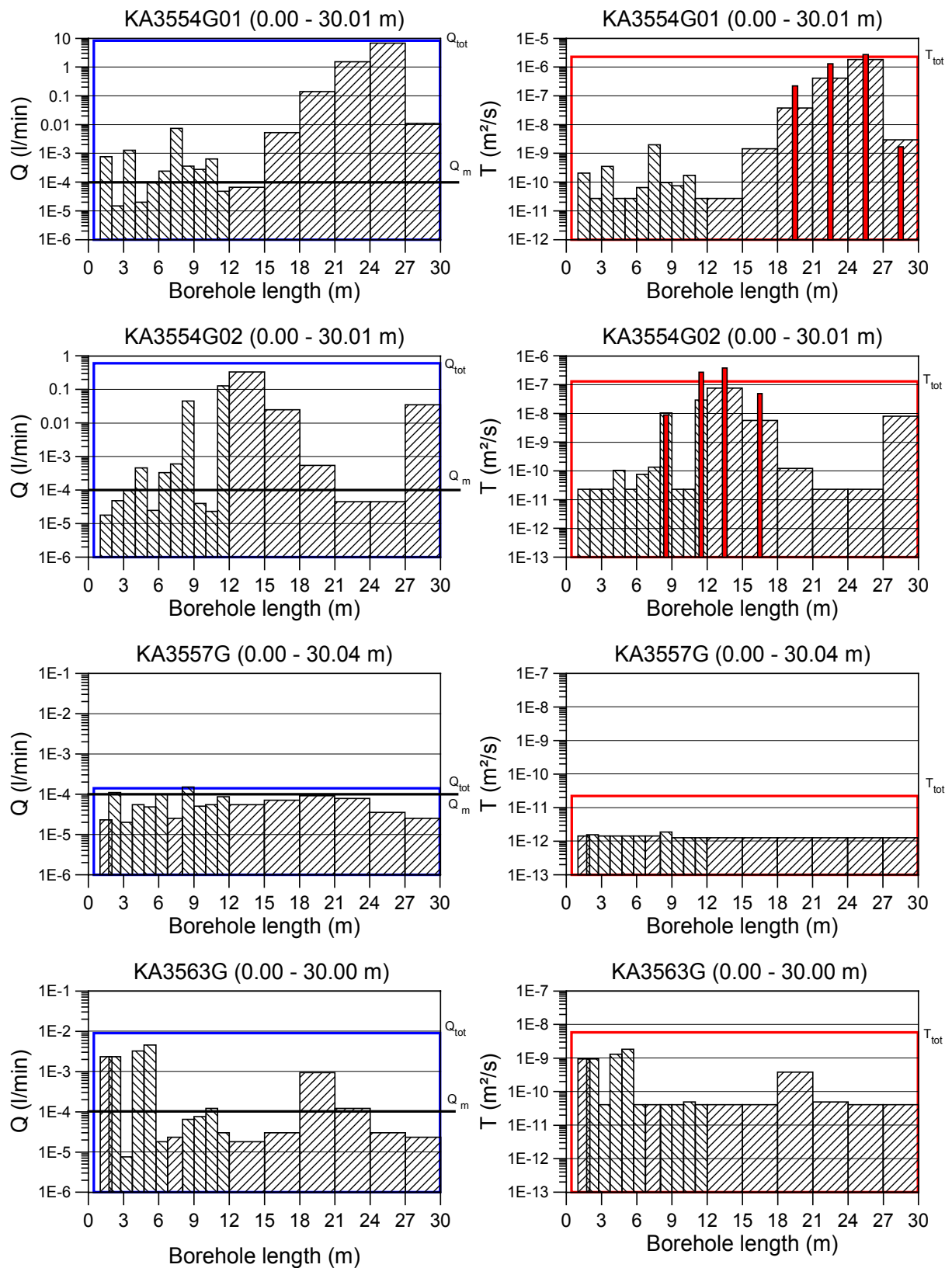


Figure 6-8 The results from flowlogging in KA3554G01, KA3554G02, KA3557G (extended) and KA3563G (extended). The red bars in the transmissivity diagrams indicate single section PBTs.

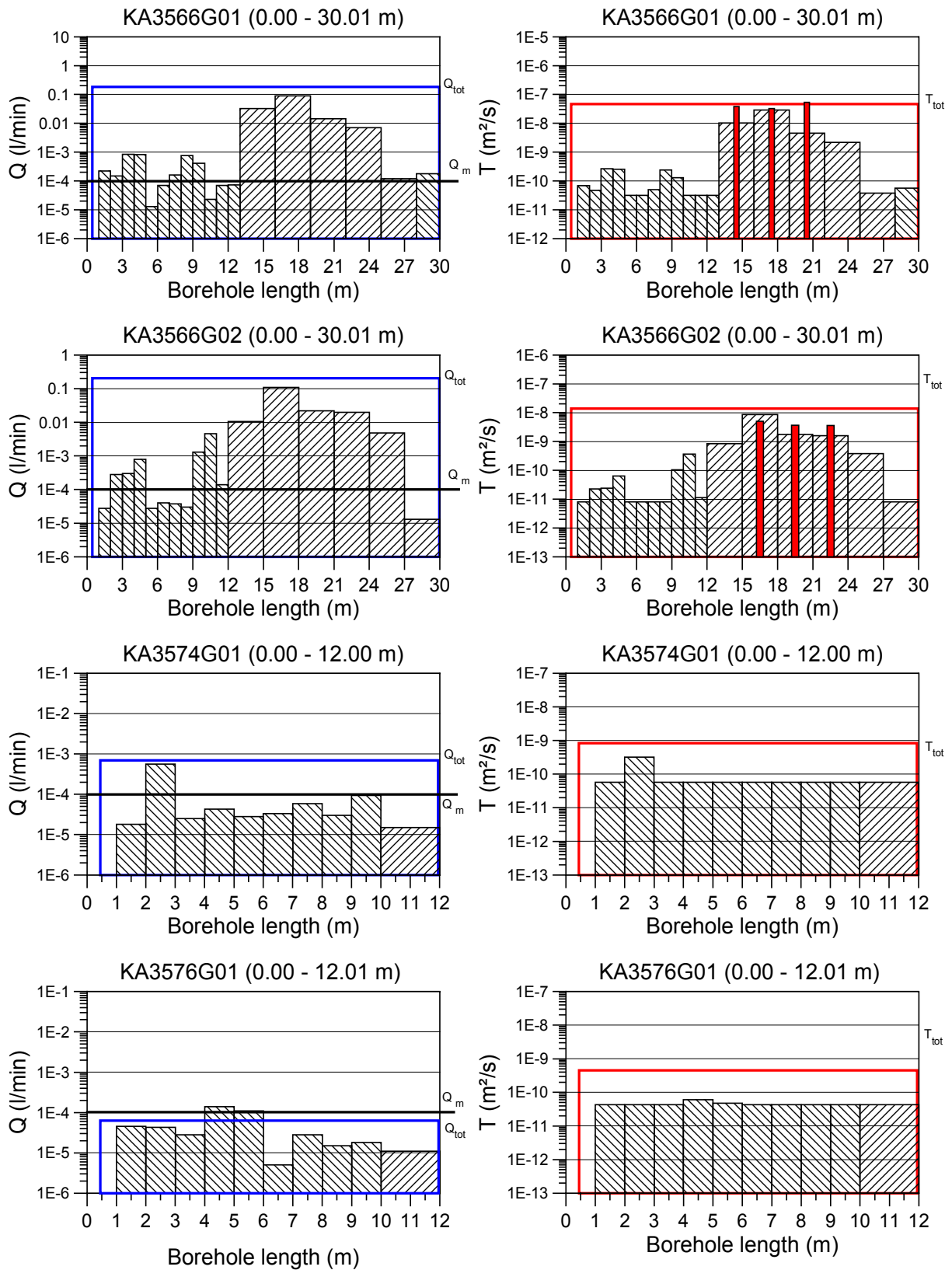


Figure 6-9 The results from flowlogging in KA3566G01, KA3566G02, KA3574G01 and KA3576G01. The red bars in the transmissivity diagrams indicate single section PBTs.

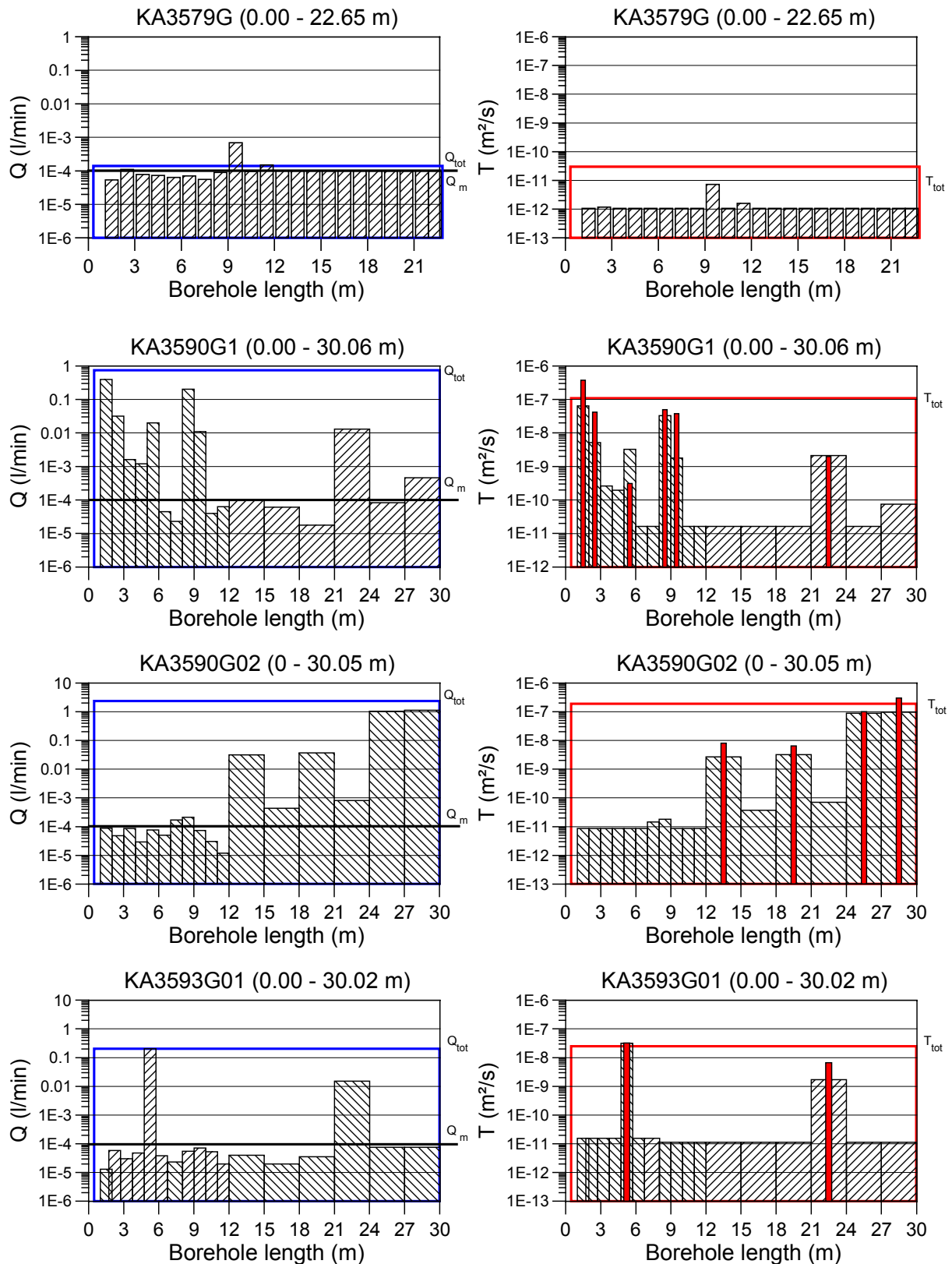


Figure 6-10 The results from flowlogging in KA3579G, KA3590G01, KA3590G02 and KA3593G (extended). The red bars in the transmissivity diagrams indicate single section PBTs.

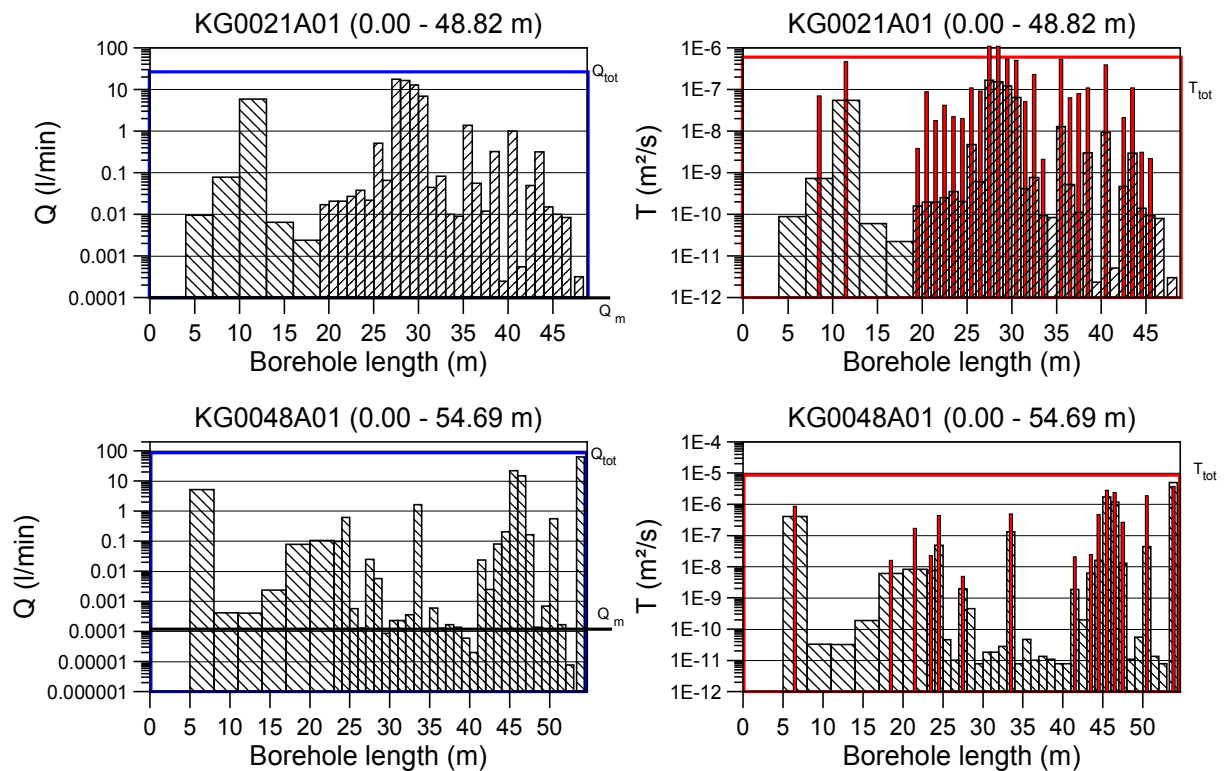


Figure 6-11 The results from flowlogging in KG0021A01 and KG0048A01. The red bars in the transmissivity diagrams indicate single section PBTs.

The flow logging produced 93 sections to be tested as a pressure build-up test. These tests are indicated in the diagrams above and described in Section 7.3.

6.4 Interference test campaign 1 after drilling campaign 3

No specific flow logging was done during the interference test campaign 1.

6.5 Interference test campaign 2 after drilling campaign 3

No specific flow logging was done during the interference test campaign 2.

6.6 Lead-through holes from G-tunnel to A-tunnel

During drilling a number of uptakes with measured increase of water-inflow were observed corresponding to possible water-bearing features. The inflow intervals are detailed in Table 6-1.

Table 6-1 Uptake with increasing inflow during drilling of the lead-through boreholes.

Borehole	Uptake (Borehole length, m)	Increase of inflow (L/min)	Flow of the entire borehole according to the drilling records (L/min)
KG0023A01	14.38 – 15.77	0.4	
KG0023A01	24.42 – 27.78	0.3	0.7
KG0027A01	8.05 – 9.92	7.2	
KG0027A01	41.57 – 44.52	1.8	9.0
KG0033A01	7.93 – 10.73	1.6	
KG0033A01	34.65 – 36.57	0.4	
KG0033A01	42.65 – 43.62	0.4	2.4

6.7 Flow logging with UCM tool

The core boreholes KA3510A, KA3539G, KA3542G01, KA3542G02, KA3548A01, KA3554G01, KA3554G02, KA3557G, KA3563G, KA3566G01, KA3566G02, KA3573A, KA3579G, KA3590G01, KA3590G02, KA3593G and KA3600F have been flow logged with a UCM probe developed by SKB (Almén and Zellman ,1991). The objectives of the UCM logging was to determine the flow along the core bore holes on order to detect anomalous in flowing and out flowing sections. The following parameters have been measured:

- Flow
- Fluid resistivity
- Temperature

The results of the UCM logging are detailed in Forsmark and Rhén (1999b) and shown in appendix.

6.8 Tunnel measurements

During the period, December 1999 to April 2000 measurement of inflow rates to the prototype repository tunnel was made in two campaigns, the first one in November - December 1999 and the second one in March - April 2000.

The result of the inflow measurements using weirs 1997 (Patél et al, 1997), 1999 and 2000 to the prototype repository tunnel is shown in Table 6-2. Do notice that the weir sections are not identical 1997 and 1999/2000. Therefore, they cannot be compared directly.

Table 6-2 Result of inflow measurements to prototype repository tunnel.

Weir sections 1997 (m)	Q 1997 (L/min)	Weir sections 1999 & 2000 (m)	Q 1999-12-01 (L/min)	Q 2000-03-30 (L/min)
3527 – 3533	0.20	-	-	-
3533 – 3539	1.17	-	-	-
3539 – 3545	0.12	-	-	-
3545 – 3551	0.03	-	-	-
3551 – 3557	0.02	-	-	-
3557 – 3562	0.05	-	-	-
3562 – 3568	0.10	3546 – 3552	0.001	0.006
3568 – 3575	0.05	3552 - 3570	0.100	0.110
3575 – 3581	1.56	3570 - 3576	0.000	0.000
3581 – 3587	1.61	3576 - 3582	2.000	1.320
3587 – 3593	0.29	3582 - 3588	1.490	1.820
3593 – 3600	0.93	3588 - 3600	1.120	1.080
SUM (3527 – 3600)	6.13	SUM (3546 – 3600)	4.711	4.336

The measurement sections are not exactly the same and it is therefore not possible to be certain about the flow rate changes during the passed time. However, the flow rate to section 3545 – 3600 and 3546 – 3600 are approximately the same during 1997 and 1999/2000.

Comparing the individual sections 3545 to 3600 indicates that possibly all sections, but 3576 – 3582 and 3582 – 3588 m have slowly decreasing flow rates. In sections 3576 – 3582 and 3582 – 3588 m, the flow rate changes rather much between the measurements, possibly due to changes of the flow rates from the flowing features.

The flow rates shown in the table above is graphically shown in Figure 6-12.

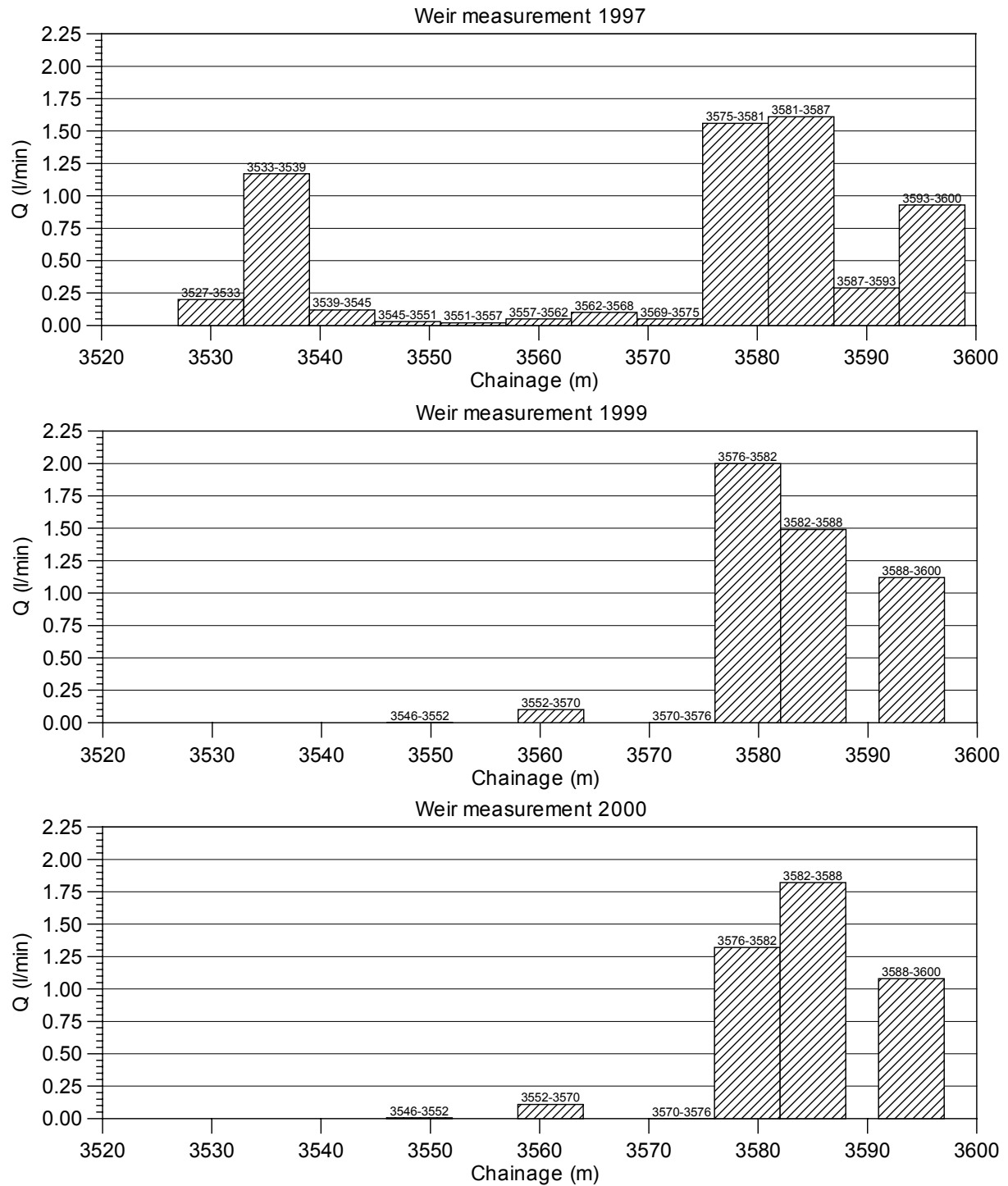


Figure 6-12 Weir measurements 1997, 1999 and 2000.

6.9 Deposition boreholes

6.9.1 Mapping and feature leakage measurements

Mapping of water-bearing features was made in January 2000. Estimations of inleakage rates from single features mapped as water-bearing and located on the hole walls were done during a measurement campaign in March/April 2000 (Forsmark et al, 2001a). In Table 6-3 the results of the detailed feature measurements are presented. In Figure 6-13 to 6-18 the mapping and position of feature inleakage measurements are shown.

Table 6-3 Inleakage measurements of features in deposition holes, see Figures 6-13 to 6-18.

Mapped feature	Q (l/min)
DA3587G01:1	1.11E-4
DA3587G01:2	1.04E-5
DA3587G01:3	0
DA3587G01:4	3.61E-5
SUM	1.58E-4
DA3581G01:1	1.67E-4
SUM	1.67E-4
DA3575G01: No feature observed	-
DA3569G01:1	0
DA3569G01:2	5.10E-5
DA3569G01:3	0
DA3569G01:4	1.38E-6
SUM	5.24E-5
DA3551G01:1	2.84E-5
DA3551G01:2	2.59E-5
DA3551G01:3	3.49E-5
DA3551G01:4	8.63E-6
DA3551G01:5	1.94E-5

Mapped feature	Q (l/min)
DA3551G01:6	1.05E-5
DA3551G01:7	1.12E-4
DA3551G01:8	1.19E-4
DA3551G01:9	0
SUM	3.59E-4
DA3545G01:1	5.45E-6
DA3545G01:2	4.16E-5
DA3545G01:3	2.17E-4
DA3545G01:4	3.85E-5
DA3545G01:5	0
DA3545G01:6	2.03E-5
DA3545G01:7	2.24E-4
DA3545G01:8	3.96E-6
DA3545G01:9	3.22E-5
DA3545G01:10	1.16E-5
SUM	5.95E-4

The measurements were made by applying plastic bags on the rock surface in order to collect water from a mapped wet feature (fracture). Once a day during approximately a period of 1 month the collected volume was measured.

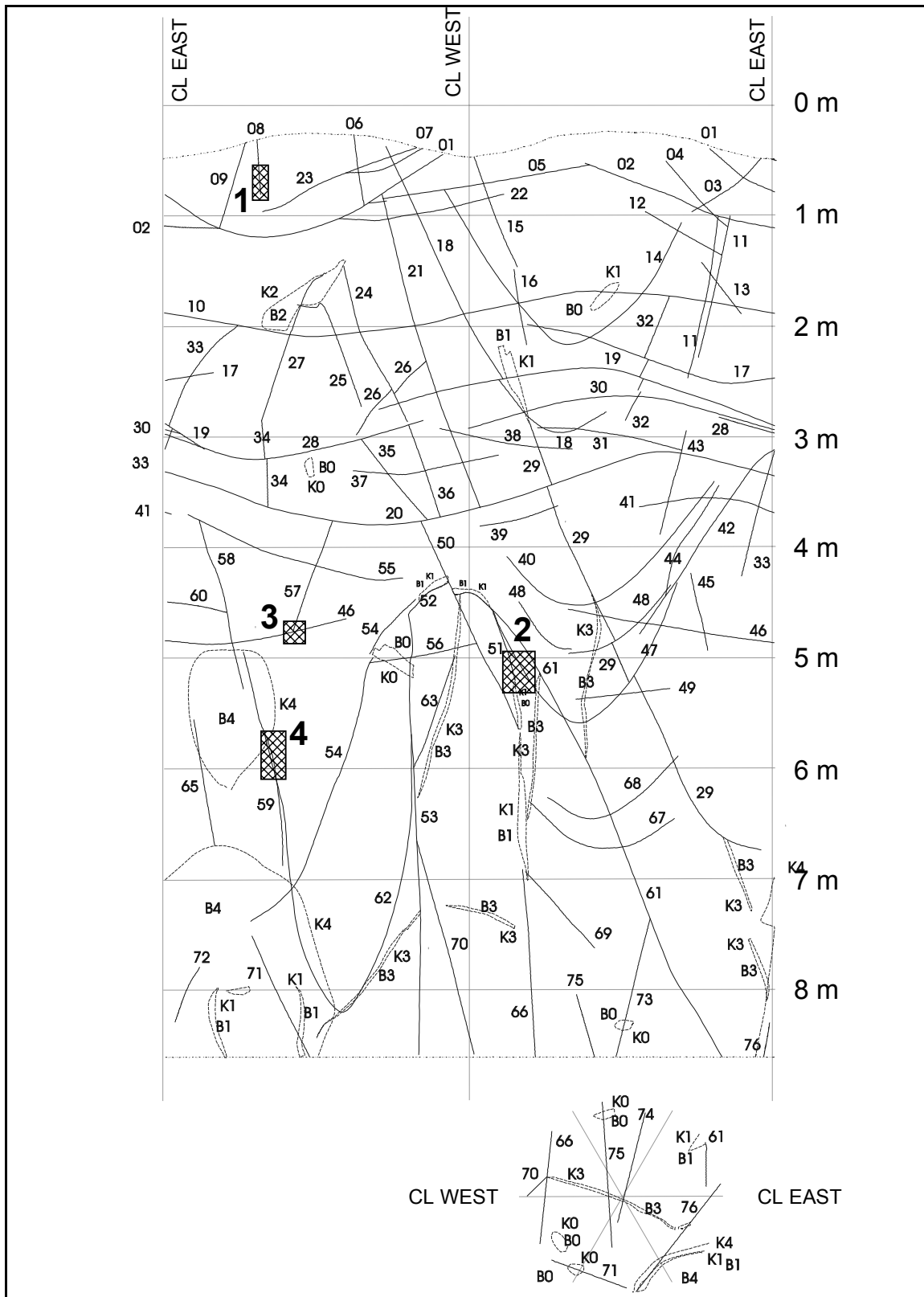


Figure 6-13 Deposition hole mapping in DA3587G01. Mapped water bearing features are marked with shaded areas.

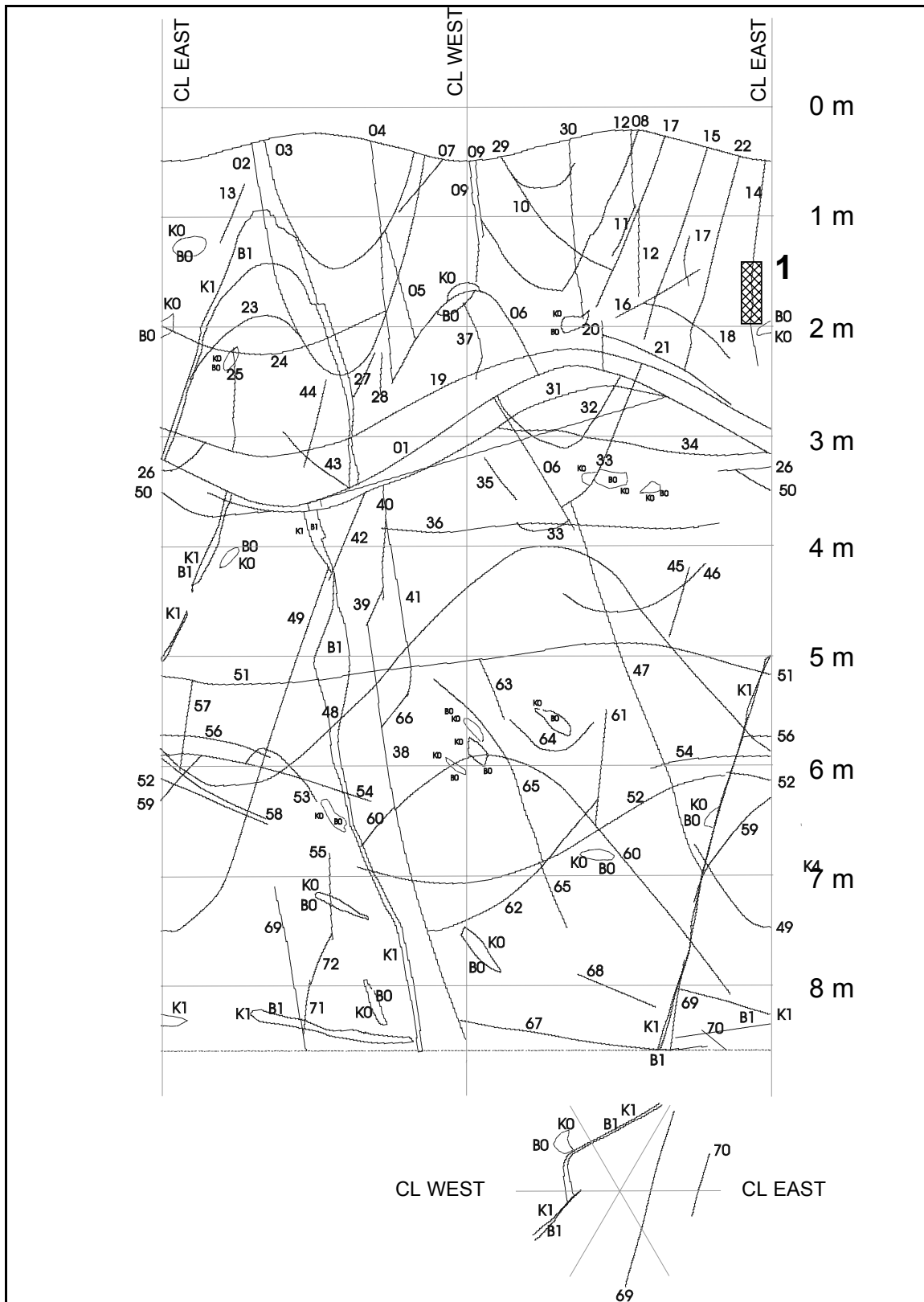


Figure 6-14 Deposition hole mapping in DA3581G01. Mapped water bearing features are marked with shaded areas.

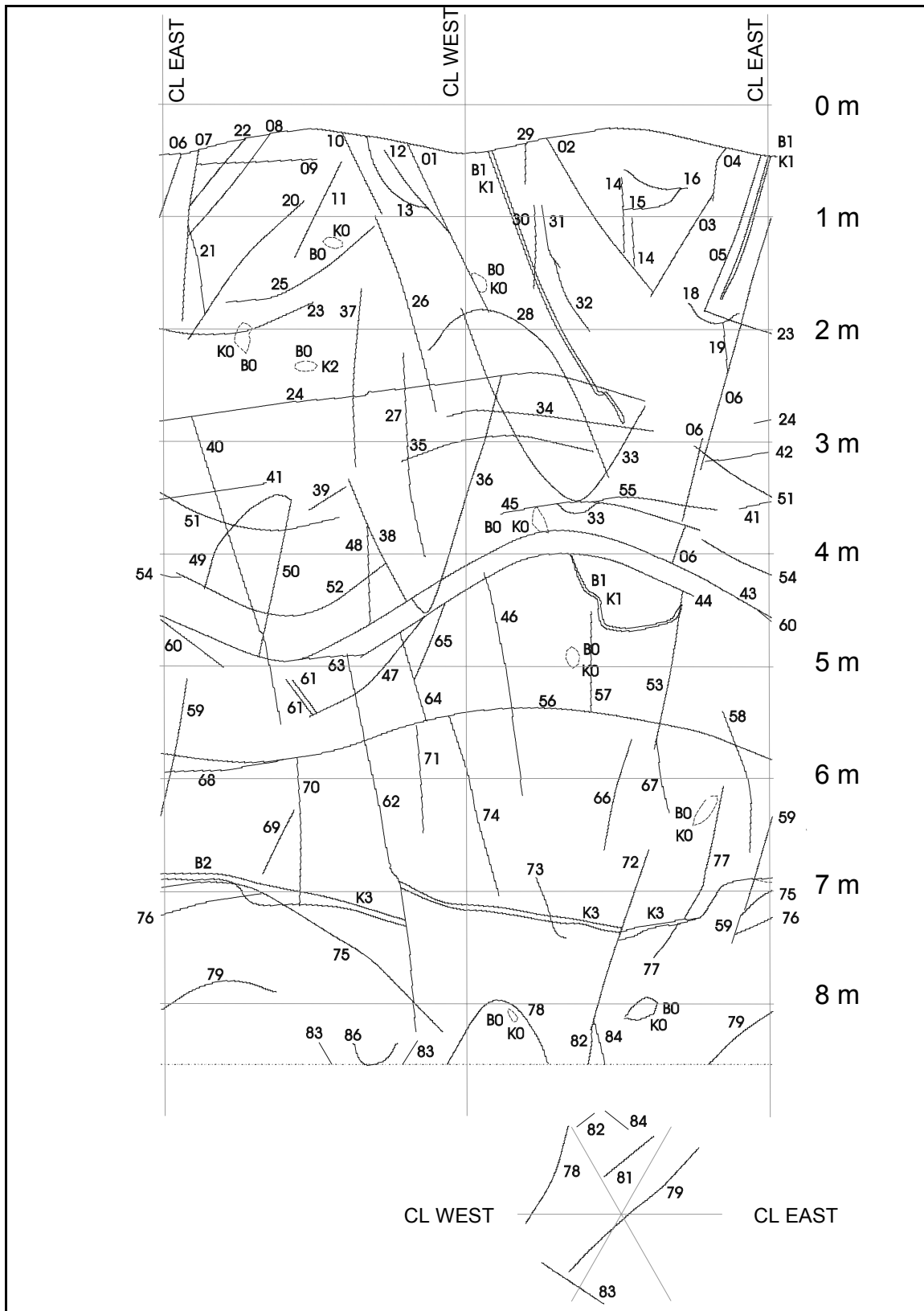


Figure 6-15 Deposition hole mapping in DA3575G01. No water bearing features was observed.

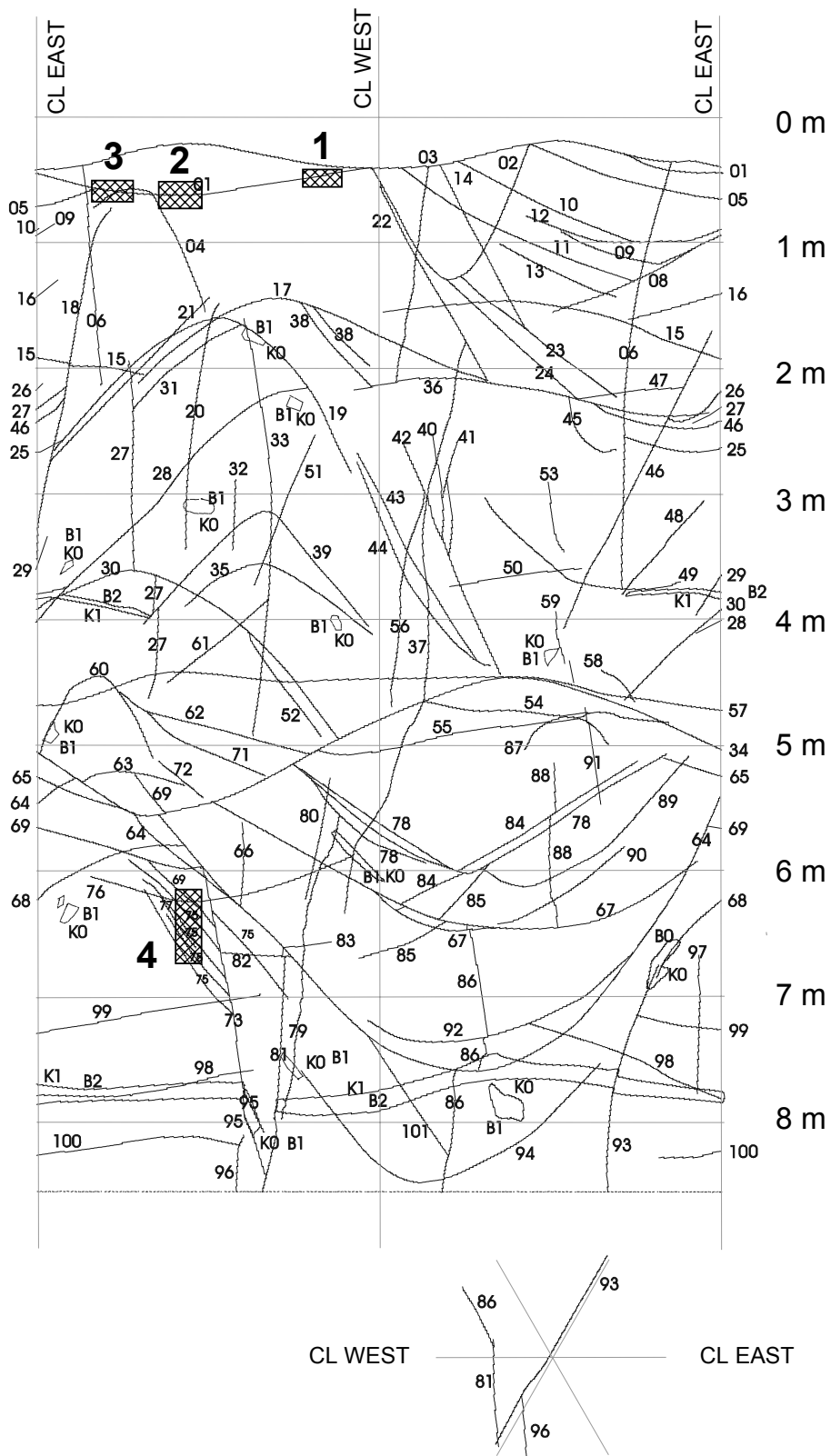


Figure 6-16 Deposition hole mapping in DA3569G01. Water bearing features are marked with shaded areas.

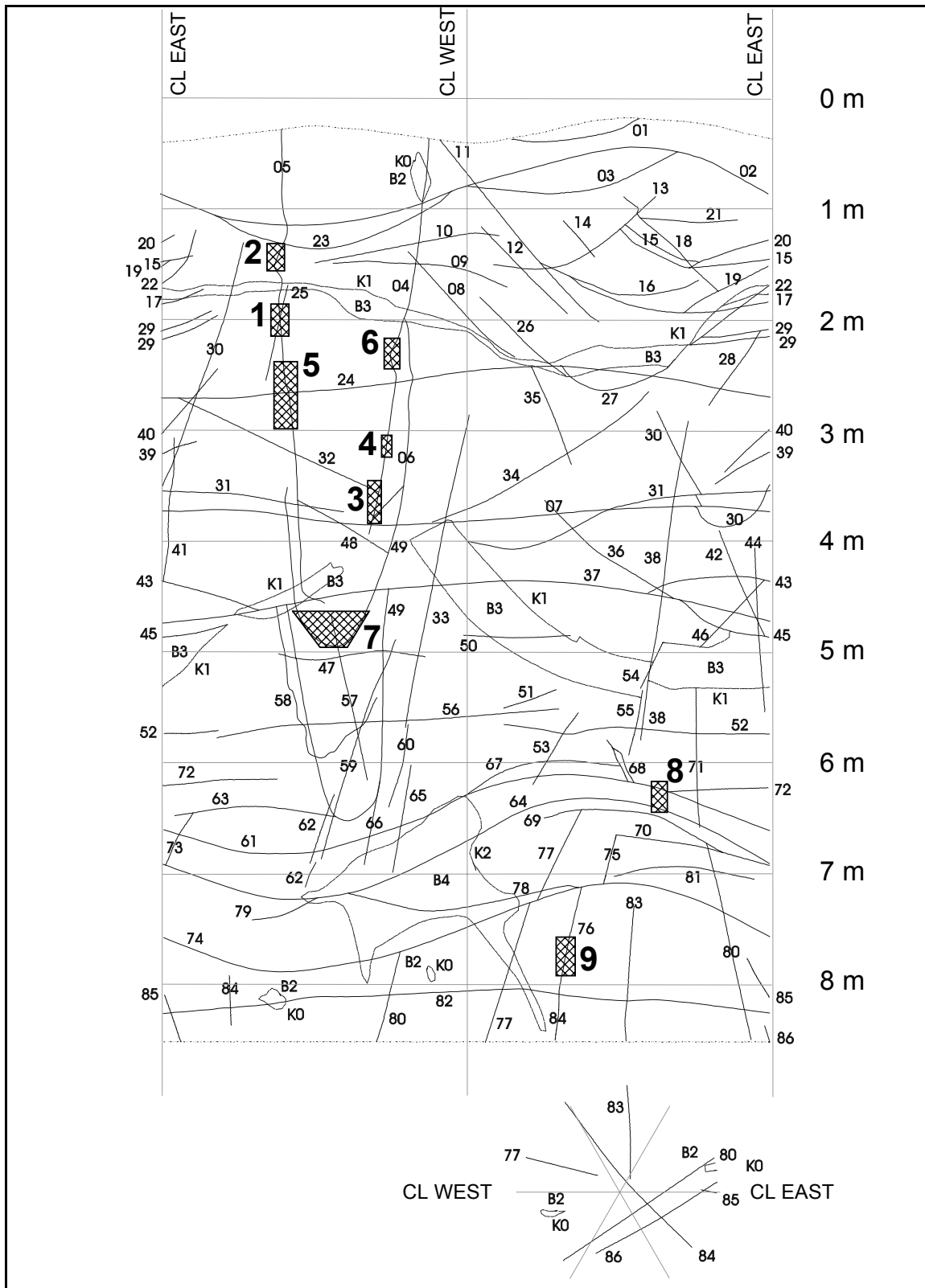


Figure 6-17 Deposition hole mapping in DA3551G01. Water bearing features are marked with shaded areas.

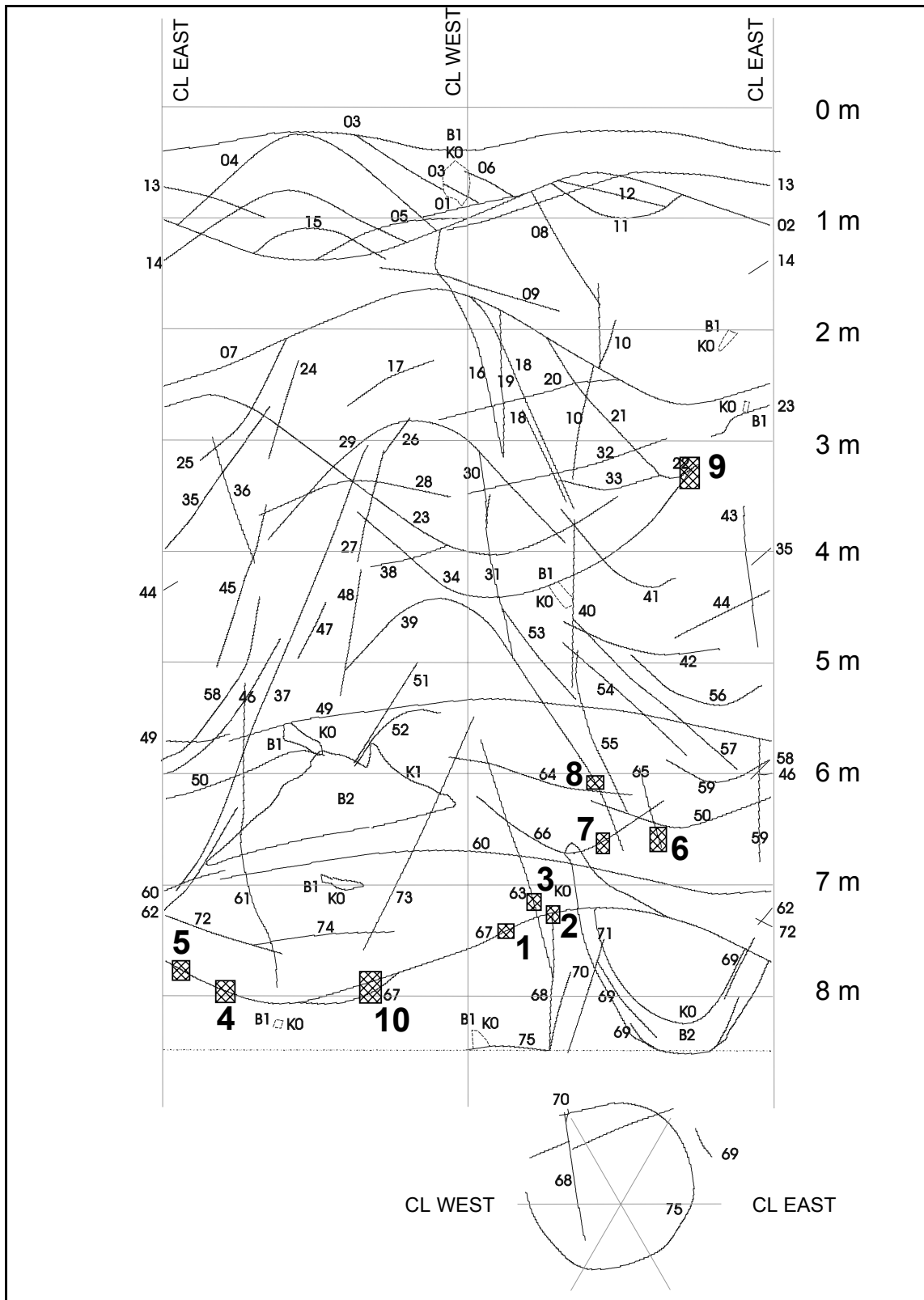


Figure 6-18 Deposition hole mapping in DA3545G01. Water bearing features are marked with shaded areas.

6.9.2 Total inflow to deposition holes

In Table 6-4, the result of the whole borehole inflow measurements in the deposition boreholes is shown.

Table 6-4 Result of inflow measurements to deposition boreholes. (Figures in bold are considered as the most representative flowrates).

Borehole	Q 1999-12-08 – 1999-12-13 (L/min)	Q 2000-03-28 – 2000-03-31 (L/min)	Q June / July 2000 (L/min)
DA3587G01	0.08000	0.07870	N/A
DA3581G01	0.00160	0.00220	0.00220*
DA3575G01	0.00280	0.00310	0.00410**
DA3569G01	0.00072	0	0.00472**
DA3551G01	0.00270	0.00155	0.00160***
DA3545G01	0.00610	0.00270	0.00740***
SUM	0.09392	0.08825	N/A

*Estimated from diaper measurements

**Measurements made 2000-06-21 to 2000-06-24

***Measurements made 2000-07-13 to 2000-07-26

There is probably some minor leakage from the tunnel floor included in the figures in Table 6-4 in all boreholes except to DA3575G01. The last two measurements in DA3551G01 are considered representative as leaking water from the tunnel floor was sealed off. Sealing was also made in DA3545G01 after the first measurement and the measurement made in March 2000 is considered the most representative. Possibly, there are new leakages from the tunnel floor during the measurement in June/July 2000.

6.9.3 Diaper measurements

In order to get an idea of the variations of inleakage to a borehole, measurements using ordinary diapers applied to the borehole walls of DA3581G01 were made during the summer of 2000 and DA3575G01 during February 2001. The measurement technique is illustrated in Figure 6-19 to 6-20. As can be seen in these figures the density of measurements was a bit higher in DA3575G01. In Figures 6-21 to 6-24, the results are shown graphically. A few measurements sections were excluded because there was some leakage from the tunnel floor. These vertical sections are blank in Figures 6-21 to 6-24.

The inleakage rates were transformed into hydraulic conductivity (K) using Thiems formula and the result is shown in Figures 6-22 and 6-24. The K-values should be seen as possible magnitudes as the estimation is based on parameters that are considered uncertain. Details of the flow measurements are found in Forsmark et al (2001a,b)

The higher inflow spots below the flowing fracture in DA3581G01, see Figure 6-21, probably reflect the water coming from that fracture. A statistical analysis of the estimated hydraulic conductivity (K) produces a geometric mean of $1.9 \cdot 10^{-13}$ m/s with a standard deviation of 0.64 for $\text{Log}_{10}(K)$.

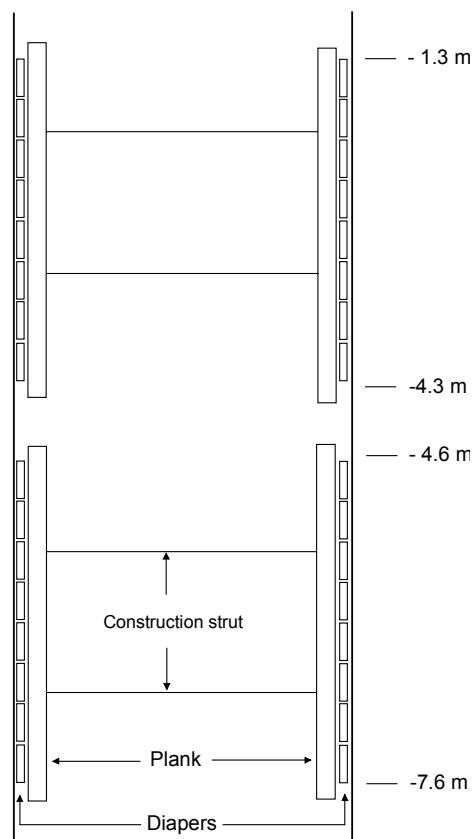


Figure 6-19 Diaper measurement arrangement in DA3581G01.

The detailed flow measurement in DA3575G01 indicated an inleakage rate to the hole to be $3 \cdot 10^{-3}$ L/min for the whole deposition hole. A statistical analysis of the estimated hydraulic conductivity (K) produces a geometric mean of $3.3 \cdot 10^{-13}$ m/s with a standard deviation of 0.67 for Log_{10} (K).



Figure 6-20 Diaphragm measurement arrangement in DA3581G01 (left) and DA3575G01 (right).

DA3581G01 - INFLOW MEASUREMENTS USING DIAPERS

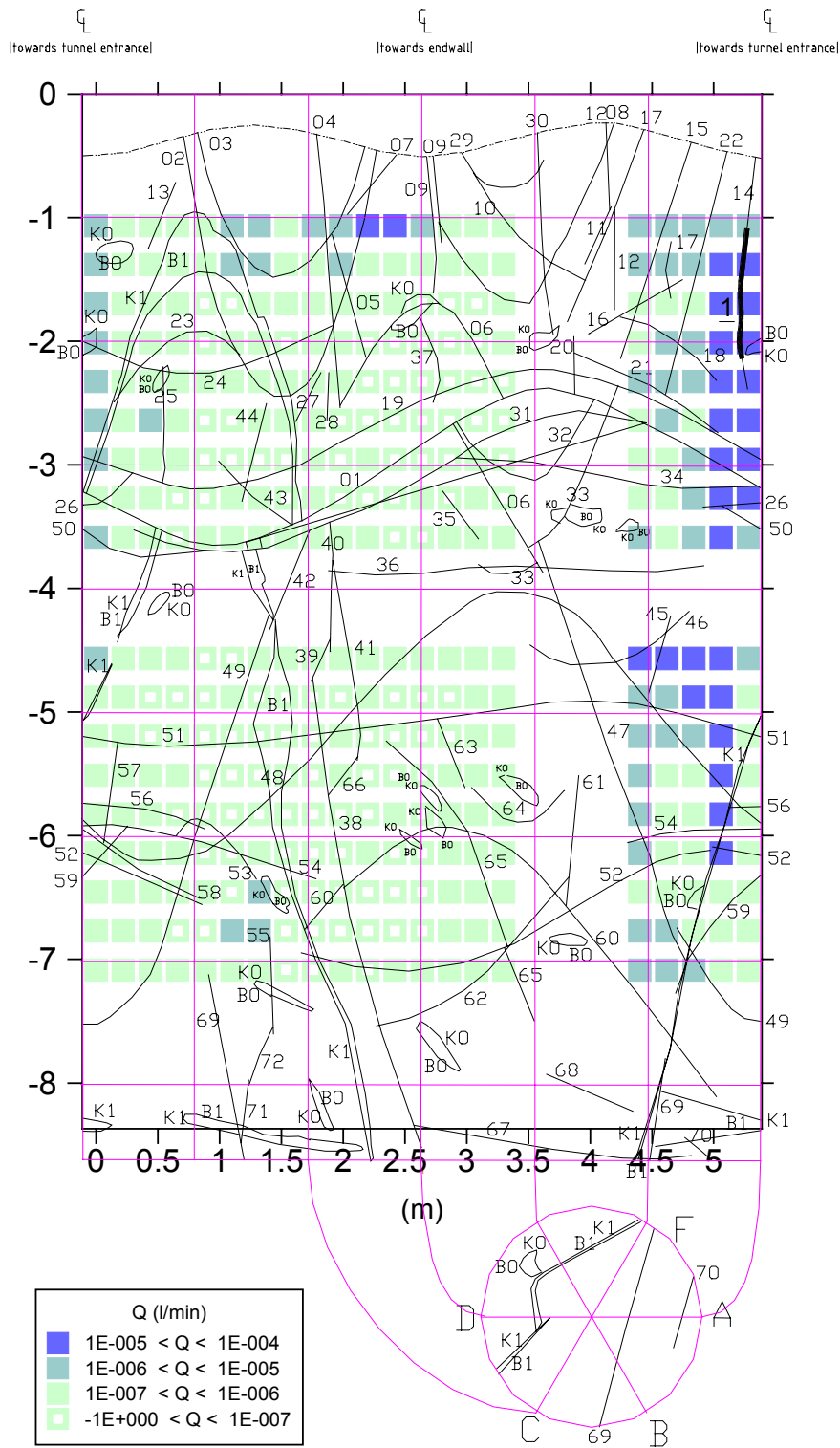


Figure 6-21 Inflow measurements in DA3581G01 using diapers. Flowing fracture shown as thick line in the upper right part of the figure.

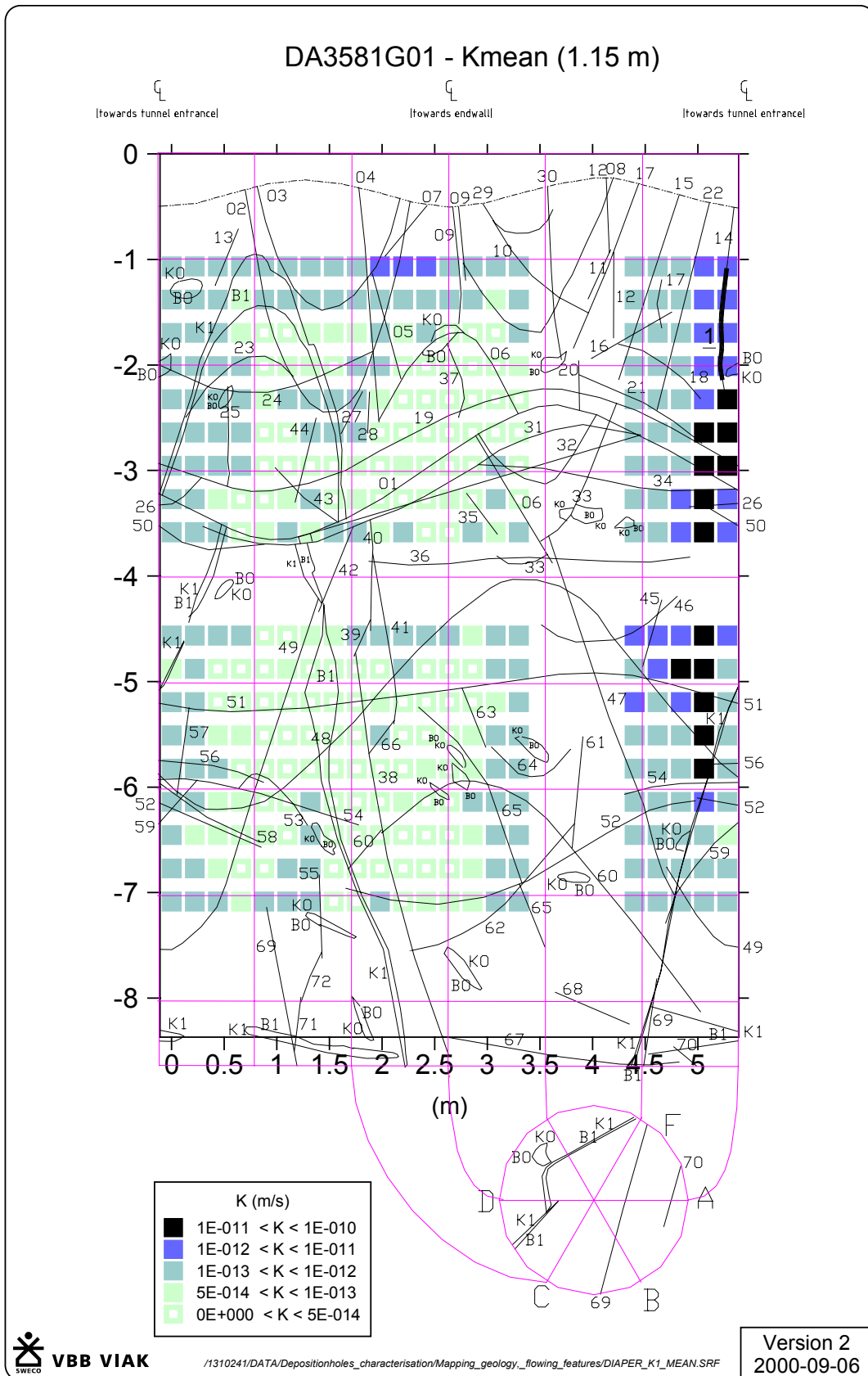


Figure 6-22 Hydraulic conductivity of DA3581G01 as estimated from diaper measurements

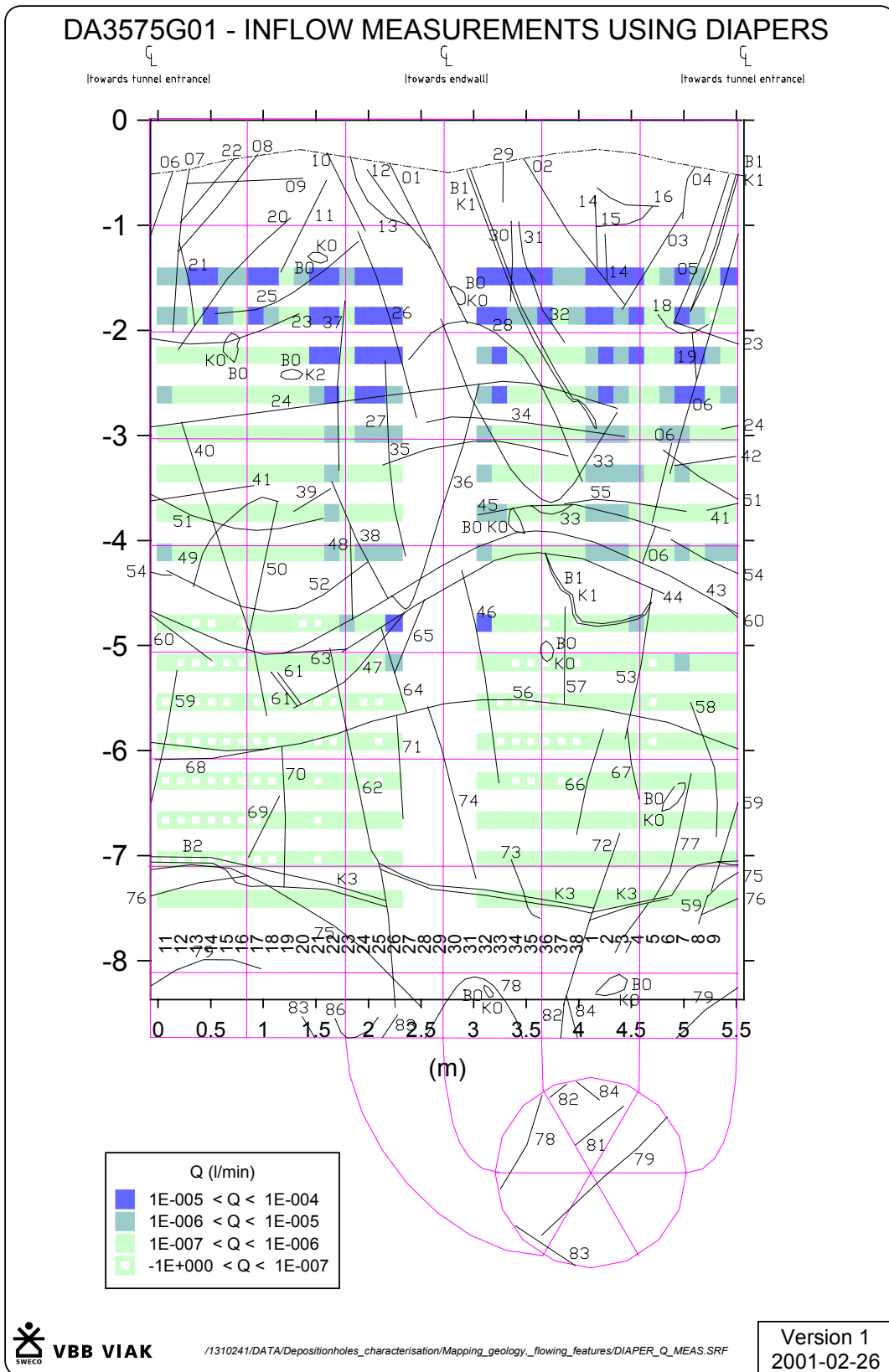


Figure 6-23 Inflow measurements in DA3575G01 using diapers. Flowing fracture shown as thick line in the upper right part of the figure.

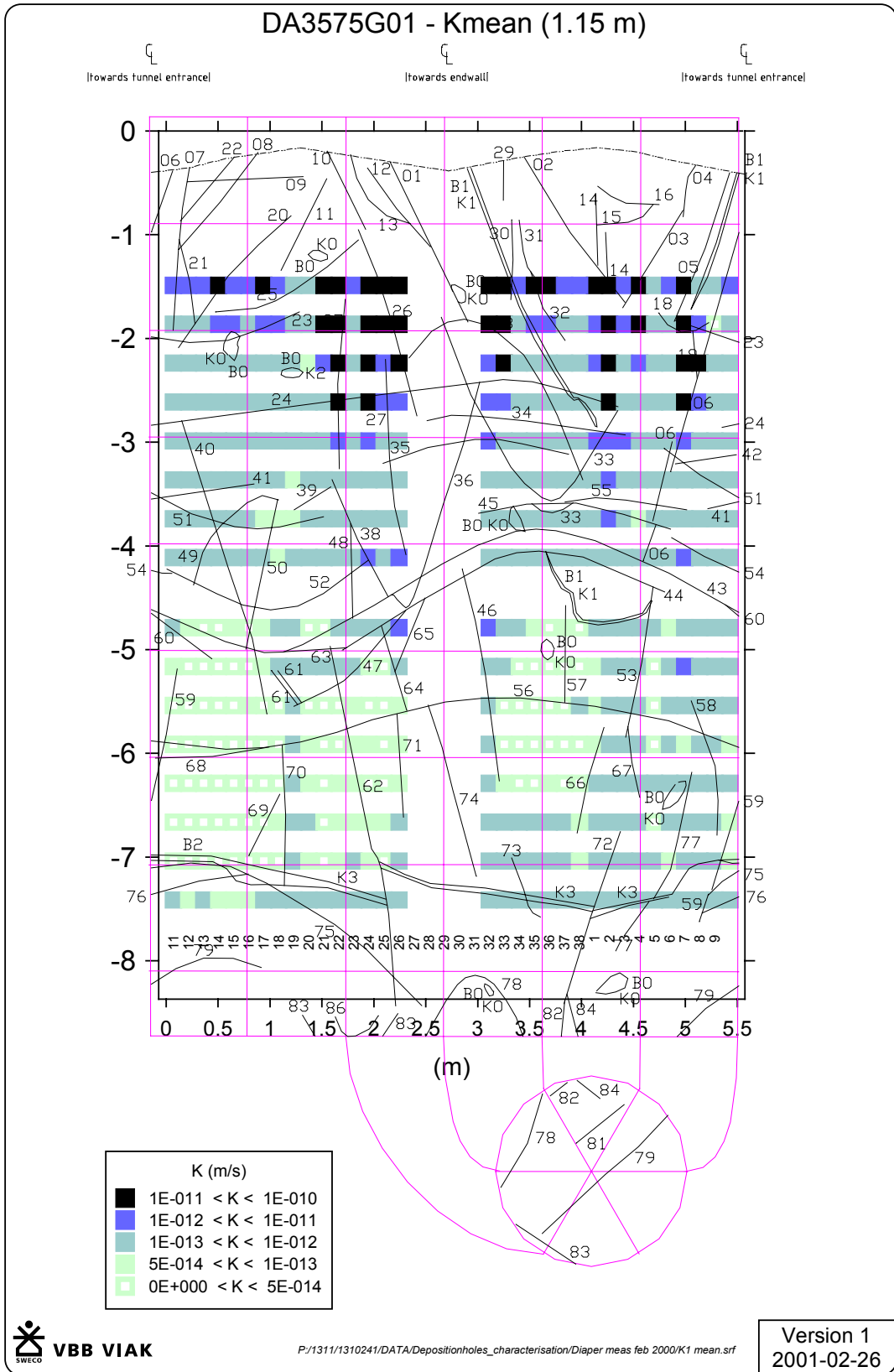


Figure 6-24 Hydraulic conductivity of DA3575G01 as estimated from diaper measurements

As can be noticed in the figures above the inflow is localised to the parts of the bore hole, which earlier has been mapped as an area with water-bearing features. But still inflow exist in a more diffuse pattern in large parts of the borehole walls, even if those parts have not and could not be mapped as water-bearing parts.

6.10 Groundwater leakage into G-, I- and J-tunnel

The intention when constructing the tunnel system was to drain water from tunnel G and J+ to weir MF0061G, while water from tunnel A, J and I should be drained to weir MA3426G, see Figure 6-25. At this moment (Autumn 2001) there are uncertainties of the flow rate and how much water from tunnel G flows to MF0061G and to MA3426G. This should be clarified. However, the measured flow rates at weirs MF0061G, MA3426G and the measured flows into the Prototype tunnel reported in Section 6.8 as well as the records of the excavation of tunnels G, I and J have been used to estimate the inflow to the different tunnel parts. See Forsmark et al (2001b) for details.

In Table 6-5, the flow rates from the discussion above are summarized. It is to be observed that the figures are approximate and should be regarded as uncertain. In Figure 6-25, the estimated inflow rates are visualized.

Three new tunnel sections (G, J+, I+) of 74 meters length created an increase of approximately 6 - 10 L/min or 0.08 – 0.14 L/min and meter tunnel.

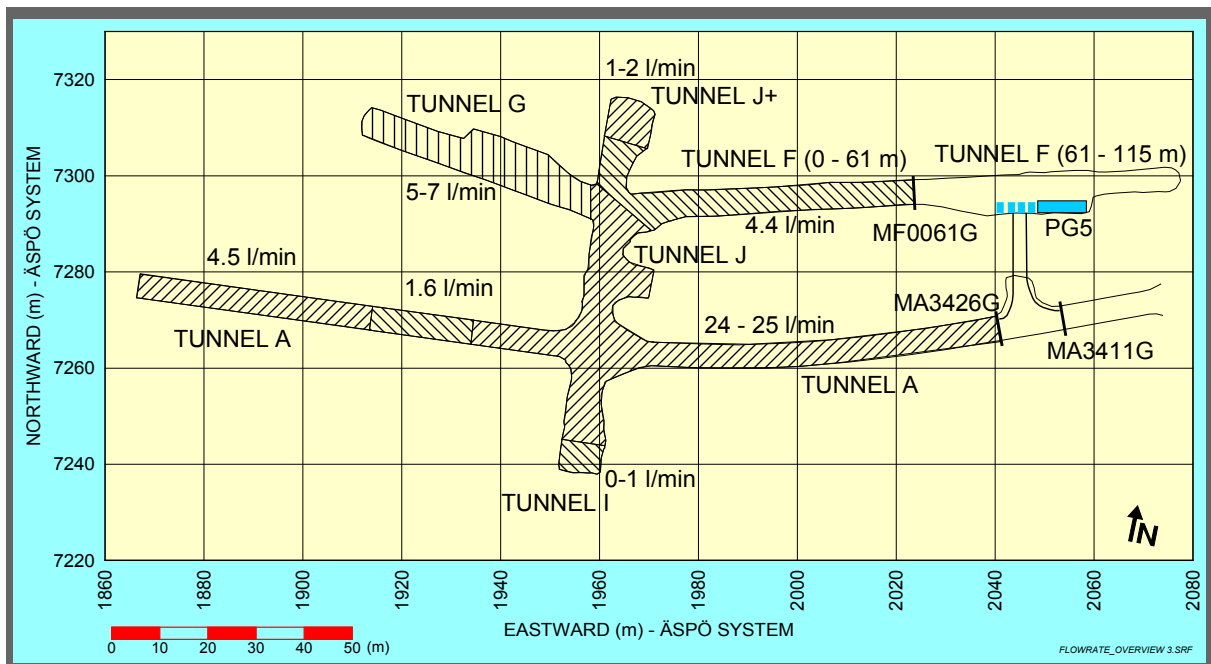


Figure 6-25 Estimated flowrates of tunnel segments

Table 6-5 Summary of flows into different tunnel sections.

Tunnel ID	Tunnel secup (m)	Tunnel secdown (m)	Meas. period	Weir	Flow rate L/min	Flow rate per m tunnel (l/(min·m))	Comments
A	3527	3600	1997	Temporary weirs	6.13	0.084	
A	3546	3600	1999-2000	Temporary weirs	4.50	0.083	
F J+	61 0	115 10.6	1995	-	6	0.11	
F J+	0 0	61 10.6	1996-07	MF0061G	4.40 (1)	0.061	Some flow from J+
F J+	0 0	61 22.6	1996-12	MF0061G	6.20 (2)	0.074	Flow from J+ prob. 1.8 L/min
J (J+)	40 (10.6)	52 (22.6)	1996-12	MF0061G	1-2 (3)	0.08 – 0.16	Estimated from measurements (2) – (1)
F J+ G	0 0 0	61 22.6 52	1999	MF0061G	7.9 (4)	-	Probably only parts of the flow from tunnel G.
A I J	3426 0 0	3600 15 26	1996-08	MA3426G	31.2 (5)	0.14	
A I J G	3426 0 0 0	3600 25 26 52	1999	MA3426G	37.6 (6)	(0.13)	Flow rate per m tunnel, not entirely correct as some water from tunnel G probably goes to MF0061G.
I	15	25	1999	MA3426G	0-1 (7)	0 – 0.1	
G	0	52	1999	MF0016G MF3426G	5-7	0.10 – 0.13	Estimated from measurements (6)-(5)-(7)+(4)-(2)-(3)

7 HYDRAULIC TESTS OF BORE HOLE SECTIONS

7.1 Drilling campaign 1

The 10 pilot holes were all pressure build-up tested. In those bore holes where radial flow occurred a Jacob semi-logarithmic evaluation of the transmissivity were made. In the remaining six bore holes the transmissivity have been estimated from the specific capacity. The following relationship have been used Rhén et al (1997).

$$\text{Log}_{10} T = 1.75 + 1.13 \cdot \text{Log}_{10} (Q/s) \quad (7-1)$$

Equation (7-1) is based on tests with test section lengths of 3 - 25 m. In one of the boreholes, a zero flow was reported (KA3557G). The pressure in this borehole was very low and could probably not generate a flow upward through the packer system. The transmissivity of the borehole section is most probably low. The boreholes are almost vertical and packer system ends some decimetres below the tunnel floor. Therefore a flow rate of $1 \cdot 10^{-7}$ L/min was used for this bore hole in the transmissivity estimation, see Table 7-1.

Table 7-1 Evaluated and estimated hydrogeological parameters (s = pressure change, Q = flow rate, Spec_cap = Specific capacity, T(Spec_cap) = transmissivity calculated from eq. 7-1, T_eval = evaluated transmissivity where possible).

Borehole	Secup (m)	Seclow (m)	s (m)	Q (l/min)	Spec_cap (m ³ /m·s)	Log ₁₀ Spec cap (m ³ /m·s)	T(Spec cap) (m ² /s)	Log T Sc (m ² /s)	T eval (m ² /s)	Log T eval (m ² /s)	T tot (m ² /s)	Log T tot (m ² /s)
KA3539G	0.70	8.04	225.94	0.128	9.4E-09	-8.02	4.8E-08	-7.32	4.8E-08	-7.32	4.8E-08	-7.32
KA3545G	0.70	8.04	232.66	0.013	9.3E-10	-9.03	3.5E-09	-8.45	2.1E-09	-8.68	2.1E-09	-8.68
KA3551G	0.70	8.04	82.16	2.20E-05	4.5E-12	-11.35	8.4E-12	-11.08	-		8.4E-12	-11.08
KA3557G	0.70	8.04	0.32	1.00E-07	5.2E-12	-11.28	1.0E-11	-11.00	-		1.0E-11	-11.00
KA3563G	0.70	8.04	5.15	0.007	2.3E-08	-7.64	1.3E-07	-6.89	1.1E-08	-7.96	1.1E-08	-7.96
KA3569G	0.70	8.04	44.14	3.80E-04	1.4E-10	-9.84	4.2E-10	-9.37	-		4.2E-10	-9.37
KA3575G	0.70	8.04	2.02	8.40E-06	6.9E-11	-10.16	1.9E-10	-9.73	-		1.9E-10	-9.73
KA3581G	0.70	8.04	4.69	1.30E-06	4.6E-12	-11.34	8.7E-12	-11.06	-		8.7E-12	-11.06
KA3587G	0.70	8.04	132.59	7.90E-05	9.9E-12	-11.00	2.1E-11	-10.68	-		2.1E-11	-10.68
KA3593G	0.70	8.04	219.43	0.265	2.0E-08	-7.70	1.1E-07	-6.95	3.2E-08	-7.49	3.2E-08	-7.49

Shadowed value = estimated value

As described earlier in Section 6.1, if the flow rate of the measurement section exceeded 10 mL/min a pressure build-up test of the section was made. The results are presented in Table 7-2. In one test, KA3539G (5.74-6.74 m), the pressure change was very low. This test was done after the test in section 6.74 - 8.04 m. The measured pressure change seems to be unreliable, if the results from the test in the entire bore hole is considered.

Table 7-2 Result from the part of bore hole pressure build-up tests (s = pressure change, Q = flow rate, Spec_cap = Specific capacity, T(Spec_cap) = transmissivity calculated from eq. 7-1, T_eval = evaluated transmissivity where possible). Shaded values : values are considered uncertain.

Borehole	Secup (m)	Seclow (m)	s (m)	Q (l/min)	Spec_cap (m ³ /m·s)	Log ₁₀ Spec cap (m ³ /m·s)	T(Spec cap) (m ² /s)	Log T Sc (m ² /s)	T eval (m ² /s)	Log T eval (m ² /s)	T tot (m ² /s)	Log T tot (m ² /s)
KA3539G	5.74	6.74	0.21	0.0825	6.5E-06	-5.18	7.8E-05	-4.11	-		-	
KA3539G	6.74	8.04	173.85	0.058	5.6E-09	-8.25	2.6E-08	-7.58	-		2.6E-08	-7.58
KA3545G	5.74	6.74	175.14	9.50E-03	9.0E-10	-9.04	3.4E-09	-8.47	-		3.4E-09	-8.47
KA3545G	6.74	8.04	170.96	1.00E-02	9.7E-10	-9.01	3.7E-09	-8.43	-		3.7E-09	-8.43
KA3593G	4.74	5.74	179.16	0.204	1.9E-08	-7.72	1.1E-07	-6.98	3.2E-08	-7.49	3.2E-08	-7.49

Shadowed values = uncertain values

7.2 Drilling campaign 2

The 10 holes were all pressure build-up tested. In those bore holes where radial flow occurred a Jacob semi-logarithmic evaluation of the transmissivity were made. In the remaining nine bore holes the transmissivity have been estimated from the specific capacity, as described in Section 7.1. The evaluated and estimated parameters are shown in Table 7-3.

Table 7-3 Evaluated and estimated hydrogeological parameters (s = pressure change, Q = flow rate, Spec_cap = Specific capacity, T(Spec_cap) = transmissivity calculated from eq. 5-1, T_eval = evaluated transmissivity where possible).

Borehole	Secup (m)	Seclow (m)	s (m)	Q (l/min)	Spec_cap (m ³ /m-s)	Log ₁₀ Spec cap (m ³ /m-s)	T(Spec cap) (m ² /s)	Log T Sc (m ² /s)	T eval (m ² /s)	Log T eval (m ² /s)	T tot (m ² /s)	Log T tot (m ² /s)
KA3544G	0.50	12.00	268.40	0.0595	3.7E-09	-8.43	1.7E-08	-7.78	-		1.7E-08	-7.78
KA3546G	0.50	12.00	202.03	0.0085	7.0E-10	-9.15	2.5E-09	-8.59	-		2.5E-09	-8.59
KA3548G	0.50	12.00	214.72	0.0125	9.7E-10	-9.01	3.7E-09	-8.43	-		3.7E-09	-8.43
KA3550G	0.50	12.00	225.71	0.0175	1.3E-09	-8.89	5.1E-09	-8.29	-		5.1E-09	-8.29
KA3552G	0.50	12.00	106.42	0.009	1.4E-09	-8.85	5.6E-09	-8.25	-		5.6E-09	-8.25
KA3572G	0.50	12.00	29.11	5.20E-04	3.0E-10	-9.53	9.7E-10	-9.01	-		9.7E-10	-9.01
KA3578G	0.50	12.00	5.31	7.60E-05	2.4E-10	-9.62	7.5E-10	-9.12	-		7.5E-10	-9.12
KA3584G	0.50	12.00	4.78	1.10E-05	3.8E-11	-10.42	9.5E-11	-10.02	-		9.5E-11	-10.02
KA3586G	0.50	8.00	25.34	1.00E-05	6.6E-12	-11.18	1.3E-11	-10.89	-		1.3E-11	-10.89
KA3588G	0.50	8.00	206.81	0.023	1.9E-09	-8.73	7.6E-09	-8.12	8.4E-09	-8.08	8.4E-09	-8.08

As described earlier in Section 6.1, if the flow rate of the measurement section exceeded 10 mL/min a pressure build-up test of the section was done. The results are presented in Table 7-4.

Table 7-4 Result from the part of bore hole pressure build-up tests (s = pressure change, Q = flow rate, Spec_cap = Specific capacity, T(Spec_cap) = transmissivity calculated from eq. 7-1, T_eval = evaluated transmissivity where possible).

Borehole	Secup (m)	Seclow (m)	s (m)	Q (l/min)	Spec_cap (m ³ /m-s)	Log ₁₀ Spec cap (m ³ /m-s)	T(Spec cap) (m ² /s)	Log T Sc (m ² /s)	T eval (m ² /s)	Log T eval (m ² /s)	T tot (m ² /s)	Log T tot (m ² /s)
KA3544G	9.70	10.70	267.93	0.048	3.0E-09	-8.52	1.3E-08	-7.88	-		1.3E-08	-7.88
KA3548G	5.70	6.70	213.98	0.011	8.6E-10	-9.07	3.2E-09	-8.50	-		3.2E-09	-8.50
KA3550G	5.70	6.70	225.08	0.015	1.1E-09	-8.95	4.3E-09	-8.37	-		4.3E-09	-8.37
KA3552G	4.70	5.70	105.98	0.0078	1.2E-09	-8.91	4.8E-09	-8.32	-		4.8E-09	-8.32
KA3588G	4.70	5.70	206.31	0.0206	1.7E-09	-8.78	6.8E-09	-8.17	1.0E-08	-8.00	1.0E-08	-8.00

7.3 Drilling campaign 3

The 18 boreholes were all pressure build-up tested. In those bore holes where radial flow occurred a Jacob semi-logarithmic evaluation of the transmissivity were made. In the remaining eight bore holes the transmissivity has been estimated from the specific capacity. The relationship above (7-1) and the following relationship have been used Rhén et al (1997).

$$25 - 50 \text{ m: } \text{Log}_{10} T = 1.17 + 1.13 \cdot \text{Log}_{10} (Q/s) \quad (7-2)$$

Equations (7-1) and (7-2) are based on tests with test section lengths of 3 - 25 and 25 - 50 m respectively. The evaluated and estimated parameters are shown in Table 7-5

Table 7-5 Evaluated and estimated hydrogeological parameters (s = pressure change, Q = flow rate, Spec_cap = Specific capacity, T(Spec_cap) = transmissivity calculated from equations 7-1 or 7-2, T_eval = evaluated transmissivity where possible).

Borehole	Secup (m)	Seclow (m)	s (m)	Q (l/min)	Spec_cap (m ³ /m·s)	Log ₁₀ Spec cap (m ³ /m·s)	T(Spec cap) (m ² /s)	Log T Sc (m ² /s)	T eval (m ² /s)	Log T eval (m ² /s)	T tot (m ² /s)	Log T tot (m ² /s)
KA3539G	0.39	30.01	291.16	5.02	2.9E-07	-6.54	6.0E-07	-6.22	-		6.0E-07	-6.22
KA3542G01	0.39	30.04	372.41	3.91	1.7E-07	-6.76	3.4E-07	-6.47	3.2E-07	-6.49	3.2E-07	-6.49
KA3542G02	0.39	30.01	304.80	4.41	2.4E-07	-6.62	4.9E-07	-6.31	-		4.9E-07	-6.31
KA3548A01	2.56	30.00	348.82	7.20	3.4E-07	-6.46	7.4E-07	-6.13	1.0E-06	-6.00	1.0E-06	-6.00
KA3554G01	0.39	30.01	382.98	8.24	3.6E-07	-6.45	7.7E-07	-6.11	2.3E-06	-5.64	2.3E-06	-5.64
KA3554G02	0.39	30.01	299.70	0.602	3.3E-08	-7.48	5.3E-08	-7.28	1.3E-07	-6.89	1.3E-07	-6.89
KA3557G	0.39	30.04	67.26	0.00014	3.5E-11	-10.46	2.2E-11	-10.65	-		2.2E-11	-10.65
KA3563G	0.39	30	9.31	0.009	1.6E-08	-7.79	2.3E-08	-7.64	5.8E-09	-8.24	5.8E-09	-8.24
KA3566G01	0.39	30.01	229.58	0.184	1.3E-08	-7.87	1.9E-08	-7.73	4.7E-08	-7.33	4.7E-08	-7.33
KA3566G02	0.39	30.01	332.67	0.203	1.0E-08	-7.99	1.4E-08	-7.86	-		1.4E-08	-7.86
KA3574G01	0.39	12	44.26	0.00069	2.6E-10	-9.59	8.3E-10	-9.08	-		8.3E-10	-9.08
KA3576G01	0.39	12.01	6.88	0.000063	1.5E-10	-9.82	4.5E-10	-9.34	-		4.5E-10	-9.34
KA3579G	0.50	22.65	168.71	0.00014	1.4E-11	-10.86	3.0E-11	-10.52	-		3.0E-11	-10.52
KA3590G01	0.39	30.06	212.36	0.75	5.9E-08	-7.23	1.0E-07	-7.00	1.1E-07	-6.96	1.1E-07	-6.96
KA3590G02	0.39	30.05	375.64	2.35	1.0E-07	-6.98	1.9E-07	-6.72	-		1.9E-07	-6.72
KA3593G	0.39	30.02	232.82	0.023	1.6E-09	-8.78	1.8E-09	-8.76	2.5E-08	-7.60	2.5E-08	-7.60
KG0021A01	0.00	48.82	314.75	26.8	1.4E-06	-5.85	3.6E-06	-5.44	6.0E-07	-6.22	6.0E-07	-6.22
KG0048A01	0.00	54.69	381.30	87.2	3.8E-06	-5.42	1.1E-05	-4.95	8.6E-06	-5.07	8.6E-06	-5.07

If the flow rate of the measurement section exceeded 10 mL/min a pressure build-up test of the section was made. The results are presented in Table 7-6 and 7-7.

Table 7-6 Result from the part of bore hole pressure build-up tests (s = pressure change, Q = flow rate, Spec_cap = Specific capacity, T(Spec_cap) = transmissivity calculated from eq. 7-1, T_eval = evaluated transmissivity where possible).

Borehole	Secup (m)	Seclow (m)	s (m)	Q (l/min)	Spec_cap (m ³ /m·s)	T(Spec_cap) (m ² /s)	T_eval (m ² /s)	T_tot (m ² /s)
KA3539G	11	12	164.00	0.088	8.9E-09	4.5E-08	4.5E-08	4.5E-08
KA3539G	12	15	160.50	0.035	3.6E-09	1.6E-08	7.6E-08	7.6E-08
KA3539G	15	18	267.00	4.062	2.5E-07	2.0E-06	2.5E-06	2.5E-06
KA3539G	18	21	112.00	0.046	6.8E-09	3.3E-08		3.3E-08
KA3539G	21	24	112.00	0.026	3.9E-09	1.8E-08	8.7E-08	8.7E-08
KA3542G01	12	15	272.50	0.044	2.7E-09	1.2E-08		1.2E-08
KA3542G01	15	18	320.00	0.538	2.8E-08	1.6E-07	2.0E-07	2.0E-07
KA3542G01	18	21	341.00	1.238	6.1E-08	3.9E-07	3.0E-07	3.0E-07
KA3542G01	21	24	322.50	1.19	6.1E-08	4.0E-07		4.0E-07
KA3542G01	27	30	372.50	0.407	1.8E-08	1.0E-07		1.0E-07
KA3542G02	3	4	192.00	0.125	1.1E-08	5.6E-08	8.4E-08	8.4E-08
KA3542G02	4	5	286.00	0.121	7.1E-09	3.5E-08	9.8E-08	9.8E-08
KA3542G02	5	6	285.00	2.535	1.5E-07	1.1E-06	4.9E-07	4.9E-07
KA3542G02	10	11	271.00	0.056	3.4E-09	1.5E-08	1.5E-08	1.5E-08
KA3542G02	11	12	258.00	0.76	4.9E-08	3.1E-07	1.9E-07	1.9E-07
KA3542G02	12	15	230.00	0.021	1.5E-09	6.1E-09		6.1E-09
KA3542G02	15	18	242.00	0.077	5.3E-09	2.5E-08		2.5E-08
KA3542G02	18	21	214.00	0.035	2.7E-09	1.2E-08		1.2E-08
KA3542G02	24	27	215.00	0.0145	1.1E-09	4.3E-09		4.3E-09
KA3548A01	5	6	280.00	0.126	7.5E-09	3.7E-08		3.7E-08
KA3548A01	6	7	113.00	0.027	4.0E-09	1.8E-08		1.8E-08
KA3548A01	9	10	368.00	1.910	8.7E-08	5.9E-07	1.1E-07	1.1E-07
KA3548A01	12	15	366.00	0.053	2.4E-09	1.0E-08	7.5E-08	7.5E-08
KA3548A01	15	18	367.00	0.212	9.6E-09	4.9E-08	7.8E-07	7.8E-07
KA3548A01	18	21	377.00	3.400	1.5E-07	1.1E-06	2.5E-06	2.5E-06
KA3548A01	21	24	375.00	0.116	5.2E-09	2.4E-08	1.7E-07	1.7E-07
KA3548A01	24	27	382.00	0.017	7.4E-10	2.7E-09		2.7E-09
KA3554G01	18	21	352.00	0.14	6.6E-09	3.2E-08	2.2E-07	2.2E-07
KA3554G01	21	24	370.00	1.53	6.9E-08	4.5E-07	1.3E-06	1.3E-06
KA3554G01	24	27	382.00	6.8	3.0E-07	2.4E-06	2.7E-06	2.7E-06
KA3554G01	27	30	368.00	0.011	5.0E-10	1.7E-09		1.7E-09
KA3554G02	8	9	344.00	0.044	2.1E-09	8.9E-09		8.9E-09
KA3554G02	11	12	317.00	0.128	6.7E-09	3.3E-08	2.9E-07	2.9E-07
KA3554G02	12	15	315.00	0.334	1.8E-08	9.8E-08	3.8E-07	3.8E-07
KA3554G02	15	18	310.00	0.0243	1.3E-09	5.1E-09	4.9E-08	4.9E-08
KA3554G02	27	30		0.0344				
KA3566G01	13	16	186.00	0.0322	2.9E-09	1.3E-08	3.8E-08	3.8E-08
KA3566G01	16	19	222.00	0.091	6.8E-09	3.3E-08		3.3E-08
KA3566G01	19	22	244.00	0.0146	1.0E-09	3.8E-09	5.3E-08	5.3E-08
KA3566G02	15	18	354.00	0.109	5.1E-09	2.4E-08	5.0E-09	5.0E-09
KA3566G02	18	21	355.00	0.021	9.9E-10	3.7E-09		3.7E-09
KA3566G02	21	24	330.00	0.019	9.6E-10	3.6E-09		3.6E-09

No data for s was possible to evaluate for KA3554G02.

Table 7-7 Result from the part of bore hole pressure build-up tests (s = pressure change, Q = flow rate, Spec_cap = Specific capacity, T(Spec_cap) = transmissivity calculated from eq. 7-1, T_eval = evaluated transmissivity where possible).

Borehole	Secup (m)	Seclow (m)	s (m)	Q (l/min)	Spec_cap (m ³ /m·s)	T(Spec_cap) (m ² /s)	T_eval (m ² /s)	T_tot (m ² /s)
KA3590G01	1	2	174.00	0.394	3.8E-08	2.3E-07	3.8E-07	3.8E-07
KA3590G01	2	3	75.00	0.032	7.1E-09	3.5E-08	4.2E-08	4.2E-08
KA3590G01	5	6	305.00	0.002	1.1E-10	3.1E-10		3.1E-10
KA3590G01	8	9	343.00	0.2	9.7E-09	5.0E-08		5.0E-08
KA3590G01	9	10	338.00	0.011	5.4E-10	1.9E-09	3.8E-08	3.8E-08
KA3590G01	21	24	361.00	0.012	5.5E-10	2.0E-09		2.0E-09
KA3590G02	12	15	126.00	0.0315	4.2E-09	1.9E-08	8.0E-09	8.0E-09
KA3590G02	18	21	210.00	0.037	2.9E-09	1.3E-08	6.4E-09	6.4E-09
KA3590G02	24	27	305.00	1.035	5.7E-08	3.6E-07	9.9E-08	9.9E-08
KA3590G02	27	30.05	279.00	1.11	6.6E-08	4.3E-07	3.0E-07	3.0E-07
KA3593G	21	24	151.00	0.0148	1.6E-09	6.6E-09		6.6E-09
KG0021A01	7	10	320.76	0.078	4.1E-09	1.8E-08	7.1E-08	7.1E-08
KG0021A01	10	13	294.36	5.78	3.3E-07	2.6E-06	4.7E-07	4.7E-07
KG0021A01	19	20	278.04	0.017	1.0E-09	3.9E-09		3.9E-09
KG0021A01	20	21	276.70	0.0205	1.2E-09	4.8E-09	8.8E-08	8.8E-08
KG0021A01	21	22	263.50	0.0212	1.3E-09	5.3E-09	1.8E-08	1.8E-08
KG0021A01	22	23	280.24	0.0272	1.6E-09	6.5E-09	4.2E-08	4.2E-08
KG0021A01	23	24	279.64	0.038	2.3E-09	9.6E-09	2.2E-08	2.2E-08
KG0021A01	24	25	256.69	0.0215	1.4E-09	5.5E-09	2.0E-08	2.0E-08
KG0021A01	26	27	276.93	0.066	4.0E-09	1.8E-08	9.2E-08	9.2E-08
KG0021A01	27	28	293.01	17.9	1.0E-06	9.5E-06	1.1E-06	1.1E-06
KG0021A01	28	29	297.19	16.41	9.2E-07	8.5E-06	1.1E-06	1.1E-06
KG0021A01	29	30	270.36	12.94	8.0E-07	7.2E-06	5.4E-07	5.4E-07
KG0021A01	30	31	266.42	6.88	4.3E-07	3.6E-06	5.0E-07	5.0E-07
KG0021A01	31	32	272.65	0.044	2.7E-09	1.2E-08	5.1E-08	5.1E-08
KG0021A01	32	33	277.96	0.0815	4.9E-09	2.3E-08	2.3E-07	2.3E-07
KG0021A01	33	34	277.53	0.01	6.0E-10	2.1E-09		2.1E-09
KG0021A01	35	36	290.84	1.38	7.9E-08	5.3E-07		5.3E-07
KG0021A01	36	37	255.93	0.056	3.6E-09	1.6E-08	6.3E-08	6.3E-08
KG0021A01	37	38	287.69	0.012	7.0E-10	2.5E-09	8.0E-08	8.0E-08
KG0021A01	38	39	279.66	0.32	1.9E-08	1.1E-07		1.1E-07
KG0021A01	40	41	280.20	1.0104	6.0E-08	3.9E-07		3.9E-07
KG0021A01	42	43	248.87	0.05	3.3E-09	1.5E-08	2.1E-08	2.1E-08
KG0021A01	43	44	258.24	0.315	2.0E-08	1.1E-07		1.1E-07
KG0021A01	44	45	290.70	0.0146	8.4E-10	3.1E-09		3.1E-09
KG0021A01	45	46	299.59	0.0112	6.2E-10	2.2E-09		2.2E-09
KG0048A01	5	8	287.63	5.2	3.0E-07	2.4E-06	8.7E-07	8.7E-07
KG0048A01	17	20	370.23	0.078	3.5E-09	1.6E-08		1.6E-08
KG0048A01	20	23	371.03	0.106	4.8E-09	2.2E-08	1.7E-07	1.7E-07
KG0048A01	23	24	324.15	0.097	5.0E-09	2.3E-08		2.3E-08
KG0048A01	24	25	372.28	0.624	2.8E-08	1.6E-07	4.4E-07	4.4E-07
KG0048A01	27	28	328.25	0.0253	1.3E-09	5.0E-09		5.0E-09
KG0048A01	33	34	368.25	1.67	7.6E-08	5.0E-07		5.0E-07
KG0048A01	41	42	354.84	0.024	1.1E-09	4.4E-09	2.1E-08	2.1E-08
KG0048A01	43	44	302.58	0.08	4.4E-09	2.0E-08	2.5E-08	2.5E-08
KG0048A01	44	45	334.52	0.204	1.0E-08	5.2E-08	4.7E-07	4.7E-07
KG0048A01	45	46	353.02	21.89	1.0E-06	9.7E-06	2.8E-06	2.8E-06
KG0048A01	46	47	342.12	15	7.3E-07	6.5E-06	2.4E-06	2.4E-06
KG0048A01	47	48	304.56	0.164	9.0E-09	4.5E-08	2.7E-07	2.7E-07
KG0048A01	50	51	282.47	0.561	3.3E-08	2.0E-07	1.9E-06	1.9E-06
KG0048A01	53	54.69	339.33	62.9	3.1E-06	3.3E-05	3.8E-06	3.8E-06

7.4 Interference test campaign 1 after drilling campaign 3

During the interference test campaign 1 after drilling campaign 3, five hole sections were used as test sections. One section was used twice. In Table 7-8, the evaluated parameters for the test sections are shown.

Table 7-8 Results from evaluation of test sections during interference test campaign 1 after drilling campaign 3.

Bore hole	Section m	Test no.	Q L/min	T m ² /s
KA3566G01:2	12.30-19.80	1:1	0.1155	$5.9 \cdot 10^{-8}$
KA3566G02:2	12.30-18.30	1:2	0.0845	$6.0 \cdot 10^{-8}$
KA3590G01:3	1.30-6.80	1:3	0.340	$1.3 \cdot 10^{-7}$
KA3590G01:2	7.80-16.30	1:4	0.398	$1.4 \cdot 10^{-7}$
KA3590G02:1	23.30-30.05	1:5	1.710	$1.5 \cdot 10^{-7}$
KA3590G01:3	1.30-6.80	1:6	0.330	$1.3 \cdot 10^{-7}$

7.5 Interference test campaign 2 after drilling campaign 3

During the interference test campaign 2 after drilling campaign 3, five hole sections were used as test sections. One section was used twice. In Table 7-8, the evaluated parameters for the test sections are shown.

Table 7-9 Results from evaluation of test sections during interference test campaign 2 after drilling campaign 3.

Bore hole	Section m	Test no.	Q L/min	T m ² /s
KG0048A01:1	49.00-54.69	2:7	2.41	$2.5 \cdot 10^{-6}$
KA3554G01:1	22.30-30.01	2:8	4.47	$1.7 \cdot 10^{-6}$
KA3554G02:2	10.30-21.30	2:9	0.482	$1.8 \cdot 10^{-7}$
KA3542G01:2	8.80-24.80	2:10	2.56	$(6.5 \cdot 10^{-6})$
KA3542G02:3	1.30-7.80	2:11	3.37	$6.1 \cdot 10^{-7}$
KA3539G:2	9.80-18.30	2:12	4.28	$5.3 \cdot 10^{-7}$
KG0021A01:1	42.50-48.82	2:13	0.38	$7.2 \cdot 10^{-7}$
KG0021A01:3	25.00-34.00	2:14	7.29	$7.3 \cdot 10^{-7}$

7.6 Injection tests

Thirty-nine injection tests were made twice, before and after the deposition holes were drilled (Forsmark and Rhén, 2000a, Forsmark et al, 2001b). The first test was performed with the UHT (Underground Hydraulic Test system) and the second with a more simply system.

In the first injection test campaign (Forsmark, Rhén, 2000a) lower measurement limit regarding the injection flow, $Q_p = 1 \cdot 10^{-4}$ L/min, prevailed. This in turn produced lower transmissivity values than was possible to evaluate in the second campaign.

In order to compare the results of the two test campaigns the 1999 test results have been recalculated using the 2001 measurement limit of the injection flow. In Table 7-10, the results of the two campaigns are shown in the same table. The measurement limit of the calculations is in both cases $Q_p = 4 \cdot 10^{-4}$ L/min.

Table 7-10 Comparison of the two test campaigns. Sections with measurement limits in italics and sections with measured value in bold. Fracture location within brackets is located outside the test section but close by.

Borehole	Secup	Seclow	Log ₁₀ T (m ² /s) 1999	Log ₁₀ T (m ² /s) 2001	Mapped open fractures in section (m)	Comments on changes (S=small or below meas. limit; R=Reliable)
KA3542G02	0.25	0.75	<i>2.3 · 10⁻¹⁰</i>	<i>1.7 · 10⁻¹⁰</i>	0.31, 0.58	S
	0.75	1.25	<i>2.2 · 10⁻¹⁰</i>	<i>1.7 · 10⁻¹⁰</i>	-	S
	1.25	1.75	3.0 · 10⁻¹⁰	3.4 · 10⁻¹⁰	(1.85)	S
KA3542G01	0.25	0.75	<i>1.0 · 10⁻¹⁰</i>	4.6 · 10⁻¹⁰	0.51, 0.63, 0.73, 0.75	R
	0.75	1.25	<i>9.4 · 10⁻¹¹</i>	<i>1.8 · 10⁻¹⁰</i>	0.75	S
	1.25	1.75	<i>9.0 · 10⁻¹¹</i>	<i>1.8 · 10⁻¹⁰</i>	-	S
KA3544G01	0.25	0.75	<i>6.9 · 10⁻¹¹</i>	<i>1.9 · 10⁻¹⁰</i>	-	S
	0.75	1.25	1.7 · 10⁻¹⁰	<i>1.9 · 10⁻¹⁰</i>	-	S
	1.25	1.75	<i>9.6 · 10⁻¹¹</i>	<i>2.1 · 10⁻¹⁰</i>	-	S
KA3546G01	0.25	0.75	<i>6.3 · 10⁻¹¹</i>	4.3 · 10⁻¹⁰	0.25, 0.28, 0.31	R
	0.75	1.25	6.2 · 10⁻¹⁰	<i>1.9 · 10⁻¹⁰</i>	0.96	R
	1.25	1.75	<i>8.4 · 10⁻¹¹</i>	<i>1.5 · 10⁻¹⁰</i>	-	S
KA3548G01	0.25	0.75	<i>9.7 · 10⁻¹¹</i>	<i>2.1 · 10⁻¹⁰</i>	-	S
	0.75	1.25	<i>5.0 · 10⁻¹¹</i>	<i>2.1 · 10⁻¹⁰</i>	1.03	S
	1.25	1.75	<i>9.6 · 10⁻¹¹</i>	<i>2.1 · 10⁻¹⁰</i>	-	S
KA3550G01	0.25	0.75	1.8 · 10⁻¹⁰	3.3 · 10⁻⁹	0.25	R
	0.75	1.25	<i>8.7 · 10⁻¹¹</i>	<i>1.8 · 10⁻¹⁰</i>	-	S
	1.25	1.75	<i>6.5 · 10⁻¹¹</i>	<i>1.9 · 10⁻¹⁰</i>	-	S
KA3552G01	0.25	0.75	<i>8.7 · 10⁻¹¹</i>	<i>1.8 · 10⁻¹⁰</i>	-	S
	0.75	1.25	<i>5.3 · 10⁻¹¹</i>	<i>1.8 · 10⁻¹⁰</i>	-	S
	1.25	1.75	<i>9.6 · 10⁻¹¹</i>	<i>1.8 · 10⁻¹⁰</i>	-	S
KA3554G02	0.25	0.75	3.9 · 10⁻¹⁰	<i>2.2 · 10⁻¹⁰</i>	0.50	R
	0.75	1.25	<i>9.6 · 10⁻¹¹</i>	<i>2.1 · 10⁻¹⁰</i>	-	S
	1.25	1.75	<i>8.3 · 10⁻¹¹</i>	<i>2.1 · 10⁻¹⁰</i>	-	S
KA3554G01	0.25	0.75	3.2 · 10⁻⁸	2.4 · 10⁻⁸	0.40, 0.42	R
	0.75	1.25	<i>7.5 · 10⁻¹¹</i>	<i>1.5 · 10⁻¹⁰</i>	0.93, 0.96	S
	1.25	1.75	<i>9.5 · 10⁻¹¹</i>	<i>1.4 · 10⁻¹⁰</i>	1.42, 1.55	S
KA3572G01	0.25	0.75	<i>9.9 · 10⁻¹¹</i>	<i>1.8 · 10⁻¹⁰</i>	-	S
	0.75	1.25	5.8 · 10⁻¹¹	<i>1.8 · 10⁻¹⁰</i>	0.91, 0.99	S
	1.25	1.75	<i>9.8 · 10⁻¹¹</i>	<i>1.8 · 10⁻¹⁰</i>	1.30	S
KA3574G01	0.25	0.75	<i>9.2 · 10⁻¹¹</i>	<i>2.0 · 10⁻¹⁰</i>	-	S
	0.75	1.25	<i>9.6 · 10⁻¹¹</i>	<i>1.8 · 10⁻¹⁰</i>	1.02, 1.06	S
	1.25	1.75	<i>8.6 · 10⁻¹¹</i>	<i>1.8 · 10⁻¹⁰</i>	-	S
KA3576G01	0.25	0.75	<i>9.7 · 10⁻¹¹</i>	<i>1.9 · 10⁻¹⁰</i>	0.62	S
	0.75	1.25	<i>9.7 · 10⁻¹¹</i>	<i>1.8 · 10⁻¹⁰</i>	-	S
	1.25	1.75	<i>9.7 · 10⁻¹¹</i>	<i>1.8 · 10⁻¹⁰</i>	-	S
KA3578G01	0.25	0.75	<i>9.3 · 10⁻¹¹</i>	<i>1.8 · 10⁻¹⁰</i>	-	S
	0.75	1.25	1.4 · 10⁻¹⁰	<i>1.8 · 10⁻¹⁰</i>	-	S
	1.25	1.75	<i>9.6 · 10⁻¹¹</i>	<i>1.7 · 10⁻¹⁰</i>	1.72	S

The values of KA3550G01, 0.25 – 0.75 m differ rather much. An increased transmissivity is evaluated in 2001, $3.3 \cdot 10^{-9} \text{ m}^2/\text{s}$ versus $1.8 \cdot 10^{-10} \text{ m}^2/\text{s}$ in 1999. An explanation to this may be a fracture located at 0.25 m in the borehole that may have been activated due to the drilling of the deposition holes and seen during the second test campaign. It is to be observed that the hole is located very close to the deposition hole DA3551G01. Another reason may be the conductive part of the fracture happens to have a good connection to the deposition hole. In such a case, one may argue that due to the close distance to the boundary (deposition hole) the increase of the specific capacity may not be comparable to the value of 1999. In Forsmark et al (2001b) it was analysed and the conclusion, based on reasonable estimates of the storativity, was that the possible error due to the deposition hole is less or much less than 30%. The increase of transmissivity, in KA3546G01 and KA3550G01 is judged real and not an artifact of the boundary conditions.

When comparing the upper end transmissivities, of 2001, with the values of 1999 in KA3554G01, 0.25 – 0.75 m, the values are within the same order of magnitude, $2.4 \cdot 10^{-8} \text{ m}^2/\text{s}$ (2001) vs $3.2 \cdot 10^{-8} \text{ m}^2/\text{s}$ (1999). There are two fractures at 0.40 m and 0.42 m in this section of the borehole.

In order to study any link between the positions of the holes in relation to the deposition holes the tested boreholes were divided into three categories:

Category 1 (holes close to a deposition hole):

KA3544G01, KA3546G01, KA3550G01, KA3552G01, KA3574G01 and KA3576G01.

Category 2 (holes more distant to a deposition hole):

KA3548G01, KA3572G01 and KA3578G01

Category 3 (inclined holes; most distant to deposition hole):

KA3542G01, KA3542G02, KA3554G01 and KA3554G02

There are only a few tests sections that indicate more reliable changes of the transmissivity due to drilling of the deposition holes. These are indicated in Table 7-10 and plotted in Figures 7-1 and 7-2. No category 2 holes show reliable changes. All other sections indicate transmissivities below $2 \cdot 10^{-10} \text{ m}^2/\text{s}$ (i.e. $K = 4 \cdot 10^{-10} \text{ m/s}$), which was the approximate measurement limit. If there are changes in these sections, they are at least small.

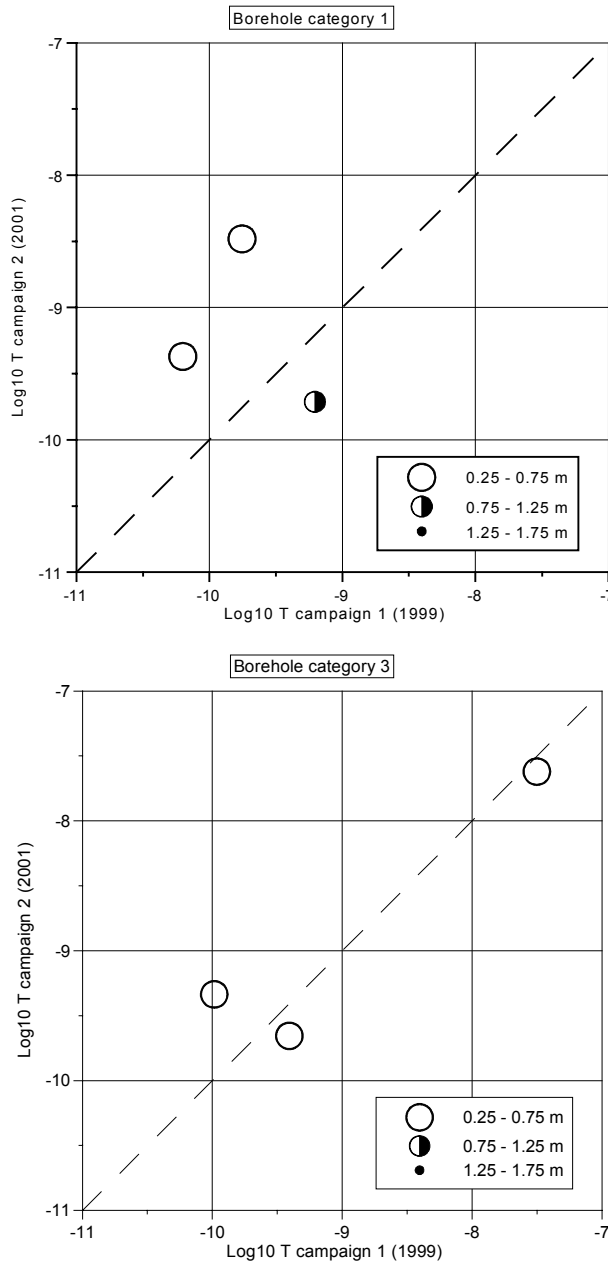


Figure 7-1 Relative overall change of transmissivities. Campaign 1: tests before the deposition holes were drilled. Campaign 2: tests after the deposition holes were drilled.

As noticed above a few of the sections show a significant transmissivity increase between the tests in 1999 and the tests in 2001.

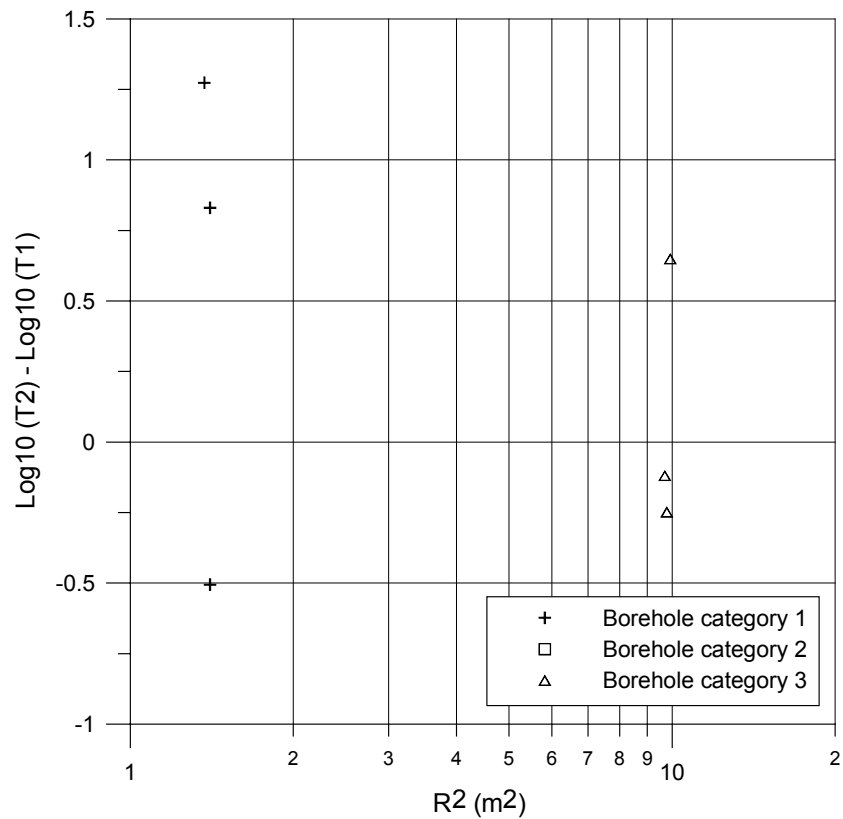


Figure 7-2 The transmissivity changes of the test section plotted against the squared distance.

In Figure 7-2, the transmissivity changes of the test section are plotted against the squared distance. The change is defined as the logarithmic value of the transmissivity of test campaign 2 minus logarithmic value of the transmissivity of test campaign 1. The group of borehole sections closest to a deposition hole indicates a larger variation of changes than the groups more distant to a deposition hole.

7.7 Lead-through holes

Four pressure build-up tests were done in three lead-through holes between tunnel G and tunnel A (Prototype Repository).

In those tests, sections where radial flow occurred, a Jacob semi-logarithmic evaluation of the transmissivity were made. In the remaining two bore holes the transmissivity have been estimated from the specific capacity. The earlier mentioned relationship (7-1) has been used.

The measured, evaluated and estimated parameters of the tests are presented in Table 7-11.

Table 7-11 Evaluated and estimated hydrogeological parameters (s = pressure change, Q = flow rate, Spec. cap = specific capacity, T(Spec. cap) = transmissivity calculated from equation 6-1, T_eval = evaluated transmissivity where radial flow occurs).

Borehole	Secup (m)	Seclow (m)	s (m)	Q (L/min)	Spec. cap (m ³ /s·m)	T(Spec. cap) (m ² /s)	T_eval (m ² /s)
KG0027A01	7.00	11.00	133.12	5.50	6.9·10 ⁻⁷	6.1·10 ⁻⁶	-
KG0033A01	9.00	13.00	3.28	0.049	2.5·10 ⁻⁷	1.9·10 ⁻⁶	3.4·10 ⁻⁷
KG0033A01	34.00	38.00	248.85	0.615	4.1·10 ⁻⁸	2.5·10 ⁻⁷	-
KG0023A01	24.00	28.00	225.59	0.39	2.9·10 ⁻⁸	1.7·10 ⁻⁷	5.9·10 ⁻⁸

The evaluated results indicate a fracture system with a transmissivity of the magnitude 1·10⁻⁷ - 5·10⁻⁷ m²/s.

8 HYDRAULIC INTERFERENCE TESTS

8.1 Drilling campaign 1

No responses could be detected in the surrounding boreholes. Interference tests are reported in Rhén and Forsmark (1998a).

8.2 Drilling campaign 2

Pressure registration was made in the neighbouring boreholes during the flowing and recovery phase of every pressure build-up test. In Table 8-1, the result of this study is presented. The hydraulic centre of the borehole (point of application) has been calculated as centre of gravity of the flow distribution in the section. The distance, r , between different borehole sections has been calculated as the spherical distance between the points of application for each section. For cases where the flow dimension was judged radial, the evaluation of T_{EVAL} and S was based on the Theis log-log type curve method. The calculation of the hydraulic diffusivity (η) is based on radial flow:

$$\eta = T / S = r^2 / [4 \cdot t_L \cdot (1 + t_L / dt) \cdot \ln(1 + dt / t_L)] \quad (8-1)$$

r : Approximate distance from flowing bore hole section to observation bore hole section

t_L : Time lag for a pressure response of 0.1 m to be registered in an observation section after shut-in

dt : Flow time of the test

As can be seen in equation the diffusivity is proportional to r^2 / t_L . S^* in the table is calculated as $S^* = T / \eta$.

Interference tests are reported in Rhén and Forsmark (1998b).

Table 8-1 Interference test results for KA3544G, KA3546G, KA3548G, KA3550G and KA3552G. (r = aprox. distance from flowing bore hole section to observation bore hole section, t_L = time lag for a pressure response of 0.1 m to be registered in an observation section, T = transmissivity, S = storage coefficient, S^* = storage coefficient from diffusivity, η .)

Flowing borehole	Hydraulic centre of borehole (m)	Flowtime dt (min)	Observation borehole	Hydraulic centre of borehole (m)	r (m)	t_L (min)	r^2 / t_L (m ² /s)	η (m ² /s)	T_{EVAL} (m ² /s)	S (-)	S^* (-)	Comments	
KA3544G	9.75	44	KA3546G	7.42	3.37	4.60	4.11E-02	3.95E-03	4.4E-09	1.6E-06	1.1E-06		
		44	KA3548G	6.18	5.30	5.40	8.67E-02	8.72E-03	2.6E-09	4.2E-07	3.0E-07		
		44	KA3550G	6.21	7.13	2.50	3.39E-01	2.74E-02	4.2E-09	2.4E-07	1.5E-07		
		44	KA3552G	4.56	9.49	6.00	2.50E-01	2.60E-02	-	-	-	Not evaluable	
		44	KA3539G	6.59	5.77	3.80	1.46E-01	1.33E-02	-	-	-	Not evaluable	
		44	KA3545G	6.25	3.66	1.10	2.03E-01	1.33E-02	3.9E-09	1.4E-06	2.9E-07		
		44	KA3510B	117.5	89.07	-	-	-	-	-	-	-	No response
		44	KA3573A:1	21.34	39.21	-	-	-	-	-	-	-	No response
		44	KA3573A:2	9.16	33.05	-	-	-	-	-	-	-	No response
		44	KA3600A:1	31.78	86.08	-	-	-	-	-	-	-	No response
44	KA3600A:2	12.51	68.26	-	-	-	-	-	-	-	No response		
KA3546G	7.42	120	KA3544G	9.75	3.37	6.20	3.05E-02	2.41E-03	7.1E-09	1.8E-06	2.9E-06		
		120	KA3548G	6.18	2.59	0.87	1.29E-01	6.46E-03	2.9E-10	5.9E-08	4.5E-08		
		120	KA3550G	6.21	4.89	1.65	2.42E-01	1.39E-02	2.8E-10	2.8E-08	2.0E-08		
		120	KA3552G	4.56	6.67	1.95	3.80E-01	2.26E-02	4.3E-10	2.5E-08	1.9E-08		
		120	KA3545G	6.25	1.53	0.77	5.07E-02	2.49E-03	3.4E-10	1.9E-07	1.4E-07		
		120	KA3551G	4.30	6.03	16.00	3.79E-02	3.90E-03	-	-	-	-	Not evaluable
		120	KA3510B	117.5	88.48	-	-	-	-	-	-	-	No response
		120	KA3573A:1	21.34	36.26	-	-	-	-	-	-	-	No response
		120	KA3573A:2	9.16	30.15	-	-	-	-	-	-	-	No response
		120	KA3600A:1	31.78	83.79	-	-	-	-	-	-	-	No response
120	KA3600A:2	12.51	66.01	-	-	-	-	-	-	-	No response		
KA3548G	6.18	61	KA3544G	9.75	5.30	5.70	8.21E-02	7.63E-03	-	-	-	Not evaluable	
		61	KA3546G	7.42	2.59	0.89	1.26E-01	7.30E-03	-	-	-	Not evaluable	
		61	KA3550G	6.21	2.39	0.44	2.16E-01	1.09E-02	2.8E-10	4.4E-08	2.6E-08		
		61	KA3552G	4.56	4.29	3.50	8.76E-02	7.11E-03	3.8E-10	8.6E-08	5.3E-08		
		61	KA3545G	6.25	2.84	0.93	1.45E-01	8.48E-03	-	-	-	-	Not evaluable
		61	KA3551G	4.30	3.52	10.00	2.07E-02	2.26E-03	-	-	-	-	Not evaluable
		61	KA3510B	117.5	88.09	-	-	-	-	-	-	-	No response
		61	KA3573A:1	21.34	34.96	-	-	-	-	-	-	-	No response
		61	KA3573A:2	9.16	28.21	-	-	-	-	-	-	-	No response
		61	KA3600A:1	31.78	81.72	-	-	-	-	-	-	-	No response
61	KA3600A:2	12.51	63.79	-	-	-	-	-	-	-	No response		
KA3550G	6.21	62	KA3544G	9.75	7.13	1.40	6.05E-01	3.88E-02	5.5E-09	2.6E-07	1.4E-07		
		62	KA3546G	7.42	4.89	0.52	7.66E-01	3.97E-02	2.1E-10	2.1E-08	5.3E-09		
		62	KA3548G	6.18	2.39	0.06	1.59E+00	5.71E-02	2.5E-10	4.4E-08	4.4E-09		
		62	KA3552G	4.56	2.81	8.30	1.59E-02	1.64E-03	2.7E-10	2.7E-07	1.7E-07		
		62	KA3551G	4.30	2.08	10.00	7.21E-03	7.86E-04	-	-	-	-	Not evaluable
		62	KA3557G	4.27	6.84	9.30	8.38E-02	8.95E-03	-	-	-	-	Not evaluable
		62	KA3510B	117.5	87.20	-	-	-	-	-	-	-	No response
		62	KA3573A:1	21.34	34.01	-	-	-	-	-	-	-	No response
		62	KA3573A:2	9.16	26.65	-	-	-	-	-	-	-	No response
		62	KA3600A:1	31.78	79.73	-	-	-	-	-	-	-	No response
62	KA3600A:2	12.51	61.69	-	-	-	-	-	-	-	No response		
KA3552G	4.56	64	KA3544G	9.75	9.49	23.40	6.41E-02	8.91E-03	-	-	-	Not evaluable	
		64	KA3546G	7.42	6.67	3.20	2.32E-01	1.81E-02	3.8E-10	2.7E-08	2.1E-08		
		64	KA3548G	6.18	4.29	5.20	5.90E-02	5.27E-03	3.8E-10	1.0E-07	7.2E-08		
		64	KA3550G	6.21	2.81	10.00	1.32E-02	1.42E-03	3.0E-10	3.5E-07	2.1E-07		
		64	KA3551G	4.30	1.26	6.60	4.01E-03	3.83E-04	-	-	-	-	Not evaluable
		64	KA3557G	4.27	5.05	39.00	1.09E-02	1.74E-03	-	-	-	-	Not evaluable
		64	KA3510B	117.5	86.44	-	-	-	-	-	-	-	No response
		64	KA3573A:1	21.34	31.43	-	-	-	-	-	-	-	No response
		64	KA3573A:2	9.16	24.08	-	-	-	-	-	-	-	No response
		64	KA3600A:1	31.78	77.68	-	-	-	-	-	-	-	No response
64	KA3600A:2	12.51	59.72	-	-	-	-	-	-	-	No response		

Table 8-2 Interference test results for KA3588G. (r = aprox. distance from flowing bore hole section to observation bore hole section, t_L = time lag for a pressure response to reach an observation section, T = transmissivity, S = storage coefficient, S^* = storage coefficient from diffusivity, η .)

Flowing borehole	Hydraulic centre of borehole (m)	Flowtime dt (min)	Observation borehole	Hydraulic centre of borehole (m)	r (m)	t_L (min)	r^2 / t_L (m ² /s)	η (m ² /s)	T_{EVAL} (m ² /s)	S (-)	S^* (-)	Comments	
KA3572G	7.67	240	No obs.										
KA3578G	7.03	240	No obs.										
KA3584G	6.24	255	No obs.										
KA3586G	4.26	251	No obs.										
KA3588G	5.18	60	KA3584G	6.24	3.75	31.60	7.42E-03	1.14E-03	-	-	-	Not evaluable	
		60	KA3586G	4.26	1.70	15.50	3.11E-03	3.90E-04	-	-	-	Not evaluable	
		60	KA3581G	4.22	6.96	-	-	-	-	-	-	-	Not evaluable
		60	KA3587G	4.30	1.37	1.90	1.65E-02	1.15E-03	-	-	-	-	Not evaluable
		60	KA3593G	5.24	5.53	0.91	5.60E-01	3.28E-02	1.1E-08	1.7E-07	3.4E-07	-	Linear flow ?
		60	KA3510B	117.5	70.51	-	-	-	-	-	-	-	No response
		60	KA3573A:1	21.34	28.62	-	-	-	-	-	-	-	No response
		60	KA3573A:2	9.16	20.19	-	-	-	-	-	-	-	No response
		60	KA3600A:1	31.78	43.82	-	-	-	-	-	-	-	No response
60	KA3600A:2	12.51	25.34	-	-	-	-	-	-	-	No response		

8.3 Drilling campaign 3

Pressure registrations were made during the pressure build-up tests of the 18 boreholes drilled during drill campaign 3. They were made in the same manner as during drilling campaign 2 described above. In Tables 8-3 to 8-7, the evaluated results are detailed.

Table 8-3 Interference test results for KA3539G, KA3542G01 and KA3542G02. (r = approx. distance from flowing bore hole section to observation bore hole section, t_L = time lag for a pressure response of 0.1 m to be registered in an observation section, T = transmissivity, S = storage coefficient, S^* = storage coefficient from diffusivity, η .)

Flowing borehole	Hydraulic centre of borehole (m)	Flowtime dt (min)	Observation borehole	Hydraulic centre of borehole (m)	r (m)	t_L (min)	r^2 / t_L (m ² /s)	η (m ² /s)	T _{EVAL} (m ² /s)	S (-)	S^* (-)	Comments		
KA3539G	16.11	64	KA3554G01	24.83	22.41	15	0.558	0.068	-	-	-	Not evaluable		
		64	KA3554G02	13.69	17.87	0.55	9.677	0.503	-	-	-	Not evaluable		
		64	KA3542G01	21.05	15.51	17	0.236	0.030	-	-	-	Not evaluable		
		64	KA3542G02	6.28	12.72	0.11	24.496	0.960	-	-	-	Not evaluable		
		64	KA3548A01	15.95	26.53	-	-	-	-	-	-	No response		
		64	KA3550G01	6.21	13.81	10	0.318	0.034	-	-	-	Not evaluable		
		64	KA3548G01	6.18	12.22	17	0.146	0.019	-	-	-	Not evaluable		
		64	KA3546G01	7.42	10.12	20	0.085	0.011	-	-	-	Not evaluable		
		64	KA3551G	4.30	15.59	13	0.312	0.036	-	-	-	Not evaluable		
		64	KA3544G01	9.75	7.23	0.26	3.351	0.151	-	-	-	Not evaluable		
		64	KA3545G	6.25	10.71	-	-	-	-	-	-	No response		
		64	KA3510B	117.50	87.74	-	-	-	-	-	-	No response		
		64	KA3573A:1	21.34	43.44	27	1.165	0.169	-	-	-	Not evaluable		
		64	KA3573A:2	9.16	38.30	17	1.438	0.182	-	-	-	Not evaluable		
		64	KA3600A:1	31.78	90.21	-	-	-	-	-	-	No response		
		64	KA3600A:2	12.51	72.79	-	-	-	-	-	-	No response		
		KA3542G01	21.05	60	KA3542G02	6.28	22.94	-	-	-	-	-	-	No response
				60	KA3554G01	24.83	12.43	0.79	3.261	0.185	9.8E-07	1.0E-05	5.3E-06	-
60	KA3554G02			13.69	28.73	1.2	11.464	0.715	-	-	-	Not evaluable		
60	KA3548A01			15.95	17.81	-	-	-	-	-	-	No response		
60	KA3550G01			6.21	20.21	-	-	-	-	-	-	No response		
60	KA3548G01			6.18	18.63	-	-	-	-	-	-	No response		
60	KA3546G01			7.42	16.83	11	0.429	0.049	1.5E-07	4.7E-06	3.1E-06	-		
60	KA3551G			4.30	20.76	-	-	-	-	-	-	No response		
60	KA3544G01			9.75	17.16	4.3	1.142	0.098	-	-	-	Not evaluable		
60	KA3545G			6.25	17.97	-	-	-	-	-	-	No response		
60	KA3539G			16.11	15.51	-	-	-	-	-	-	No response		
60	KA3510B			117.50	81.08	3.5	31.304	2.551	-	-	-	Not evaluable		
60	KA3573A:1			21.34	35.67	2.6	8.157	0.614	2.6E-06	3.9E-06	4.2E-06	-		
60	KA3573A:2			9.16	35.02	1.7	12.025	0.814	1.2E-06	1.6E-06	1.5E-06	-		
60	KA3600A:1			31.78	87.03	23	5.489	0.773	-	-	-	Not evaluable		
60	KA3600A:2			12.51	71.22	10	8.453	0.931	-	-	-	Not evaluable		
KA3542G02	6.28			64	KA3542G01	21.05	22.94	31	0.283	0.043	-	-	-	Not evaluable
				64	KA3554G01	24.83	29.00	14	1.001	0.120	-	-	-	Not evaluable
		64	KA3554G02	13.69	13.89	0.12	26.788	1.064	1.5E-07	1.7E-07	1.4E-07	-		
		64	KA3548A01	15.95	24.91	10	1.034	0.112	-	-	-	Not evaluable		
		64	KA3550G01	6.21	9.25	7.9	0.181	0.018	-	-	-	Not evaluable		
		64	KA3548G01	6.18	7.94	16	0.066	0.008	-	-	-	Not evaluable		
		64	KA3546G01	7.42	7.50	20	0.047	0.006	1.4E-08	5.0E-06	2.2E-06	-		
		64	KA3551G	4.30	10.08	4.7	0.360	0.031	-	-	-	Not evaluable		
		64	KA3544G01	9.75	7.01	0.26	3.149	0.142	1.0E-07	3.4E-06	7.0E-07	-		
		64	KA3545G	6.25	6.09	24	0.026	0.004	-	-	-	Not evaluable		
		64	KA3539G	16.11	12.72	0.16	16.841	0.701	-	-	-	Not evaluable		
		64	KA3510B	117.50	95.39	-	-	-	-	-	-	No response		
		64	KA3573A:1	21.34	42.20	22	1.349	0.184	-	-	-	Not evaluable		
		64	KA3573A:2	9.16	35.06	14	1.464	0.175	-	-	-	Not evaluable		
		64	KA3600A:1	31.78	88.43	-	-	-	-	-	-	-		
		64	KA3600A:2	12.51	70.12	-	-	-	-	-	-	-		

Table 8-4 Interference test results for KA3548A01, KA3554G01, KA3554G02 and KA3566G01.

Flowing borehole	Hydraulic centre of borehole (m)	Flowtime dt (min)	Observation borehole	Hydraulic centre of borehole (m)	r (m)	t _L (min)	r ² /t _L (m ² /s)	η (m ² /s)	T _{eval} (m ² /s)	S (-)	S [*] (-)	Comments	
KA3548A01	15.95	64	KA3554G01	13.69	15.02	1.1	3.418	0.206	1.9E-08	4.8E-06	9.2E-08		
		64	KA3554G02	24.83	41.54	30	0.959	0.143	-	-	-	-	Not evaluable
		64	KA3542G01	21.05	17.81	0.17	31.084	1.306	6.7E-07	3.2E-07	5.1E-07	-	
		64	KA3542G02	6.28	24.91	18	0.574	0.074	-	-	-	-	Not evaluable
		64	KA3550G01	6.21	20.77	44	0.163	0.027	-	-	-	-	Not evaluable
		64	KA3548G01	6.18	19.94	44	0.151	0.025	-	-	-	-	Not evaluable
		64	KA3546G01	7.42	19.80	41	0.159	0.026	-	-	-	-	Not evaluable
		64	KA3551G	4.30	19.52	26	0.244	0.035	-	-	-	-	Not evaluable
		64	KA3544G01	9.75	22.64	22	0.388	0.053	-	-	-	-	Not evaluable
		64	KA3545G	6.25	20.28	-	-	-	-	-	-	-	No response
		64	KA3539G	16.11	26.53	17	0.690	0.087	-	-	-	-	Not evaluable
		64	KA3510B	117.50	86.11	4.9	25.221	2.216	1.9E-05	3.7E-06	8.6E-06	-	
		64	KA3573A:1	21.34	24.78	0.52	19.681	1.012	5.2E-06	4.9E-06	5.1E-06	-	
		64	KA3573A:2	9.16	25.08	0.1	104.834	4.049	2.4E-06	1.9E-06	5.9E-07	-	
		64	KA3600A:1	31.78	79.30	19	5.516	0.721	-	-	-	-	Not evaluable
		64	KA3600A:2	12.51	70.64	2.9	28.678	2.185	-	-	-	-	Not evaluable
KA3554G01	24.83	64	KA3554G02	13.69	29.35	0.5	28.710	1.465	-	-	-	Not evaluable	
		64	KA3566G01	17.15	14.48	1.4	2.496	0.159	2.7E-06	9.3E-06	1.7E-05	-	
		64	KA3566G02	17.29	33.83	22	0.867	0.118	2.7E-07	4.9E-06	2.3E-06	-	
		64	KA3557G	11.40	19.47	35	0.180	0.028	-	-	-	-	Not evaluable
		64	KA3552G01	4.56	21.73	6	1.312	0.122	-	-	-	-	Not evaluable
		64	KA3550G01	6.21	22.38	-	-	-	-	-	-	-	No response
		64	KA3548G01	6.18	22.06	-	-	-	-	-	-	-	No response
		64	KA3551G	4.30	22.63	10	0.854	0.092	-	-	-	-	Not evaluable
		64	KA3548A01	15.95	19.87	0.33	19.940	0.941	2.2E-06	2.3E-06	2.3E-06	-	
		64	KA3542G01	21.05	12.43	0.72	3.578	0.197	1.2E-06	1.1E-05	6.1E-06	-	
		64	KA3542G02	6.28	29.00	14	1.001	0.120	9.1E-07	1.3E-05	7.6E-06	-	
		64	KA3510B	117.50	69.81	1.2	67.692	4.158	1.9E-05	3.3E-06	4.6E-06	-	
		64	KA3573A:1	21.34	27.38	0.06	208.164	7.456	4.0E-06	2.6E-05	5.4E-07	-	
		64	KA3573A:2	9.16	27.79	0.01	1287.233	36.713	2.4E-06	7.8E-07	6.5E-08	-	
		64	KA3600A:1	31.78	76.00	16	6.017	0.748	-	-	-	-	Not evaluable
		64	KA3600A:2	12.51	61.03	3.1	20.026	1.553	1.8E-05	3.7E-06	1.2E-05	-	
KA3554G02	13.69	64	KA3554G01	24.83	29.35	-	-	-	-	-	-	No response	
		64	KA3566G01	17.15	25.96	22	0.511	0.070	-	-	-	-	Not evaluable
		64	KA3566G02	17.29	12.55	1.8	1.459	0.099	1.3E-07	9.5E-07	1.3E-06	-	
		64	KA3557G	11.40	11.05	22	0.092	0.013	-	-	-	-	Not evaluable
		64	KA3552G01	4.56	12.38	-	-	-	-	-	-	-	No response
		64	KA3550G01	6.21	10.71	4.9	0.390	0.034	6.9E-08	2.1E-06	2.0E-06	-	
		64	KA3548G01	6.18	12.32	10	0.253	0.027	3.5E-08	1.6E-06	1.3E-06	-	
		64	KA3551G	4.30	11.90	12	0.197	0.022	-	-	-	-	Not evaluable
		64	KA3548A01	15.95	31.25	-	-	-	-	-	-	-	No response
		64	KA3542G01	21.05	28.73	-	-	-	-	-	-	-	No response
		64	KA3542G02	6.28	13.89	0.52	6.182	0.318	3.1E-07	3.2E-07	9.7E-07	-	Linear flow ?
		64	KA3510B	117.50	87.99	-	-	-	-	-	-	-	No response
		64	KA3573A:1	21.34	40.33	-	-	-	-	-	-	-	No response
		64	KA3573A:2	9.16	30.89	-	-	-	-	-	-	-	No response
		64	KA3600A:1	31.78	79.35	-	-	-	-	-	-	-	No response
		64	KA3600A:2	12.51	60.80	-	-	-	-	-	-	-	No response
KA3557G	11.40		No obs.										
KA3563G	5.60		No obs.										
KA3566G01	17.15	63	KA3566G02	17.29	25.64	-	-	-	-	-	-	No response	
		63	KA3590G01	4.33	27.19	0.91	13.535	0.785	8.1E-08	5.5E-08	1.0E-07	-	
		63	KA3590G02	26.73	40.75	-	-	-	-	-	-	-	No response
		63	KA3574G01	4.93	17.38	-	-	-	-	-	-	-	No response
		63	KA3554G01	13.69	12.58	10	0.264	0.029	-	-	-	-	Not evaluable
		63	KA3554G02	24.83	33.53	-	-	-	-	-	-	-	No response
		63	KA3548A01	15.95	23.13	-	-	-	-	-	-	-	No response
		63	KA3569G	4.00	15.36	7.4	0.531	0.053	1.1E-08	2.5E-07	2.1E-07	-	
		63	KA3557G	11.40	15.12	20	0.190	0.025	-	-	-	-	Not evaluable
		63	KA3563G	5.60	14.73	-	-	-	-	-	-	-	No response
		63	KA3572G01	7.67	14.62	-	-	-	-	-	-	-	No response
		63	KA3510B	117.50	67.64	-	-	-	-	-	-	-	No response
		63	KA3573A:1	21.34	18.80	0.4	14.733	0.722	-	-	-	-	Not evaluable
		63	KA3573A:2	9.16	15.53	0.1	40.207	1.557	-	-	-	-	Not evaluable
		63	KA3600A:1	31.78	63.02	-	-	-	-	-	-	-	No response
		63	KA3600A:2	12.51	47.08	-	-	-	-	-	-	-	No response

Table 8-5 Interference test results for KA3566G02, KA3590G01, KA3590G02 and KA3593G.

Flowing borehole	Hydraulic centre of borehole (m)	Flowtime dt (min)	Observation borehole	Hydraulic centre of borehole (m)	r (m)	t _L (min)	r ² /t _L (m ² /s)	η (m ² /s)	T _{eval} (m ² /s)	S (-)	S [*] (-)	Comments	
KA3566G02	17.29	63	KA3566G01	17.15	25.64	5	2.191	0.194	-	-	-	Not evaluable	
		63	KA3590G01	4.33	30.53	3	5.180	0.400	-	-	-	Not evaluable	
		63	KA3590G02	26.73	25.65	-	-	-	-	-	-	-	No response
		63	KA3574G01	4.93	16.36	10	0.446	0.048	-	-	-	-	Not evaluable
		63	KA3554G01	24.83	33.83	43	0.444	0.073	-	-	-	-	Not evaluable
		63	KA3554G02	13.69	12.55	3.2	0.821	0.064	2.3E-07	1.4E-06	3.6E-06	-	Not evaluable
		63	KA3548A01	15.95	38.50	40	0.618	0.100	-	-	-	-	Not evaluable
		63	KA3569G	4.00	15.43	6.3	0.630	0.060	-	-	-	-	Not evaluable
		63	KA3557G	11.40	15.43	37	0.107	0.017	-	-	-	-	Not evaluable
		63	KA3563G	5.60	14.52	0.96	3.662	0.215	-	-	-	-	Not evaluable
		63	KA3572G01	7.67	14.95	12	0.311	0.036	-	-	-	-	Not evaluable
		63	KA3510B	117.50	82.22	52	2.167	0.374	-	-	-	-	Not evaluable
		63	KA3573A:1	21.34	39.76	50	0.527	0.090	-	-	-	-	Not evaluable
		63	KA3573A:2	9.16	29.06	0.03	469.125	15.323	-	-	-	-	Not evaluable
		63	KA3600A:1	31.78	69.92	38	2.144	0.342	-	-	-	-	Not evaluable
		63	KA3600A:2	12.51	51.39	44	1.000	0.166	-	-	-	-	Not evaluable
KA3574G01	4.93	No obs.											
KA3576G01	5.99	No obs.											
KA3590G01	4.33	62	KA3590G02	26.73	28.06	9.3	1.411	0.151	-	-	-	Not evaluable	
		62	KA3593G	6.45	6.01	1.9	0.317	0.022	-	-	-	Not evaluable	
		62	KA3588G01	5.18	4.43	10	0.033	0.004	-	-	-	Not evaluable	
		62	KA3566G01	17.15	27.19	0.45	27.371	1.377	1.2E-07	5.2E-08	8.7E-08	-	Not evaluable
		62	KA3566G02	17.29	30.53	4.5	3.453	0.299	-	-	-	-	Not evaluable
		62	KA3548A01	15.95	44.56	4.5	7.352	0.636	-	-	-	-	Not evaluable
		62	KA3586G01	4.26	5.47	-	-	-	-	-	-	-	No response
		62	KA3587G	4.30	5.11	-	-	-	-	-	-	-	No response
		62	KA3581G	4.22	9.97	-	-	-	-	-	-	-	No response
		62	KA3579G	7.62	12.294	-	-	-	-	-	-	-	No response
		62	KA3510B	117.50	69.95	-	-	-	-	-	-	-	No response
		62	KA3573A:1	21.34	27.20	12	1.028	0.118	-	-	-	-	Not evaluable
		62	KA3573A:2	9.16	20.04	3.1	2.159	0.169	-	-	-	-	Not evaluable
		62	KA3600A:1	31.78	40.24	-	-	-	-	-	-	-	No response
62	KA3600A:2	12.51	21.80	-	-	-	-	-	-	-	No response		
KA3590G02	26.73	60	KA3590G01	4.33	28.06	-	-	-	-	-	-	No response	
		60	KA3593G	6.45	23.37	21	0.433	0.059	-	-	-	Not evaluable	
		60	KA3588G01	5.18	24.43	24	0.415	0.059	-	-	-	Not evaluable	
		60	KA3566G01	17.15	40.75	8.7	3.180	0.336	-	-	-	Not evaluable	
		60	KA3566G02	17.29	25.65	0.72	15.230	0.848	6.2E-08	1.2E-07	7.3E-08	-	Not evaluable
		60	KA3548A01	15.95	59.93	6.90	8.674	0.856	-	-	-	-	Not evaluable
		60	KA3586G01	4.26	24.15	-	-	-	-	-	-	-	No response
		60	KA3587G	4.30	24.36	-	-	-	-	-	-	-	No response
		60	KA3581G	4.22	25.87	-	-	-	-	-	-	-	No response
		60	KA3579G	7.62	24.858	-	-	-	-	-	-	-	No response
		60	KA3510B	117.50	75.70	-	-	-	-	-	-	-	No response
		60	KA3573A:1	21.34	51.10	20	2.176	0.294	-	-	-	-	Not evaluable
		60	KA3573A:2	9.16	41.43	14	2.043	0.249	-	-	-	-	Not evaluable
		60	KA3600A:1	31.78	56.52	25	2.130	0.307	-	-	-	-	Not evaluable
60	KA3600A:2	12.51	40.32	35	0.774	0.122	-	-	-	-	Not evaluable		
KA3593G	6.45	64	KA3590G01	4.33	6.01	3.3	0.182	0.014	-	-	-	Not evaluable	
		64	KA3590G02	26.73	23.37	-	-	-	-	-	-	No response	
		64	KA3588G01	5.18	5.86	0.79	0.724	0.041	8.4E-09	2.3E-07	2.1E-07	-	Not evaluable
		64	KA3566G01	17.15	30.63	5.5	2.843	0.258	-	-	-	-	Not evaluable
		64	KA3566G02	17.29	30.71	-	-	-	-	-	-	-	No response
		64	KA3548A01	15.95	49.36	-	-	-	-	-	-	-	No response
		64	KA3586G01	4.26	6.98	-	-	-	-	-	-	-	No response
		64	KA3587G	4.30	6.75	-	-	-	-	-	-	-	No response
		64	KA3581G	4.22	12.63	-	-	-	-	-	-	-	No response
		64	KA3579G	7.62	14.111	-	-	-	-	-	-	-	No response
		64	KA3510B	117.50	68.82	-	-	-	-	-	-	-	No response
		64	KA3573A:1	21.34	32.76	-	-	-	-	-	-	-	No response
		64	KA3573A:2	9.16	25.45	-	-	-	-	-	-	-	No response
		64	KA3600A:1	31.78	39.22	-	-	-	-	-	-	-	No response
64	KA3600A:2	12.51	20.97	-	-	-	-	-	-	-	No response		

Table 8-6 Interference test results for KG0021A01 and KG0048A01.

Flowing borehole	Hydraulic centre of borehole (m)	Flowtime dt (min)	Observation borehole	Hydraulic centre of borehole (m)	r (m)	t _L (min)	r ² /t _L (m ² /s)	η (m ² /s)	T _{eval} (m ² /s)	S (-)	S [*] (-)	Comments
KG0021A01	27.41	85	KA3590G01	4.33	51.00	-	-	-	-	-	-	No logger
		85	KA3590G02	26.73	57.10	4.00	13.587	1.046	4.1E-07	4.0E-07	3.9E-07	
		85	KA3566G01	17.15	39.83	26.90	0.983	0.131	1.4E-06	1.7E-05	1.1E-05	
		85	KA3566G02	17.29	33.64	9.30	2.029	0.197	2.2E-07	1.6E-06	1.1E-06	
		85	KA3554G01	24.83	41.59	0.96	30.031	1.652	-	-	-	Not evaluable
		85	KA3554G02	13.69	24.54	7.10	1.414	0.127	3.6E-06	3.2E-05	2.8E-05	
		85	KA3548A01:1	19.56	33.18	6.20	2.959	0.256	2.7E-06	1.2E-05	1.1E-05	
		85	KA3548A01:2	13.49	27.50	5.20	2.423	0.200	-	-	-	Not evaluable
		85	KA3542G01	21.05	36.37	7.90	2.790	0.259	-	-	-	Not evaluable
		85	KA3542G02	6.28	21.64	0.48	16.262	0.780	-	-	-	Not evaluable
		85	KA3510A:1	122.50	111.98	16.00	13.062	1.492	-	-	-	Not evaluable
		85	KA3510A:2	117.50	107.22	53.70	3.568	0.576	-	-	-	Not evaluable
		85	KA3510A:3	45.00	44.32	7.10	4.612	0.415	1.9E-06	6.3E-06	4.6E-06	
		85	KA3573A:1	21.34	45.26	10.00	3.415	0.339	6.5E-06	2.0E-05	1.9E-05	
		85	KA3573A:2	9.16	37.28	4.70	4.928	0.396	3.0E-06	9.3E-06	7.6E-06	
		85	KA3600F:1	31.78	89.36	28.20	4.720	0.637	-	-	-	Not evaluable
		85	KA3600F:2	12.51	70.74	18.20	4.582	0.544	-	-	-	Not evaluable
		85	KG0048A01:1	53.81	45.24	8.00	4.264	0.397	2.8E-06	6.0E-06	7.1E-06	
		85	KG0048A01:2	45.89	39.07	3.00	8.479	0.606	2.9E-06	3.7E-06	4.8E-06	
		85	KG0048A01:3	33.50	31.05	1.90	8.455	0.541	5.0E-07	1.2E-06	9.2E-07	
85	KG0048A01:4	23.64	27.12	1.70	7.213	0.450	2.2E-07	6.7E-07	4.9E-07			
85	KG0048A01:5	6.50	28.32	1.40	9.546	0.570	-	-	-	Not evaluable		
KG0048A01	48.25	65.8	KA3590G01	4.33	20.10	0.30	22.454	1.036	-	-	-	Not evaluable
		65.8	KA3590G02	26.73	41.23	0.66	42.931	2.304	-	-	-	Not evaluable
		65.8	KA3566G01	17.15	33.51	0.38	49.245	2.372	-	-	-	Not evaluable
		65.8	KA3566G02	17.29	35.28	16.60	1.249	0.156	-	-	-	Not evaluable
		65.8	KA3554G01	24.83	46.27	0.28	127.413	5.805	1.5E-06	4.7E-07	2.6E-07	
		65.8	KA3554G02	13.69	39.74	13.20	1.994	0.232	-	-	-	Not evaluable
		65.8	KA3548A01:1	19.56	41.66	0.02	1701.525	51.477	2.1E-06	9.4E-08	4.1E-08	
		65.8	KA3548A01:2	13.49	39.05	1.95	13.032	0.892	1.1E-06	1.4E-06	1.2E-06	
		65.8	KA3542G01	21.05	51.99	3.00	15.015	1.146	9.2E-07	8.8E-07	8.0E-07	
		65.8	KA3542G02	6.28	45.15	9.80	3.467	0.369	-	-	-	Not evaluable
		65.8	KA3510B	117.50	87.79	1.66	77.380	5.093	-	-	-	Not evaluable
		65.8	KA3573A:1	21.34	27.34	0.03	498.317	15.812	2.8E-06	2.0E-06	1.8E-07	
		65.8	KA3573A:2	9.16	19.00	0.00	6016.667	135.577	1.4E-06	3.2E-07	1.0E-08	
		65.8	KA3600F:1	31.78	50.13	1.50	27.922	1.794	-	-	-	Not evaluable
		65.8	KA3600F:2	12.51	32.35	0.20	87.210	3.748	9.5E-06	4.1E-06	2.5E-06	
		65.8	KG0021A01:1	29.13	39.60	0.36	72.596	3.462	-	-	-	Not evaluable
		65.8	KG0021A01:2	11.72	53.42	0.29	164.024	7.520	1.3E-06	2.0E-07	1.7E-07	

8.4 Interference test campaign 1 after drilling campaign 3

Interference test campaign 1 is reported in Forsmark and Rhén (1999a).

8.4.1 Interference test 1:1

The test was carried out in KA3566G01, section 12.30 - 19.80 m, with a flow period of 364 minutes with a final flow of 0.1155 L/min, while the pressure build-up time was 2155 minutes. In Figure 8-1 and Figure 8-2, the pressure drawdown recordings are shown and in Table 8-8, the interference test results are presented.

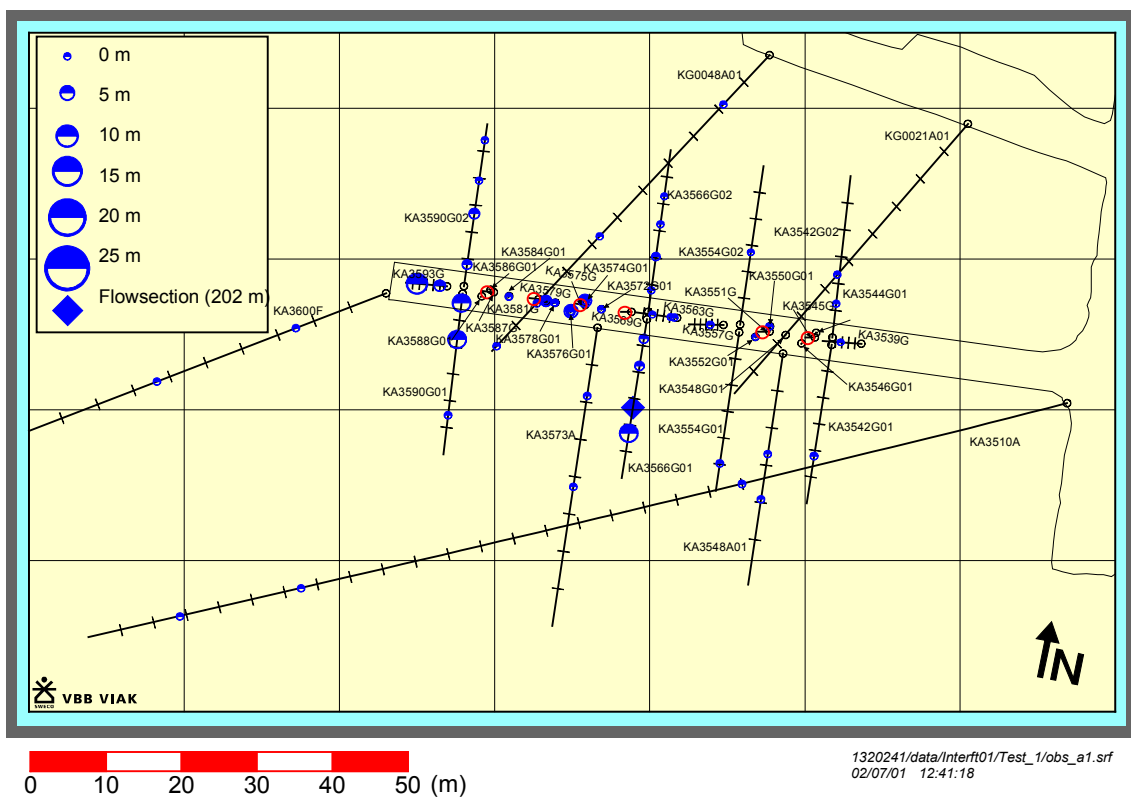


Figure 8-1 Drawdown during flowing of KA3566G01:2 (Interference test 1:1) - plan view.

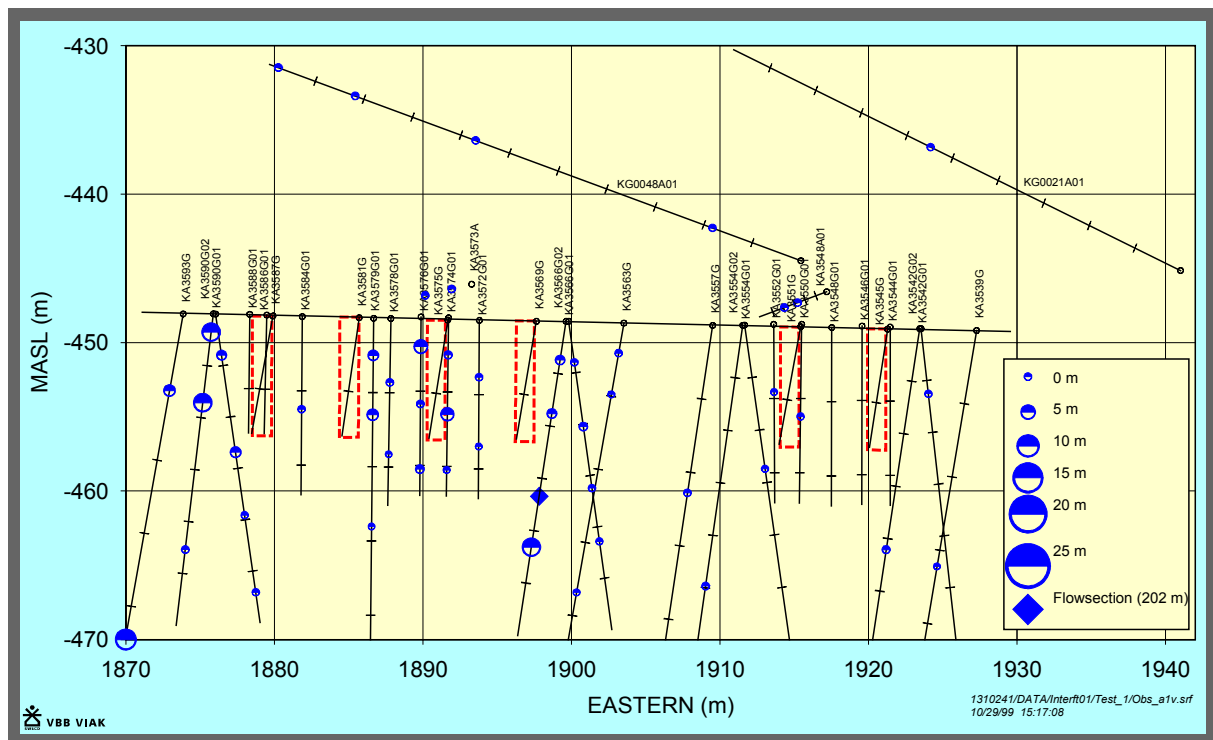


Figure 8-2 Drawdown during flowing of KA3566G01:2 (Interference test 1:1) - vertical view.

This test indicates a hydraulic feature, striking approximately WNW, south of the tunnel and westward from the test section, with distinct responses in KA3590G01 with short response times, t_L , see Table 4-1. East of the flow section, the responses are more diffuse and the response times are considerably longer. It is noted that neither KG0048A01 nor KA3573A responds until very late. There does not seem to exist a direct connection between these boreholes and KA3590G01 or KA3566G01.

The evaluated transmissivity for the test section is $5.9 \cdot 10^{-8} \text{ m}^2/\text{s}$, with the evaluation time for this section being 5 - 50 minutes. In most cases the evaluation time of the observation sections are within that interval.

The evaluated transmissivity and storage coefficient KA3590G01:3 are $7.8 \cdot 10^{-8} \text{ m}^2/\text{s}$ and $4.0 \cdot 10^{-8}$ respectively. These values are close to the parameters evaluated, in KA3566G01:2, during test 1:3.

Table 8-7 Interference test results for KA3566G01, 12.30 - 19.80 m. (r = aprox. distance from flowing bore hole section to observation bore hole section, tL = time lag for a pressure response of 0.1 m to be registered in an observation section, T = transmissivity, S = storage coefficient, S* = storage coefficient from diffusivity, η) The response is classified as 1 = no response (< 0.1 m), 2 = some response (0.1 m - 1.0 m) and 3 = good response (> 1.0 m). P0 = Initial pressure before opening of the valve, Pp = Pressure just before closing the valve, Pf = Pressure at the end of the pressure build-up period.

Observation borehole	Secup (m)	Seclow (m)	Hydraulic centre of borehole (m)	r (m)	t _L (recovery) (min)	r ² / t _L (m ² /s)	η (m ² /s)	T _{eval} (m ² /s)	S (-)	S* (-)	Response (0 = no, 1 = some, 2 =good response)	Po - Pp (kPa)	Pf - Pp (kPa)	Comments
KA3510A:1	122.02	150.00	136.00	85.71	200	6.12E-01	9.53E-02	-	-	-	1	0	2.8	Not evaluable
KA3510A:2	114.02	121.02	117.50	67.99	140	5.50E-01	7.76E-02	-	-	-	1	0	2.4	Not evaluable
KA3510A:3	4.52	113.02	50.00	21.91	26	3.08E-01	2.65E-02	9.0E-07	6.3E-06	3.4E-05	1	1.9	4.3	
KA3539G:1	0.30	30.01	16.11	28.54	-	-	-	-	-	-	0	-4.9	-26.4	No response
KA3542G01:1	0.30	30.04	21.05	24.48	-	-	-	-	-	-	0	3.1	2.5	No response
KA3542G02:1	0.30	30.01	6.28	30.40	50	3.08E-01	3.20E-02	-	-	-	1	-1.1	-26.6	Not evaluable
KA3548A01:1	15.00	30.00	19.56	24.12	50	1.94E-01	2.02E-02	-	-	-	1	0.8	3.3	Not evaluable
KA3548A01:2	10.00	14.00	13.49	22.59	60	1.42E-01	1.56E-02	-	-	-	1	0.7	2.5	Not evaluable
KA3550G01:1	0.30	12.03	6.21	21.31	-	-	-	-	-	-	0	-1	3.9	No response
KA3552G01:1	0.30	12.01	4.56	19.66	-	-	-	-	-	-	0	-4.3	-14.4	No response
KA3554G01:1	0.30	30.01	24.83	14.72	250	1.45E-02	2.38E-03	-	-	-	1	1.2	3	Not evaluable
KA3554G02:1	0.30	30.01	13.69	25.66	90	1.22E-01	1.51E-02	-	-	-	1	-3.7	-20.9	Not evaluable
KA3557G:1	0.30	30.04	11.40	14.85	-	-	-	-	-	-	0	-0.2	-4.5	No response
KA3563G01:1	9.30	30.00	18.42	14.16	26	1.29E-01	1.11E-02	-	-	-	2	-3.7	30.5	Not evaluable
KA3563G01:2	3.80	8.30	4.87	14.67	29	1.24E-01	1.10E-02	-	-	-	2	-3.7	30.3	Not evaluable
KA3563G01:3	1.30	2.80	2.05	16.26	270	1.63E-02	2.74E-03	-	-	-	1	-0.4	0.6	Not evaluable
KA3566G01:1	20.80	30.01	21.57	4.86	0.15	2.62E+00	8.41E-02	-	-	-	2	73	74.3	Not evaluable
KA3566G01:2	12.30	19.80	16.71	0.00	-	-	-	5.9E-08	-	-	-	2019.8	2003.1	
KA3566G01:3	7.30	11.30	8.81	7.90	0.15	6.93E+00	2.22E-01	-	-	-	2	14.9	116.7	Not evaluable
KA3566G01:4	1.30	6.30	3.70	13.01	0.15	1.88E+01	6.03E-01	-	-	-	2	13.5	40.3	Not evaluable
KA3566G02:1	19.30	30.01	21.41	28.46	100	1.35E-01	1.73E-02	-	-	-	1	-2.5	-11.1	Not evaluable
KA3566G02:2	12.30	18.30	16.23	24.57	110	9.15E-02	1.20E-02	-	-	-	1	-0.8	-0.4	Not evaluable
KA3566G02:3	7.80	11.30	10.25	20.78	90	8.00E-02	9.91E-03	-	-	-	2	7	17.6	Not evaluable
KA3566G02:4	1.30	6.80	3.99	18.13	190	2.88E-02	4.43E-03	-	-	-	1	-0.8	3.9	Not evaluable
KA3572G01:1	6.30	12.00	8.49	14.04	31	1.06E-01	9.60E-03	-	-	-	2	-5.5	49.3	Not evaluable
KA3572G01:2	1.30	5.30	3.82	15.83	240	1.74E-02	2.84E-03	-	-	-	1	-0.2	3.9	Not evaluable
KA3573A:1	18.00	40.07	21.34	18.77	121	4.85E-02	6.56E-03	-	-	-	1	0.2	2.5	Not evaluable
KA3573A:2	4.50	17.00	9.16	15.23	51	7.58E-02	7.93E-03	-	-	-	1	0.4	3.3	Not evaluable
KA3574G01:1	8.80	12.00	10.25	15.56	26	1.55E-01	1.34E-02	-	-	-	2	-4.7	27	Not evaluable
KA3574G01:2	5.30	7.80	6.50	16.42	-	-	-	-	-	-	0	38.5	-173.1	No response
KA3574G01:3	1.30	4.30	2.50	18.16	282	1.95E-02	3.31E-03	-	-	-	1	4.3	0.8	Not evaluable
KA3576G01:1	8.80	12.01	10.25	15.12	-	-	-	-	-	-	0	7.6	-29	No response
KA3576G01:2	3.80	7.80	5.86	16.27	-	-	-	-	-	-	0	0.6	-3.1	No response
KA3576G01:3	1.30	2.80	2.00	18.12	-	-	-	-	-	-	0	43.1	-190.6	No response
KA3578G01:1	6.80	12.58	9.14	17.41	29	1.74E-01	1.55E-02	-	-	-	2	-6.5	42.2	Not evaluable
KA3578G01:2	1.30	5.80	4.30	18.79	-	-	-	-	-	-	0	0.8	-3.5	No response
KA3579G01:1	9.30	22.65	14.02	18.24	46	1.21E-01	1.22E-02	-	-	-	2	-4.9	45.1	Not evaluable
KA3579G01:2	5.30	8.30	6.50	18.87	-	-	-	-	-	-	0	27.1	-435.6	No response
KA3579G01:3	1.30	4.30	2.50	20.36	-	-	-	-	-	-	0	21.3	-98.4	No response
KA3584G01:1	0.30	12.00	6.24	22.51	280	3.02E-02	5.12E-03	-	-	-	1	-0.4	0.6	Not evaluable
KA3590G01:1	17.30	30.06	22.70	24.11	70	1.38E-01	1.59E-02	-	-	-	1	0.8	4.5	Not evaluable
KA3590G01:2	7.80	16.30	8.56	25.18	0.8	1.32E+01	5.38E-01	8.5E-08	4.8E-08	1.6E-07	2	73.5	70	
KA3590G01:3	1.30	6.80	1.76	28.32	0.8	1.67E+01	6.81E-01	7.8E-08	4.0E-08	1.1E-07	2	73.5	70.5	
KA3590G02:1	23.30	30.05	27.06	40.77	110	2.52E-01	3.31E-02	-	-	-	1	-1	3.3	Not evaluable
KA3590G02:2	17.30	22.30	19.56	36.06	90	2.41E-01	2.98E-02	-	-	-	1	-1.6	7.6	Not evaluable
KA3590G02:3	8.30	16.30	13.44	32.98	50	3.63E-01	3.77E-02	3.1E-08	9.2E-07	8.2E-07	2	22.7	23.7	
KA3590G02:4	1.20	7.20	4.00	30.12	-	-	-	-	-	-	0	16.1	-30.5	No response
KA3593G01:1	8.30	30.02	22.13	33.70	2.8	6.76E+00	3.44E-01	3.0E-08	5.4E-08	8.7E-08	2	89.9	88.1	
KA3593G01:2	1.30	7.30	5.24	30.52	25	6.21E-01	5.29E-02	5.1E-08	2.7E-05	9.6E-07	2	27.4	30.7	
KA3600F:1	22.00	50.10	31.78	62.98	160	4.13E-01	6.05E-02	-	-	-	1	-0.1	2.1	Not evaluable
KA3600F:2	4.50	21.00	12.51	46.96	150	2.45E-01	3.52E-02	-	-	-	1	0.2	2.4	Not evaluable
KG0021A01:1	0.00	48.82	27.41	39.48	100	2.60E-01	3.32E-02	-	-	-	1	-1.1	6	Not evaluable
KG0048A01:1	49.00	54.69	53.81	34.77	40	5.04E-01	4.91E-02	-	-	-	1	1	4.6	Not evaluable
KG0048A01:2	41.00	48.00	45.90	32.74	50	3.57E-01	3.71E-02	-	-	-	1	0.5	4.6	Not evaluable
KG0048A01:3	30.00	40.00	33.50	33.30	90	2.05E-01	2.54E-02	-	-	-	1	-0.5	4.1	Not evaluable
KG0048A01:4	4.00	29.00	9.12	45.58	90	3.85E-01	4.77E-02	-	-	-	1	-1.6	6.5	Not evaluable

8.4.2 Interference test 1:2

The test was carried out in KA3566G02, section 12.30 - 18.30 m . The flow period was for 377 minutes with a final flow of 0.0845 L/min, while the pressure build-up time was 1037 minutes. In Figure 8-3 and Figure 8-4, the pressure drawdown recordings are shown and in Table 8-9, the interference test results are presented.

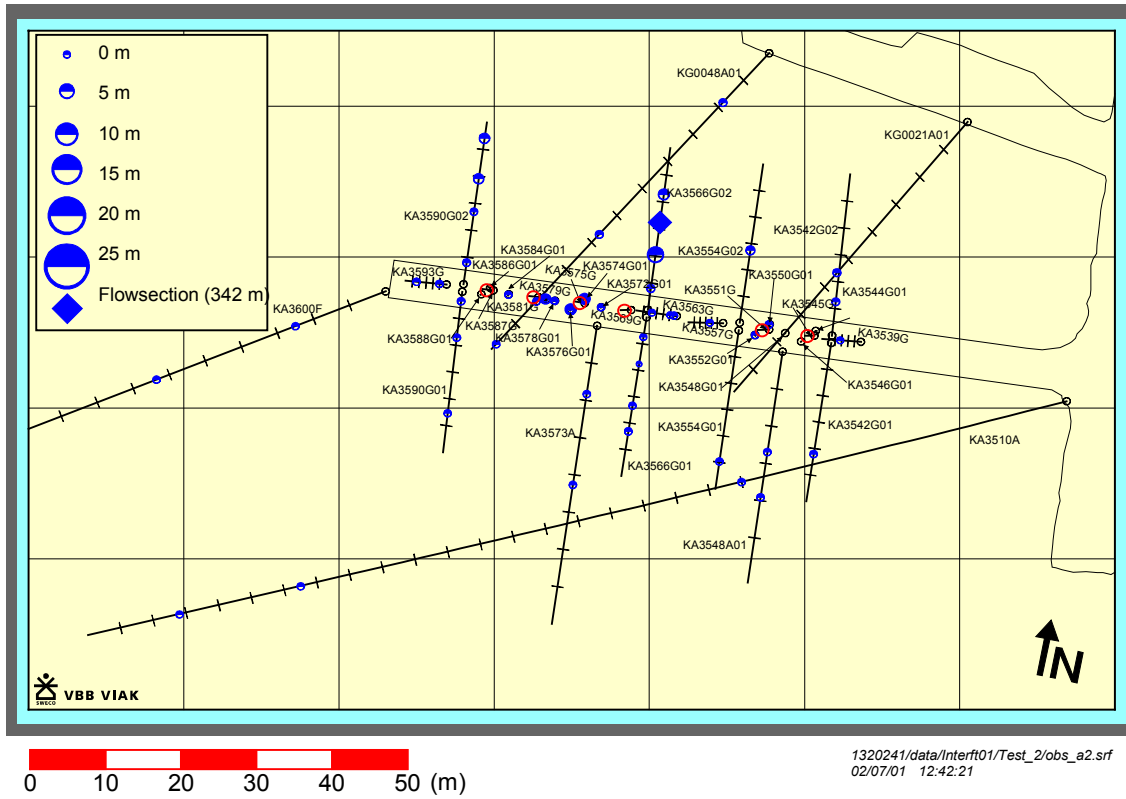


Figure 8-3 Drawdown during flowing of KA3566G02:2 (Interference test 1:2) - plan view.

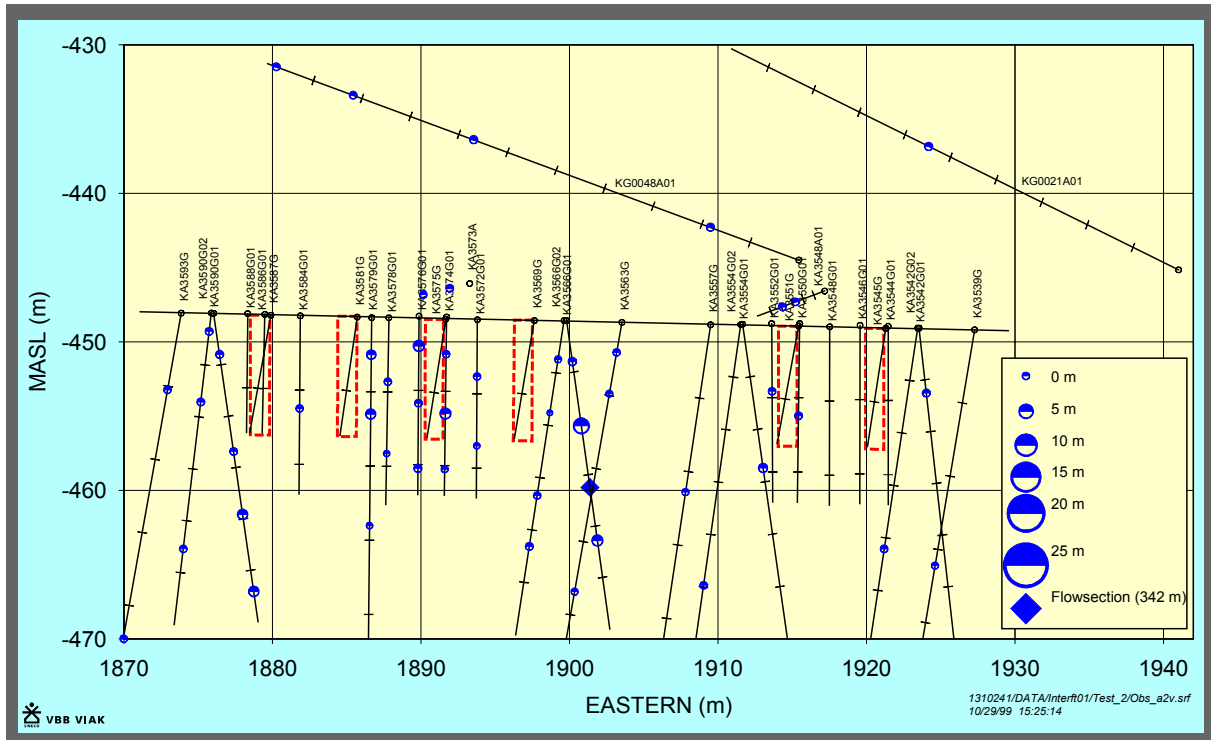


Figure 8-4 Drawdown during flowing of KA3566G02:2 (Interference test 1:2) - vertical view.

This test indicates a hydraulic feature, striking WNW, north of the tunnel. The responses west of the flow section are not as distinct as for the feature south of the tunnel during test 1:1, but they are certain enough to make this feature probable. East of the flow section, the responses are again more diffuse than to the west but there is a possible feature or system of subvertical features striking approximately WNW.

The evaluated transmissivity for the test section is $6.0 \cdot 10^{-8} \text{ m}^2/\text{s}$, with the evaluation time for this section being 200 - 250 minutes. In most cases the evaluation time of the observation sections are within that time interval.

The evaluated transmissivity and storage coefficient KA3590G02:1 is $9.3 \cdot 10^{-8} \text{ m}^2/\text{s}$ and $2.8 \cdot 10^{-7}$ respectively.

Table 8-8 Interference test results for KA3566G02, 12.30 - 18.30 m. (r = aprox. distance from flowing bore hole section to observation bore hole section, t_L = time lag for a pressure response of 0.1 m to be registered in an observation section, T = transmissivity, S = storage coefficient, S^* = storage coefficient from diffusivity, η .) The response is classified as 1 = no response (< 0.1 m), 2 = some response (0.1 m - 1.0 m) and 3 = good response (> 1.0 m). P_0 = Initial pressure before opening of the valve, P_p = Pressure just before closing the valve, P_f = Pressure at the end of the pressure build-up period.

Observation borehole	Secup (m)	Seclow (m)	Hydraulic centre of borehole (m)	r (m)	t_L (recovery) (min)	r^2/t_L (m ² /s)	η (m ² /s)	T_{EVAL} (m ² /s)	S (-)	S^* (-)	Response (0 = no, 1 = some, 2 = good response)	$P_0 - P_p$ (kPa)	$P_f - P_p$ (kPa)	Comments
KA3510A:1	122.02	150.00	136.00	98.85	250	6.51E-01	1.07E-01	-	-	-	1	-0.4	1.1	Not evaluable
KA3510A:2	114.02	121.02	117.50	82.13	220	5.11E-01	8.08E-02	-	-	-	1	0.4	1.6	Not evaluable
KA3510A:3	4.52	113.02	50.00	38.61	60	4.14E-01	4.50E-02	-	-	-	1	1.4	3.3	Not evaluable
KA3539G:1	0.30	30.01	16.11	28.49	14	9.66E-01	7.00E-02	-	-	-	1	-2	-14.5	Not evaluable
KA3542G01:1	0.30	30.04	21.05	36.79	33	6.83E-01	6.24E-02	3.7E-07	1.8E-06	5.9E-06	1	1.8	3.9	
KA3542G02:1	0.30	30.01	6.28	25.77	-	-	-	-	-	-	0	3.9	-28.8	No response
KA3548A01:1	15.00	30.00	19.56	40.56	55	4.98E-01	5.28E-02	-	-	-	1	1.3	3.7	Not evaluable
KA3548A01:2	10.00	14.00	13.49	35.71	40	5.31E-01	5.12E-02	-	-	-	1	1.8	4.1	Not evaluable
KA3550G01:1	0.30	12.03	6.21	20.10	-	-	-	-	-	-	0	2	6.1	No response
KA3552G01:1	0.30	12.01	4.56	20.39	-	-	-	-	-	-	0	1	11	No response
KA3554G01:1	0.30	30.01	24.83	33.27	30	6.15E-01	5.46E-02	-	-	-	1	1.2	3.1	Not evaluable
KA3554G02:1	0.30	30.01	13.69	12.30	5	5.04E-01	2.87E-02	2.1E-07	1.9E-06	7.3E-06	1	11.6	-13.5	
KA3557G:1	0.30	30.04	11.40	14.79	-	-	-	-	-	-	0	-2.4	9	No response
KA3563G01:1	9.30	30.00	18.42	13.91	70	4.61E-02	5.24E-03	-	-	-	2	-2.4	10.3	Not evaluable
KA3563G01:2	3.80	8.30	4.87	13.88	80	4.01E-02	4.75E-03	-	-	-	2	-2.7	10	Not evaluable
KA3563G01:3	1.30	2.80	2.05	15.44	-	-	-	-	-	-	0	0.5	0.7	No response
KA3566G01:1	20.80	30.01	21.57	28.29	45	2.96E-01	2.96E-02	-	-	-	1	2.3	2.7	Not evaluable
KA3566G01:2	12.30	19.80	16.71	24.57	-	-	-	-	-	-	0	0	0.4	No response
KA3566G01:3	7.30	11.30	8.81	19.62	15	4.28E-01	3.15E-02	-	-	-	2	-11.4	35.6	Not evaluable
KA3566G01:4	1.30	6.30	3.70	17.60	-	-	-	-	-	-	0	-2.3	12.3	No response
KA3566G02:1	19.30	30.01	21.41	5.18	0.1	4.47E+00	1.36E-01	-	-	-	2	24.7	17.4	Not evaluable
KA3566G02:2	12.30	18.30	16.23	0.00	-	-	-	6.0E-08	-	-	-	3417.9	3417.9	
KA3566G02:3	7.80	11.30	10.25	5.98	0.1	5.96E+00	1.81E-01	-	-	-	2	56.7	62.2	Not evaluable
KA3566G02:4	1.30	6.80	3.99	12.24	0.1	2.50E+01	7.58E-01	-	-	-	2	6	11.9	Not evaluable
KA3572G01:1	6.30	12.00	8.49	13.91	25	1.29E-01	1.09E-02	-	-	-	2	-6.1	21.9	Not evaluable
KA3572G01:2	1.30	5.30	3.82	15.51	50	8.01E-02	8.25E-03	-	-	-	1	-0.48	3.1	Not evaluable
KA3573A:1	18.00	40.07	21.34	38.80	20	1.25E+00	9.97E-02	-	-	-	1	0.9	2.7	Not evaluable
KA3573A:2	4.50	17.00	9.16	28.06	50	2.62E-01	2.70E-02	-	-	-	1	1.2	3.4	Not evaluable
KA3574G01:1	8.80	12.00	10.25	14.15	25	1.33E-01	1.13E-02	-	-	-	2	-2.6	16.4	Not evaluable
KA3574G01:2	5.30	7.80	6.50	14.90	-	-	-	-	-	-	0	24.4	-48.9	No response
KA3574G01:3	1.30	4.30	2.50	16.63	100	4.61E-02	5.83E-03	-	-	-	2	0	41.9	Not evaluable
KA3576G01:1	8.80	12.01	10.25	16.46	-	-	-	-	-	-	0	3.9	-0.8	No response
KA3576G01:2	3.80	7.80	5.86	17.31	-	-	-	-	-	-	0	0.6	-0.2	No response
KA3576G01:3	1.30	2.80	2.00	18.88	-	-	-	-	-	-	0	24.9	-59.1	No response
KA3578G01:1	6.80	12.58	9.14	17.36	-	-	-	-	-	-	0	-7.1	26.4	No response
KA3578G01:2	1.30	5.80	4.30	18.55	-	-	-	-	-	-	0	0.6	-0.2	No response
KA3579G01:1	9.30	22.65	14.02	18.14	25	2.19E-01	1.85E-02	-	-	-	2	-6.3	18.6	Not evaluable
KA3579G01:2	5.30	8.30	6.50	18.58	-	-	-	-	-	-	0	19.2	-45.2	No response
KA3579G01:3	1.30	4.30	2.50	20.00	-	-	-	-	-	-	0	13.5	-57	No response
KA3584G01:1	0.30	12.00	6.24	22.41	-	-	-	-	-	-	0	0.2	0.2	No response
KA3590G01:1	17.30	30.06	22.70	37.51	100	2.34E-01	2.97E-02	-	-	-	1	0.6	5.1	Not evaluable
KA3590G01:2	7.80	16.30	8.56	30.87	-	-	-	-	-	-	0	2.3	0	No response
KA3590G01:3	1.30	6.80	1.76	29.61	-	-	-	-	-	-	0	2.1	-0.2	No response
KA3590G02:1	23.30	30.05	27.06	26.18	5	2.28E+00	1.30E-01	9.3E-08	2.8E-07	7.2E-07	2	20.7	31.5	
KA3590G02:2	17.30	22.30	19.56	24.15	12	8.10E-01	5.64E-02	5.9E-08	5.1E-07	1.0E-06	2	19.5	30.9	
KA3590G02:3	8.30	16.30	13.44	24.15	90	1.08E-01	1.32E-02	-	-	-	1	1.8	5.1	Not evaluable
KA3590G02:4	1.20	7.20	4.00	27.02	-	-	-	-	-	-	0	3.7	3.5	No response
KA3593G01:1	8.30	30.02	22.13	33.90	150	1.28E-01	1.82E-02	-	-	-	1	1.2	1.4	Not evaluable
KA3593G01:2	1.30	7.30	5.24	30.30	120	1.28E-01	1.70E-02	-	-	-	1	0.6	4.2	Not evaluable
KA3600F:1	22.00	50.10	31.78	69.45	200	4.02E-01	6.20E-02	-	-	-	1	0.8	2.8	Not evaluable
KA3600F:2	4.50	21.00	12.51	50.88	210	2.05E-01	3.21E-02	-	-	-	1	0.4	2.2	Not evaluable
KG0021A01:1	0.00	48.82	27.41	33.04	20	9.10E-01	7.23E-02	-	-	-	2	4.7	28.6	Not evaluable
KG0048A01:1	49.00	54.69	53.81	38.85	30	8.38E-01	7.45E-02	-	-	-	1	1.9	3.7	Not evaluable
KG0048A01:2	41.00	48.00	45.90	32.59	30	5.90E-01	5.24E-02	-	-	-	1	1.8	4.1	Not evaluable
KG0048A01:3	30.00	40.00	33.50	24.75	20	5.10E-01	4.05E-02	-	-	-	2	4.6	12.2	Not evaluable
KG0048A01:4	4.00	29.00	9.12	25.01	22	4.74E-01	3.86E-02	-	-	-	2	4.1	24.5	Not evaluable

8.4.3 Interference test 1:3

The test was carried out in KA3590G01, section 1.30 - 6.80 m. The flow period was for 363 minutes with a final flow of 0.340 L/min, while the pressure build-up time was 1027 minutes. In Figure 8-5 and Figure 8-6 the pressure drawdown recordings are shown and in Table 8-10 the interference test results are presented.

During this test one of the packers, enclosing the flow section, was leaking causing the pressure data of KA3590G01:2 to be unreliable. This circumstance does not however affect the pressure responses in the observation sections. The test was later carried out once more as test 1:6.

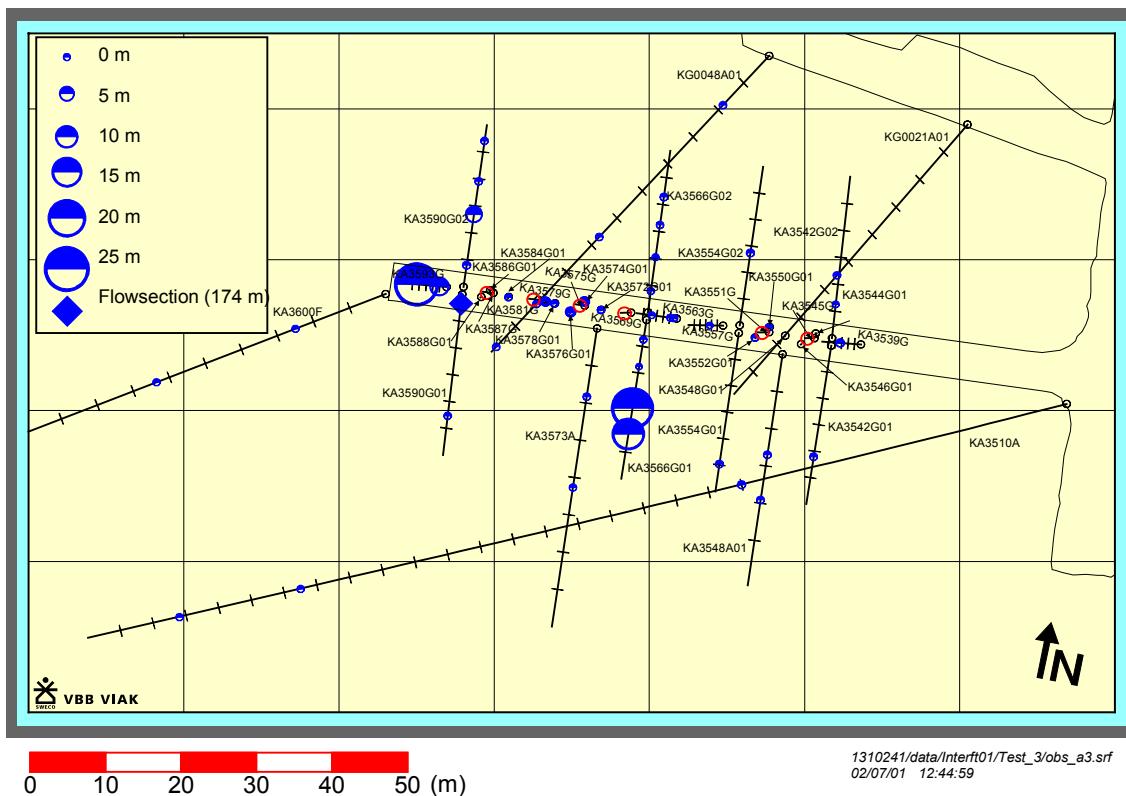


Figure 8-5 Drawdown during flowing of KA3590G01:3 (Interference test 1:3) - plan view.

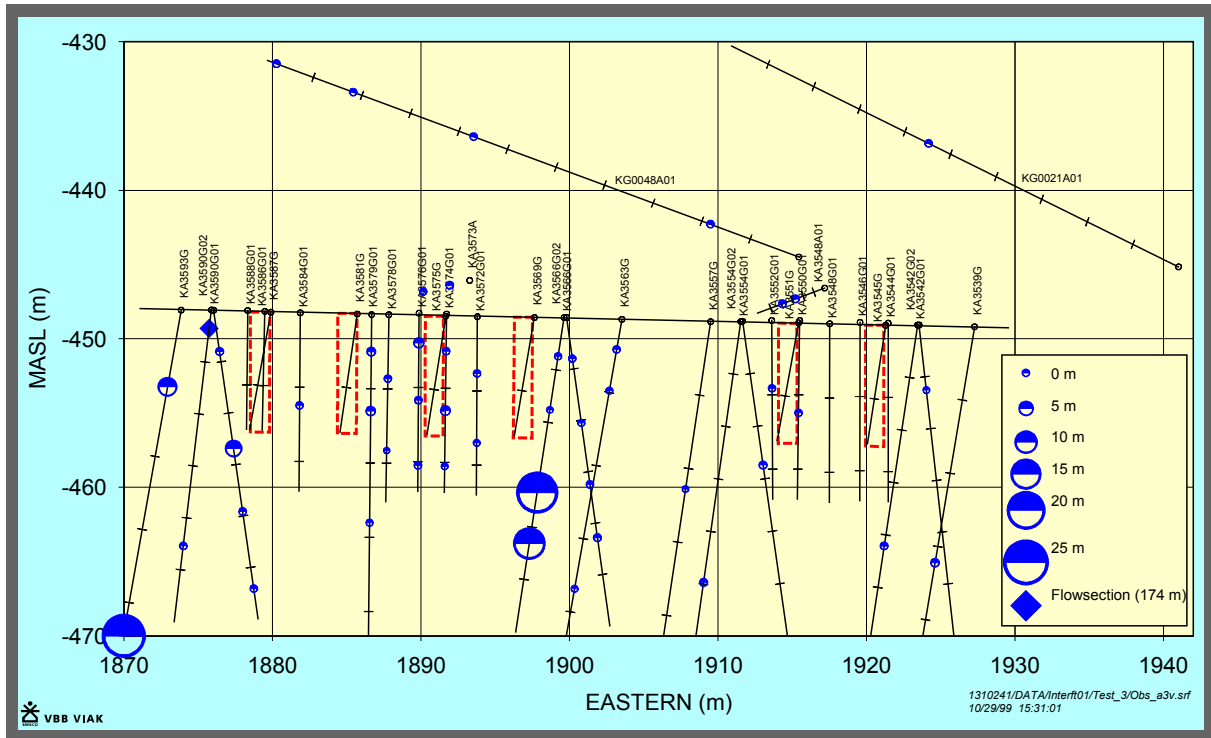


Figure 8-6 Drawdown during flowing of KA3590G01:3 (Interference test 1:3) - vertical view.

The test gives a certain indication of the same hydraulic feature, observed during test 1:1, located south of the tunnel. The response time in KA3566G01 is as short as the response time in KA3590G01 during test 1:1. The evaluated transmissivity for the tests section is $1.3 \cdot 10^{-7} \text{ m}^2/\text{s}$, with the evaluation time for this section being 3 - 8 minutes. In most cases the evaluation time of the observation sections are within that time interval. The evaluated transmissivity is twice as high as the transmissivity from test 1:1. The values are still within the same order of magnitude. It is noted that as during test 1:1 neither KG0048A01 nor KA3573A responds until very late. There does not seem to exist a direct connection between these bore holes and KA3566G01 or KA3590G01.

The evaluated transmissivity and storage coefficient KA3566G01:2 are $8.0 \cdot 10^{-8} \text{ m}^2/\text{s}$ and $4.7 \cdot 10^{-8}$ respectively. These values are close to the parameters evaluated, in KA3590G01:3, during test 1:1.

Table 8-9 Interference test results for KA3590G01, 1.30 - 6.80 m. (r = aprox. distance from flowing bore hole section to observation bore hole section, t_L = time lag for a pressure response of 0.1 m to be registered in an observation section, T = transmissivity, S = storage coefficient, S^* = storage coefficient from diffusivity, η .) The response is classified as 1 = no response (< 0.1 m), 2 = some response (0.1 m - 1.0 m) and 3 = good response (> 1.0 m). P_0 = Initial pressure before opening of the valve, P_p = Pressure just before closing the valve, P_f = Pressure at the end of the pressure build-up period.

Observation borehole	Secup (m)	Seclow (m)	Hydraulic centre of borehole (m)	r (m)	t_L (recovery) (min)	r^2 / t_L (m ² /s)	η (m ² /s)	T_{EVAL} (m ² /s)	S (-)	S^* (-)	Response (0 = no, 1 = some, 2 = good response)	$P_0 - P_p$ (kPa)	$P_f - P_p$ (kPa)	Comments
KA3510A:1	122.02	150.00	136.00	87.08	250	5.06E-01	8.34E-02	-	-	-	1	-0.2	1	Not evaluable
KA3510A:2	114.02	121.02	117.50	72.40	-	-	-	-	-	-	0	0	0.7	No response
KA3510A:3	4.52	113.02	50.00	49.81	10	4.13E+00	2.78E-01	-	-	-	1	5.6	6.6	Not evaluable
KA3539G:1	0.30	30.01	16.11	51.61	-	-	-	-	-	-	0	7.2	2	No response
KA3542G01:1	0.30	30.04	21.05	51.87	40	1.12E+00	1.09E-01	-	-	-	1	2.5	3.5	Not evaluable
KA3542G02:1	0.30	30.01	6.28	48.47	-	-	-	-	-	-	0	-3.7	3.6	No response
KA3548A01:1	15.00	30.00	19.56	46.57	30	1.20E+00	1.08E-01	3.2E-06	4.1E-06	3.0E-05	1	2	3.6	
KA3548A01:2	10.00	14.00	13.49	44.30	35	9.35E-01	8.76E-02	-	-	-	1	2.4	4	Not evaluable
KA3550G01:1	0.30	12.03	6.21	40.20	-	-	-	-	-	-	0	0	0.4	No response
KA3552G01:1	0.30	12.01	4.56	38.37	-	-	-	-	-	-	0	-0.8	5.2	No response
KA3554G01:1	0.30	30.01	24.83	43.04	15	2.06E+00	1.53E-01	2.8E-06	2.4E-06	1.8E-05	1	3.3	4.9	
KA3554G02:1	0.30	30.01	13.69	38.99	120	2.11E-01	2.85E-02	-	-	-	1	3.9	3.9	Not evaluable
KA3557G:1	0.30	30.04	11.40	33.96	-	-	-	-	-	-	0	-5.1	0.6	No response
KA3563G01:1	9.30	30.00	18.42	30.25	75	2.03E-01	2.39E-02	-	-	-	1	-3	9.7	Not evaluable
KA3563G01:2	3.80	8.30	4.87	27.33	70	1.78E-01	2.05E-02	-	-	-	1	-2.9	9.9	Not evaluable
KA3563G01:3	1.30	2.80	2.05	27.53	-	-	-	-	-	-	0	0.2	0	No response
KA3566G01:1	20.80	30.01	21.57	31.19	0.9	1.80E+01	7.48E-01	8.0E-08	7.5E-08	1.1E-07	2	161.4	141.1	
KA3566G01:2	12.30	19.80	16.71	28.32	0.5	2.67E+01	1.01E+00	8.0E-08	4.7E-08	7.9E-08	2	225	196.3	
KA3566G01:3	7.30	11.30	8.81	25.01	1.5	6.95E+00	3.15E-01	1.8E-06	6.6E-07	5.7E-06	2	-5.7	30.9	
KA3566G01:4	1.30	6.30	3.70	24.04	1.9	5.07E+00	2.40E-01	4.1E-06	1.0E-06	1.7E-05	1	-1.2	9.4	
KA3566G02:1	19.30	30.01	21.41	32.89	160	1.13E-01	1.65E-02	-	-	-	1	3.1	3.3	Not evaluable
KA3566G02:2	12.30	18.30	16.23	29.61	200	7.31E-02	1.14E-02	-	-	-	1	0.6	2.5	Not evaluable
KA3566G02:3	7.80	11.30	10.25	26.58	200	5.89E-02	9.17E-03	-	-	-	1	-1.7	3.9	Not evaluable
KA3566G02:4	1.30	6.80	3.99	24.59	230	4.38E-02	7.08E-03	-	-	-	1	-0.6	1.1	Not evaluable
KA3572G01:1	6.30	12.00	8.49	19.61	110	5.83E-02	7.67E-03	-	-	-	1	-3.9	9.6	Not evaluable
KA3572G01:2	1.30	5.30	3.82	18.31	250	2.24E-02	3.69E-03	-	-	-	1	0.2	1	Not evaluable
KA3573A:1	18.00	40.07	21.34	28.41	250	5.38E-02	8.88E-03	-	-	-	1	0.2	1.4	Not evaluable
KA3573A:2	4.50	17.00	9.16	20.55	30	2.35E-01	2.11E-02	-	-	-	1	1.6	3.7	Not evaluable
KA3574G01:1	8.80	12.00	10.25	18.38	85	6.62E-02	8.07E-03	-	-	-	2	-3.9	10.2	Not evaluable
KA3574G01:2	5.30	7.80	6.50	16.84	-	-	-	-	-	-	0	17	-45.4	No response
KA3574G01:3	1.30	4.30	2.50	16.03	-	-	-	-	-	-	0	0.6	-0.8	No response
KA3576G01:1	8.80	12.01	10.25	16.85	-	-	-	-	-	-	0	1.1	-3.4	No response
KA3576G01:2	3.80	7.80	5.86	14.93	-	-	-	-	-	-	0	0.4	-0.7	No response
KA3576G01:3	1.30	2.80	2.00	14.19	-	-	-	-	-	-	0	19.6	-50.5	No response
KA3578G01:1	6.80	12.58	9.14	14.51	65	5.40E-02	6.07E-03	-	-	-	2	-7.6	20.9	Not evaluable
KA3578G01:2	1.30	5.80	4.30	12.50	-	-	-	-	-	-	0	0.6	-0.2	No response
KA3579G01:1	9.30	22.65	14.02	16.97	190	2.53E-02	3.88E-03	-	-	-	1	-2.3	9	Not evaluable
KA3579G01:2	5.30	8.30	6.50	12.22	-	-	-	-	-	-	0	14.8	-38.2	No response
KA3579G01:3	1.30	4.30	2.50	11.03	-	-	-	-	-	-	0	9.4	-26.2	No response
KA3584G01:1	0.30	12.00	6.24	8.05	-	-	-	-	-	-	0	-0.2	0.2	No response
KA3590G01:1	17.30	30.06	22.70	20.94	0.1	7.31E+01	2.23E+00	-	-	-	1	0.8	3.3	Not evaluable
KA3590G01:2	7.80	16.30	8.56	6.80	0.05	1.54E+01	4.33E-01	-	-	-	2	-2010	16.8	Not evaluable
KA3590G01:3	1.30	6.80	1.76	0.00	-	-	-	1.3E-07	-	-	-	1743.8	1595.3	
KA3590G02:1	23.30	30.05	27.06	27.97	230	5.67E-02	9.16E-03	-	-	-	1	0.6	1.3	Not evaluable
KA3590G02:2	17.30	22.30	19.56	20.51	170	4.12E-02	6.14E-03	-	-	-	1	1.8	3.3	Not evaluable
KA3590G02:3	8.30	16.30	13.44	14.45	55	6.33E-02	6.77E-03	4.3E-08	6.9E-06	6.4E-06	2	61.4	45.4	
KA3590G02:4	1.20	7.20	4.00	5.39	-	-	-	-	-	-	0	4	-3.8	No response
KA3593G01:1	8.30	30.02	22.13	21.51	1.7	4.54E+00	2.10E-01	4.3E-08	1.6E-07	2.0E-07	2	238	206.3	
KA3593G01:2	1.30	7.30	5.24	5.35	12	3.98E-02	2.80E-03	-	-	-	2	76	59.7	Not evaluable
KA3600F:1	22.00	50.10	31.78	40.71	-	-	-	-	-	-	0	0	0.9	No response
KA3600F:2	4.50	21.00	12.51	21.86	250	3.19E-02	5.26E-03	-	-	-	1	-0.2	0.6	Not evaluable
KG0021A01:1	0.00	48.82	27.41	50.15	130	3.22E-01	4.45E-02	-	-	-	1	0.9	0.9	Not evaluable
KG0048A01:1	49.00	54.69	53.81	19.26	20	3.09E-01	2.48E-02	-	-	-	1	1.4	3.5	Not evaluable
KG0048A01:2	41.00	48.00	45.90	18.63	30	1.93E-01	1.73E-02	-	-	-	1	0.9	3.2	Not evaluable
KG0048A01:3	30.00	40.00	33.50	23.71	40	2.34E-01	2.28E-02	-	-	-	1	1.1	2.7	Not evaluable
KG0048A01:4	4.00	29.00	9.12	43.38	220	1.43E-01	2.28E-02	-	-	-	1	0.9	0.7	Not evaluable

8.4.4 Interference test 1:4

The test was carried out in KA3590G01, section 7.80 - 16.30 m . The flow period was for 10 minutes with a final flow of 0.398 L/min, while the pressure build-up time was 30 minutes. In Figure 8-7 and Figure 8-8, the pressure drawdown recordings are shown and in Table 8-11, the interference test results are presented. Diagrams of evaluated borehole sections are presented in Appendix 5.

This test was carried out as a function test due to the malfunction of one of the packers during test 1:3.

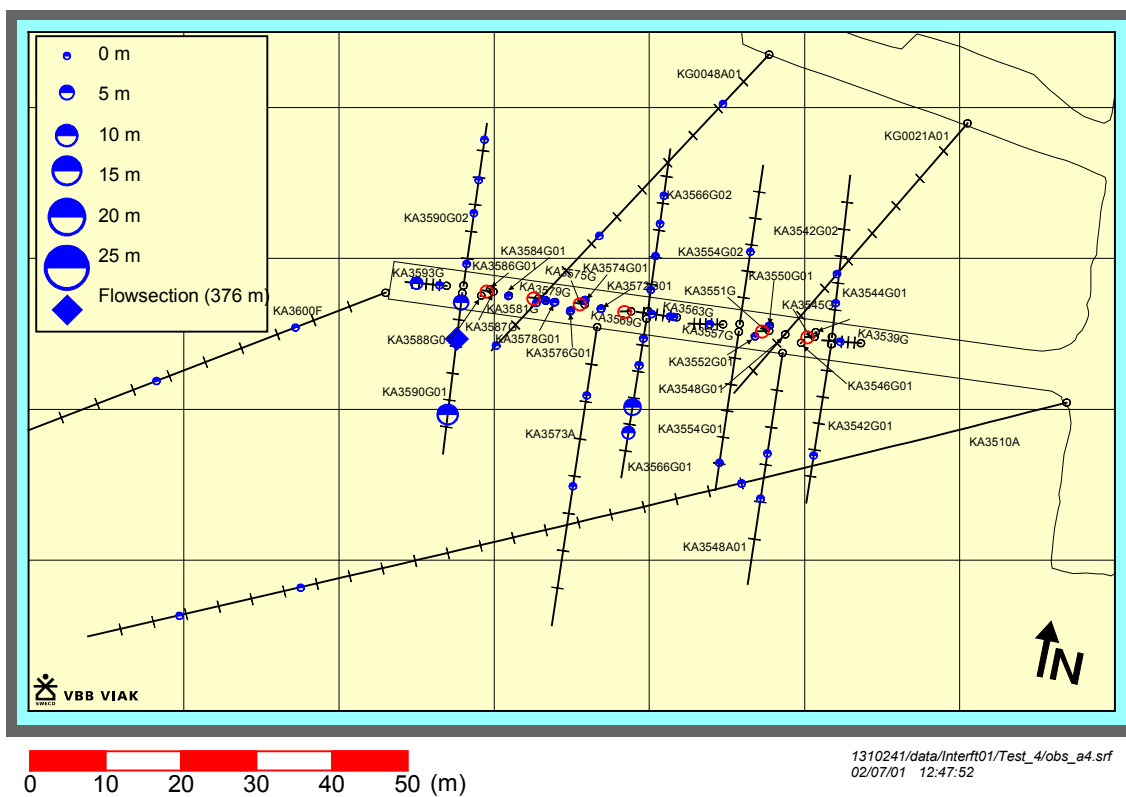


Figure 8-7 Drawdown during flowing of KA3590G01:2 (Interference test 1:4) - plan view.

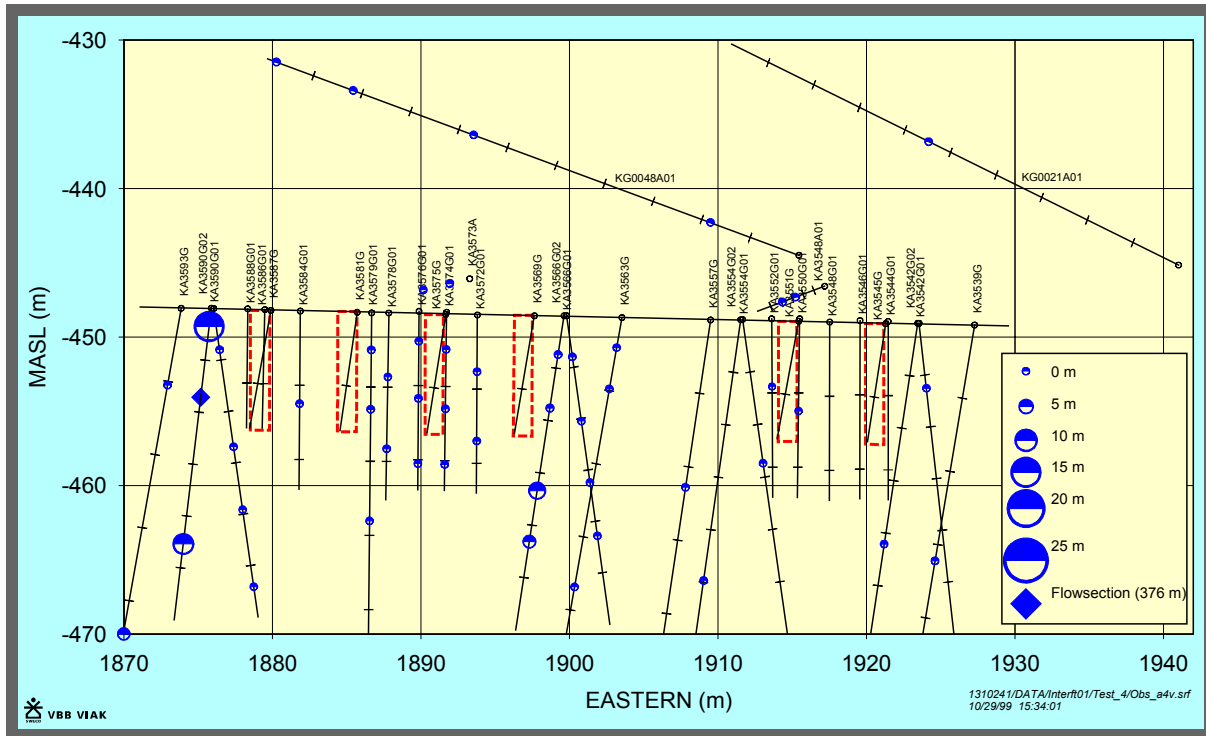


Figure 8-8 Drawdown during flowing of KA3590G01:2 (Interference test 1:4) - vertical view.

This very short test still show the indication of the south feature indicated in test 1:1 and 1:3. The evaluated transmissivity of the test section is $1.4 \cdot 10^{-7} \text{ m}^2/\text{s}$, with the evaluation time for this section being 1 - 2 minutes. The evaluated transmissivity is in the same order of magnitude as the evaluated transmissivity of test 1:1, 1:3 and 1:6.

Table 8-10 Interference test results for KA3590G01, 7.80 - 16.30 m. (r = aprox. distance from flowing bore hole section to observation bore hole section, t_L = time lag for a pressure response of 0.1 m to be registered in an observation section, T = transmissivity, S = storage coefficient, S^* = storage coefficient from diffusivity, η .) The response is classified as 1 = no response (< 0.1 m), 2 = some response (0.1 m - 1.0 m) and 3 = good response (> 1.0 m). P_0 = Initial pressure before opening of the valve, P_p = Pressure just before closing the valve, P_f = Pressure at the end of the pressure build-up period.

Observation borehole	Secup (m)	Seclow (m)	Hydraulic centre of borehole (m)	r (m)	t_L (recovery) (min)	r^2 / t_L (m ² /s)	η (m ² /s)	T_{EVAL} (m ² /s)	S (-)	S^* (-)	Response (0 = no, 1 = some, 2 = good response)	$P_0 - P_p$ (kPa)	$P_f - P_p$ (kPa)	Comments
KA3510A:1	122.02	150.00	136.00	80.91	-	-	-	-	-	-	0	0	0.2	No response
KA3510A:2	114.02	121.02	117.50	65.93	-	-	-	-	-	-	0	0	0.3	No response
KA3510A:3	4.52	113.02	50.00	45.86	-	-	-	-	-	-	0	2.3	0	No response
KA3539G:1	0.30	30.01	16.11	50.64	-	-	-	-	-	-	0	1.5	-0.8	No response
KA3542G01:1	0.30	30.04	21.05	49.53	-	-	-	-	-	-	0	0.2	-0.8	No response
KA3542G02:1	0.30	30.01	6.28	49.08	7	5.74E+00	9.51E-01	-	-	-	1	0	9	Not evaluable
KA3548A01:1	15.00	30.00	19.56	44.98	-	-	-	-	-	-	0	1.4	0	No response
KA3548A01:2	10.00	14.00	13.49	43.35	-	-	-	-	-	-	0	0.4	-0.4	No response
KA3550G01:1	0.30	12.03	6.21	40.29	-	-	-	-	-	-	0	-1.6	3.1	No response
KA3552G01:1	0.30	12.01	4.56	38.47	-	-	-	-	-	-	0	-3.5	-2.7	No response
KA3554G01:1	0.30	30.01	24.83	39.60	-	-	-	-	-	-	0	1.4	0.4	No response
KA3554G02:1	0.30	30.01	13.69	39.82	-	-	-	-	-	-	0	-0.2	0.4	No response
KA3557G:1	0.30	30.04	11.40	33.25	-	-	-	-	-	-	0	0.4	-0.2	No response
KA3563G01:1	9.30	30.00	18.42	28.42	-	-	-	-	-	-	0	0.2	0.4	No response
KA3563G01:2	3.80	8.30	4.87	27.67	-	-	-	-	-	-	0	-0.1	0.2	No response
KA3563G01:3	1.30	2.80	2.05	28.34	-	-	-	-	-	-	0	-0.3	0	No response
KA3566G01:1	20.80	30.01	21.57	27.18	3	4.10E+00	5.38E-01	1.6E-08	5.5E-08	3.0E-08	2	36.8	37.7	No response
KA3566G01:2	12.30	19.80	16.71	25.18	0.8	1.32E+01	1.18E+00	-	-	-	2	64.2	68.1	Not evaluable
KA3566G01:3	7.30	11.30	8.81	23.77	1.4	6.73E+00	7.04E-01	-	-	-	1	4.1	5.3	Not evaluable
KA3566G01:4	1.30	6.30	3.70	24.23	2	4.89E+00	5.69E-01	-	-	-	1	2.5	2.9	Not evaluable
KA3566G02:1	19.30	30.01	21.41	34.06	-	-	-	-	-	-	0	0	0.2	No response
KA3566G02:2	12.30	18.30	16.23	30.87	-	-	-	-	-	-	0	0.3	0	No response
KA3566G02:3	7.80	11.30	10.25	27.93	-	-	-	-	-	-	0	0	0	No response
KA3566G02:4	1.30	6.80	3.99	25.99	-	-	-	-	-	-	0	0.3	0.5	No response
KA3572G01:1	6.30	12.00	8.49	19.23	-	-	-	-	-	-	0	0	-0.6	No response
KA3572G01:2	1.30	5.30	3.82	19.11	-	-	-	-	-	-	0	0.4	0.4	No response
KA3573A:1	18.00	40.07	21.34	25.65	-	-	-	-	-	-	0	0.4	0	No response
KA3573A:2	4.50	17.00	9.16	19.89	-	-	-	-	-	-	0	0.8	0.3	No response
KA3574G01:1	8.80	12.00	10.25	17.79	-	-	-	-	-	-	0	0.2	-1	No response
KA3574G01:2	5.30	7.80	6.50	17.27	-	-	-	-	-	-	0	0.8	-3	No response
KA3574G01:3	1.30	4.30	2.50	17.60	-	-	-	-	-	-	0	0	-0.2	No response
KA3576G01:1	8.80	12.01	10.25	15.71	-	-	-	-	-	-	0	0.5	-1.6	No response
KA3576G01:2	3.80	7.80	5.86	15.11	-	-	-	-	-	-	0	0	0	No response
KA3576G01:3	1.30	2.80	2.00	15.61	-	-	-	-	-	-	0	0.4	-2.5	No response
KA3578G01:1	6.80	12.58	9.14	13.86	-	-	-	-	-	-	0	0.4	-0.3	No response
KA3578G01:2	1.30	5.80	4.30	13.57	-	-	-	-	-	-	0	0	0	No response
KA3579G01:1	9.30	22.65	14.02	15.01	-	-	-	-	-	-	0	-0.2	0	No response
KA3579G01:2	5.30	8.30	6.50	12.56	-	-	-	-	-	-	0	1.4	-0.7	No response
KA3579G01:3	1.30	4.30	2.50	12.96	-	-	-	-	-	-	0	1.1	-2	No response
KA3584G01:1	0.30	12.00	6.24	8.75	-	-	-	-	-	-	0	0	0	No response
KA3590G01:1	17.30	30.06	22.70	14.14	0.10	3.33E+01	1.79E+00	-	-	-	2	89.7	86.2	Not evaluable
KA3590G01:2	7.80	16.30	8.56	0.00	-	-	-	1.4E-07	-	-	-	3759.7	1718.6	
KA3590G01:3	1.30	6.80	1.76	6.80	0.1	7.71E+00	4.13E-01	-	-	-	2	1358.5	1487.4	Not evaluable
KA3590G02:1	23.30	30.05	27.06	29.55	-	-	-	-	-	-	0	0.1	-0.3	No response
KA3590G02:2	17.30	22.30	19.56	22.55	-	-	-	-	-	-	0	0.1	0	No response
KA3590G02:3	8.30	16.30	13.44	17.15	-	-	-	-	-	-	0	0.2	-0.6	No response
KA3590G02:4	1.20	7.20	4.00	10.52	5	3.69E-01	5.59E-02	-	-	-	2	0.2	-1.2	Not evaluable
KA3593G01:1	8.30	30.02	22.13	18.21	-	-	-	-	-	-	0	33.7	31.9	No response
KA3593G01:2	1.30	7.30	5.24	7.51	-	-	-	-	-	-	0	1.4	0	No response
KA3600F:1	22.00	50.10	31.78	39.82	-	-	-	-	-	-	0	0	0	No response
KA3600F:2	4.50	21.00	12.51	22.36	-	-	-	-	-	-	0	-0.2	-0.2	No response
KG0021A01:1	0.00	48.82	27.41	52.64	-	-	-	-	-	-	0	0	-0.9	No response
KG0048A01:1	49.00	54.69	53.81	23.16	-	-	-	-	-	-	0	2.2	0.4	No response
KG0048A01:2	41.00	48.00	45.90	23.57	-	-	-	-	-	-	0	1.6	0.5	No response
KG0048A01:3	30.00	40.00	33.50	28.93	-	-	-	-	-	-	0	0.3	0	No response
KG0048A01:4	4.00	29.00	9.12	47.82	-	-	-	-	-	-	0	-0.6	-0.6	No response

8.4.5 Interference test 1:5

The test was carried out in KA3590G02, section 23.30 - 30.05 m . The flow period was for 445 minutes with a final flow of 1.710 L/min, while the pressure build-up time was 3840 minutes. In Figure 8-9 and Figure 8-10, the pressure drawdown recordings are shown and in Table 8-12, the interference test results are presented.

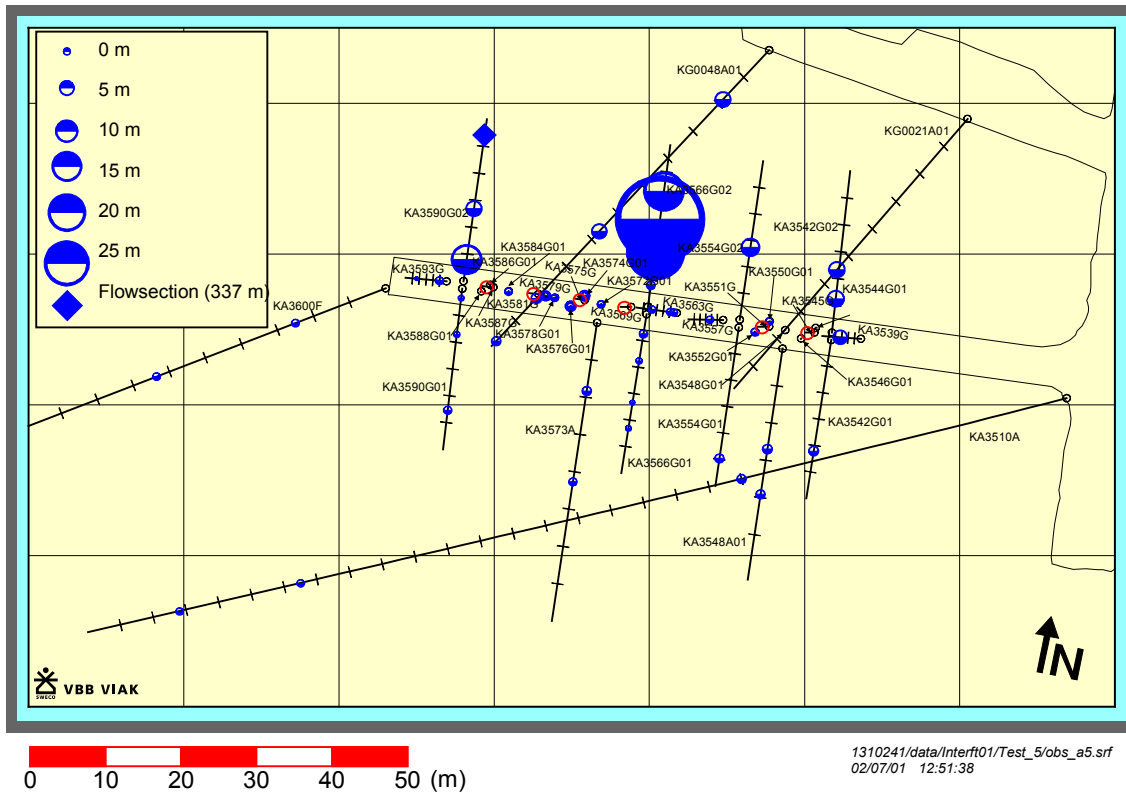


Figure 8-9 Drawdown during flowing of KA3590G02:1 (Interference test 1:5) - plan view.

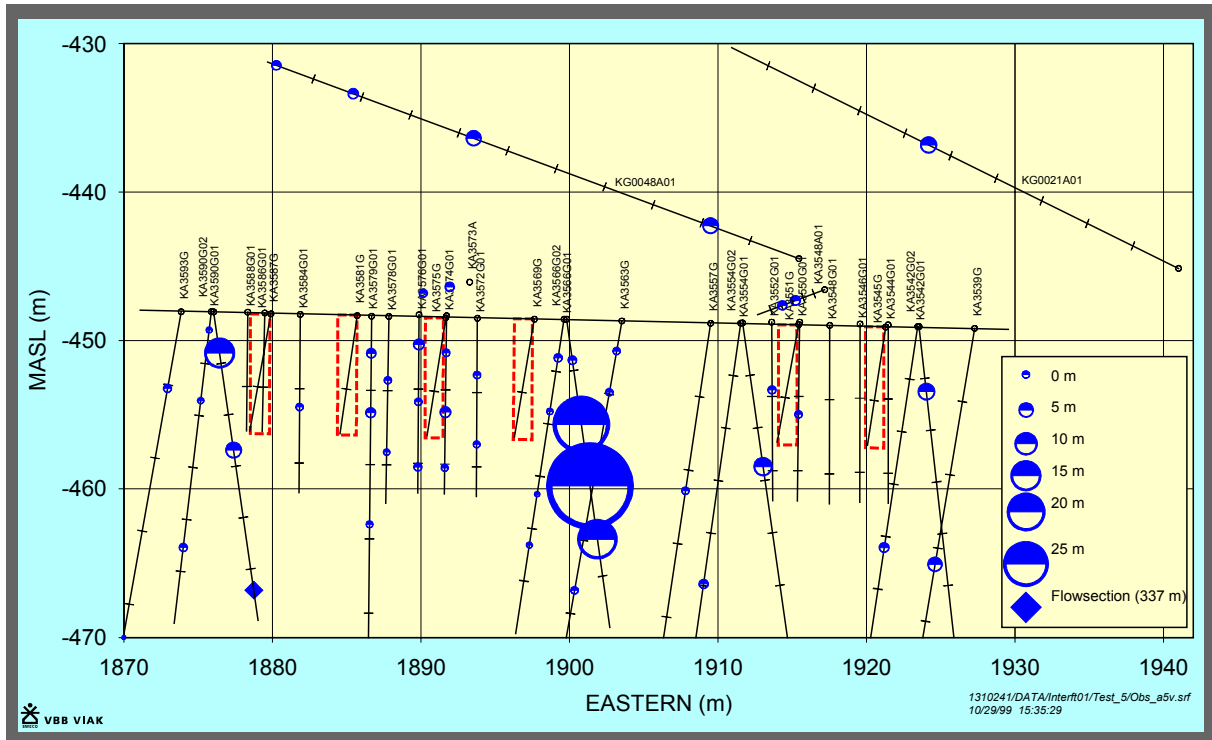


Figure 8-10 Drawdown during flowing of KA3590G02:1 (Interference test 1:5) - vertical view.

This test indicates a hydraulic feature, striking WNW, north of the tunnel. The response time in KA3566G02 is almost as short as for the tests south of the tunnel. Further east the responses are again more diffuse as noted in test 1:2 but still there may exist a hydraulic feature or system of hydraulic features.

The evaluated transmissivity for the test section is $1.5 \cdot 10^{-7} \text{ m}^2/\text{s}$, with the evaluation time for this section being 0.5 - 1.8 minutes.

The evaluated transmissivity and storage coefficient of KA3566G02:2 are $5.8 \cdot 10^{-8} \text{ m}^2/\text{s}$ and $1.5 \cdot 10^{-7}$ respectively.

Table 8-11 Interference test results for KA3590G02, 23.30 - 30.05 m. (r = aprox. distance from flowing bore hole section to observation bore hole section, t_L = time lag for a pressure response of 0.1 m to be registered in an observation section, T = transmissivity, S = storage coefficient, S^* = storage coefficient from diffusivity, η .) The response is classified as 1 = no response (< 0.1 m), 2 = some response (0.1 m - 1.0 m) and 3 = good response (> 1.0 m). P_0 = Initial pressure before opening of the valve, P_p = Pressure just before closing the valve, P_f = Pressure at the end of the pressure build-up period.

Observation borehole	Secup (m)	Seclow (m)	Hydraulic centre of borehole (m)	r (m)	t_L (recovery) (min)	r^2 / t_L (m ² /s)	η (m ² /s)	T_{EVAL} (m ² /s)	S (-)	S^* (-)	Response (0 = no, 1 = some, 2 = good response)	$P_0 - P_p$ (kPa)	$P_f - P_p$ (kPa)	Comments
KA3510A:1	122.02	150.00	136.00	89.53	250	5.34E-01	8.37E-02	-	-	-	1	0.6	0.1	Not evaluable
KA3510A:2	114.02	121.02	117.50	75.77	250	3.83E-01	5.99E-02	-	-	-	1	1.8	2.3	Not evaluable
KA3510A:3	4.52	113.02	50.00	56.77	20	2.69E+00	2.04E-01	-	-	-	2	12.7	5.9	Not evaluable
KA3539G:1	0.30	30.01	16.11	53.13	35	1.34E+00	1.19E-01	5.7E-07	2.2E-06	4.8E-06	2	46.4	61.9	
KA3542G01:1	0.30	30.04	21.05	59.68	27	2.20E+00	1.81E-01	1.5E-06	4.4E-06	8.3E-06	2	16.2	17.2	
KA3542G02:1	0.30	30.01	6.28	51.95	10	4.50E+00	2.88E-01	6.3E-07	1.2E-06	2.2E-06	2	62.2	60.7	
KA3548A01:1	15.00	30.00	19.56	62.45	20	3.25E+00	2.47E-01	2.7E-06	4.5E-06	1.1E-05	2	12.3	14.1	
KA3548A01:2	10.00	14.00	13.49	58.66	28	2.05E+00	1.70E-01	1.3E-06	4.4E-06	7.6E-06	2	15.8	17.2	
KA3550G01:1	0.30	12.03	6.21	45.77	-	-	-	-	-	-	0	1.1	2.9	No response
KA3552G01:1	0.30	12.01	4.56	45.61	-	-	-	-	-	-	0	5.5	10.2	No response
KA3554G01:1	0.30	30.01	24.83	52.46	20	2.29E+00	1.74E-01	2.8E-06	8.5E-06	1.6E-05	2	11.7	13.3	
KA3554G02:1	0.30	30.01	13.69	38.28	7	3.49E+00	2.06E-01	4.8E-07	1.3E-06	2.3E-06	2	72.8	81.2	
KA3557G:1	0.30	30.04	11.40	38.57	-	-	-	-	-	-	0	1.3	3.9	No response
KA3563G01:1	9.30	30.00	18.42	31.63	7	2.38E+00	1.41E-01	-	-	-	2	1	31.2	Not evaluable
KA3563G01:2	3.80	8.30	4.87	36.05	8	2.71E+00	1.65E-01	-	-	-	2	1.1	31.3	Not evaluable
KA3563G01:3	1.30	2.80	2.05	37.53	300	7.82E-02	1.28E-02	-	-	-	1	0.5	0.2	Not evaluable
KA3566G01:1	20.80	30.01	21.57	43.16	30	1.03E+00	8.78E-02	-	-	-	1	-9.4	1.8	Not evaluable
KA3566G01:2	12.30	19.80	16.71	40.77	40	6.93E-01	6.37E-02	-	-	-	1	-14.5	-0.4	Not evaluable
KA3566G01:3	7.30	11.30	8.81	37.91	65	3.68E-01	3.90E-02	-	-	-	2	-5.7	39.6	Not evaluable
KA3566G01:4	1.30	6.30	3.70	36.85	7	3.23E+00	1.91E-01	-	-	-	2	6.1	21.9	Not evaluable
KA3566G02:1	19.30	30.01	21.41	24.54	3	3.35E+00	1.66E-01	2.0E-07	9.9E-07	1.2E-06	2	213.4	338.1	
KA3566G02:2	12.30	18.30	16.23	26.18	1.2	9.52E+00	4.01E-01	5.8E-08	1.5E-07	1.4E-07	2	528.4	679.8	
KA3566G02:3	7.80	11.30	10.25	29.13	55	2.57E-01	2.59E-02	2.7E-08	1.4E-06	1.0E-06	2	328.1	970.4	Slow !!
KA3566G02:4	1.30	6.80	3.99	33.10	3.5	5.22E+00	2.67E-01	-	-	-	2	8.4	569	Not evaluable
KA3572G01:1	6.30	12.00	8.49	28.72	220	6.25E-02	9.45E-03	-	-	-	2	-2.9	31.3	Not evaluable
KA3572G01:2	1.30	5.30	3.82	30.63	100	1.56E-01	1.88E-02	-	-	-	1	0.6	7.1	Not evaluable
KA3573A:1	18.00	40.07	21.34	51.39	40	1.10E+00	1.01E-01	-	-	-	1	5.5	6.3	Not evaluable
KA3573A:2	4.50	17.00	9.16	41.72	18	1.61E+00	1.19E-01	2.9E-06	9.2E-06	2.4E-05	2	12.5	14.3	
KA3574G01:1	8.80	12.00	10.25	26.20	150	7.63E-02	1.04E-02	-	-	-	2	-2.6	32.5	Not evaluable
KA3574G01:2	5.30	7.80	6.50	27.62	-	-	-	-	-	-	0	23	-151.2	No response
KA3574G01:3	1.30	4.30	2.50	29.58	100	1.46E-01	1.76E-02	-	-	-	1	1.5	1.6	Not evaluable
KA3576G01:1	8.80	12.01	10.25	26.63	-	-	-	-	-	-	0	4.7	-17.6	No response
KA3576G01:2	3.80	7.80	5.86	28.28	-	-	-	-	-	-	0	0.2	-1.2	No response
KA3576G01:3	1.30	2.80	2.00	30.18	-	-	-	-	-	-	0	22.5	-138.6	No response
KA3578G01:1	6.80	12.58	9.14	25.14	50	2.11E-01	2.07E-02	-	-	-	2	-6	62.2	Not evaluable
KA3578G01:2	1.30	5.80	4.30	27.31	-	-	-	-	-	-	0	0.5	-1.4	No response
KA3579G01:1	9.30	22.65	14.02	23.07	90	9.86E-02	1.15E-02	-	-	-	2	-3.4	34.1	Not evaluable
KA3579G01:2	5.30	8.30	6.50	25.66	-	-	-	-	-	-	0	17.3	-237.7	No response
KA3579G01:3	1.30	4.30	2.50	27.77	-	-	-	-	-	-	0	14.7	-193.1	No response
KA3584G01:1	0.30	12.00	6.24	24.33	300	3.29E-02	5.40E-03	-	-	-	1	0.4	0	Not evaluable
KA3590G01:1	17.30	30.06	22.70	36.87	40	5.66E-01	5.21E-02	-	-	-	1	6	-494.9	Not evaluable
KA3590G01:2	7.80	16.30	8.56	29.55	60	2.43E-01	2.51E-02	-	-	-	1	-6.8	-0.4	Not evaluable
KA3590G01:3	1.30	6.80	1.76	27.97	60	2.17E-01	2.25E-02	-	-	-	1	-9.4	0.4	Not evaluable
KA3590G02:1	23.30	30.05	27.06	0.00	-	-	-	1.5E-07	-	-	-	3368.9	3371.2	
KA3590G02:2	17.30	22.30	19.56	7.50	0.1	9.37E+00	2.79E-01	-	-	-	2	1155.1	1167.1	Not evaluable
KA3590G02:3	8.30	16.30	13.44	13.62	0.1	3.09E+01	9.20E-01	-	-	-	2	56.4	64	Not evaluable
KA3590G02:4	1.20	7.20	4.00	23.06	-	-	-	-	-	-	0	150.8	152.6	No response
KA3593G01:1	8.30	30.02	22.13	21.16	35	2.13E-01	1.89E-02	-	-	-	1	-23.9	1.6	Not evaluable
KA3593G01:2	1.30	7.30	5.24	24.30	4	2.46E+00	1.29E-01	-	-	-	2	4.7	21.8	Not evaluable
KA3600F:1	22.00	50.10	31.78	56.76	200	2.68E-01	3.95E-02	-	-	-	1	2.7	3.3	Not evaluable
KA3600F:2	4.50	21.00	12.51	40.60	100	2.75E-01	3.31E-02	-	-	-	1	3	3.6	Not evaluable
KG0021A01:1	0.00	48.82	27.41	57.27	3	1.82E+01	9.04E-01	7.3E-07	5.9E-07	8.1E-07	2	58.6	62	
KG0048A01:1	49.00	54.69	53.81	44.69	17	1.96E+00	1.43E-01	3.1E-06	7.6E-06	2.2E-05	2	13.3	13.8	
KG0048A01:2	41.00	48.00	45.90	40.38	9	3.02E+00	1.89E-01	2.0E-06	4.5E-06	1.1E-05	2	20	19.3	
KG0048A01:3	30.00	40.00	33.50	36.16	5	4.36E+00	2.39E-01	-	-	-	2	51.9	53.1	Not evaluable
KG0048A01:4	4.00	29.00	9.12	39.62	5	5.23E+00	2.88E-01	6.7E-07	1.7E-06	2.3E-06	2	55.2	58	

8.4.6 Interference test 1:6

The test was carried out in KA3590G01, section 1.30 - 6.80 m. It was a repeat test for test 1:3. Before this all packers of KA3590G01 was checked and then reinstalled. The flow period was for 362 minutes with a final flow of 0.330 L/min, while the pressure build-up time was 840 minutes. In Figure 8-11 and Figure 8-12, the pressure drawdown recordings are shown and in Table 8-13, the interference test results are presented.

It is to be observed that KA3566G02:3 was opened for water sampling on March 29 with a pressure drawdown of approximately 2700 kPa and with a flow rate of 0.006 L/min. It is also to be noted that less than an hour before the test start the bottom section of KA3578G01 and the upper section of KA3572G01 were opened for water sampling. The section pressures fell from c. 950 kPa and 250 kPa respectively. The flow rates were low (less than or equal to c. 1 mL/min). The sections were kept open during the whole test period. As a consequence of these activities the following sections show lower initial pressures, P_0 , when compared with interference test 1:3; KA3566G02:3, KA3572G01:2, KA3574G01:2, KA3578G01:1, KA3579G01:2 and KA3579G01:3.

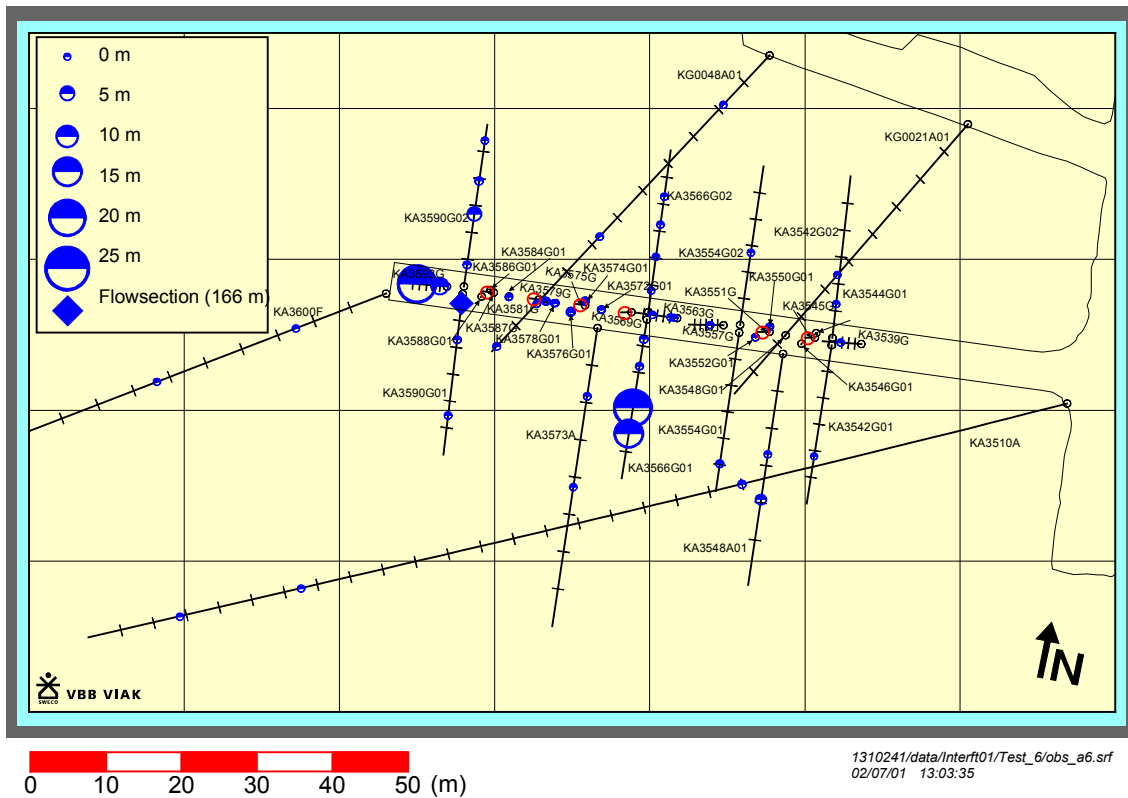


Figure 8-11 Drawdown during flowing of KA3590G01:3 (Interference test 1:6) - plan view.

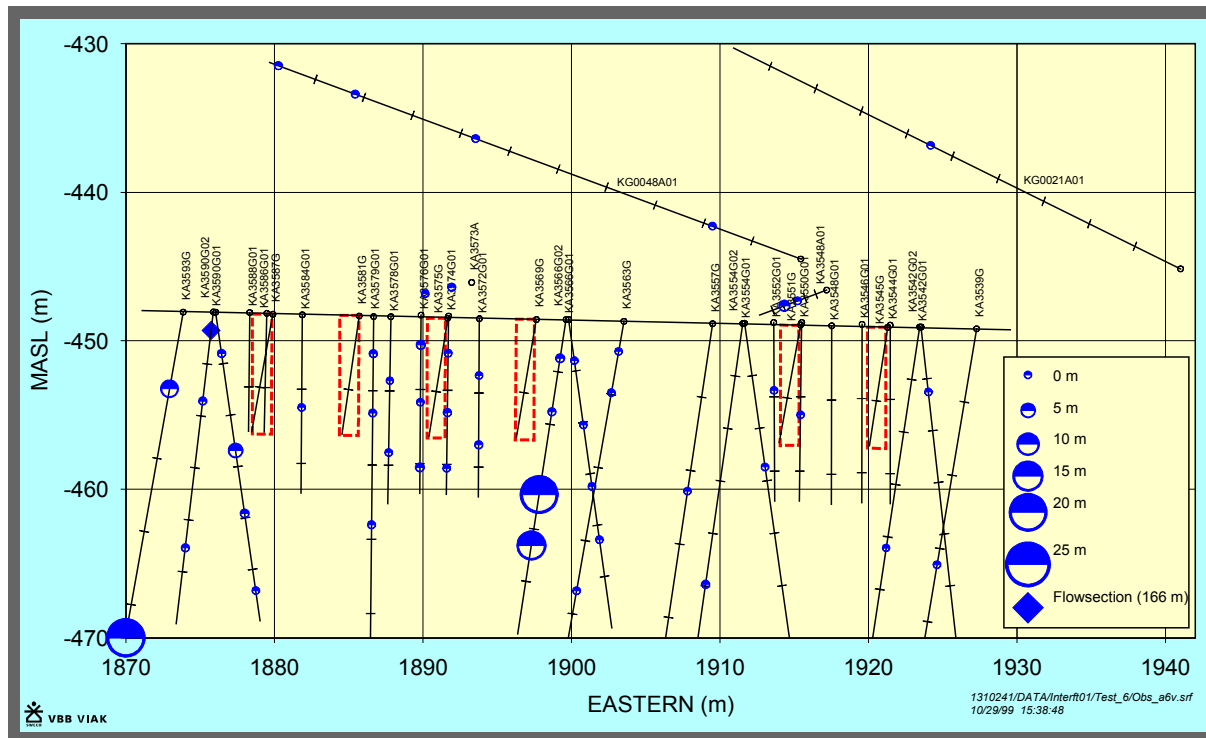


Figure 8-12 Drawdown during flowing of KA3590G01:3 (Interference test 1:6) - vertical view.

The test gives a certain indication of the same hydraulic feature, observed during test 1:1, 1:3 and 1:4 located south of the tunnel. The response time in KA3566G01 is as short as the response time in KA3566G01 during test 1:3. The evaluated transmissivity for the test section is $1.3 \cdot 10^{-7} \text{ m}^2/\text{s}$, with the evaluation time for this section being 3 - 8 minutes. In most cases the evaluation time of the observation sections are within that time interval. The evaluated transmissivity is twice as high as the transmissivity from test 1:1 but the same as in test 1:3. The values are still within the same order of magnitude. It is noted that as during test 1:1 and 1:3 neither KG0048A01 nor KA3573A responds until very late. There does not exist a direct connection between these boreholes and KA3566G01 or KA3590G01.

The evaluated transmissivity and storage coefficient of KA3566G01:2 are $7.5 \cdot 10^{-8} \text{ m}^2/\text{s}$ and $4.3 \cdot 10^{-8}$ respectively. These values are close to the parameters evaluated during test 1:1 and almost identical to the evaluated parameters of test 1:3.

Table 8-12 Interference test results for KA3590G01, 1.30 - 6.80 m. (r = aprox. distance from flowing bore hole section to observation bore hole section, t_L = time lag for a pressure response of 0.1 m to be registered in an observation section, T = transmissivity, S = storage coefficient, S* = storage coefficient from diffusivity, η.) The response is classified as 1 = no response (< 0.1 m), 2 = some response (0.1 m - 1.0 m) and 3 = good response (> 1.0 m). P₀ = Initial pressure before opening of the valve, P_p = Pressure just before closing the valve, P_f = Pressure at the end of the pressure build-up period.

Observation borehole	Secup (m)	Seclow (m)	Hydraulic centre of borehole (m)	r (m)	t _L (recovery) (min)	r ² / t _L (m ² /s)	η (m ² /s)	T _{EVAl} (m ² /s)	S (-)	S* (-)	Response (0 = no, 1 = some, 2 = good response)	Po - Pp (kPa)	Pf - Pp (kPa)	Comments
KA3510A:1	122.02	150.00	136.00	87.08	-	-	-	-	-	-	0	0.9	0.6	No response
KA3510A:2	114.02	121.02	117.50	72.40	200	4.37E-01	6.81E-02	-	-	-	1	0.4	1	Not evaluable
KA3510A:3	4.52	113.02	50.00	49.81	10	4.13E+00	2.78E-01	1.5E-06	1.1E-06	5.4E-06	1	7.2	7	
KA3539G:1	0.30	30.01	16.11	51.61	-	-	-	-	-	-	0	1	0.2	No response
KA3542G01:1	0.30	30.04	21.05	51.87	35	1.28E+00	1.20E-01	-	-	-	2	-1.8	4.1	Not evaluable
KA3542G02:1	0.30	30.01	6.28	48.47	-	-	-	-	-	-	0	0.8	0.6	No response
KA3548A01:1	15.00	30.00	19.56	46.57	25	1.45E+00	1.23E-01	2.4E-06	3.2E-06	1.9E-05	1	24	24.4	
KA3548A01:2	10.00	14.00	13.49	44.30	-	-	-	-	-	-	0	1.3	-0.2	No response
KA3550G01:1	0.30	12.03	6.21	40.20	-	-	-	-	-	-	0	0.4	-0.8	No response
KA3552G01:1	0.30	12.01	4.56	38.37	-	-	-	-	-	-	0	0.6	-0.6	No response
KA3554G01:1	0.30	30.01	24.83	43.04	16	1.93E+00	1.46E-01	2.2E-06	2.7E-06	1.5E-05	1	4.8	4.4	
KA3554G02:1	0.30	30.01	13.69	38.99	150	1.69E-01	2.43E-02	-	-	-	1	0.8	1	Not evaluable
KA3557G:1	0.30	30.04	11.40	33.96	-	-	-	-	-	-	0	0.2	-0.8	No response
KA3563G01:1	9.30	30.00	18.42	30.25	-	-	-	-	-	-	0	1.4	-0.6	No response
KA3563G01:2	3.80	8.30	4.87	27.33	-	-	-	-	-	-	0	1.6	-0.5	No response
KA3563G01:3	1.30	2.80	2.05	27.53	-	-	-	-	-	-	0	0	-0.8	No response
KA3566G01:1	20.80	30.01	21.57	31.19	0.9	1.80E+01	7.49E-01	8.0E-08	7.9E-08	1.1E-07	2	144.2	146.7	
KA3566G01:2	12.30	19.80	16.71	28.32	0.5	2.67E+01	1.01E+00	7.5E-08	4.3E-08	7.4E-08	2	203.3	206.8	
KA3566G01:3	7.30	11.30	8.81	25.01	1.8	5.79E+00	2.71E-01	-	-	-	1	4.3	5.5	Not evaluable
KA3566G01:4	1.30	6.30	3.70	24.04	2.2	4.38E+00	2.13E-01	-	-	-	1	9	-2.2	Not evaluable
KA3566G02:1	19.30	30.01	21.41	32.89	130	1.39E-01	1.92E-02	-	-	-	1	1.1	1.5	Not evaluable
KA3566G02:2	12.30	18.30	16.23	29.61	120	1.22E-01	1.64E-02	-	-	-	1	1.2	1.8	Not evaluable
KA3566G02:3	7.80	11.30	10.25	26.58	-	-	-	-	-	-	0	0.4	-0.8	No response
KA3566G02:4	1.30	6.80	3.99	24.59	-	-	-	-	-	-	0	0.4	-3.7	No response
KA3572G01:1	6.30	12.00	8.49	19.61	-	-	-	-	-	-	0	3.7	-10.6	No response
KA3572G01:2	1.30	5.30	3.82	18.31	-	-	-	-	-	-	0	0.2	-1	No response
KA3573A:1	18.00	40.07	21.34	28.41	100	1.35E-01	1.72E-02	-	-	-	1	1.2	1.6	Not evaluable
KA3573A:2	4.50	17.00	9.16	20.55	25	2.82E-01	2.40E-02	-	-	-	1	3.4	3.6	Not evaluable
KA3574G01:1	8.80	12.00	10.25	18.38	150	3.75E-02	5.40E-03	-	-	-	1	0.4	3.2	Not evaluable
KA3574G01:2	5.30	7.80	6.50	16.84	-	-	-	-	-	-	0	4.5	-6.5	No response
KA3574G01:3	1.30	4.30	2.50	16.03	-	-	-	-	-	-	0	1.6	-2.3	No response
KA3576G01:1	8.80	12.01	10.25	16.85	-	-	-	-	-	-	0	8.6	-16.8	No response
KA3576G01:2	3.80	7.80	5.86	14.93	-	-	-	-	-	-	0	0.2	0.4	No response
KA3576G01:3	1.30	2.80	2.00	14.19	-	-	-	-	-	-	0	10.8	-21.9	No response
KA3578G01:1	6.80	12.58	9.14	14.51	-	-	-	-	-	-	0	0.2	-0.8	No response
KA3578G01:2	1.30	5.80	4.30	12.50	200	1.30E-02	2.03E-03	-	-	-	1	-1.2	1.1	Not evaluable
KA3579G01:1	9.30	22.65	14.02	16.97	-	-	-	-	-	-	0	3.4	-4.1	No response
KA3579G01:2	5.30	8.30	6.50	12.22	-	-	-	-	-	-	0	2.1	-2.6	No response
KA3579G01:3	1.30	4.30	2.50	11.03	-	-	-	-	-	-	0	3.7	-4.3	No response
KA3584G01:1	0.30	12.00	6.24	8.05	-	-	-	-	-	-	0	0	-0.9	No response
KA3590G01:1	17.30	30.06	22.70	20.94	0.1	7.31E+01	2.23E+00	-	-	-	2	3.2	3.7	Not evaluable
KA3590G01:2	7.80	16.30	8.56	6.80	0.1	7.71E+00	2.35E-01	-	-	-	2	4.1	4.5	Not evaluable
KA3590G01:3	1.30	6.80	1.76	0.00	-	-	-	1.3E-07	-	-	-	1524.1	1527.8	
KA3590G02:1	23.30	30.05	27.06	27.97	100	1.30E-01	1.67E-02	-	-	-	1	1	2	Not evaluable
KA3590G02:2	17.30	22.30	19.56	20.51	70	1.00E-01	1.15E-02	2.4E-07	5.6E-06	2.1E-05	1	8.2	9.2	
KA3590G02:3	8.30	16.30	13.44	14.45	48	7.25E-02	7.46E-03	4.4E-08	7.0E-06	5.9E-06	2	47.4	43.1	
KA3590G02:4	1.20	7.20	4.00	5.39	-	-	-	-	-	-	0	4.3	3.1	No response
KA3593G01:1	8.30	30.02	22.13	21.51	1.5	5.14E+00	2.33E-01	4.2E-08	1.5E-07	1.8E-07	2	207.5	210.6	Not evaluable
KA3593G01:2	1.30	7.30	5.24	5.35	10	4.77E-02	3.21E-03	-	-	-	2	68.1	62.8	Not evaluable
KA3600F:1	22.00	50.10	31.78	40.71	200	1.38E-01	2.15E-02	-	-	-	1	0.2	1	Not evaluable
KA3600F:2	4.50	21.00	12.51	21.86	140	5.69E-02	8.03E-03	-	-	-	1	1	1.4	Not evaluable
KG0021A01:1	0.00	48.82	27.41	50.15	100	4.19E-01	5.37E-02	-	-	-	1	-0.2	3	Not evaluable
KG0048A01:1	49.00	54.69	53.81	19.26	25	2.47E-01	2.11E-02	-	-	-	1	3.5	4.2	Not evaluable
KG0048A01:2	41.00	48.00	45.90	18.63	45	1.29E-01	1.30E-02	-	-	-	1	2.5	2.7	Not evaluable
KG0048A01:3	30.00	40.00	33.50	23.71	55	1.70E-01	1.83E-02	-	-	-	1	1.9	2.5	Not evaluable
KG0048A01:4	4.00	29.00	9.12	43.38	100	3.14E-01	4.01E-02	-	-	-	1	0.4	2.9	Not evaluable

8.5 Interference test campaign 2 after drilling campaign 3

Interference test campaign 2 is reported in Forsmark and Rhén (2000b).

8.5.1 Interference test 2:7

The test was carried out in KG0048A01, section 49.00 - 54.69 metres. The flow period was for 85 minutes with a final flow of 2.410 L/min, while the pressure build-up time was 275 minutes. In Figure 8-13 and Figure 8-13, the pressure drawdown recordings are shown and in Table 8-14, the interference test results are presented.

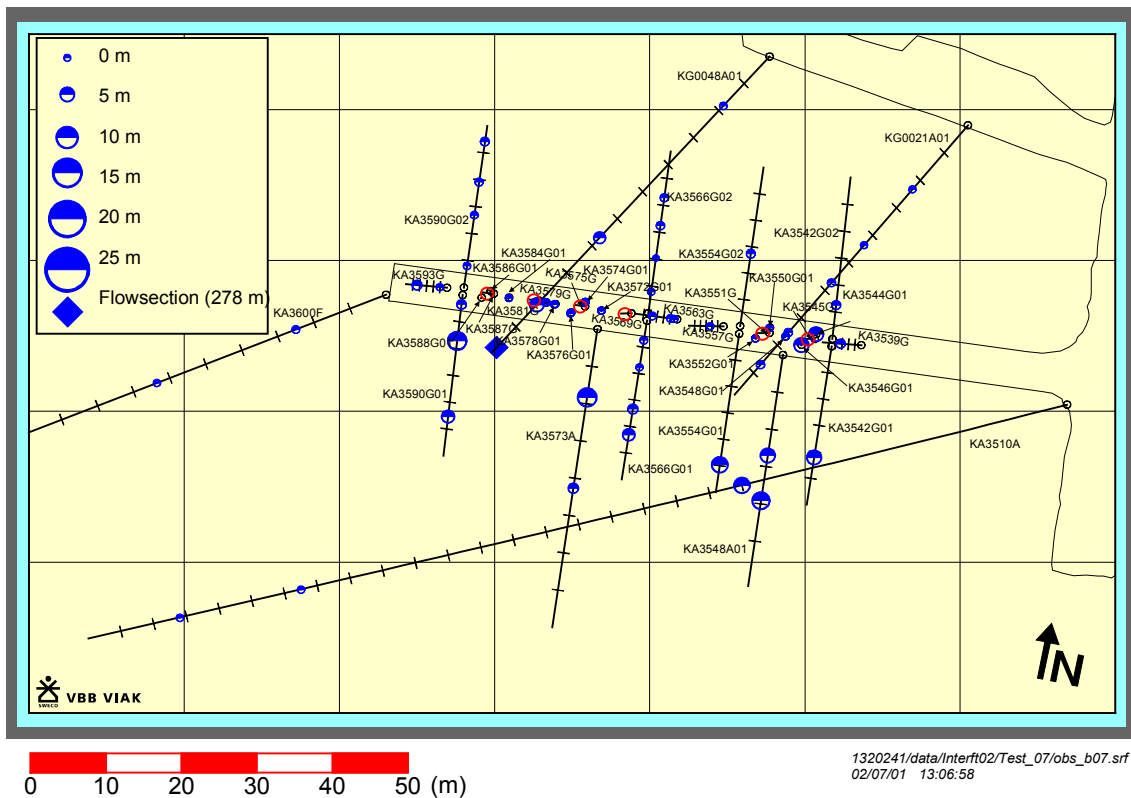


Figure 8-13 Drawdown during flowing of KG0048A01:1 (Interference test 2:7) - plan view.

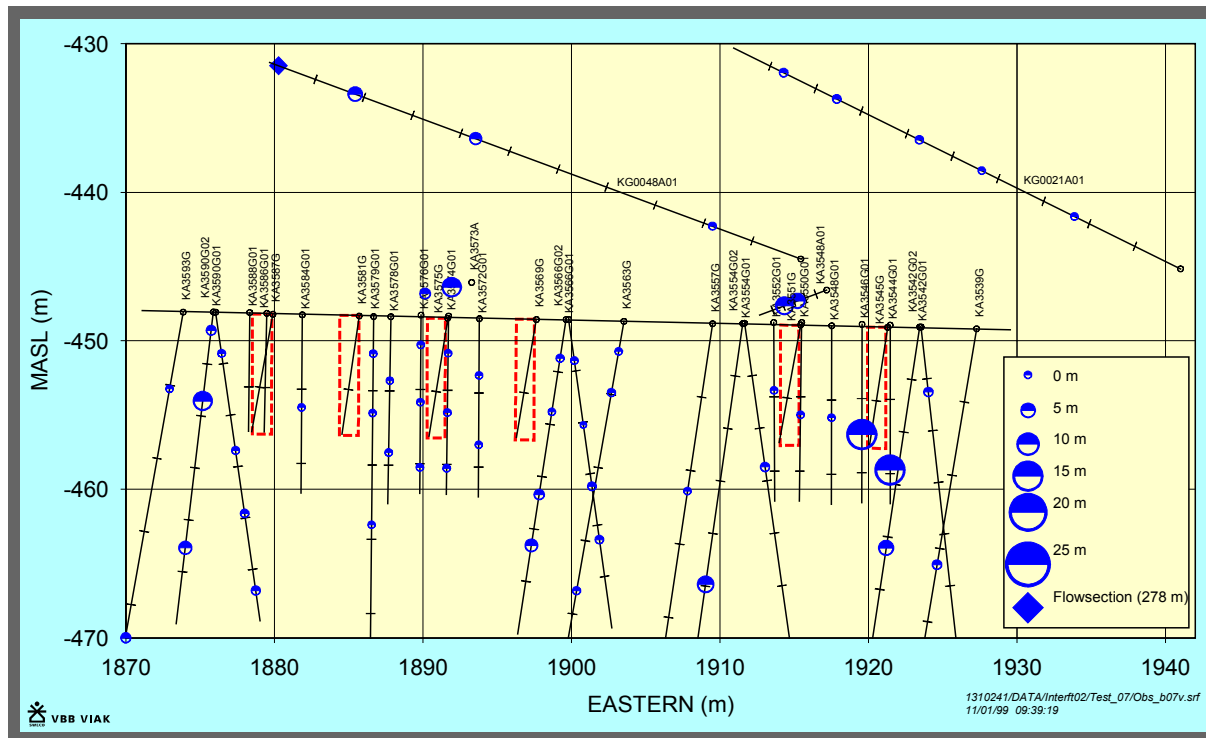


Figure 8-14 Drawdown during flowing of KG0048A01:1 (Interference test 2:7) - vertical view.

This test shows a good connection between the flow section and KA3590G01:2, KA3573A:2, KA3554G01 (whole borehole), KA3510A:3 and finally a very quick and good response in KA3548A01:1. In comparison with the tests during the first interference test campaign, especially 1:1, 1:3 and 1:6 this test seem to activate a structure situated parallel or in the vicinity to the one activated during the earlier test. The sections, which respond during this test, do not respond at all or poorly during the earlier tests. The pressure responses of the sections in KA3566G01 are slow, while the response was fast and distinct during the earlier tests.

The transmissivity of the observation sections with response times less than 1 minute, i.e. the sections mentioned above with the exception of KA3510A:3, is within the range $9.4 \cdot 10^{-7} - 2.9 \cdot 10^{-6} \text{ m}^2/\text{s}$. The transmissivity of the flowing section is evaluated to be $2.5 \cdot 10^{-6} \text{ m}^2/\text{s}$ with the evaluation period 1 – 3 minutes.

The structure activated during this test seem to be a more conductive than the one observed during the earlier tests. The higher flow rate and the higher evaluated values of the transmissivity indicate this.

8.5.2 Interference test 2:8

The test was carried out in KA3554G01, section 22.30 – 30.01 metres. The flow period was for 364 minutes with a final flow of 4.47 L/min, while the pressure build-up time was 1011 minutes. In Figure 8-15 and Figure 8-16, the pressure drawdown recordings are shown and in Table 8-15, the interference test results are presented.

The two lowest sections of KA3539G show almost exactly the same pressures during this test and during the tests 2:9 – 2:14 as well. This was a consequence of a leakage between the two measurement sections.

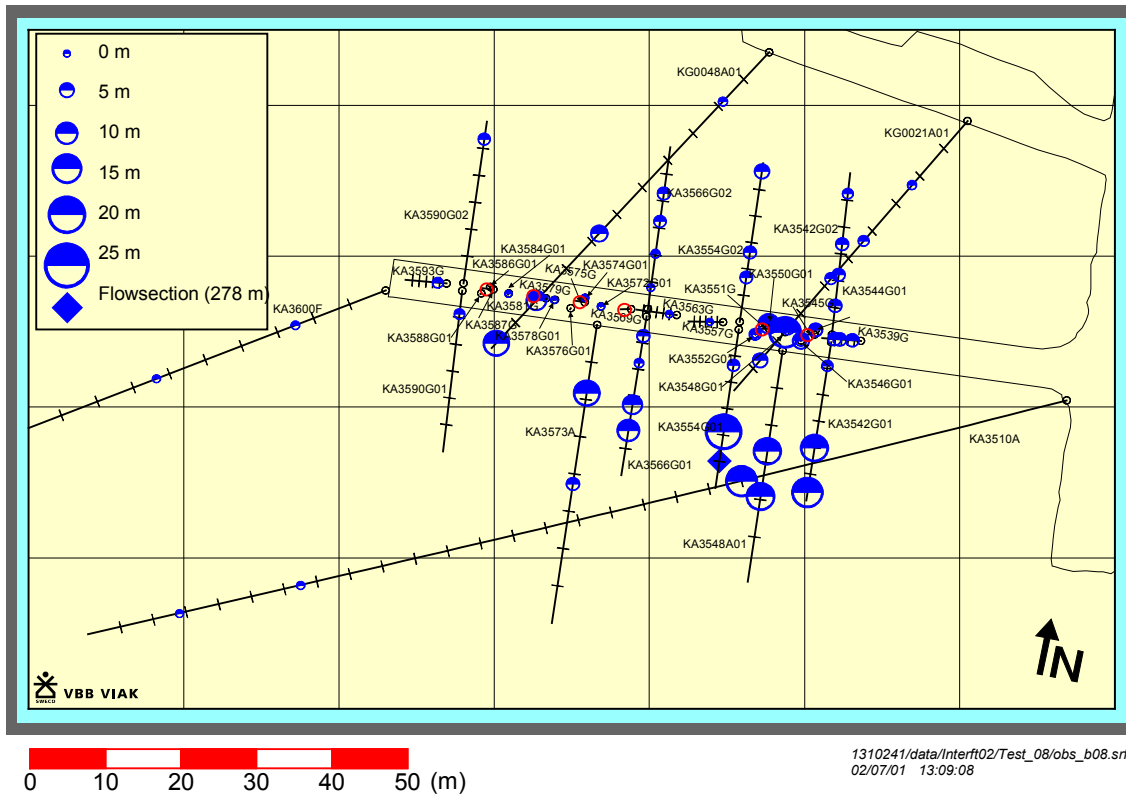


Figure 8-15 Drawdown during flowing of KA3554G01:1 (Interference test 2:8) - plan view.

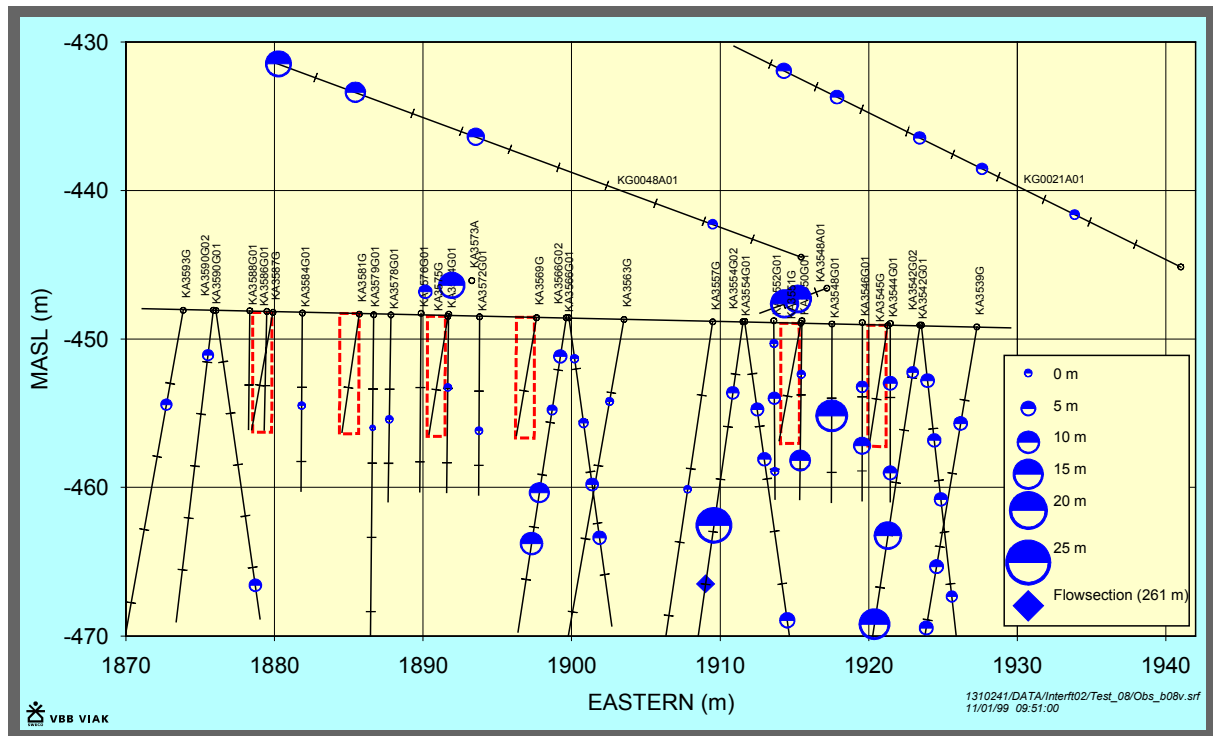


Figure 8-16 Drawdown during flowing of KA3554G01:1 (Interference test 2:8) - vertical view.

This test shows good connection, i.e. short response times, between the flow section and KA3510A:3, KA3542G01:1, KA3548A01:1, KA3573A:2 and KG0048A01:1. It is probably the same hydraulic structure that is activated during this test as during the 2:7.

The transmissivity of the observation sections with response times less than 1 minute, i.e. the sections mentioned above, is within the range $1.3 - 1.5 \cdot 10^{-6} \text{ m}^2/\text{s}$. The transmissivity of the flowing section is evaluated to be $1.7 \cdot 10^{-6} \text{ m}^2/\text{s}$ with the evaluation period 2 – 6 minutes.

The same conclusion, as the one drawn from test 2:7, can be made from this test; that the structure activated from the flowing of KA3554G01:1 is more conductive than the one observed from the test series of interference test campaign 1.

8.5.3 Interference test 2:9

The test was carried out in KA3554G02, section 10.30 - 21.80 meters. The flow period was for 364 minutes with a final flow of 0.482 L/min, while the pressure build-up time was 974 minutes. In Figure 8-17 and Figure 8-18, the pressure drawdown recordings are shown and in Table 8-16, the interference test results are presented.

The two lowest sections of KA3539G show almost exactly the same pressures during this test. This was a consequence of a leakage between the two measurement sections.

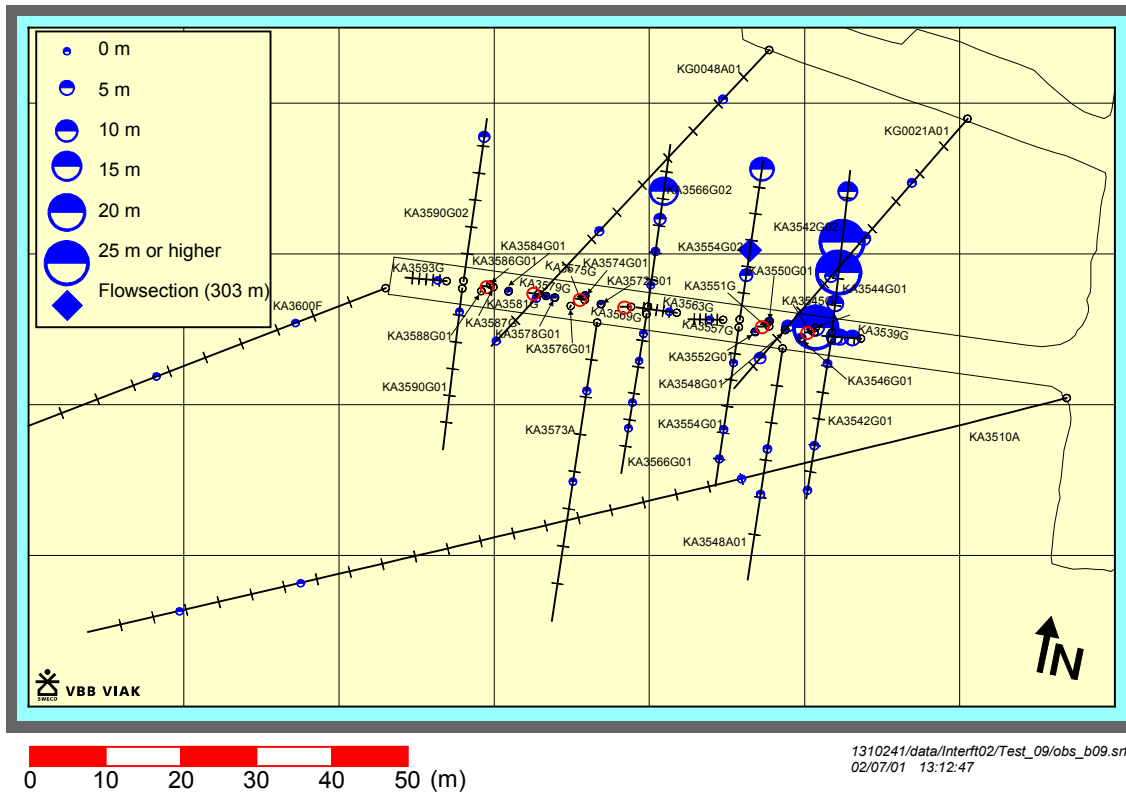


Figure 8-17 Drawdown during flowing of KA3554G02:2 (Interference test 2:9) - plan view.

This test coincided with a major earthquake in Turkey the night between 1999-08-16 and 1999-08-17. Several of the observation sections responded to this event.

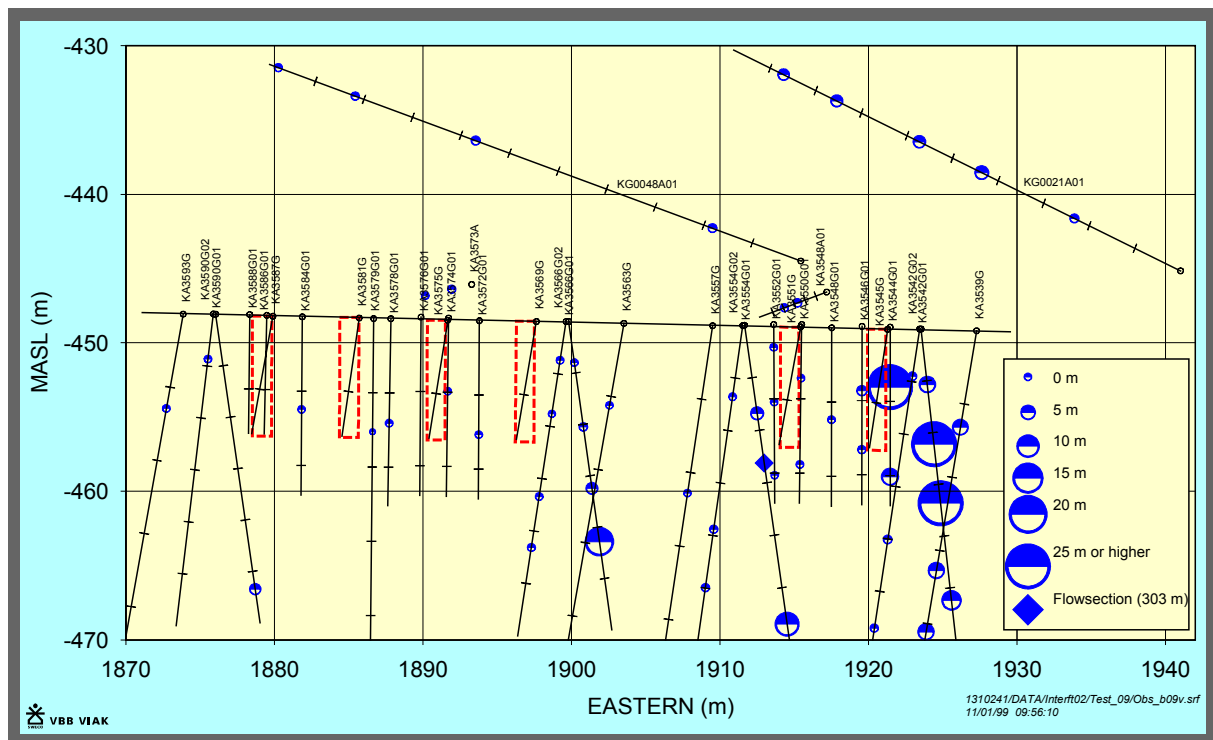


Figure 8-18 Drawdown during flowing of KA3554G02:2 (Interference test 2:9) - vertical view.

Three of the observation boreholes respond rather well, with relatively short response times, during this test. The best connection exist between the flow section and the observation sections KA3566G02:1, KA3542G02:3 and the sections of KA3539G which all show similar responses. Altogether, this is evidence of probably several hydraulic structures on the north side of the tunnel. It may be in close contact with the structure activated during test 1:2 and 1:5.

The transmissivity of the flowing section is evaluated to be $1.8 \cdot 10^{-7} \text{ m}^2/\text{s}$ with the evaluation period 0.6 – 2 minutes. The transmissivity of KA3566G02:1 and KA3542G02:3 is $1.2 \cdot 10^{-7} \text{ m}^2/\text{s}$ and $1.8 \cdot 10^{-7} \text{ m}^2/\text{s}$ respectively. This is within the same order of magnitude as the structure observed during the earlier tests at the north side of the prototype repository.

8.5.4 Interference test 2:10

The test was carried out in KA3542G01, section 8.80 - 24.80 meters. The flow period was for 365 minutes with a final flow of 2.556 L/min, while the pressure build-up time was 365 minutes. In Figure 8-19 and Figure 8-20, the pressure drawdown recordings are shown and in Table 8-17, the interference test results are presented.

The two lowest sections of KA3539G show almost exactly the same pressures during this test. This was a consequence of a leakage between the two measurement sections.

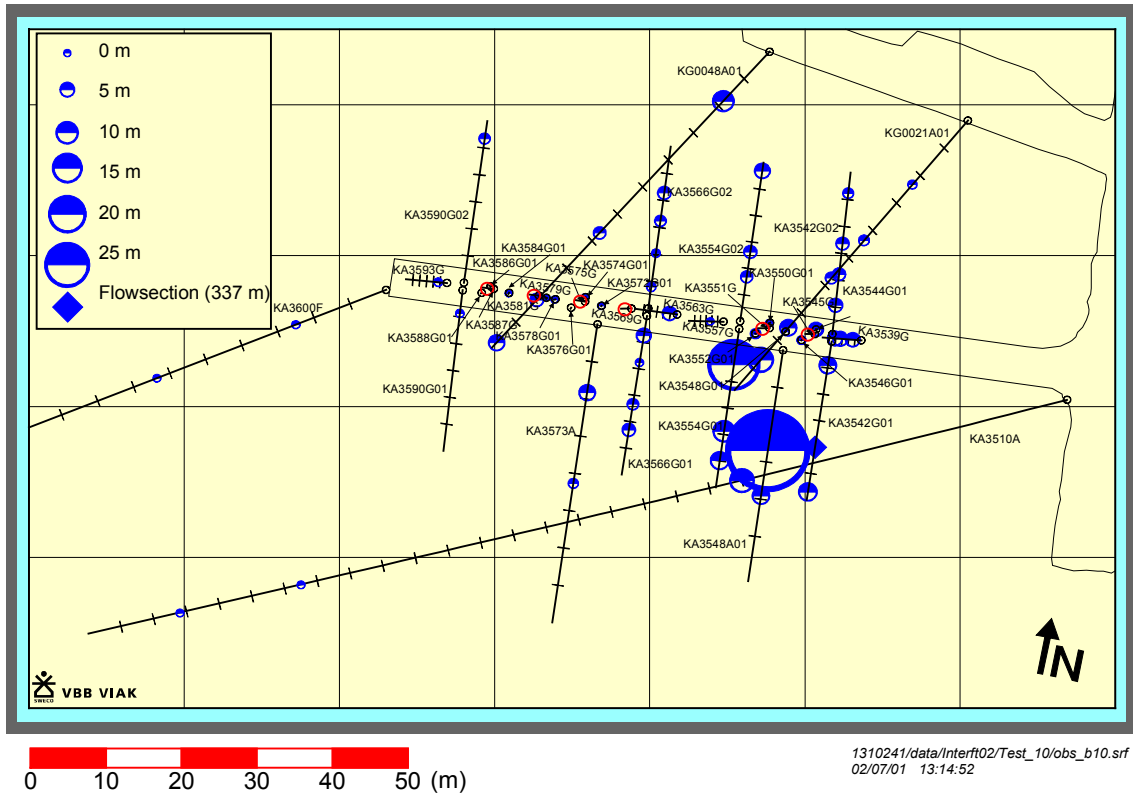


Figure 8-19 Drawdown during flowing of KA3542G01:2 (Interference test 2:10) - plan view.

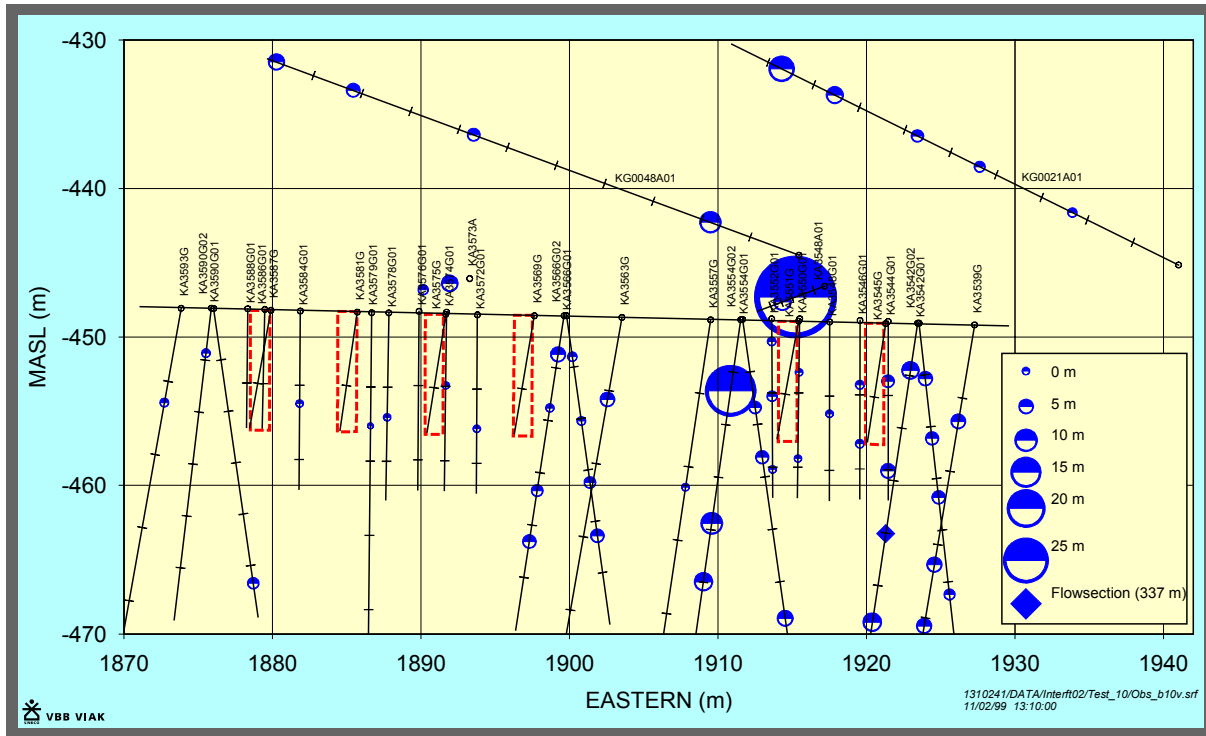


Figure 8-20 Drawdown during flowing of KA3542G01:2 (Interference test 2:10) - vertical view.

The pressure responses of this test show only a few with short response times, i.e. less than 1 minute. Good connection exists between the flow section, KA3510A:3, and KA3548A01:2.

During this test, no radial flow occurred into the flow section until late in test period ($T = 6.5 \cdot 10^{-6} \text{ m}^2/\text{s}$ with the evaluation time 200 – 250 minutes). Therefore, the evaluated transmissivity of the flowing borehole section is estimated to include several hydraulic structures and not a single one. The observed pressure response in KA3548A01:2, however, is a good one and evaluated to be $5.4 \cdot 10^{-7} \text{ m}^2/\text{s}$ while the storativity is $2.4 \cdot 10^{-7}$.

8.5.5 Interference test 2:11

The test was carried out in KA3542G02, section 1.30 - 7.80 m. The flow period was for 361 minutes with a final flow of 3.37 L/min, while the pressure build-up time was 1014 minutes. In Figure 8-21 and Figure 8-22, the pressure drawdown recordings are shown and in Table 8-18, the interference test results are presented.

The two lowest sections of KA3539G show almost exactly the same pressures during this test. This was a consequence of a leakage between the two measurement sections.

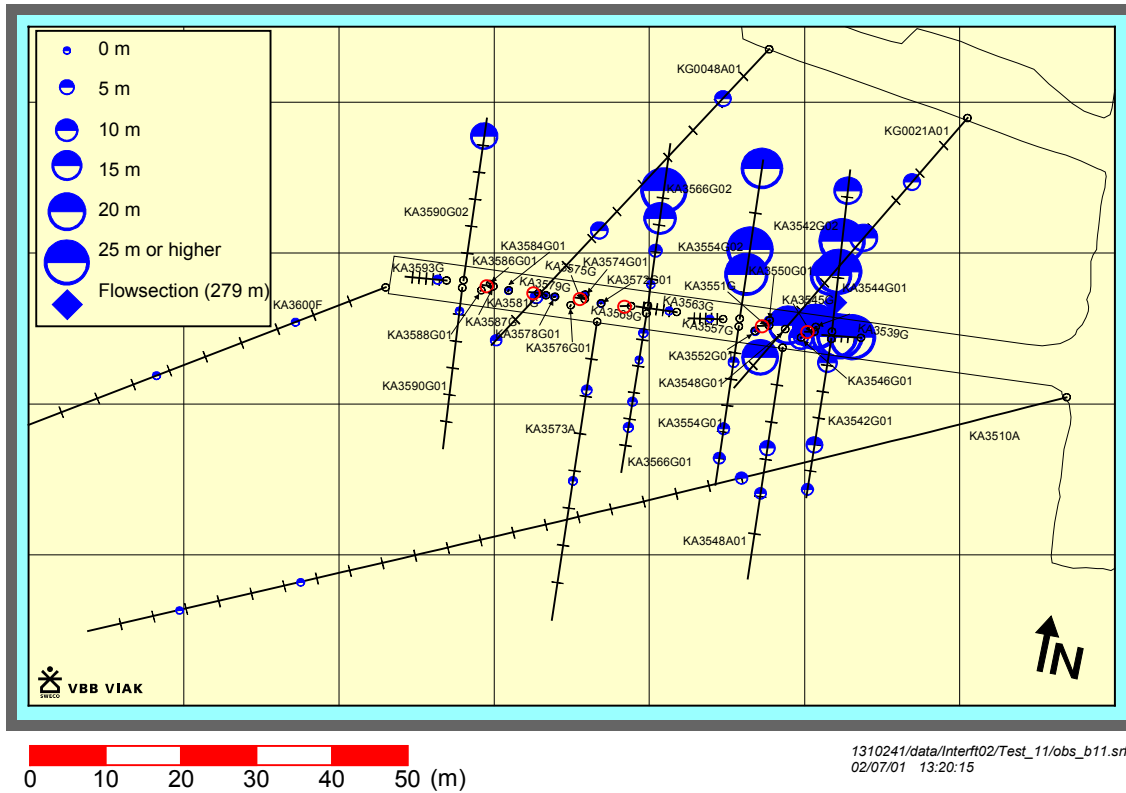


Figure 8-21 Drawdown during flowing of KA3542G02:4 (Interference test 2:11) - plan view.

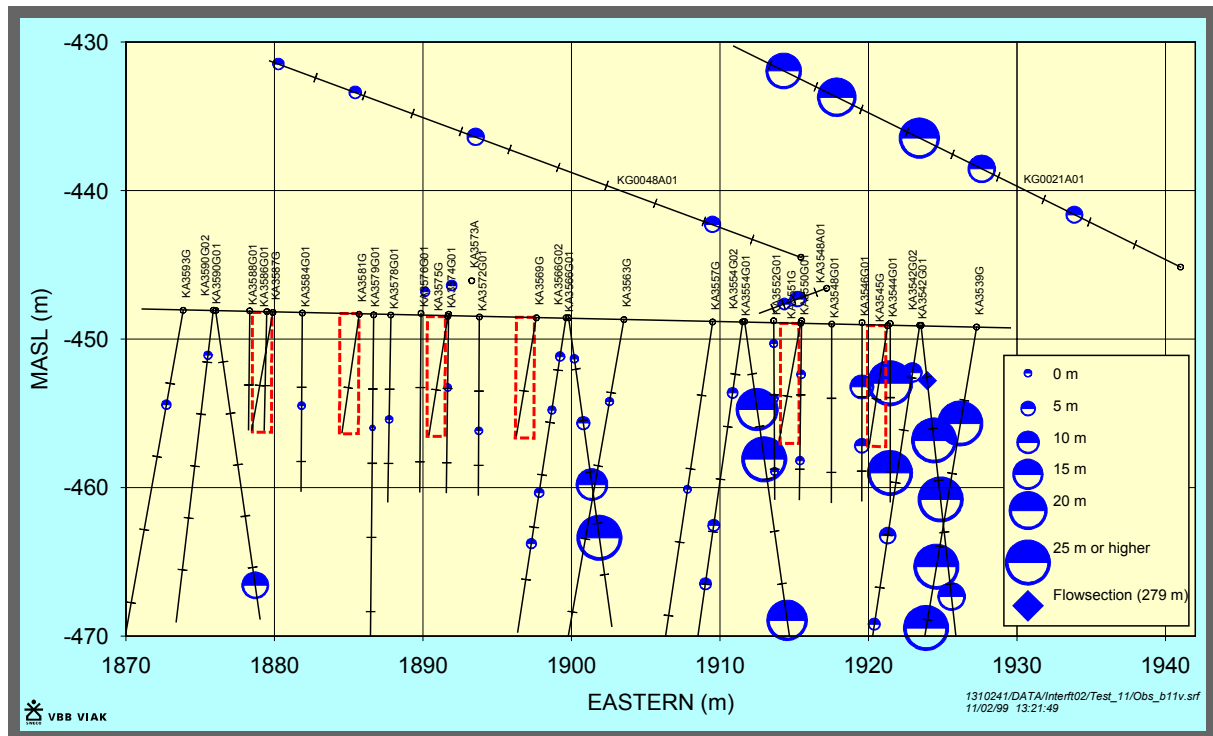


Figure 8-22 Drawdown during flowing of KA3542G02:4 (Interference test 2:11) - vertical view.

The closest observation section, KA3544G01:2, to the flow section are located with a distance of approximately 4 meters to it. The response time is very short, less than 5 seconds. The hydraulic properties of this hydraulic connection is evaluated to be $T = 9.7 \cdot 10^{-6} \text{ m}^2/\text{s}$ and $S = 1.1 \cdot 10^{-4}$. This may be the result of a feature being rather horizontal. The value of storativity is high and may indicate of the involvement of several hydraulic features. The lower section of KA3544G01 responds rather fast as well, indicating a connection with the dominating hydraulic feature at the north side of the prototype tunnel.

This is consistent with the results of the rest of the observation sections with rather short response times. The flow section has good connection with KG0021A01:3, KA3554G02:2 and the sections of KA3539G. The transmissivity of these sections is within the range $4 \cdot 10^{-7}$ and $2 \cdot 10^{-6} \text{ m}^2/\text{s}$ with a storativity range of $2 - 7 \cdot 10^{-7}$. The evaluated transmissivity of the flow section is $T = 6.1 \cdot 10^{-7} \text{ m}^2/\text{s}$ with the evaluation period 0.7 – 3 minutes.

8.5.6 Interference test 2:12

The test was planned to be carried out in KA3539G, section 9.80 - 18.30 m. Since there was a leak between the two lowest sections, this test in fact included sections 9.80 – 18.30 meters plus 19.30 – 30.01 meters. The flow period was for 61 minutes with a final flow rate of 4.278 L/min, while the pressure build-up time was 529 minutes. In Figure 8-23 and Figure 8-24, the pressure drawdown recordings are shown and in Table 8-19, the interference test results are presented.

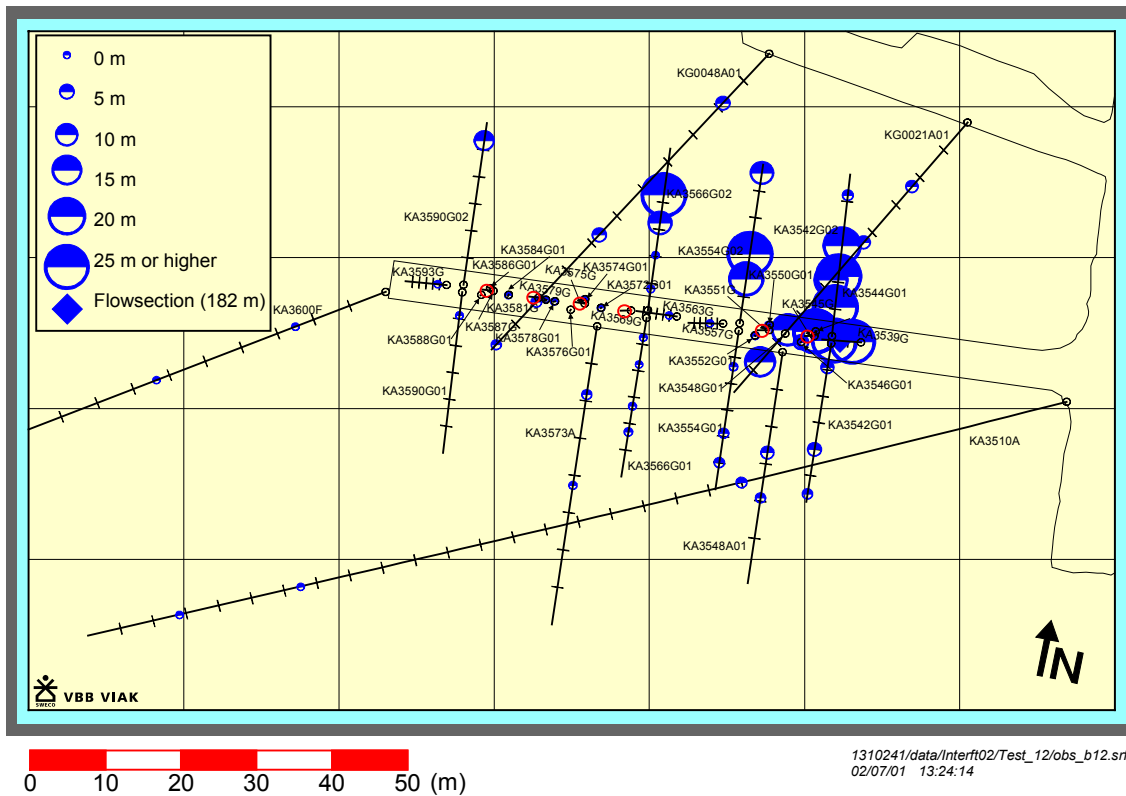


Figure 8-23 Drawdown during flowing of KA3539G:2 (Interference test 2:12) - plan view.

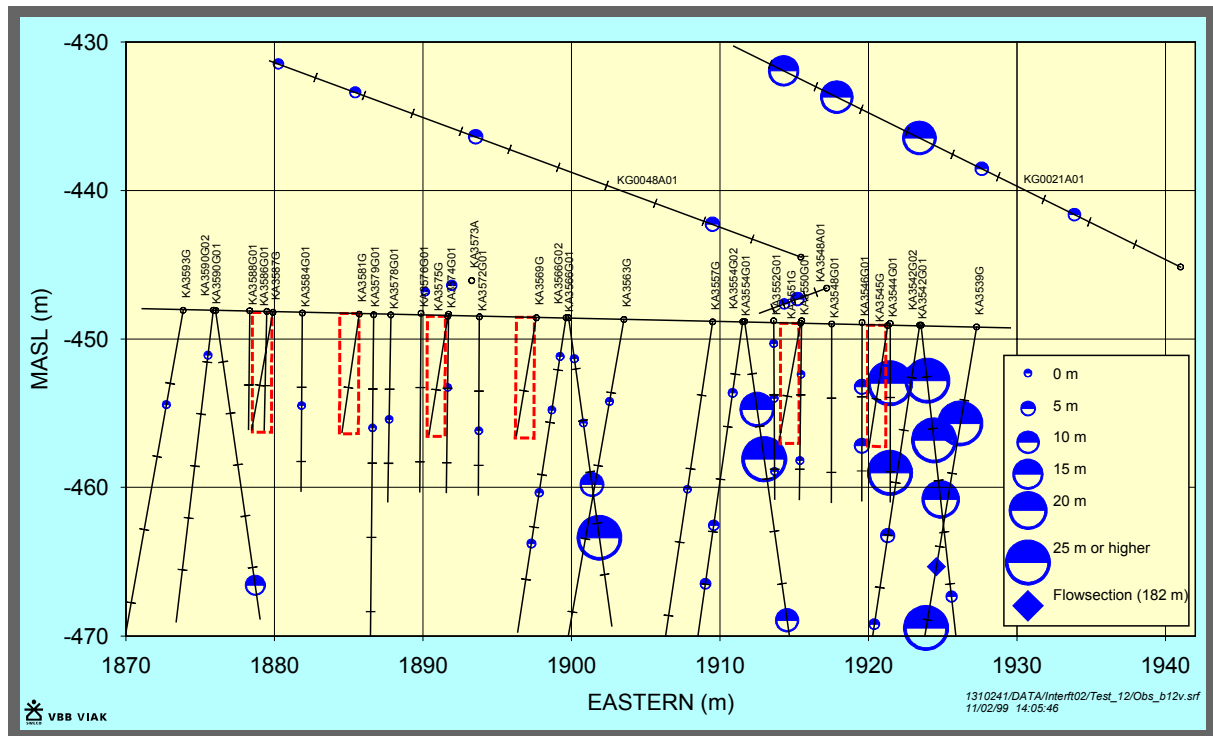


Figure 8-24 Drawdown during flowing of KA3539G:2 (Interference test 2:12) - vertical view.

This test shows good connection, with short response times, between the flow section and KA3542G02:4, KA3544G01:1, KA3554G02:2 and KG0021A01:3. The transmissivity of these sections is within the range $9 \cdot 10^{-7}$ and $3 \cdot 10^{-6}$ m²/s while the storativity is between $3 \cdot 10^{-7}$ and $3 \cdot 10^{-6}$. The evaluated transmissivity of the flow section is $5.3 \cdot 10^{-7}$ m²/s with the evaluation period 0.4 – 2 minutes.

Considering the short response times and the magnitude of the evaluated hydraulic properties it seems plausible that the same structure, or system of hydraulic features, is activated in all of these borehole sections.

8.5.7 Interference test 2:13

The test was carried out in KG0021A01, section 42.50 – 48.82 m. Flow period was for 362 minutes with a final flow of 0.380 L/min, while the pressure build-up time was 1013 minutes. In Figure 8-25 and Figure 8-26, the pressure drawdown recordings are shown and in Table 8-20, the interference test results are presented.

The two lowest sections of KA3539G show almost exactly the same pressures during this test. This was a consequence of a leakage between the two measurement sections.

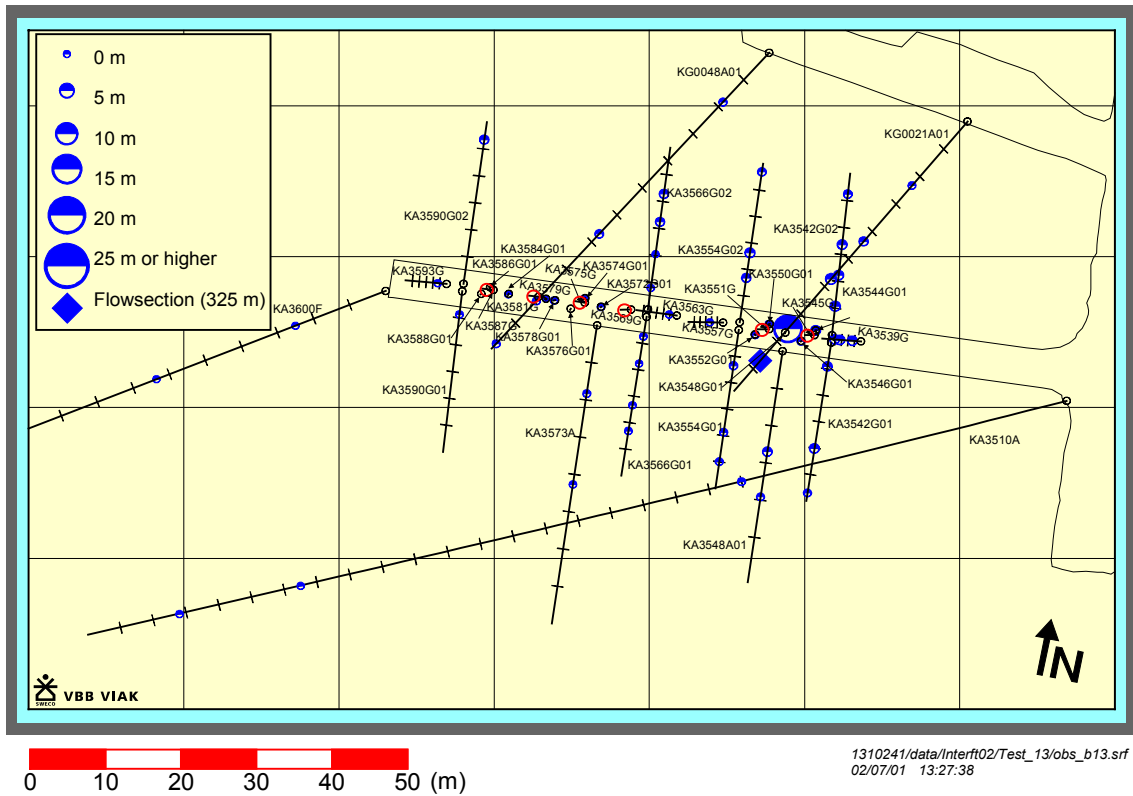


Figure 8-25 Drawdown during flowing of KG0021A01:1 (Interference test 2:13) - plan view.

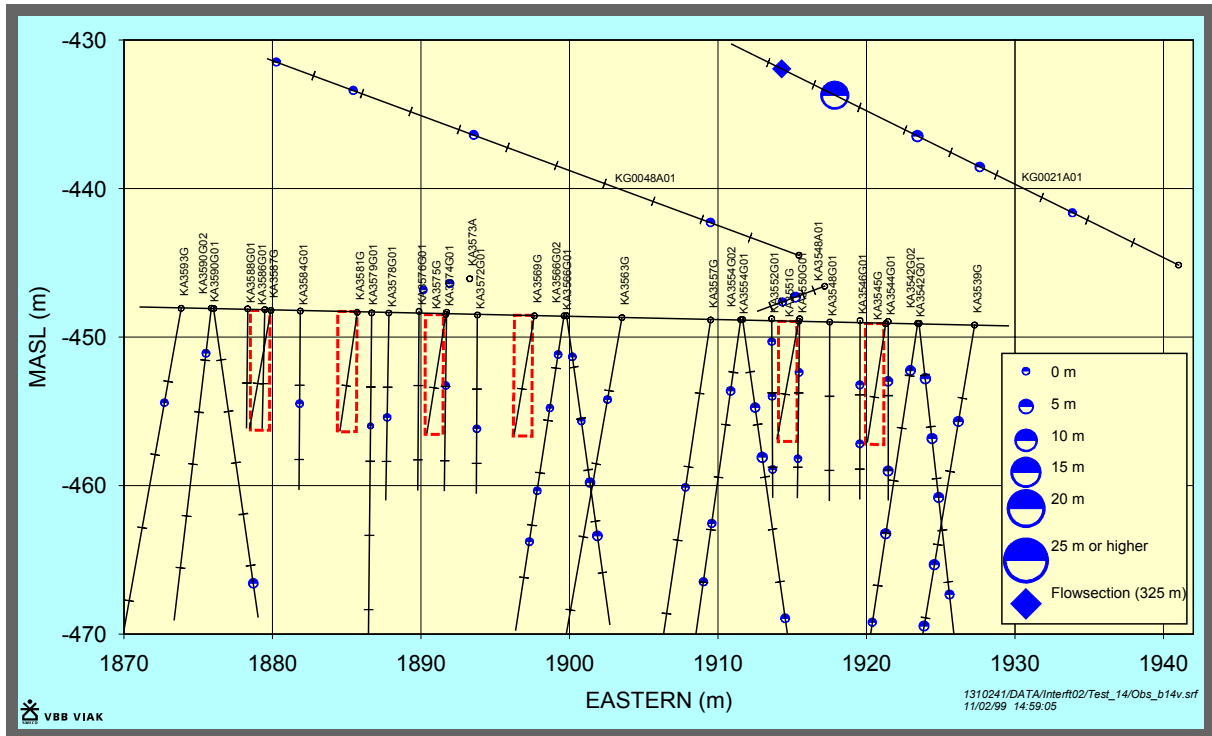


Figure 8-26 Drawdown during flowing of KG0021A01:1 (Interference test 2:13) - vertical view.

The pressure responses in the observation borehole sections of this test have all very slow response times. No direct hydraulic connection between the flow section and the observation sections has been established.

The evaluated transmissivity of the flow section is $7.2 \cdot 10^{-7} \text{ m}^2/\text{s}$ with the evaluation period 120 – 150 minutes. Due to the late time evaluation, this value probably represents more than one hydraulic structure.

Table 8-19 Interference test results for KG0021A01:1, 42.50 – 48.82 m. . (r = aprox. distance from flowing bore hole section to observation bore hole section, t_L = time lag for a pressure response of 0.1 m to be registered in an observation section, T = transmissivity, S = storage coefficient, S^* = storage coefficient from diffusivity, η .) The response is classified as 1 = no response (< 0.1 m), 2 = some response (0.1 m - 1.0 m) and 3 = good response (> 1.0 m). P_0 = Initial pressure before opening of the valve, P_p = Pressure just before closing the valve, P_f = Pressure at the end of the pressure build-up period.

Observation borehole	Secup (m)	Seclow (m)	Hydraulic centre of borehole (m)	r (m)	t_L (recovery) (min)	r^2/t_L (m ² /s)	η (m ² /s)	T_{EVAL} (m ² /s)	S (-)	S^* (-)	Response (0 = no, 1 = some, 2 =good response)	Po - Pp (kPa)	Pf - Pp (kPa)
KA3510A:1	122.02	150.00	136.00	117.93	-	-	-	-	-	-	0	-0.2	0.2
KA3510A:2	114.02	121.02	117.50	100.51	-	-	-	-	-	-	0	-0.8	0.2
KA3510A:3	4.52	113.02	50.00	44.86	65	0.516	5.81E-02	-	-	-	1	3.9	2.9
KA3539G:1	19.30	30.01	20.56	38.83	60	0.419	4.61E-02	-	-	-	2	15.9	16.9
KA3539G:2	9.80	18.30	16.37	35.05	60	0.341	3.75E-02	-	-	-	2	16.4	17.2
KA3539G:3	1.30	8.80	6.59	26.69	35	0.339	3.19E-02	-	-	-	2	15.9	17.6
KA3542G01:1	25.80	30.04	28.50	41.63	70	0.413	4.75E-02	-	-	-	1	3.9	2.3
KA3542G01:2	8.80	24.80	20.06	34.12	55	0.353	3.78E-02	-	-	-	2	16.2	15.6
KA3542G01:3	1.30	7.80	4.50	22.10	75	0.109	1.28E-02	-	-	-	2	14.3	13.7
KA3542G02:1	22.30	30.01	26.21	43.24	90	0.346	4.29E-02	-	-	-	2	8.8	11.5
KA3542G02:2	13.80	21.30	16.83	34.38	60	0.328	3.61E-02	-	-	-	2	16.8	17.8
KA3542G02:3	8.80	12.80	11.13	29.17	65	0.218	2.46E-02	-	-	-	2	17.1	17.7
KA3542G02:4	1.30	7.80	5.36	24.11	58	0.167	1.82E-02	-	-	-	2	18.8	18.6
KA3544G01:1	6.30	12.00	10.07	28.30	65	0.205	2.31E-02	-	-	-	2	15.7	15.7
KA3544G01:2	1.30	5.30	4.03	22.59	68	0.125	1.43E-02	-	-	-	2	11.9	13.8
KA3546G01:1	6.80	12.00	8.30	25.93	95	0.118	1.49E-02	-	-	-	1	1.9	3.1
KA3546G01:2	1.30	5.80	4.33	22.08	105	0.077	1.00E-02	-	-	-	1	2.4	4.7
KA3548A01:1	15.00	30.00	19.56	23.91	75	0.127	1.49E-02	-	-	-	1	3.3	2.5
KA3548A01:2	10.00	14.00	13.49	19.55	55	0.116	1.24E-02	-	-	-	2	14.6	13.8
KA3548G01:1	0.30	12.01	6.18	23.75	-	-	-	-	-	-	-	-	-
KA3550G01:1	6.30	12.03	9.42	26.72	110	0.108	1.42E-02	-	-	-	1	-1.8	6.4
KA3550G01:2	1.30	5.30	3.61	21.05	-	-	-	-	-	-	0	1.2	-1.9
KA3552G01:1	8.80	12.01	10.15	27.21	210	0.059	9.28E-03	-	-	-	1	0.4	1.8
KA3552G01:2	4.05	7.80	5.22	22.33	200	0.042	6.48E-03	-	-	-	1	0.8	1.2
KA3552G01:3	1.30	3.05	1.53	18.70	280	0.021	3.54E-03	-	-	-	1	0	1
KA3554G01:1	22.30	30.01	24.95	37.41	70	0.333	3.84E-02	-	-	-	1	3.7	2.6
KA3554G01:2	12.30	21.30	19.39	32.39	80	0.219	2.62E-02	-	-	-	1	4.1	2.7
KA3554G01:3	1.30	11.30	6.78	21.97	75	0.107	1.26E-02	-	-	-	1	6.7	5.9
KA3554G02:1	22.30	30.01	28.47	44.69	85	0.392	4.78E-02	-	-	-	2	8	11.2
KA3554G02:2	10.30	21.01	13.13	29.85	61	0.243	2.69E-02	-	-	-	2	17.7	18.5
KA3554G02:3	1.30	9.30	8.39	25.38	72	0.149	1.73E-02	-	-	-	2	12.1	12.7
KA3557G:1	0.30	30.04	11.40	29.36	240	0.060	9.79E-03	-	-	-	1	-0.2	1.5
KA3563G01:1	0.30	30.00	5.60	25.90	130	0.086	1.19E-02	1.3E-06	5.7E-05	1.1E-04	1	0.6	1
KA3566G01:1	20.80	30.01	21.57	37.26	100	0.231	2.96E-02	-	-	-	1	1.8	1.6
KA3566G01:2	12.30	19.80	16.71	33.36	105	0.177	2.29E-02	-	-	-	1	0.4	2.3
KA3566G01:3	7.30	11.30	8.81	27.66	150	0.085	1.22E-02	-	-	-	1	-1.2	2.7
KA3566G01:4	1.30	6.30	3.70	24.63	120	0.084	1.14E-02	5.0E-07	4.0E-05	4.4E-05	1	0.6	2.9
KA3566G02:1	19.30	30.01	21.41	40.40	65	0.418	4.71E-02	-	-	-	2	13.5	17
KA3566G02:2	12.30	18.30	16.23	35.80	70	0.305	3.51E-02	-	-	-	2	11.9	13.7
KA3566G02:3	7.80	11.30	10.25	30.73	150	0.105	1.51E-02	4.1E-08	4.9E-06	2.7E-06	1	-1.8	7
KA3566G02:4	1.30	6.80	3.99	25.84	250	0.045	7.35E-03	-	-	-	1	0.4	0.6
KA3572G01:1	0.30	12.00	7.67	32.55	220	0.080	1.28E-02	-	-	-	1	-0.6	1.1
KA3573A:1	18.00	40.07	21.34	32.75	120	0.149	2.01E-02	-	-	-	1	0.5	1.1
KA3573A:2	4.50	17.00	9.16	26.96	75	0.162	1.90E-02	-	-	-	1	3.1	2.1
KA3574G01:1	0.30	12.00	4.93	32.17	-	-	-	-	-	-	0	-0.2	0
KA3576G01:1	0.30	12.01	5.99	33.81	-	-	-	-	-	-	-	-	-
KA3578G01:1	0.30	12.58	7.03	36.33	-	-	-	-	-	-	0	0	0.2
KA3579G01:1	0.30	22.65	7.62	37.58	20	1.177	9.45E-02	-	-	-	2	-11.5	14.3
KA3584G01:1	0.30	12.00	6.24	40.49	-	-	-	-	-	-	0	0.2	0.4
KA3590G01:1	0.30	30.06	4.33	43.66	-	-	-	-	-	-	0	0.9	-0.6
KA3590G02:1	0.30	30.05	26.73	57.67	60	0.924	1.02E-01	-	-	-	2	12.7	14.5
KA3593G01:1	0.30	30.02	6.45	48.35	130	0.300	4.14E-02	6.1E-07	1.1E-05	1.5E-05	1	0	2.5
KA3600F:1	22.00	50.10	31.78	79.20	-	-	-	-	-	-	0	-0.8	-0.2
KA3600F:2	4.50	21.00	12.51	61.69	-	-	-	-	-	-	0	-0.5	0.6
KG0021A01:1	42.50	48.82	43.53	0.00	-	-	-	7.2E-07	-	-	2	3251.1	3249.9
KG0021A01:2	35.00	41.50	37.70	5.83	20	0.028	2.27E-03	-	-	-	2	136.7	137.9
KG0021A01:3	25.00	34.00	28.64	14.89	50	0.074	7.70E-03	-	-	-	2	24.2	26
KG0021A01:4	17.00	24.00	21.80	21.73	44	0.179	1.79E-02	-	-	-	2	12.3	16.2
KG0021A01:5	4.00	16.00	11.64	31.89	80	0.212	2.54E-02	-	-	-	1	2.9	5.7
KG0048A01:1	49.00	54.69	53.81	34.09	70	0.277	3.19E-02	-	-	-	1	3.1	2.3
KG0048A01:2	41.00	48.00	45.90	29.95	70	0.214	2.46E-02	-	-	-	1	3.9	3.9
KG0048A01:3	30.00	40.00	33.50	27.06	60	0.203	2.24E-02	-	-	-	1	8.4	8.8
KG0048A01:4	4.00	29.00	9.12	36.14	80	0.272	3.26E-02	-	-	-	1	5.7	5.5

8.5.8 Interference test 2:14

The test was carried out in KG0021A01, section 25.00 – 34.00 m. Flow period was for 360 minutes with a final flow of 7.29 L/min, while the pressure build-up time was 1135 minutes. In Figure 8-27 and Figure 8-28, the pressure drawdown recordings are shown and in Table 8-21, the interference test results are presented.

The two lowest sections of KA3539G show almost exactly the same pressures during this test. This was a consequence of a leakage between the two measurement sections.

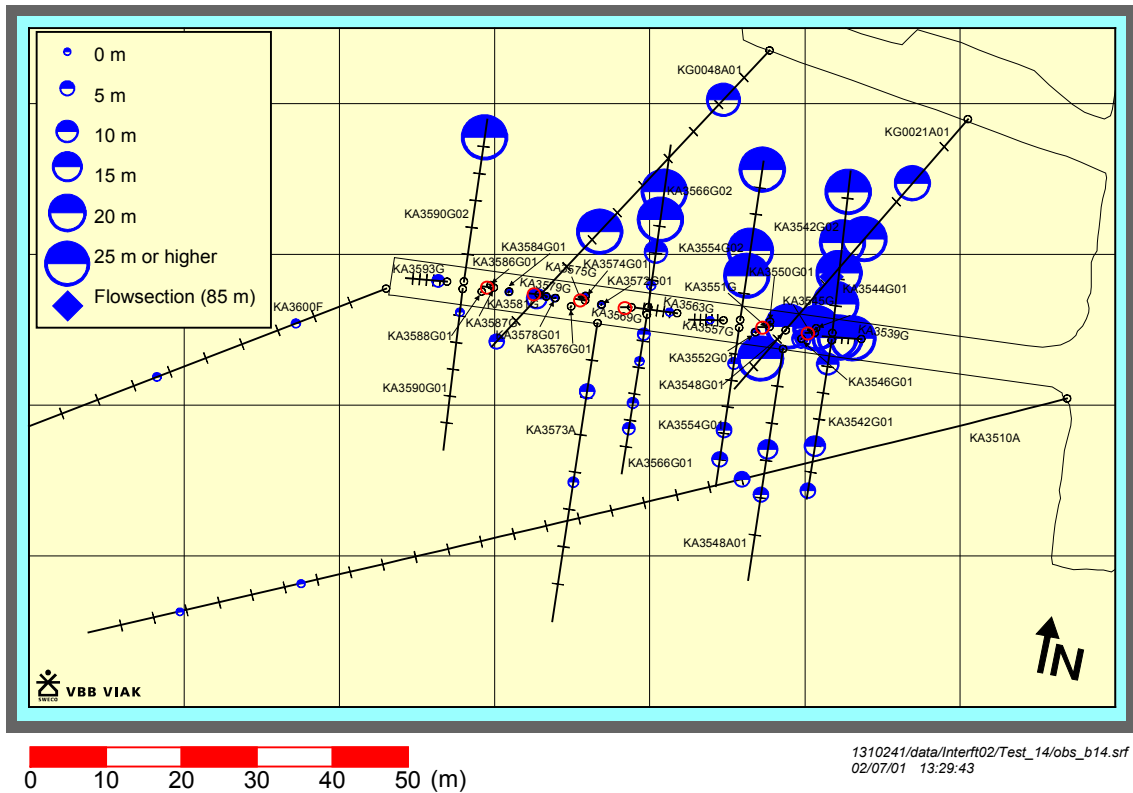


Figure 8-27 Drawdown during flowing of KG0021A01:3 (Interference test 2:14) - plan view.

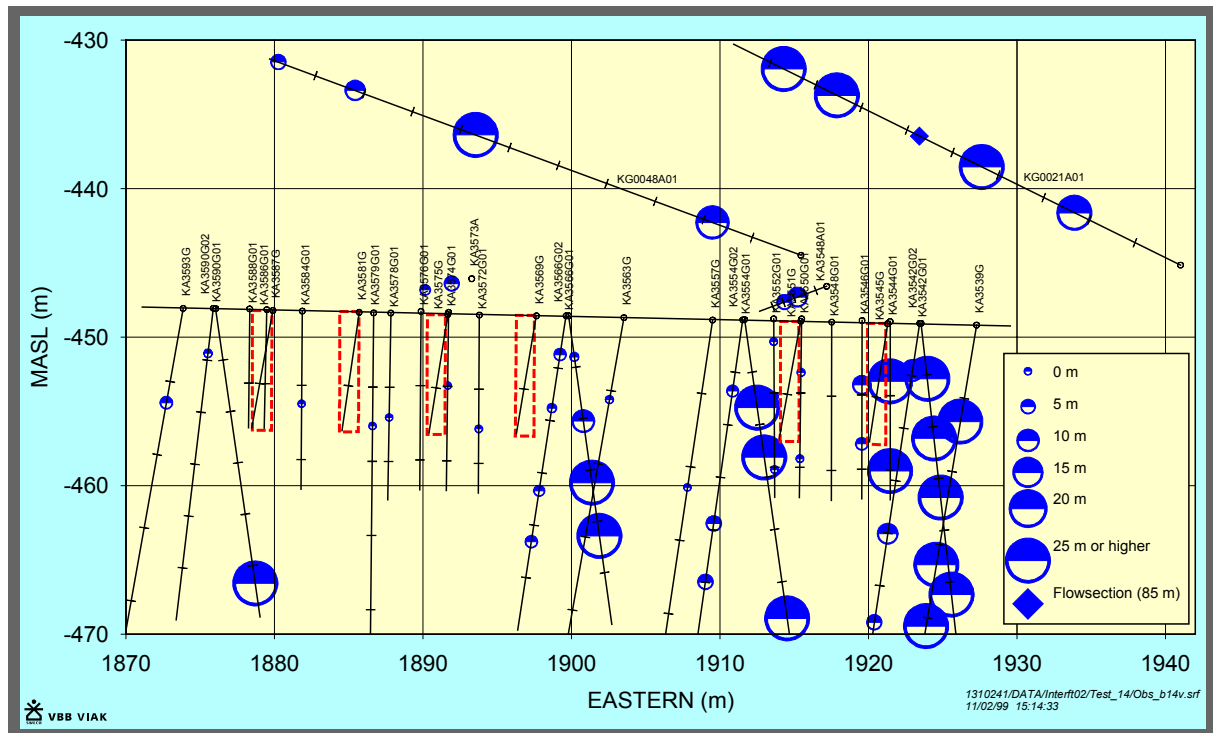


Figure 8-28 Drawdown during flowing of KG0021A01:3 (Interference test 2:14) - vertical view.

This test shows good connection, with short response times, between the flow section and KA3542G02:4, KA3544G01:2, KA3554G02:2, KG0048A01:3 and the sections of KA3539G. The transmissivity of these sections is within the range $2 \cdot 10^{-6}$ and $5 \cdot 10^{-6}$ m²/s while the storativity is between $3 \cdot 10^{-7}$ and $2 \cdot 10^{-6}$. The evaluated transmissivity of the flow section is $7.3 \cdot 10^{-7}$ m²/s with the evaluation period 7 –15 minutes.

Considering the short response times and the magnitude of the evaluated hydraulic properties is seem probable that the same structure, or system of hydraulic features, is activated in all of these borehole sections.

9 BLASTING

In the preparations for the concrete plug construction, blasting of niches were made at two chainage locations in the Prototype Repository Tunnel, namely 3537 and 3560. Pressure registrations were made in KA3510A, KG0021A01 and KG0048A01 during the blasting period, 2000-08-24 – 2000-09-05.

A result is that at several blasting occasions the pressure rises in the observation sections after almost every blasting round, see Figure 9-1 for an example. At most, the increase was approximately 8 – 10 meters in four out of five sections in KG0021A01 when the first round went off. In KG0048A01 the corresponding pressure, increase was 1 – 4 meters in all four sections. The pressure increase seems to be somewhat higher for sections closer to the constructed niche.

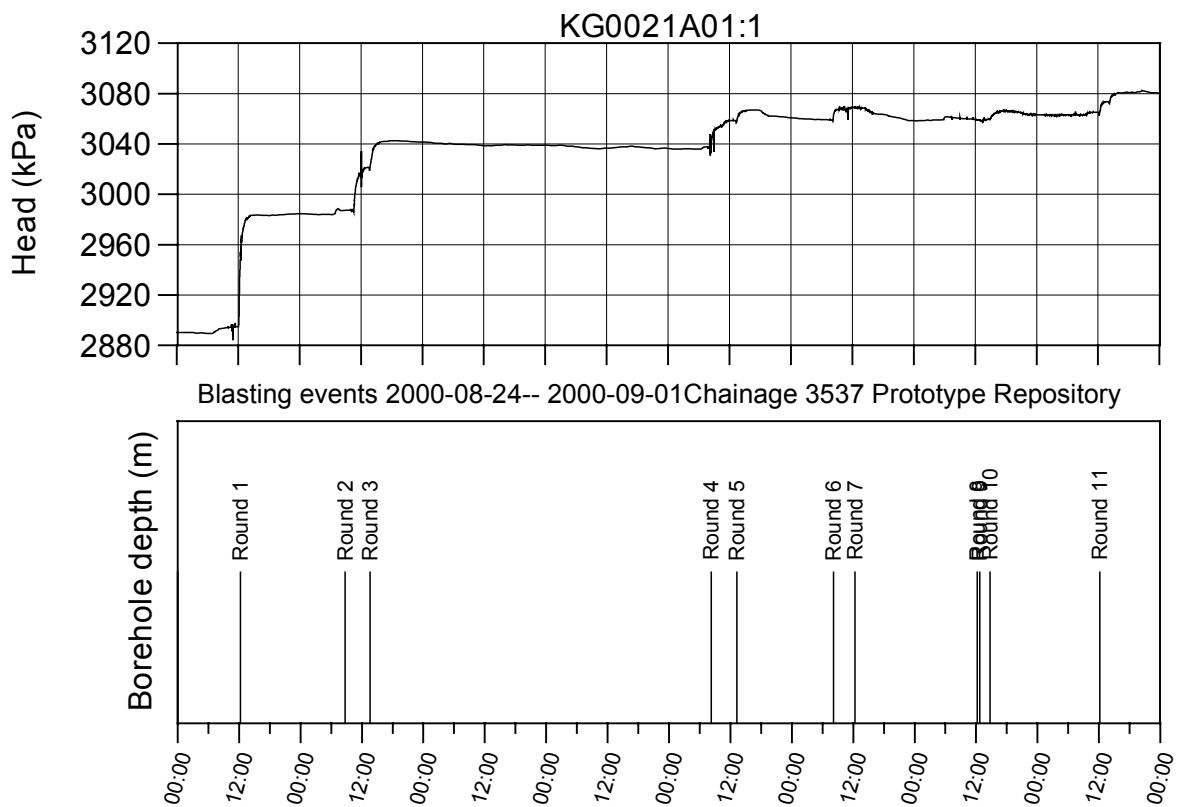


Figure 9-1 Example of pressure response due to blasting.

The total increase of the pressure in available observation sections after the blasting of the two niches is shown in Table 9-1.

Table 9-1 Total increase of the pressure in available observation sections after the blasting of the two niches.

Observation section of observation borehole	Increase of the pressure in KA3510A1 (m)	Increase of the pressure in KG0021A01 (m)	Increase of the pressure in KG0048A01 (m)
1	0.2	31.0	5.0
2	0.7	36.5	9.0
3	6.0	37.5	15.0
4	-	19.0	-0.5
5	-	24.0	-

These measurements clearly show that the blasting affects the hydraulic system. A probable cause is that the vibrations from the blasting make the gauge material in the fracture move. The inter-connected fracture system will then become less permeable and the pressure will increase in fracture systems up gradient of the clogged fractures.

The pressure increase after each blasting round is of similar magnitude in several sections indicating the possibility of the clogging of major flowing features.

10 Laboratory measurements of porosity in the deposition holes

Micro fracturing and porosity in the excavation damage zone has been studied by using ^{14}C -polymethylmethacrylate (^{14}C -PMMA) method (Autio et al, 2001). A total of 12 samples (from short cores holes) from the deposition holes 3 and 4 were taken from the Prototype Repository Tunnel in Äspö HRL. The samples representing Äspö diorite were taken from different depths and orientations with respect to the of stress field. The micro fracturing and spatial distribution of porosity adjacent to the surface of the deposition holes in the samples has been studied in laboratory by using ^{14}C -PMMA method and scanning electron microscopy. The laboratory tests and analytical work has been carried out and the work is being reported. According to the results the porosity of undisturbed rock is 0.2-0.4 vol. %.

The thickness of the crushed zone with significantly higher porosity is few millimetres and the depth of the Excavation Disturbed Zone (EDZ) is from 10 to 20 mm (or even 30 mm in some samples). The porosity profiles of the samples form holes 3 and 4 are shown below in Figure 10-1. The profiles are measured perpendicular to the disturbed surface (surface of the deposition holes). The EDZ adjacent to the surface looks similar to what have been seen at Olkiluoto – the hydraulic conductivities might not be therefore very different from those.

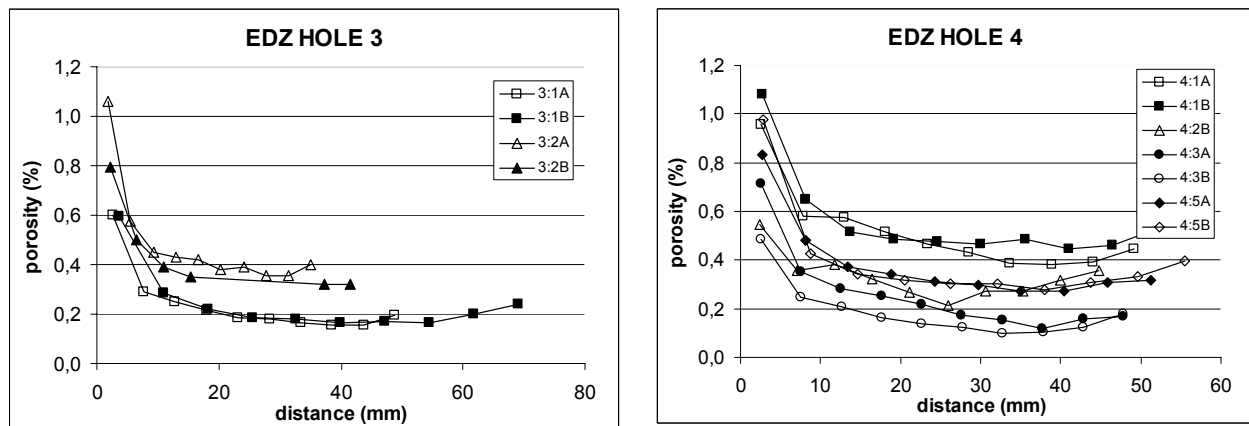


Figure 10-1 Porosity of rock determined by using ^{14}C -PMMA-method with respect to the distance from the surface of the experimental deposition holes 3 and 4 in the Prototype Repository tunnel at Äspö Hard Rock Laboratory.

11 HYDRAULIC PROPERTIES OF ROCK MASS

11.1 Transmissivity

11.1.1 Distance between features

In this analysis the distance between features exceeding a predefined magnitude of transmissivity were studied. Features exceeding six different orders of magnitude of the transmissivity were analysed: $T > 10^{-11}$, 10^{-10} , 10^{-9} , 10^{-8} , 10^{-7} and 10^{-6} m²/s. In this analysis all boreholes drilled during the Prototype Repository Project (drill batch 1 - 3) were used, totally 34 bore holes. The evaluation is based on the transmissivity evaluated for the 1 m and 3 m sections assigning the midpoint of the section as a feature. The transmissivity for each section is the T_{tot} value in the tables in Chapter 7.

The statistical analysis used was method C in Figure 11-1. The difference between Methods A, B, and Method C are that in C every available borehole meter is used in the estimations of distance between different features. Five different data sets were created with the 34 (or fewer in subclasses) boreholes randomly ranked in a "long" borehole. The beginning (d1) plus the end (d10) of the "long" bore hole make up one distance in the analysis according to method C.

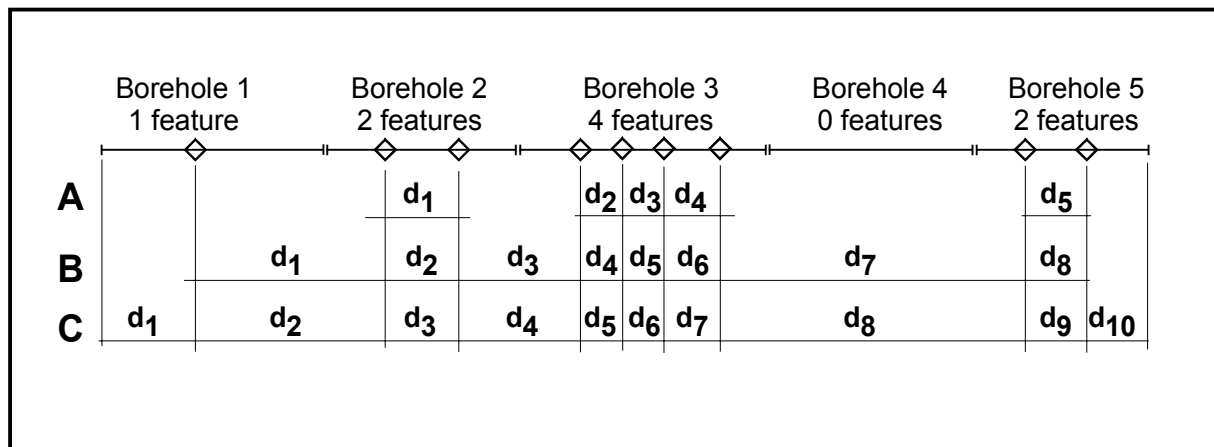


Figure 11-1 Methods for calculation of distance between features in several boreholes.

The available boreholes were divided into the following subclasses and analysed:

1. All boreholes drilled during drilling campaign 1, 2 and 3 (34 boreholes)
2. Sub-vertical bore holes (23 boreholes)
3. Sub-horizontal boreholes (KG0021A01, KG0048A01 and KA3548A01)

4. Southerly inclined boreholes (KA3542G01, KA3554G01, KA3566G01 and KA3590G01)
5. Northerly inclined boreholes (KA3542G02, KA3554G02, KA3566G02 and KA3590G02)

In Table 11-1 and Figures 11-7 to 11-9 a summary of the results of the distance analysis are presented. In Forsmark and Rhén (1999b) the details of the analysis are presented.

As an example of a lognormal distribution of the distances, Figure 11-2 is presented which shows the lognormal probability plot for distances between features with a transmissivity greater than $1 \cdot 10^{-9} \text{ m}^2/\text{s}$ for data set 1. The distances between the features are approximately lognormal distributed in several cases.

Normal Probability Plot for LogD1_9

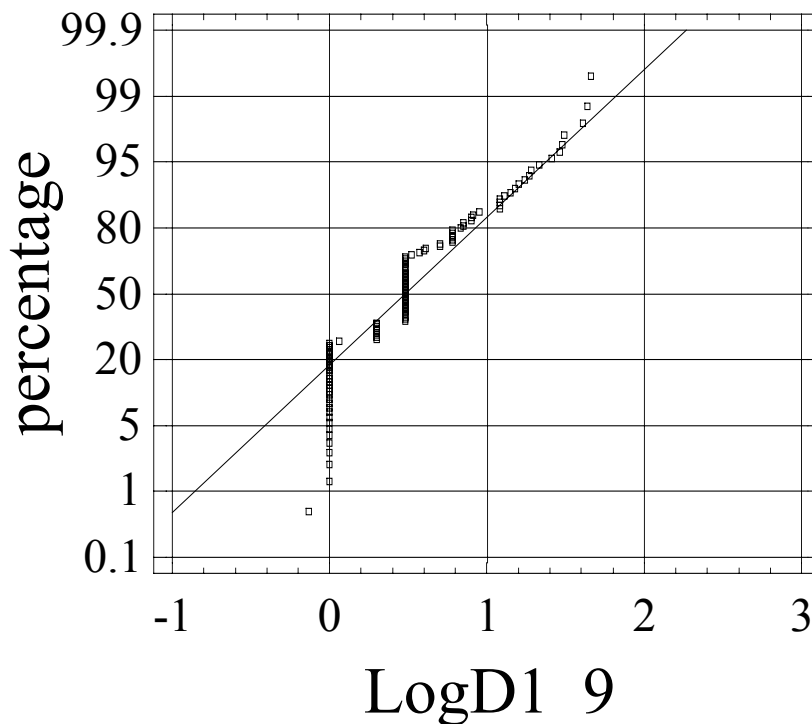


Figure 11-2 Log normal probability plot for distances between features with a transmissivity greater than $1 \cdot 10^{-9} \text{ m}^2/\text{s}$ for data set 1.

The difference between the data sets 1 - 5 are generally very small and the average values presented in Table 6-2 can be considered to be representative for the rock volume around the prototype repository. Possibly a somewhat larger standard deviation ($S(\text{Log}_{10} D)$) could be used for features with a low transmissivity considering that all directions are censored for distances shorter than 1 m, see Figure 11-2, and Forsmark and Rhén (1999b). Possibly ($S(\text{Log}_{10} D)$) should not be less than around 0.4 - 0.5 for transmissivity $< 10^{-8} \text{ m}^2/\text{s}$.

Table 11-1 Distance between hydraulic features with $T > 10^{-6}$, $T > 10^{-7}$, $T > 10^{-8}$, $T > 10^{-9}$, $T > 10^{-10}$ and $T > 10^{-11}$ m²/s respectively. Summary of data set 1 - 5. (n = sample size, D_a = arithmetic mean, D_{median} = median, D_g = geometric mean, $S(\text{Log10 D})$ = standard deviation.

SUMMARY DATASET 1 - 5						
	LogT>-6	LogT>-7	LogT>-8	LogT>-9	LogT>-10	LogT>-11
SUBCLASS 1						
n	11	40	80	117	175	377
Da	63.73	17.02	8.63	5.99	4.00	1.89
Dmedian	10.23	3.02	3.02	3.02	3.02	1.00
Dg	14.08	5.93	3.24	3.11	2.43	1.42
S(Log10 D)	0.90	0.61	0.53	0.45	0.39	0.26
SUBCLASS 2						
n	2	2	10	23	52	172
Da	163.79	134.03	27.81	12.59	5.84	1.93
Dmedian	56.89	56.89	3.51	3.85	2.00	1.00
Dg	56.89	56.89	8.20	5.67	2.93	1.28
S(Log10 D)	1.05	1.05	0.74	0.61	0.51	0.27
SUBCLASS 3						
n	7	25	43	50	56	78
Da	19.07	7.27	4.08	3.34	2.71	1.78
Dmedian	3.98	3.02	1.00	1.00	1.00	1.00
Dg	6.89	3.41	2.02	1.90	1.74	1.43
S(Log10 D)	0.74	0.42	0.37	0.34	0.32	0.24
SUBCLASS 4						
n	2	8	15	20	30	59
Da	60.00	15.00	8.00	6.00	4.00	2.03
Dmedian	18.84	3.72	3.02	3.02	3.02	1.00
Dg	18.84	6.83	4.54	4.26	2.94	1.70
S(Log10 D)	1.12	0.52	0.45	0.36	0.34	0.26
SUBCLASS 5						
n	0	5	12	25	37	64
Da	-	22.24	9.60	5.04	3.39	1.88
Dmedian	-	19.32	3.02	3.02	3.02	1.00
Dg	-	13.37	4.18	3.67	2.59	1.55
S(Log10 D)	-	0.60	0.57	0.33	0.29	0.23

As mentioned above hydraulic feature in the calculations is per measurement section (1 or 3 m sections). One or more conductive fractures may of course intersect a test section. This means that the conductive fracture frequency should be somewhat higher, at least for low conductive fractures, but also that the transmissivity for individual fractures will be lower as the measured transmissivity in some cases should be divided on a number of fractures.

In a few cases, in nearby sections which all have a high transmissivity, it is possible that the evaluated transmissivity of these sections represent only a single major fracture.

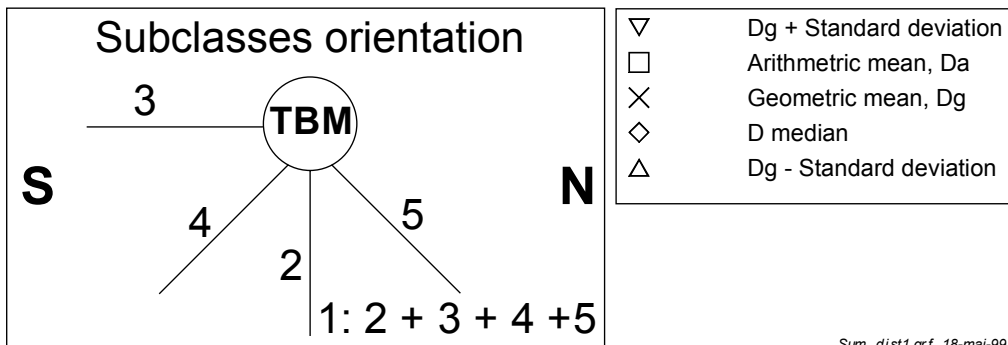
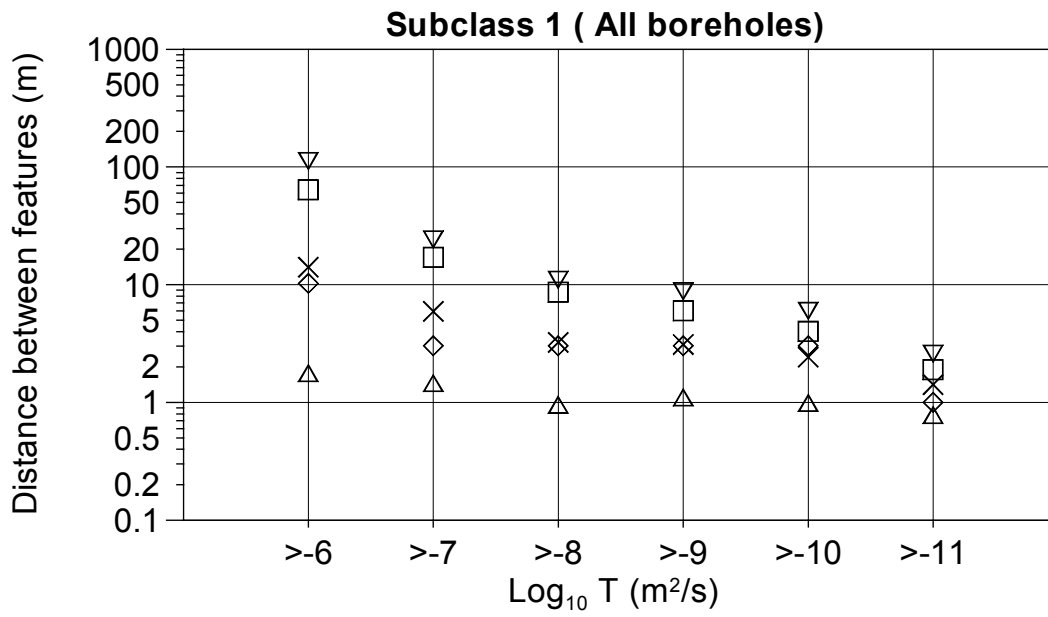
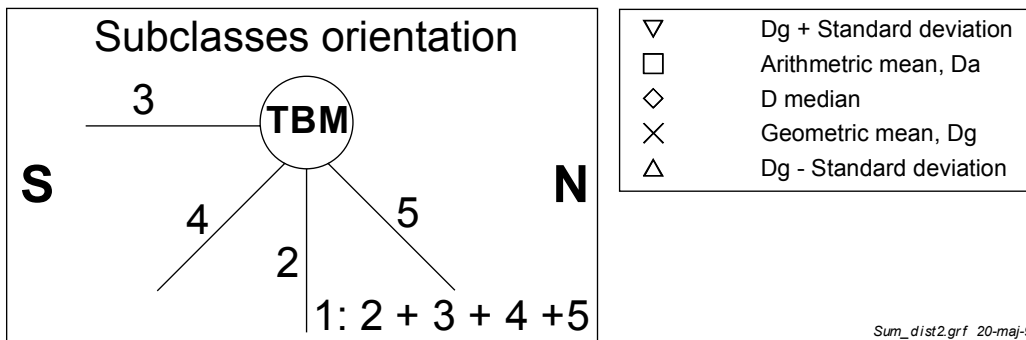
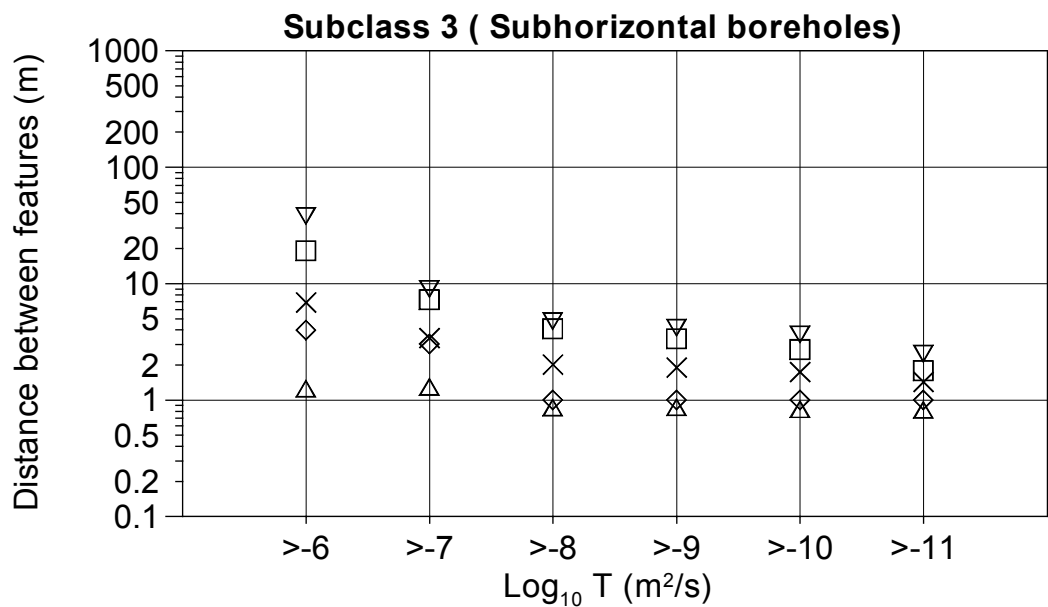
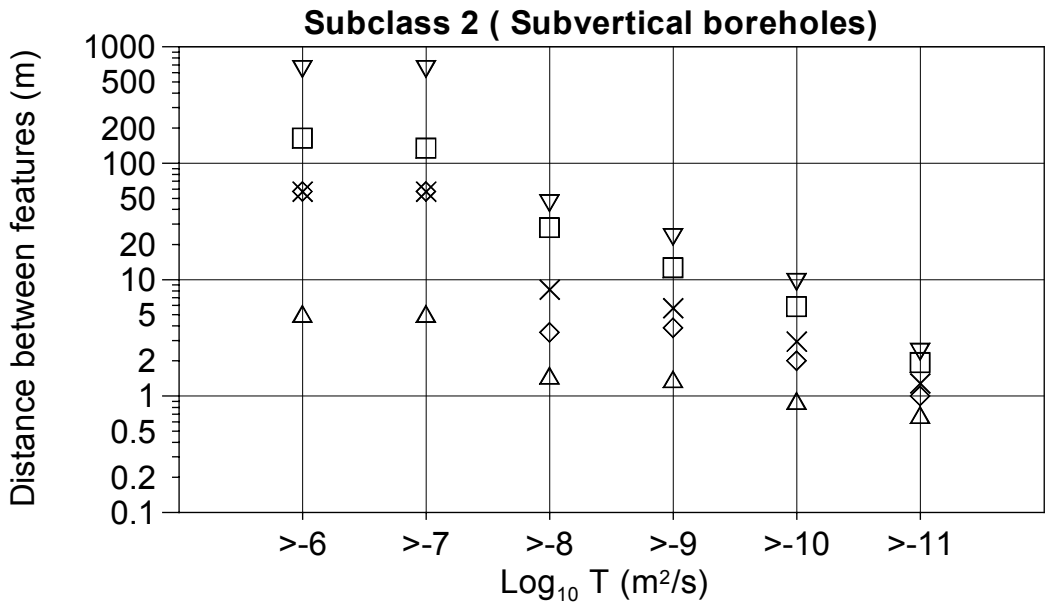


Figure 11-3 Distances between features. Summary of data set 1- 5 for subclass 1 (all boreholes).



Sum_dist2.grf 20-maj-99

Figure 11-4 Distances between features. Summary of data set 1- 5 for subclass 2 and 3 (vertical and horizontal boreholes).

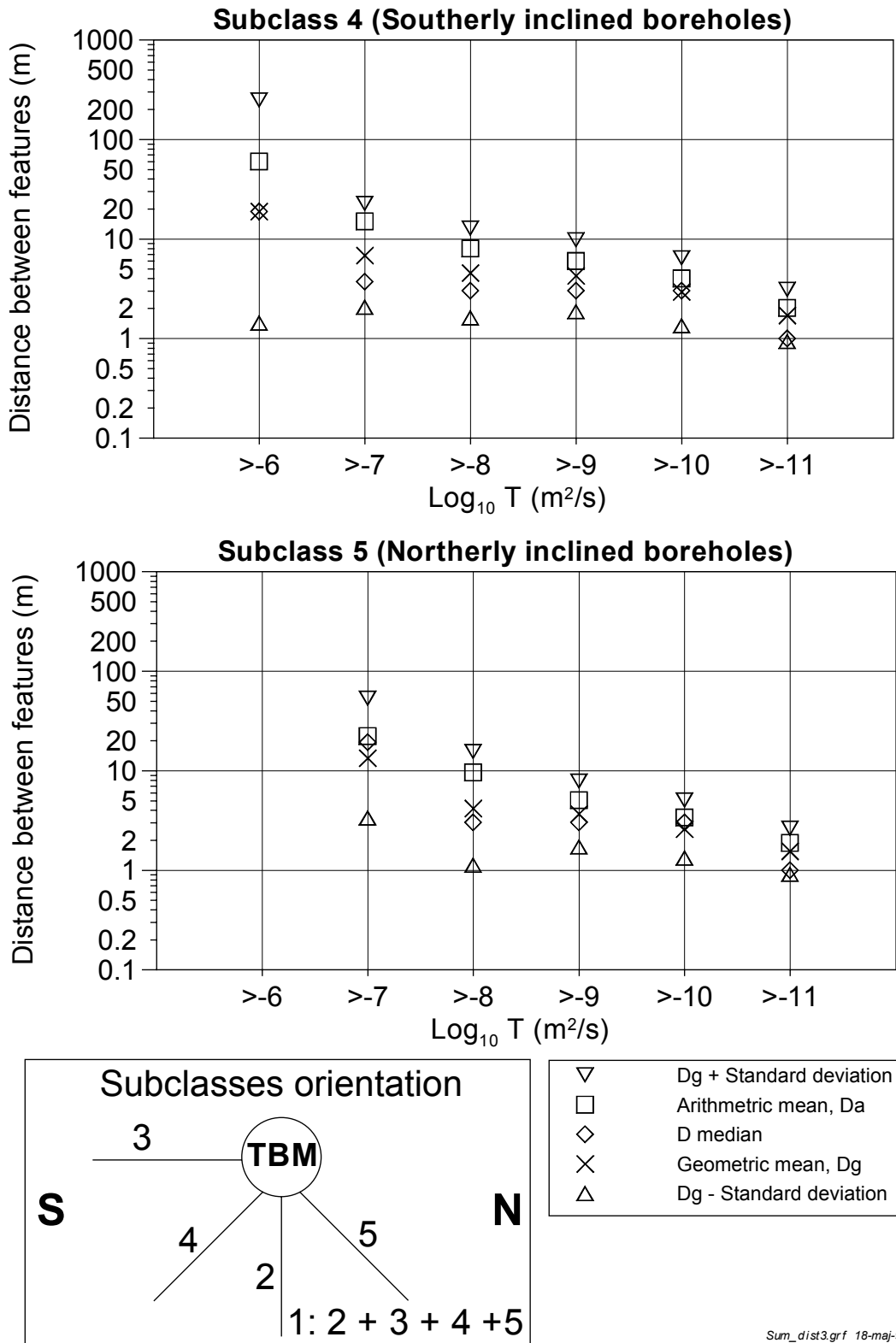


Figure 11-5 Distances between features. Summary of data set 1- 5 for subclass 2 and 3 (southerly and northerly inclined boreholes).

11.1.2 Measurement limit of transmissivity

The measurement limit for the flow rate measured with the double-packer system, reported in Chapter 6, was estimated to $1 \cdot 10^{-4}$ L/min. This was the minimum value that was given to the tests. The undisturbed water pressure could mostly be estimated and then an approximate estimate of the upper limit of the transmissivity for test sections with flow rates at measurement limit could be made. The statistics for the measurement limit of the transmissivity shown in Chapter 6 is shown in Figure 11-6.

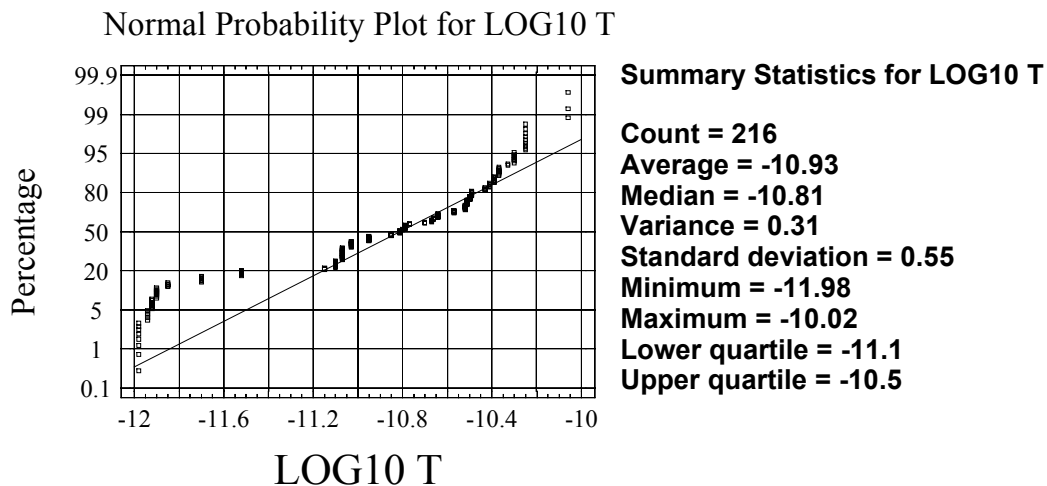


Figure 11-6 Probability distribution of Log10 T.

11.1.3 DFN properties

In Stigsson et al (2001) the fracture network and the hydraulic tests were analysed and a numerical model was made.

Fractures with low transmissivity have little influence on the flow solution but still require computer power to calculate the flow solution. In Stigsson et al (2001) the assumed cut-off for T of “natural” fractures is $3 \cdot 10^{-11}$ m²/s. This is the value that is assumed to be the cut-off for the simulated fractures that will be mapped as “natural” in the deposition holes. Fractures with a lower transmissivity are assumed to be “sealed”. The “natural” fractures still contain fractures that have little impact for the flow solution. In Stigsson et al (2001) the highest truncation value that was possible to use without losing accuracy for the flow was $5 \cdot 10^{-10}$ m²/s. Conductive fractures were therefore defined as fractures with a transmissivity larger than or equal to $5 \cdot 10^{-10}$ m²/s.

The fracture frequency along boreholes does not by itself explain how fractured the rock mass is as boreholes are only line samples. Maps of outcrops and tunnel walls show two-dimensional intersections with fractures in the network and are also subject of sampling bias. From a DFN point of view, intensity is best described by a three-dimensional measure, fracture area per unit volume (m²/m³), P₃₂. The fracture intensity measure, P₃₂ (fracture area density), cannot be measured directly in the field. However, Dershowitz and Herda (1992)

have shown that P_{21} (trace length density, fracture length per unit area, m/m^2) and P_{10} (linear frequency, fractures per unit length, No/m) is linearly correlated to P_{32} according to the equations:

$$P_{32} = C_{21} \cdot P_{21} \quad \text{or}$$

$$P_{32} = C_{10} \cdot P_{10}$$

Where C is an unknown constant of proportionality. This constant depends only upon the orientation and size distribution of the fractures in the rock mass, and the orientation of the surface (P_{21}) or along the line (P_{10}) in which the fractures have been mapped. Applying its linear relationship with P_{10} , P_{32} can be calculated from borehole data by means of generating a DFN model based on the orientation and size distributions derived with a hypothetical $P_{32,sim}$. See Stigsson et al (2001) for further details.

Table 11-2 shows the fracture intensity, P_{32} , for all, natural- and conductive fractures. The measured and simulated fracture frequency for different transmissivity cut-off is shown in Figure 11-7. One can see a good match for measured and simulated frequencies for the sub-vertical holes, sub-horizontal holes and holes inclined towards north, but the southerly inclined holes is intersected by approximately 30% too few fractures. The variation of the fracture frequency between the boreholes is rather large, which can be seen in Figure 11-9.

Table 11-2. P_{32} for the three different fracture sets with different truncation level.

	<i>Set 1</i>	<i>Set 2</i>	<i>Set 3</i>	Σ
$P_{32, all}$	0.85	1.59	0.97	3.41
$P_{32, natural}$	0.26	0.85	0.18	1.25
$P_{32, conductive}$	0.15	0.51	0.06	0.71

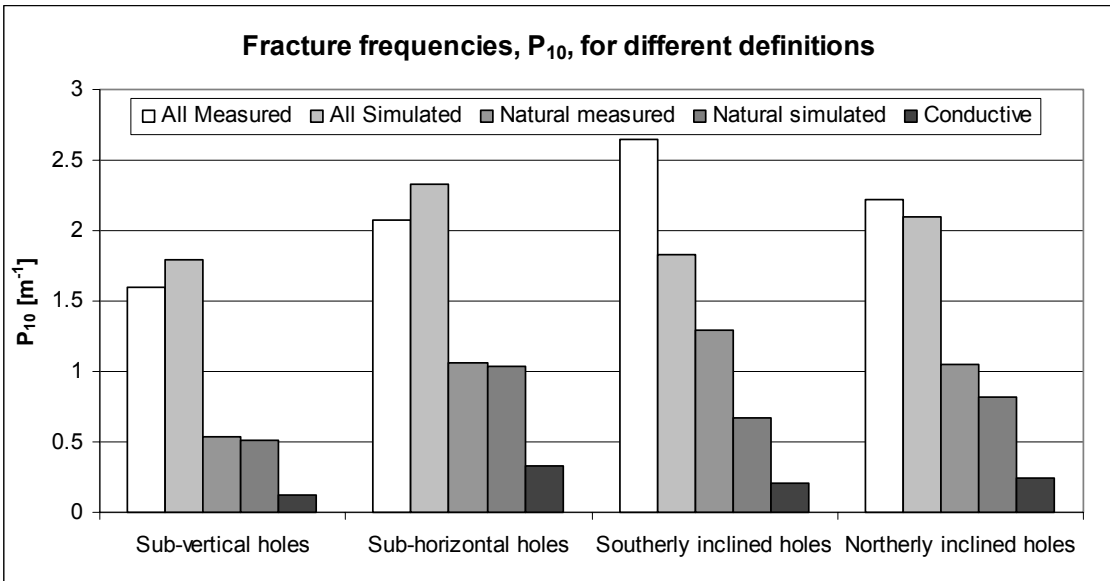


Figure 11-7. The fracture frequency in different borehole directions for different transmissivity cut-off.

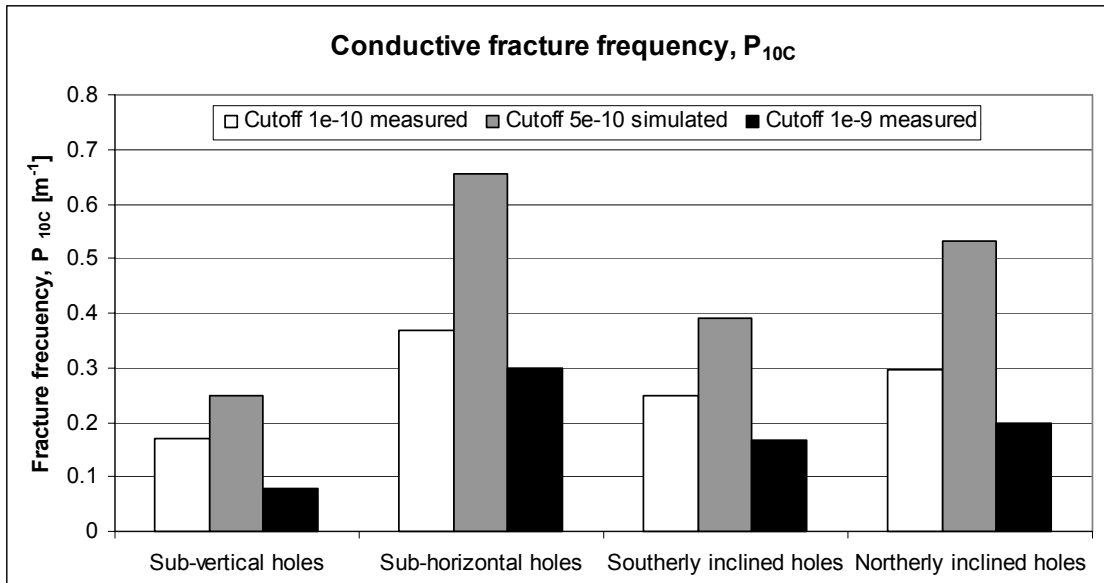


Figure 11-8. Estimated conductive fracture frequencies by Forsmark and Rhén (1999) and simulated frequency.

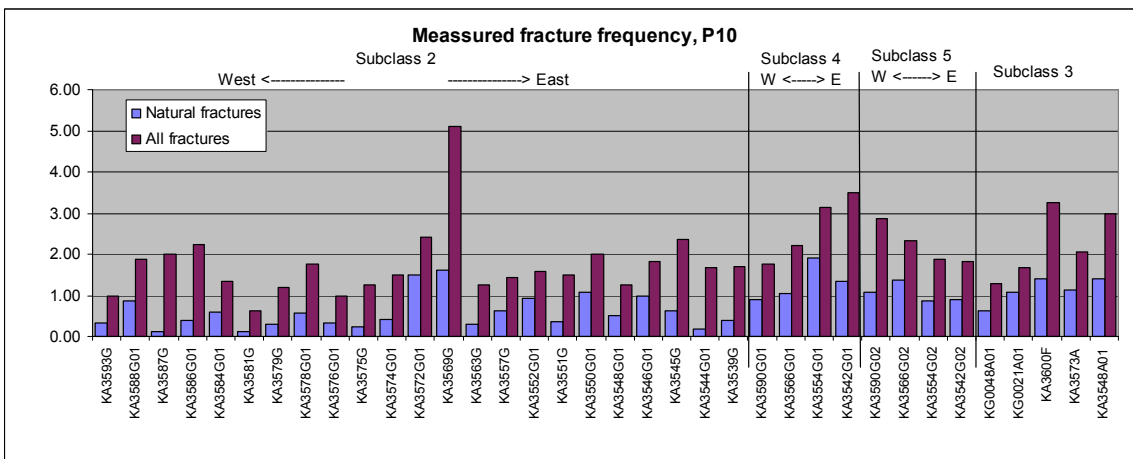


Figure 11-9. Fracture frequency in the 36 pilot and exploratory holes in the vicinity of the Prototype repository of the TBM tunnel.

As mentioned above the flow solution is made with only the conductive fractures present in the model, i.e. a model with a P_{32C} equal to $0.71 \text{ m}^2/\text{m}^3$. As a comparison Hermanson et al. (1999), used a DFN model with a conductive P_{32C} of $0.7 \text{ m}^2/\text{m}^3$. A comparison with the estimated fracture frequency at different transmissivities done by Forsmark and Rhén (1999b) shows that the DFN model produces twice as many fractures, see Figure 11-8. This can be an effect that Forsmark and Rhén (1999b) assumed that there only was one feature (fracture) per packer section and that the DFN model simulate a bit too many fractures with transmissivity in the mid range.

Table 11-3 is a summary of the calibrated parameters in the DFN model that was used for the sensitivity analysis and the predictions. A few results from the modelling are shown in Chapter 15.

Table 11-3. Summary of used parameters for the DFN model.(mean= arithmetic mean of the distribution).

<i>Parameter</i>	<i>Used data</i>				<i>Data from</i>	<i>Reference</i>
Orientation	Set	Strike	Dip	K	Pilot and Exploratory holes	Stigsson et al (2001)
	1	219	83.7	4.84		
	2	127	84.2	8.35		
	3	20.6	6	8.33		
Size, (m)	Set	mean	Std dev		TBM tunnel	Follin and Hermanson (1996)
	1	2	2			
	2	8	2			
	3	5	4			
Location model	Poisson distributed Enhanced Baecher				TBM tunnel	Follin and Hermanson (1996)
Conductive intensity, P_{32c}	0.71				Exploratory holes 1 m and 3 m test	Stigsson et al (2001)
Transmissivity distribution $\log_{10}(T)$ (m/s)	Set	mean	Std dev	Upper trunc	Pilot and Exploratory holes	Stigsson et al (2001)
	1	-11.5	2.30	-5		
	2	-10.3	2.07	-6		
	3	-11.6	1.47	-7		
Model size	100 x 175 x 100 m (North, East, Up)					
Centre point in Äspö96 Co-ordinates	North = 7271 m East = 1899 m Z = -448 m					
Outer boundary conditions	Specified head boundary				site scale model	Svensson (1997)
Inner boundaries	Tunnels as head simulating atmospheric pressure $p = 0$. Boreholes no flow or head according to performed tests				Performed tests	Gentzschein (personal communication 1998) and Forsmark and Rhén (1999b)

11.2 Hydraulic conductivity

11.2.1 Undisturbed rock mass

Each of the subclasses defined in Section 11.1.1 were statistically analysed using the criteria's below

- Log_{10} K for 1 m sections (tested as such)
- Log_{10} K for 3 m sections (tested as such)
- Log_{10} K for 3 m sections, where the transmissivity of the 1 meter tested sections were added together in series of three to create artificial 3 m sections and then divided by 3 meters. In this manner, Log_{10} K for the entire bore hole length was created. In Table 11-4, the results are detailed. In Figure 11-10, the results of the group (1*3 + 3 m) are illustrated.

Table 11-4. Statistical analysis of Log_{10} K. Scale 1 m and 3 m.

Subclass (see above)	Geometric mean (m/s) 1 m	Standard deviation (Log_{10} K) 1 m	Geometric mean (m/s) 3 m	Standard deviation (Log_{10} K) 3 m	Geometric mean (m/s) 1*3 + 3 m	Standard deviation (Log_{10} K) 1*3 + 3 m
1	$8.5 \cdot 10^{-11}$	1.48	$4.1 \cdot 10^{-10}$	1.83	$3.2 \cdot 10^{-10}$	1.76
2	$2.6 \cdot 10^{-11}$	1.09	$2.5 \cdot 10^{-11}$	1.71	$3.7 \cdot 10^{-11}$	1.47
3	$2.6 \cdot 10^{-9}$	1.91	$2.5 \cdot 10^{-9}$	1.98	$8.7 \cdot 10^{-9}$	1.70
4	$9.0 \cdot 10^{-11}$	1.08	$9.4 \cdot 10^{-10}$	1.83	$6.2 \cdot 10^{-10}$	1.62
5	$1.9 \cdot 10^{-10}$	1.26	$9.1 \cdot 10^{-10}$	1.19	$8.1 \cdot 10^{-10}$	1.28

As can be noted the horizontal bore holes show considerably higher values of hydraulic conductivity than vertical bore holes. Observe that the tested sections for the 1 m and 3 m tests are not in the same part of the boreholes, see Chapter 6. To a minor extent probably the data is biased as the same feature (fracture or fracture system) and may have been tested in an adjacent test section due to a local hydraulically well - interconnected fracture network or long intersections between a conductive fracture and the bore hole.

In Forsmark and Rhén (1999b) the statistical analysis results are detailed. Some distributions are approximately log-normal (generally subclasses with (1*3 + 3 m) and 3 m data sets, but some deviate rather strongly from the log-normal distribution (almost all subclasses with 1 m data sets). For the near field of the prototype tunnel the distributions based on 1*3 + 3 m tests in Table 11-4 should be used preferably.

Bore holes KA3573A, KA3600F and the first 50 metres of KA3510A was not included in the analysis since no hydraulic tests have been made in those boreholes. The tests in section below 50 m in KA3510A, with test section lengths of 5 m, were not either included in the analysis.

In Section 15.2.3 the average hydraulic conductivity around the deposition holes is estimated.

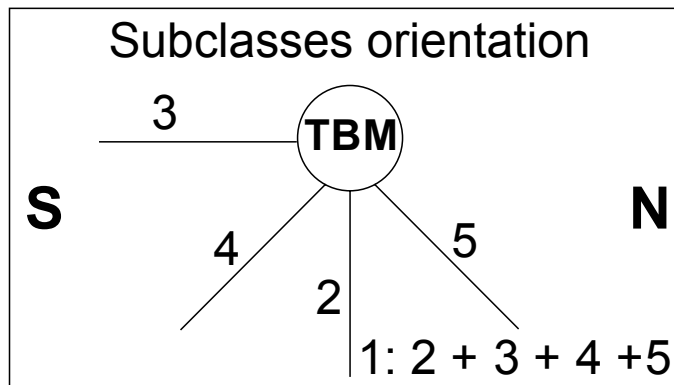
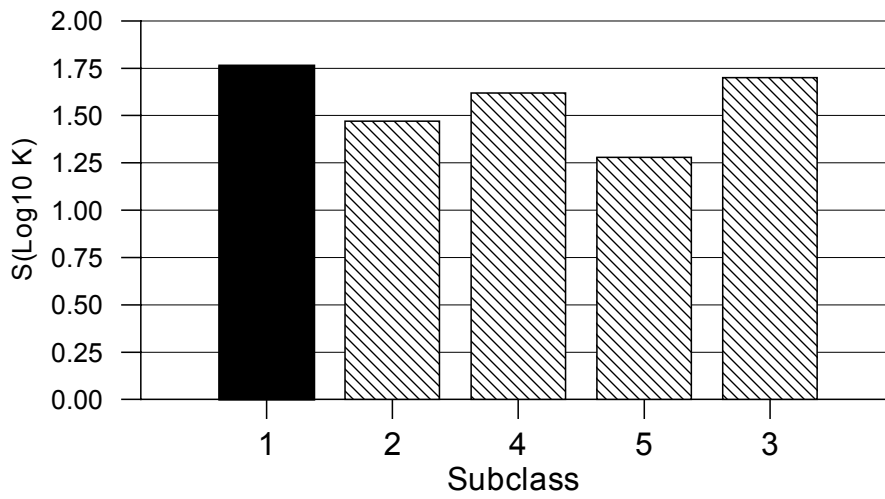
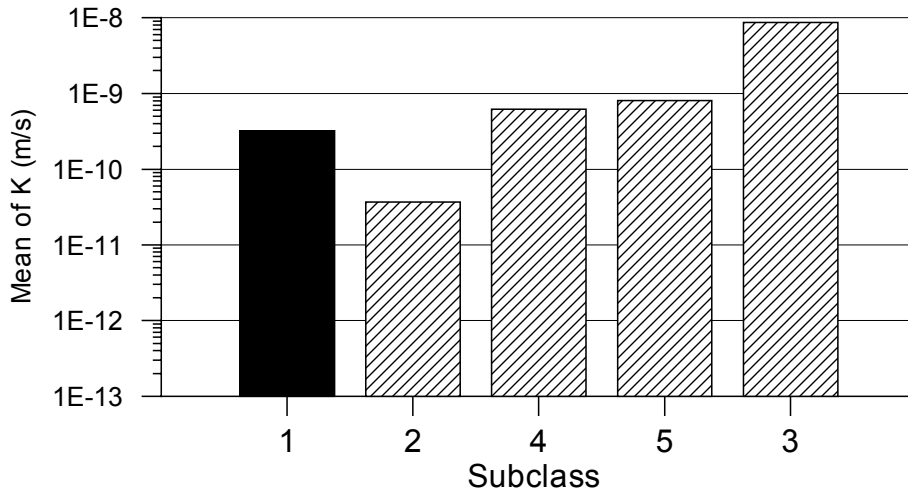


Fig_6_4B.GRF 16-Aug-01

Figure 11-10 Statistical analysis of Log10 K (1*3 + 3 m), geometric mean and standard deviation.

11.3 Hydraulic diffusivity

The diffusivity, η , versus the distance, r , and the timelag versus the distance, r , are shown in Figure 11-11 below. Data are from all 14 interference tests performed during the two test campaigns.

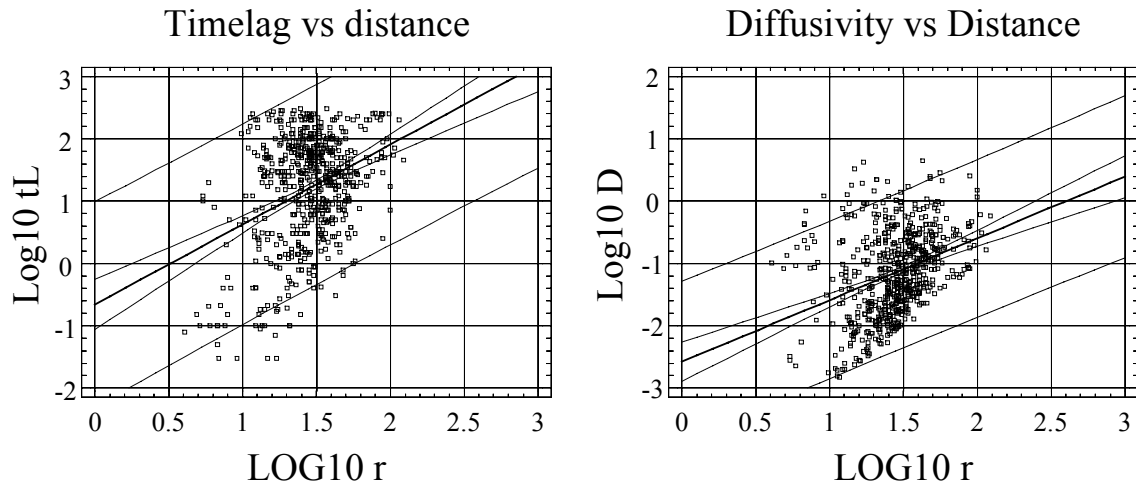


Figure 11-11 Linear regression plots of timelag, t_L (min) and diffusivity versus distance, r , (m).

The equations of the regression lines in Figure 11-11 are

$$\text{Log}_{10} t_L = 1.282 * \text{Log}_{10} r - 0.655$$

$$\text{Log}_{10} \eta = 0.991 * \text{Log}_{10} r - 2.579$$

11.4 Storativity

The storativity is not always received from a hydraulic test. In order to estimate an approximate value of the parameter a relationship between the evaluated transmissivity T_{EVAL} and the evaluated storativity S is established from the fourteen evaluated interference tests 1:1-2:14. The results are shown in Figure 11-12.

Linear regression of T and S

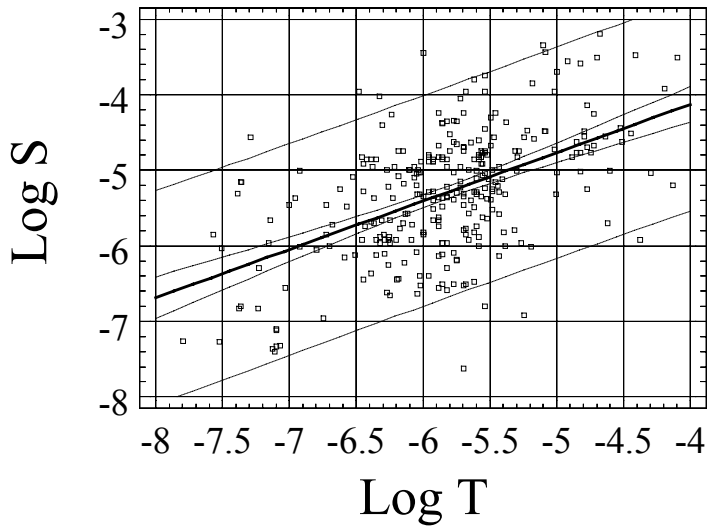


Figure 11-12 Linear regression of T_{EVAL} and S .

The equation of the regression line in Figure 11-12 is

$$\text{Log}_{10} S = 0.640 * \text{Log}_{10} T_{EVAL} - 1.570$$

The relationship between T_{EVAL} and the storativity estimated from the diffusivity, η (see Section 8.2), is shown in Figure 11-13. Results from all fourteen tests 1:1 to 2:14 are included.

Linear regression of T and S star

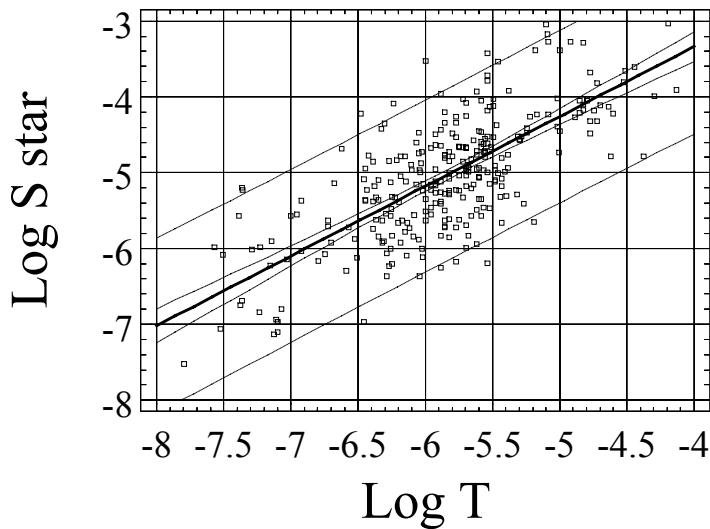


Figure 11-13 Linear regressions of T_{EVAL} and S^* .

The equation of the regression line in Figure 11-13 is

$$\text{Log}_{10} S^* = 0.919 * \text{Log}_{10} T + 0.338$$

11.5 Connectivity

The connectivity of the rock around the prototype repository is analyzed in this chapter. In Table 11-5, the responses from the 14 interference tests are summarized. The flow period was about 6 to 7 h for most of the tests and about 1 h a for two tests and 10 minutes for one test, see Sections 8.4 and 8.5.

The Table 11-5 and Figure 11-14 show that about 25 % of the test sections show no responses and about 33 % of the test sections only show small responses ($0.1 \text{ m} < dP < 1 \text{ m}$) after flow time of the test. The rest or 42 % percent of the responses are larger than 1 meter or show good response.

Table 11-5 Summary of responses in 14 interference tests. The response is classified as 0 = no response ($< 0.1 \text{ m}$), 1 = some response ($0.1 - 1.0 \text{ m}$) and 2 = good response ($> 1.0 \text{ m}$).

Test	Test index	Distance to test section, r, (m)	r-index	No response (=0)	Some response (=1)	Good response (=2)	Sum
1:1	1	0 – 10	1	0	0	2	2
1:1	1	10 – 15	2	1	1	4	6
1:1	1	15 – 20	3	7	6	3	16
1:1	1	20 – 25	4	3	6	1	10
1:1	1	25 – 30	5	1	2	2	5
1:1	1	30 – 35	6	1	4	3	8
1:1	1	35 – 40	7	0	2	0	2
1:1	1	40 – 45	8	0	1	0	1
1:1	1	45 – 50	9	0	2	0	2
1:1	1	50 – 60	10	0	0	0	0
1:1	1	60 – 75	11	0	2	0	2
1:1	1	75 – 90	12	0	1	0	1
1:1	1	90 – 110	13	0	0	0	0
1:1	1	110 – 130	14	0	0	0	0
	Sum			13	27	15	55
1:2	2	0 – 10	1	0	0	2	2
1:2	2	10 – 15	2	2	1	5	8
1:2	2	15 – 20	3	8	1	3	12
1:2	2	20 – 25	4	5	1	2	8
1:2	2	25 – 30	5	3	3	2	8
1:2	2	30 – 35	6	1	4	1	6
1:2	2	35 – 40	7	0	6	0	6
1:2	2	40 – 45	8	0	1	0	1
1:2	2	45 – 50	9	0	0	0	0
1:2	2	50 – 60	10	0	1	0	1
1:2	2	60 – 75	11	0	1	0	1
1:2	2	75 – 90	12	0	1	0	1
1:2	2	90 – 110	13	0	1	0	1
1:2	2	110 – 130	14	0	0	0	0
	Sum			19	21	15	55
1:3	3	0 – 10	1	2	0	2	4
1:3	3	10 – 15	2	5	0	2	7
1:3	3	15 – 20	3	3	5	1	9
1:3	3	20 – 25	4	0	7	1	8
1:3	3	25 – 30	5	1	5	2	8
1:3	3	30 – 35	6	1	2	1	4

Test	Test index	Distance to test section, r, (m)	r-index	No response (=0)	Some response (=1)	Good response (=2)	Sum
1:3	3	35 – 40	7	1	1	0	2
1:3	3	40 – 45	8	2	3	0	5
1:3	3	45 – 50	9	1	2	0	3
1:3	3	50 – 60	10	1	2	0	3
1:3	3	60 – 75	11	1	0	0	1
1:3	3	75 – 90	12	0	1	0	1
1:3	3	90 – 110	13	0	0	0	0
1:3	3	110 – 130	14	0	0	0	0
	Sum			18	28	9	55
1:4	4	0 – 10	1	2	0	1	3
1:4	4	10 – 15	2	4	0	2	6
1:4	4	15 – 20	3	12	0	0	12
1:4	4	20 – 25	4	4	2	0	6
1:4	4	25 – 30	5	8	0	2	10
1:4	4	30 – 35	6	3	0	0	3
1:4	4	35 – 40	7	4	0	0	4
1:4	4	40 – 45	8	3	0	0	3
1:4	4	45 – 50	9	3	1	0	4
1:4	4	50 – 60	10	2	0	0	2
1:4	4	60 – 75	11	1	0	0	1
1:4	4	75 – 90	12	1	0	0	1
1:4	4	90 – 110	13	0	0	0	0
1:4	4	110 – 130	14	0	0	0	0
	Sum			47	3	5	55
1:5	5	0 – 10	1	0	0	1	1
1:5	5	10 – 15	2	0	0	1	1
1:5	5	15 – 20	3	0	0	0	0
1:5	5	20 – 25	4	1	2	3	6
1:5	5	25 – 30	5	6	0	5	11
1:5	5	30 – 35	6	1	0	2	3
1:5	5	35 – 40	7	1	0	6	7
1:5	5	40 – 45	8	0	0	3	3
1:5	5	45 – 50	9	2	0	0	2
1:5	5	50 – 60	10	0	2	7	9
1:5	5	60 – 75	11	0	0	1	1
1:5	5	75 – 90	12	0	2	0	2
1:5	5	90 – 110	13	0	0	0	0
1:5	5	110 – 130	14	0	0	0	0
	Sum			11	6	29	46
1:6	6	0 – 10	1	2	0	2	4
1:6	6	10 – 15	2	5	1	1	7
1:6	6	15 – 20	3	6	3	0	9
1:6	6	20 – 25	4	1	5	2	8
1:6	6	25 – 30	5	3	3	1	7
1:6	6	30 – 35	6	2	1	1	4
1:6	6	35 – 40	7	1	2	0	3
1:6	6	40 – 45	8	2	3	0	5
1:6	6	45 – 50	9	0	2	0	2
1:6	6	50 – 60	10	0	1	1	2
1:6	6	60 – 75	11	0	1	0	1
1:6	6	75 – 90	12	0	0	0	0
1:6	6	90 – 110	13	0	0	0	0
1:6	6	110 – 130	14	0	0	0	0
	Sum			22	22	8	52
2:7	7	0 – 10	1	0	0	1	1
2:7	7	10 – 15	2	0	0	0	0
2:7	7	15 – 20	3	0	0	1	1
2:7	7	20 – 25	4	6	2	3	11

Test	Test index	Distance to test section, r, (m)	r-index	No response (=0)	Some response (=1)	Good response (=2)	Sum
2:7	7	25 – 30	5	4	7	1	12
2:7	7	30 – 35	6	0	4	4	8
2:7	7	35 – 40	7	1	1	4	6
2:7	7	40 – 45	8	1	4	6	11
2:7	7	45 – 50	9	0	2	3	5
2:7	7	50 – 60	10	0	1	3	4
2:7	7	60 – 75	11	0	0	0	0
2:7	7	75 – 90	12	0	1	0	1
2:7	7	90 – 110	13	0	1	0	1
2:7	7	110 – 130	14	0	0	0	0
	Sum			12	23	26	61
2:8	8	0 – 10	1	0	0	2	2
2:8	8	10 – 15	2	0	0	4	4
2:8	8	15 – 20	3	2	0	1	3
2:8	8	20 – 25	4	6	4	7	17
2:8	8	25 – 30	5	0	3	6	9
2:8	8	30 – 35	6	4	0	4	8
2:8	8	35 – 40	7	0	0	5	5
2:8	8	40 – 45	8	0	0	4	4
2:8	8	45 – 50	9	0	0	3	3
2:8	8	50 – 60	10	0	0	3	3
2:8	8	60 – 75	11	0	1	1	2
2:8	8	75 – 90	12	0	2	0	2
2:8	8	90 – 110	13	0	0	0	0
2:8	8	110 – 130	14	0	0	0	0
	Sum			12	10	40	62
2:9	9	0 – 10	1	0	1	1	2
2:9	9	10 – 15	2	3	7	6	16
2:9	9	15 – 20	3	0	4	5	9
2:9	9	20 – 25	4	4	1	2	7
2:9	9	25 – 30	5	2	8	2	12
2:9	9	30 – 35	6	1	4	0	5
2:9	9	35 – 40	7	1	2	1	4
2:9	9	40 – 45	8	0	2	0	2
2:9	9	45 – 50	9	0	0	0	0
2:9	9	50 – 60	10	0	0	0	0
2:9	9	60 – 75	11	0	1	0	1
2:9	9	75 – 90	12	0	2	0	2
2:9	9	90 – 110	13	1	0	0	1
2:9	9	110 – 130	14	0	0	0	0
	Sum			12	32	17	61
2:10	10	0 – 10	1	0	0	1	1
2:10	10	10 – 15	2	0	0	4	4
2:10	10	15 – 20	3	2	3	9	14
2:10	10	20 – 25	4	1	2	4	7
2:10	10	25 – 30	5	0	1	5	6
2:10	10	30 – 35	6	1	1	5	7
2:10	10	35 – 40	7	3	1	6	10
2:10	10	40 – 45	8	1	0	1	2
2:10	10	45 – 50	9	1	0	1	2
2:10	10	50 – 60	10	0	1	5	6
2:10	10	60 – 75	11	0	1	0	1
2:10	10	75 – 90	12	0	2	0	2
2:10	10	90 – 110	13	0	1	0	1
2:10	10	110 – 130	14	0	0	0	0
	Sum			9	13	41	63
2:11	11	0 – 10	1	1	0	7	8
2:11	11	10 – 15	2	0	4	4	8

Test	Test index	Distance to test section, r, (m)	r-index	No response (=0)	Some response (=1)	Good response (=2)	Sum
2:11	11	15 – 20	3	0	1	4	5
2:11	11	20 – 25	4	0	2	8	10
2:11	11	25 – 30	5	0	1	7	8
2:11	11	30 – 35	6	1	2	4	7
2:11	11	35 – 40	7	1	1	1	3
2:11	11	40 – 45	8	1	1	1	3
2:11	11	45 – 50	9	0	1	1	2
2:11	11	50 – 60	10	0	0	2	2
2:11	11	60 – 75	11	0	1	0	1
2:11	11	75 – 90	12	0	1	0	1
2:11	11	90 – 110	13	0	1	0	1
2:11	11	110 – 130	14	0	1	0	1
	Sum			4	17	39	60
2:12	12	0 – 10	1	0	0	4	4
2:12	12	10 – 15	2	0	2	7	9
2:12	12	15 – 20	3	2	3	4	9
2:12	12	20 – 25	4	0	1	4	5
2:12	12	25 – 30	5	1	5	5	11
2:12	12	30 – 35	6	1	0	3	4
2:12	12	35 – 40	7	2	1	2	5
2:12	12	40 – 45	8	1	1	2	4
2:12	12	45 – 50	9	0	0	0	0
2:12	12	50 – 60	10	0	2	3	5
2:12	12	60 – 75	11	0	1	0	1
2:12	12	75 – 90	12	0	1	0	1
2:12	12	90 – 110	13	0	0	0	0
2:12	12	110 – 130	14	0	0	0	0
	Sum			7	17	34	58
2:13	13	0 – 10	1	0	0	1	1
2:13	13	10 – 15	2	0	0	1	1
2:13	13	15 – 20	3	0	1	1	2
2:13	13	20 – 25	4	1	5	4	10
2:13	13	25 – 30	5	0	10	5	15
2:13	13	30 – 35	6	1	7	2	10
2:13	13	35 – 40	7	1	3	4	8
2:13	13	40 – 45	8	2	2	3	7
2:13	13	45 – 50	9	0	0	0	0
2:13	13	50 – 60	10	0	0	1	1
2:13	13	60 – 75	11	1	1	0	2
2:13	13	75 – 90	12	1	2	0	3
2:13	13	90 – 110	13	1	0	0	1
2:13	13	110 – 130	14	1	0	0	1
	Sum			9	31	22	62
2:14	14	0 – 10	1	0	0	2	2
2:14	14	10 – 15	2	0	0	1	1
2:14	14	15 – 20	3	1	1	5	7
2:14	14	20 – 25	4	0	2	8	10
2:14	14	25 – 30	5	0	3	5	8
2:14	14	30 – 35	6	0	0	7	7
2:14	14	35 – 40	7	1	1	7	9
2:14	14	40 – 45	8	1	1	5	7
2:14	14	45 – 50	9	0	1	1	2
2:14	14	50 – 60	10	0	1	2	3
2:14	14	60 – 75	11	0	0	1	1
2:14	14	75 – 90	12	0	1	0	1
2:14	14	90 – 110	13	0	1	0	1
2:14	14	110 – 130	14	0	1	0	1
	Sum			3	13	44	60

Test	Test index	Distance to test section, r, (m)	r-index	No response (=0)	Some response (=1)	Good response (=2)	Sum
	Total Sum			201	271	344	816

In Figure 11-14, the distribution within each radius index group is visualized.

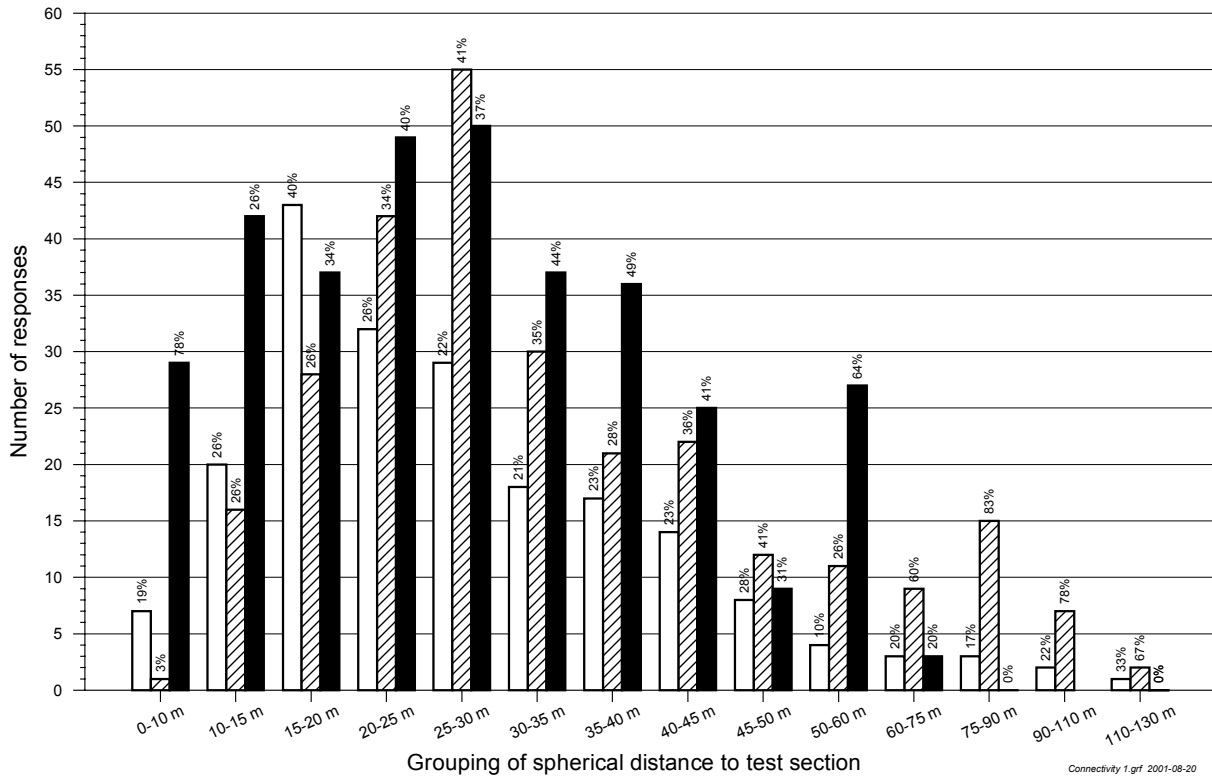


Figure 11-14 Distribution of responses versus distance to test section. White: No responses, Line screen: Some response (0.1-1.0m), Black: god response(>1.0m)

11.6 Preliminary model of deterministic features

Two major and six minor hydraulic features have been located. In Figure 11-15, Figure 11-16 and Table 1 the location of the features are shown.

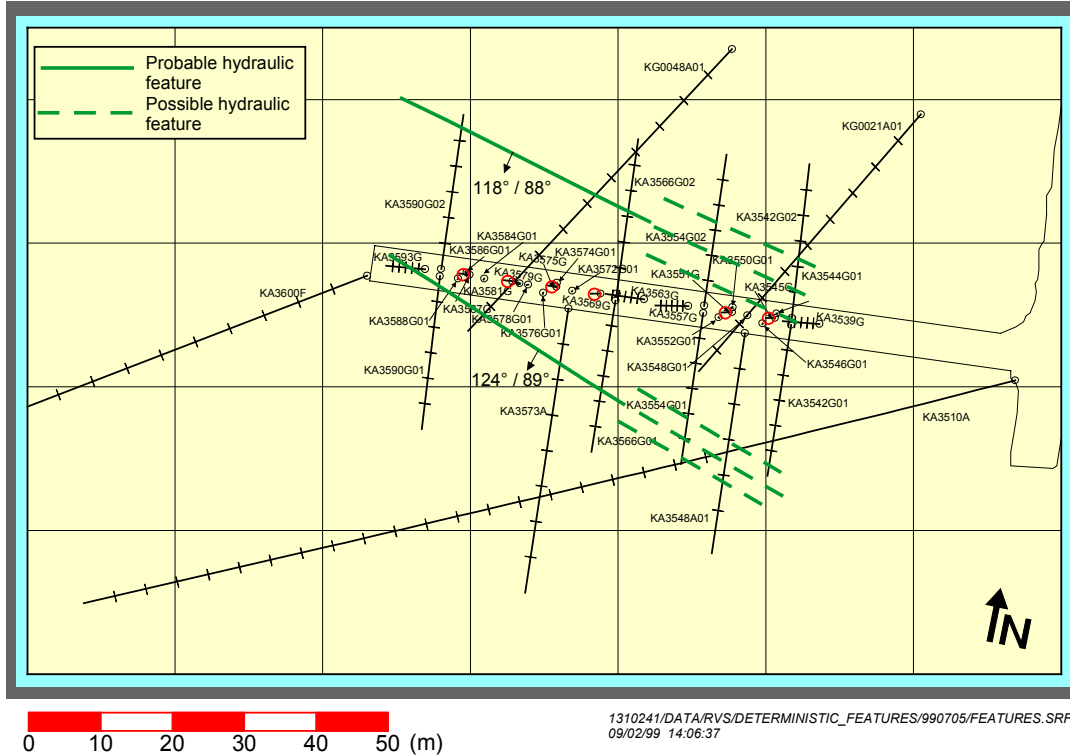


Figure 11-15 Major hydraulic features located during interference tests 1:1 - 1:6.

North major feature

This feature is located north of the prototype repository, most notably observed in bore holes KA3566G02 and KA3590G02. The strike and dip of this feature is approximately 118° and 88° respectively. The location of the centre with an estimated hydraulic radius of 20 m, of this feature, is estimated to be at

X (East) = 1892 m

Y (North) = 7289 m

Z = -449 mamsl (meters above mean sea level)

This feature has a transmissivity of $5 - 10 \cdot 10^{-8} \text{ m}^2/\text{s}$ and a storage coefficient of $1 - 3 \cdot 10^{-7}$.

South major feature

This feature is located south of the prototype repository, most notably observed in bore holes KA3566G01 and KA3590G01. It does not intersect KA3573A or KG0048A01. The strike and dip of this feature is approximately 124° and 89° respectively. The location of the centre with an estimated hydraulic radius of 20 m, of this feature, is estimated to be at

X (East) = 1887 m

Y (North) = 7266 m

Z = -449 mamsl (meters above mean sea level)

This feature has a transmissivity of $7 - 9 \cdot 10^{-8} \text{ m}^2/\text{s}$ and a storage coefficient of $4 - 5 \cdot 10^{-8}$.

Minor features

In Figure 11-16 and Table 11-6 the properties of the six minor features are shown.

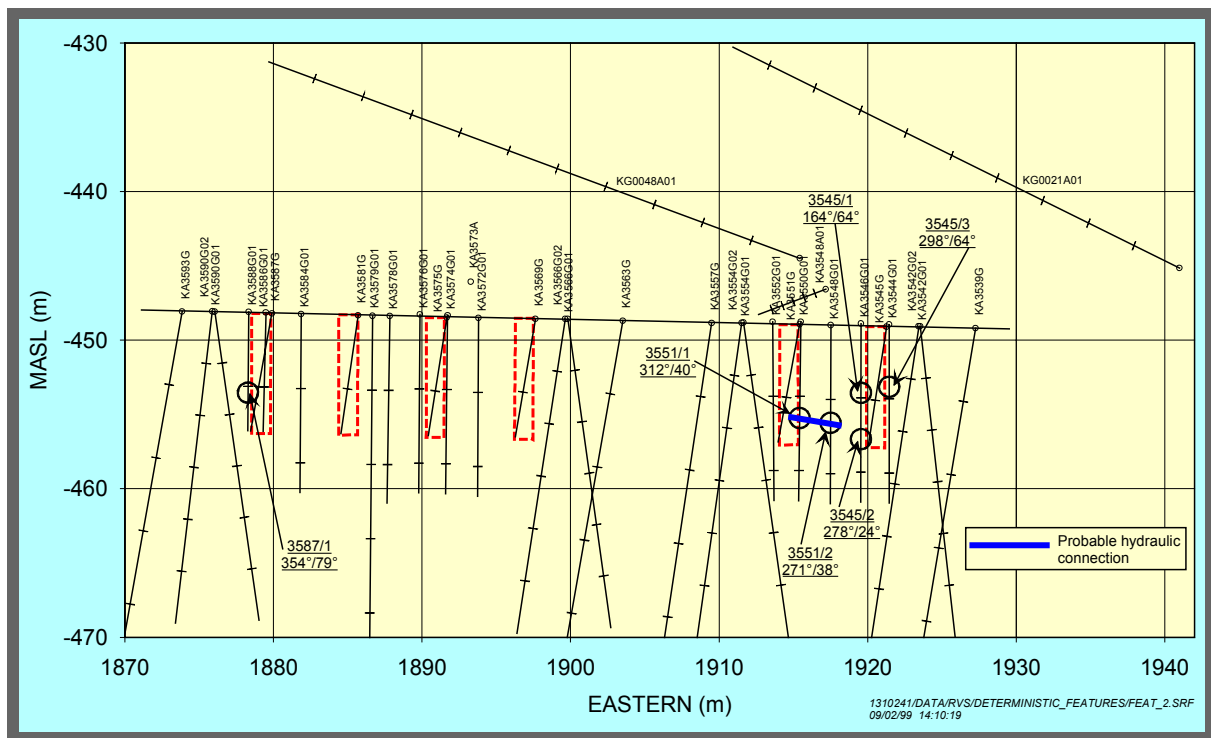


Figure 11-16 Minor identified features in the close vicinity of the deposition bore holes labelled with feature name and strike/dip.

Table 11-6 Data of minor features. The co-ordinates indicate the centre of the feature plane.

Feature	X (east) (m)	Y (north) (m)	Z (mamsl)	Strike (°)	Dip (°)	Radius (m)	T (m ² /s)	S (-)
3587/1	1878.28	7275.03	-453.53	354	79	2	$8.1 \cdot 10^{-9}$	$3 \cdot 10^{-7}$
3551/1	1915.42	7271.06	-455.24	312	40	2	$4.7 \cdot 10^{-9}$	$3 \cdot 10^{-7}$
3551/2	1917.50	7269.90	-455.56	271	38	2	$3.3 \cdot 10^{-9}$	$2 \cdot 10^{-7}$
3445/2	1919.55	7268.80	-456.66	278	24	2	$1.7 \cdot 10^{-9}$	$2 \cdot 10^{-7}$
3445/1	1919.55	7268.80	-453.54	164	64	2	$2.8 \cdot 10^{-10}$	$9 \cdot 10^{-8}$
3445/3	1921.45	7270.22	-453.14	298	64	2	$1.3 \cdot 10^{-8}$	$4 \cdot 10^{-7}$

12 UNDISTURBED HYDRAULIC PRESSURE

The “undisturbed hydraulic pressure” presented in this chapter is the measured pressures that are judged represent the static water pressure around the tunnel, assumed to not be affected of hydraulic tests, water sampling etc.

12.1 Before the deposition holes were drilled

An analysis of the undisturbed pressure in the rock has been done within this project for a limited period, namely between 1999-03-01 and the end of June 1999. The purpose of this has been to try detecting any time correlated trends of the levels of the hydraulic pressure in the rock. As a summary Table 12-1 and Figure 12-1 is presented.

In Figure 12-1 five different pressures are shown

- P_0 , as reported in Forsmark and Rhén (1999a) for sections of the interference test campaign 1 that coincide with sections of the drilling campaign 1 - 3 of pilot and exploratory bore holes of the prototype repository.
- Pressure 1999-03-01
- Pressure 1999-06-19
- Maximum pressure of a section during the time period 1999-03-01 to 1999-06-19
- Minimum pressure of a section during the time period 1999-03-01 to 1999-06-19

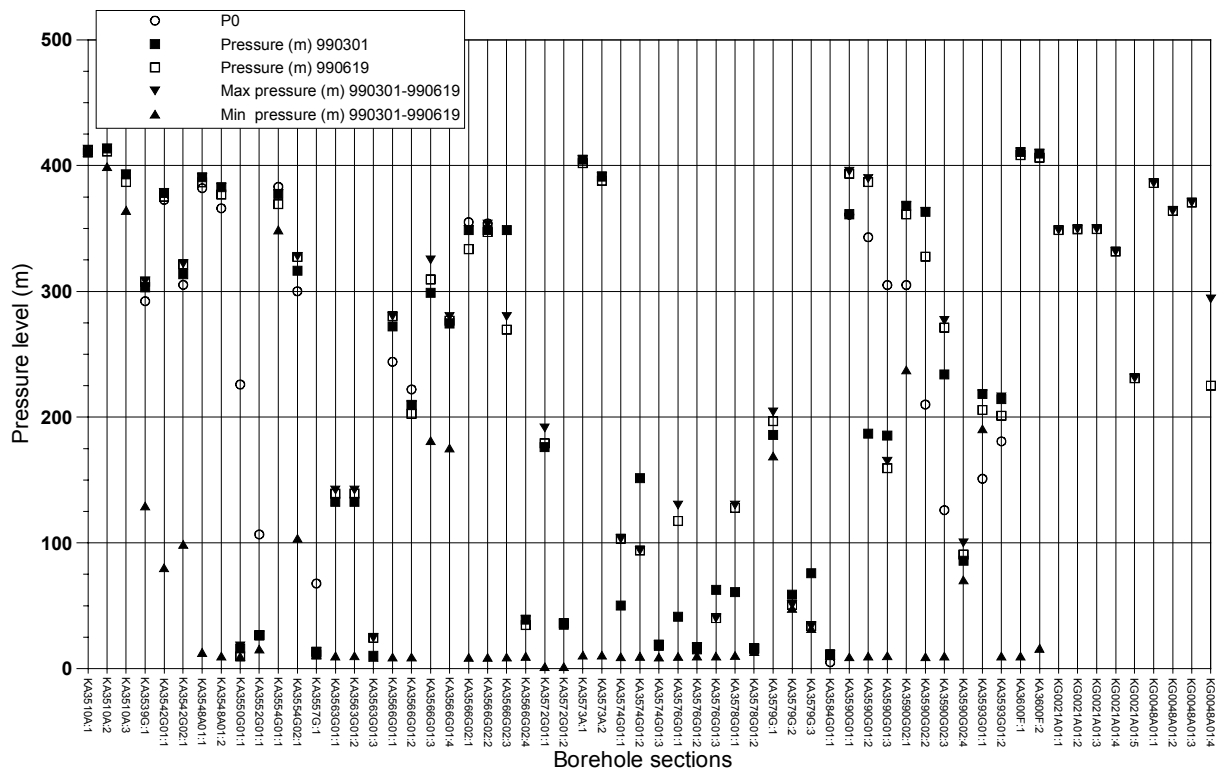


Figure 12-1 Pressures based on different times and methods of selection

Table 12-1 Undisturbed pressure. Estimated high pressures are marked with grey boxes and uncertain values are italicised.

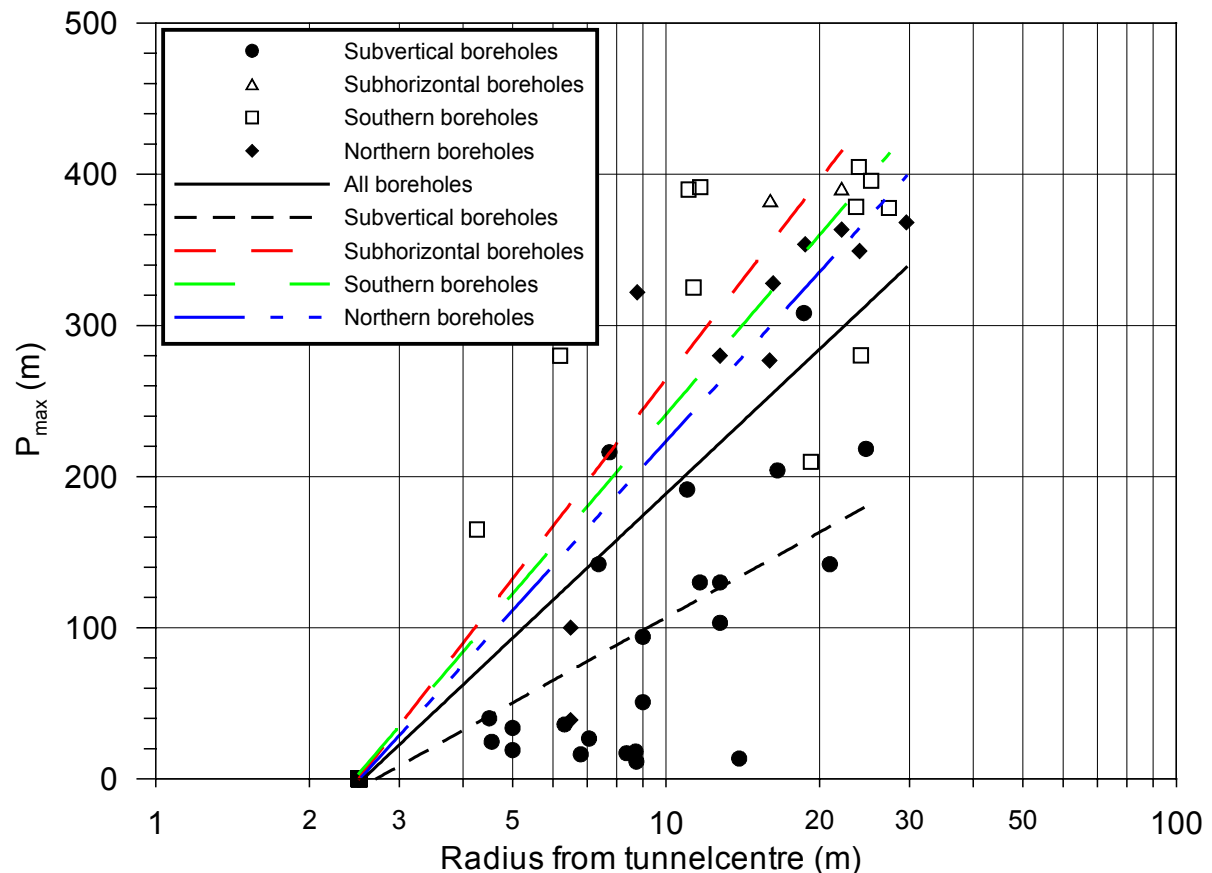
Bh	Secup_P0	Seclow_P0	P0 (m)	Secup	Seclow	P_990301 (m)	P_990619 (m)	P_min (m)	P_max (m)	Comment
KA3510A:1	-	-	-	122.02	150.00	410.29	412.38	410.29	413.03	
KA3510A:2	-	-	-	114.02	121.02	413.68	411.27	399.09	413.79	
KA3510A:3	-	-	-	4.52	113.02	393.13	386.89	364.39	393.23	
KA3539G:1	0.39	30.01	292.18	0.30	30.01	303.26	307.61	129.32	308.20	
KA3542G01:1	0.39	30.04	372.75	0.30	30.04	378.34	375.35	80.24	378.44	
KA3542G02:1	0.39	30.01	305.16	0.30	30.01	313.72	321.47	98.67	321.90	
KA3548A01:1	24.00	27.00	382	15.00	30.00	390.67	386.60	12.86	390.67	
KA3548A01:2	12.00	15.00	366	10.00	14.00	382.72	377.01	9.98	382.72	
KA3550G01:1	0.50	12.03	225.91	0.30	12.03	15.97	9.71	9.59	18.14	
KA3552G01:1	0.50	12.01	106.67	0.30	12.01	26.73	26.43	15.58	26.73	
KA3554G01:1	0.39	30.01	383.14	0.30	30.01	377.54	369.32	348.86	377.62	
KA3554G02:1	0.39	30.01	300.04	0.30	30.01	316.41	327.37	103.65	327.80	
KA3557G:1	0.39	30.04	67.67	0.30	30.04	11.12	13.41	10.87	13.51	Low conductive section
KA3563G01:1	-	-	-	9.30	30.00	132.57	139.10	10.09	142.04	Short cut with KA3563G01:2
KA3563G01:2	-	-	-	3.80	8.30	132.61	139.16	10.15	142.08	Short cut with KA3563G01:1
KA3563G01:3	-	-	-	1.30	2.80	10.34	24.38	9.09	24.61	
KA3566G01:1	19.00	22.00	244	20.80	30.01	272.13	280.25	9.24	280.25	
KA3566G01:2	16.00	19.00	222	12.30	19.80	209.76	202.66	9.29	209.76	
KA3566G01:3	-	-	-	7.30	11.30	298.92	309.44	181.19	325	Low conductive section
KA3566G01:4	-	-	-	1.30	6.30	274.56	276.59	175.46	280	Low conductive section
KA3566G02:1	18.00	21.00	355	19.30	30.01	348.84	333.59	8.92	349.18	
KA3566G02:2	15.00	18.00	354	12.30	18.30	348.80	347.08	8.95	353.61	
KA3566G02:3	-	-	-	7.80	11.30	348.67	269.54	9.16	280	Low conductive section
KA3566G02:4	-	-	-	1.30	6.80	38.98	34.72	9.79	38.98	Low conductive section
KA3572G01:1	-	-	-	6.30	12.00	176.18	179.11	1.54	191.46	
KA3572G01:2	-	-	-	1.30	5.30	35.00	36.06	1.54	36.06	
KA3573A:1	-	-	-	18.00	40.07	404.78	401.94	10.58	404.86	
KA3573A:2	-	-	-	4.50	17.00	391.35	387.85	10.69	391.45	
KA3574G01:1	-	-	-	8.80	12.00	50.23	103.26	9.54	103.26	Low conductive section
KA3574G01:2	-	-	-	5.30	7.80	151.52	94.01	9.82	94.01	Low conductive section
KA3574G01:3	-	-	-	1.30	4.30	18.19	19.09	9.28	19.09	Low conductive section
KA3576G01:1	-	-	-	8.80	12.01	41.28	117.46	9.64	130	Low conductive section
KA3576G01:2	-	-	-	3.80	7.80	15.37	17.03	10.10	17.03	Low conductive section
KA3576G01:3	-	-	-	1.30	2.80	62.66	40.11	9.85	40.11	Low conductive section
KA3578G01:1	-	-	-	6.80	12.58	60.96	127.89	10.47	130	Low conductive section
KA3578G01:2	-	-	-	1.30	5.80	15.27	16.30	13.43	16.30	Low conductive section
KA3579G01:1	-	-	-	9.30	22.65	185.91	196.80	169.12	204.09	Low conductive section
KA3579G01:2	-	-	-	5.30	8.30	58.74	50.79	47.89	50.79	Low conductive section
KA3579G01:3	-	-	-	1.30	4.30	75.79	33.75	31.86	33.75	Low conductive section
KA3584G01:1	1.21	12.00	5.08	0.30	12.00	10.85	11.30	10.69	11.51	Low conductive section
KA3590G01:1	21.00	24.00	361	17.30	30.06	361.34	393.56	9.29	395.63	
KA3590G01:2	8.00	9.00	343	7.80	16.30	186.93	386.98	10.01	389.83	
KA3590G01:3	5.00	6.00	305	1.30	6.80	185.23	159.34	10.11	165	Reinstrumentation of borehole
KA3590G02:1	24.00	27.00	305	23.30	30.05	367.93	361.24	237.61	368.05	
KA3590G02:2	18.00	21.00	210	17.30	22.30	363.22	327.69	9.45	363.42	
KA3590G02:3	12.00	15.00	126	8.30	16.30	233.86	271.21	9.95	276.83	
KA3590G02:4	-	-	-	1.20	7.20	85.83	90.68	70.43	100.09	
KA3593G01:1	21.00	24.00	151	8.30	30.02	218.35	205.68	190.69	218.35	
KA3593G01:2	4.74	5.74	180.7	1.30	7.30	214.41	201.09	9.87	216.09	
KA3600F:1	-	-	-	22.00	50.10	410.87	408.40	9.85	410.87	
KA3600F:2	-	-	-	4.50	21.00	409.62	406.37	16.15	409.70	
KG0021A01:1	-	-	-	42.50	48.82	-	348.70	-	348.70	Low conductive section
KG0021A01:2	-	-	-	35.00	41.50	-	349.40	-	349.55	
KG0021A01:3	-	-	-	25.00	34.00	-	349.52	-	349.59	
KG0021A01:4	-	-	-	17.00	24.00	-	331.68	-	331.70	
KG0021A01:5	-	-	-	4.00	16.00	-	230.83	-	231.07	
KG0048A01:1	-	-	-	49.00	54.69	-	386.17	-	386.21	
KG0048A01:2	-	-	-	41.00	48.00	-	363.96	-	364.02	
KG0048A01:3	-	-	-	30.00	40.00	-	370.69	-	370.73	
KG0048A01:4	-	-	-	4.00	29.00	-	225.01	-	293.97	

Some boreholes have very low hydraulic conductivity, among them KA3576G01, KA3579G and the upper parts of KA3566G01 and KA3566G02. A consequence of this fact is that a very high pressure may be registered when an activity occurs concerning a change in the hydraulic head around the tunnel.

In some cases, the measured values of a pressure are believed to be uncertain and are indicated as such in the Table 12-1. The values in the column P_max have for a number of low conductive borehole sections been estimated instead of using the measured values during the period.

In Figure 12-2 maximum pressures are plotted as function of the distance to the tunnel centre. The tunnel radius is estimated to be 2.5 meters. The equations for the different relationships (plotted lines) in the figure are shown below:

- All boreholes: $P_{max} = 317.71 * \text{Log}_{10}(D_t) - 128.92$
- Subvertical boreholes: $P_{max} = 187.62 * \text{Log}_{10}(D_t) - 80.82$
- Subhorizontal borehole: $P_{max} = 438.62 * \text{Log}_{10}(D_t) - 174.12$
- Southern boreholes: $P_{max} = 394.57 * \text{Log}_{10}(D_t) - 153.36$
- Northern boreholes: $P_{max} = 372.13 * \text{Log}_{10}(D_t) - 148.62$



1310241\data\hms\p0-data\r_pmax.grf 26-nov-99

Figure 12-2 Maximum pressures plotted as function of the distance to the tunnel centre.

In Table 12-1, P_0 may differ from the pressures measured during the period 1999-03-01 to 1999-06-19 because some of the P_0 pressures were measured within 3 meters packer enclosure. In that case, it is possible to isolate a single open fracture and thereby measuring a higher or lower pressure than measuring with longer packer distances.

During the period 1999-03-01 to 1999-06-19 different kinds of activities, such as water sampling, dilution tests and flow tests within the TRUE BLOCK SCALE, PROTOTYPE and GWCM projects, were on going in the prototype repository area or in the vicinity of it. These activities include water sampling, packer installations etc. It is to be noted that during the actual period there are approximately only two short periods of no activities, namely 1999-03-01 to 1999-03-03 and 1999-03-30 to 1999-04-05.

The following boreholes have what appears to be a systematic pressure head change trend; KA3510A, KA3542G01, KA3548A01, KA3554G01, KA3557G01, KA3566G01, KA3579G01, KA3584G01, KA3590G01 and KA3593G01.

The levels of HAS04, 05, 11, 19 and 20 were studied for the period 1996 up to date (Nyberg et al, 1997, 1998, 1999 and 2000). It was noticed there still is a decreasing trend of pietzometric levels of the rock mass above the Äspö Hard Rock Laboratory. HAS04 has a decreasing trend for the years 1996 and 1997, mainly during the first part of the year, but has stabilised during 1998. The other boreholes had no discernible trend of increasing or decreasing levels. When compared with the tunnel boreholes that have a pressure head change trend no direct correlation seem to exist.

The difference between the maximum registered pressures, start, and stop values of the studied time period is plotted in Figure 11-3.

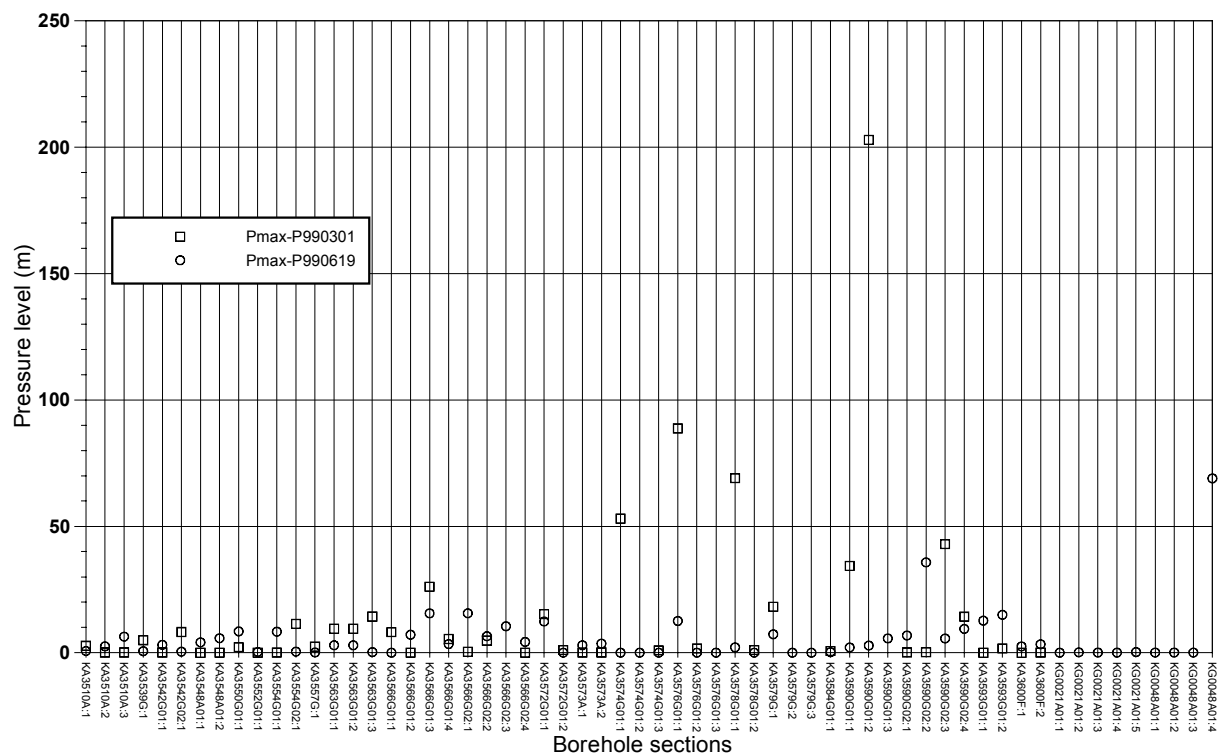


Figure 12-3 Difference between the maximum registered pressures and start and stop values of the studied period, 1999-03-01 and 1999-06-19.

As a guideline for values of undisturbed pressure the following is recommended ;

- For the use of numerical modelling without deposition bore holes P_{max} in Table 12-1 is the best estimate. It is assumed to best represent the undisturbed conditions before the deposition boreholes were drilled.
- For the use of numerical modelling initial pressure as P_{990619} in Table 12-1 is an alternative to P_{max} to study the pressure change during drilling of the deposition boreholes.

12.2 After the deposition holes were drilled

In Section 5.7 the pressure responses during the drilling of the deposition holes were presented and in Forsmark and Rhén (2001a) all details are shown. Generally, only small pressure changes were recorded. The few sections with greater changes can be seen in Table 5-5.

During the period between the drilling of deposition hole 4 (DA3569G01) and deposition hole 5 (DA3551G01) most of the observation hole was re-monitored. Thereby the monitoring sections available after the completion of the drilling were not the same as before the start of the drillings, except for KA3548A01, KA3557G, KA3566G01, KA3566G02 and KA3584G01. The borehole sections available and used are shown in Table 12-2.

Table 12-2 Pressures 1999-12-01 after deposition holes were drilled. CLASS: refers to main borehole direction, see below in text and Figure 11-3.

Bh	Secup (m)	Seclow (m)	Estimated point of hydraulic conductor (m)	CLASS	P_{max} in Table 12-1 for same section (m)	Pressure measured 1999-12-01 (m)
KA3539G:1	19.30	30.01	20.60	2		266.8
KA3539G:1	9.80	18.30	16.37	2		266.8
KA3539G:1	1.30	8.80	6.59	2		199.8
KA3542G01:1	25.80	30.04	28.50	4		382.7
KA3542G01:1	8.80	24.80	20.06	4		371.6
KA3542G01:1	1.30	7.80	4.50	4		110.7
KA3542G02:1	22.30	30.01	26.20	5		294.8
KA3542G02:1	13.80	21.30	17.43	5		316.3
KA3542G02:1	8.80	12.80	11.13	5		303.8
KA3542G02:1	1.30	7.80	5.36	5		283.3
KA3544G01	6.30	12.00	10.16	2		234.5
KA3544G01	1.30	5.30	4.03	2		105.6
KA3546G01	6.80	12.00	8.30	2		19.5
KA3546G01	1.30	5.80	4.33	2		6.3
KA3548A01:1	15.00	30.00	19.56	3	390.6	384.0
KA3548A01:2	10.00	14.00	13.49	3	382.7	374.7
KA3548G01	0.30	12.00	6.18	2		8.9
KA3550G01:1	6.30	12.03	9.42	2		4.9
KA3550G01:1	1.30	5.30	3.61	2		5.1

Bh	Secup (m)	Seclow (m)	Estimated point of hydraulic conductor (m)	CLASS	P _{max} in Table 12-1 for same section (m)	Pressure measured 1999-12-01 (m)
KA3552G01:1	8.80	12.01	10.15	2		50.5
KA3552G01:1	4.05	7.80	5.22	2		11.9
KA3552G01:1	1.30	3.05	1.53	2		17.0
KA3554G01:1	22.30	30.01	24.95	4		382.3
KA3554G01:1	12.30	21.30	19.39	4		380.8
KA3554G01:1	1.30	11.30	6.78	4		107.1
KA3554G02:1	22.30	30.01	28.47	5		328.9
KA3554G02:1	10.30	21.01	13.13	5		303.8
KA3554G02:1	1.30	9.30	8.39	5		326.5
KA3557G	0.30	30.04	11.40	2	13.5	17.1
KA3563G01	0.30	30.04	5.60	2		26.6
KA3566G01:1	20.80	30.01	21.57	4	280.2	256.0
KA3566G01:2	12.30	19.80	16.71	4	209.8	195.1
KA3566G01:3	7.30	11.30	8.81	4	325	321.9
KA3566G01:4	1.30	6.30	3.70	4	280	272.7
KA3566G02:1	19.30	30.01	21.41	5	349.2	319.2
KA3566G02:2	12.30	18.30	16.23	5	353.6	340.2
KA3566G02:3	7.80	11.30	10.25	5	280	265.5
KA3566G02:4	1.30	6.80	3.99	5	39.0	32.3
KA3572G01	0.30	12.00	5.77	2		34.5
KA3573A:1	18.00	40.07	21.34	4	404.9	398.8
KA3573A:2	4.50	17.00	9.16	4	391.5	384.8
KA3574G01	0.30	12.00	4.93	2		10.9
KA3578G01	0.30	12.58	7.03	2		9.1
KA3579G	0.30	22.65	11.44	2		54.7
KA3584G01	0.30	12.00	6.24	2	11.5	10.5
KA3590G01	0.30	30.06	4.33	4		69.1
KA3590G02	0.30	30.05	26.73	5		350.3
KA3593G01	0.30	30.02	6.45	2		145.1

In Figure 12-4 pressures chosen 1999-12-01 are plotted versus the distance to tunnel centre. The equations for the different relationships (plotted lines) in the figure are shown below:

- All boreholes (Class 1): $P_{\max} = 299.79 * \text{Log}_{10}(D_t) - 123.79$
- Subvertical boreholes (Class 2): $P_{\max} = 144.80 * \text{Log}_{10}(D_t) - 62.80$
- Subhorizontal borehole (Class 3): $P_{\max} = 430.31 * \text{Log}_{10}(D_t) - 170.79$
- Southern boreholes (Class 4): $P_{\max} = 357.87 * \text{Log}_{10}(D_t) - 141.77$
- Northern boreholes (Class 5): $P_{\max} = 346.18 * \text{Log}_{10}(D_t) - 136.25$

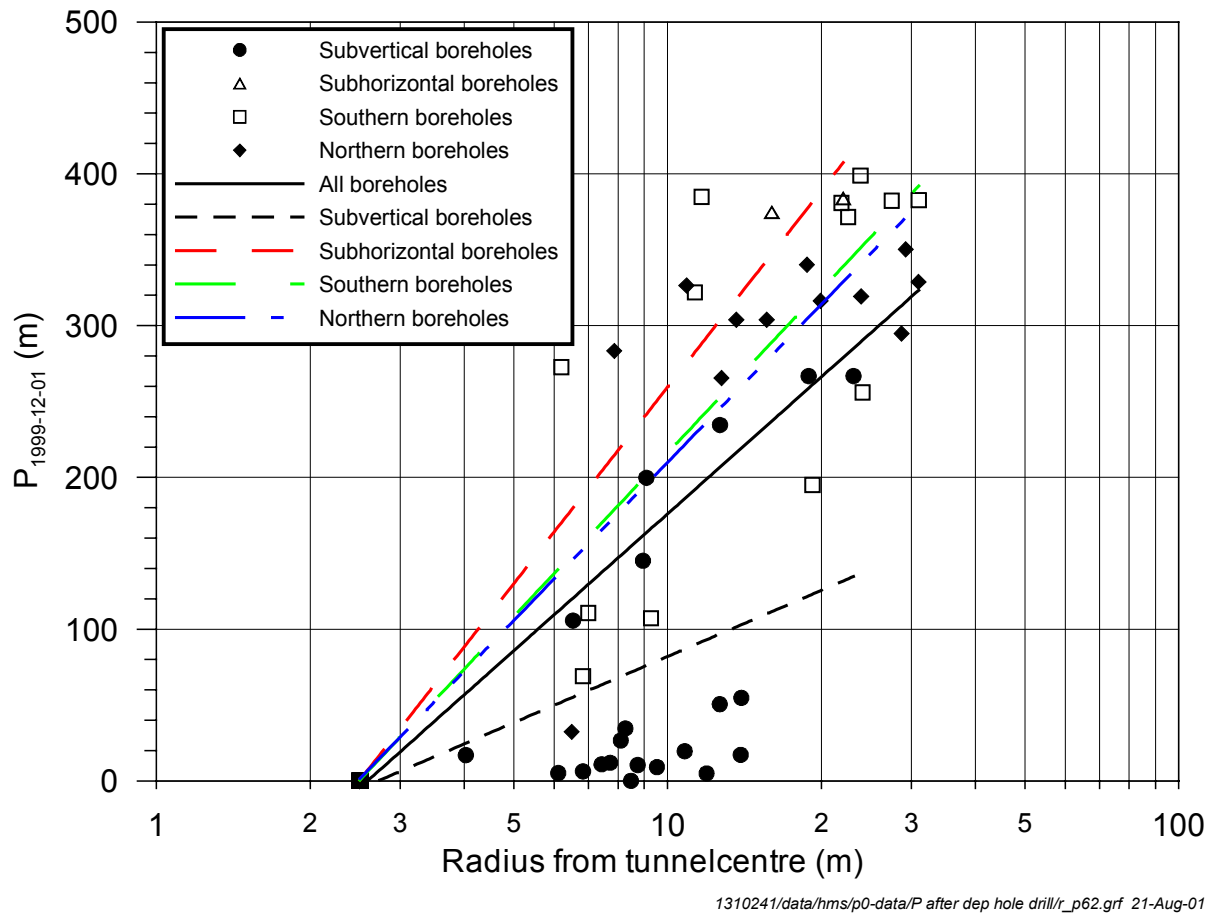


Figure 12-4 Pressures 1999-12-01 plotted as function of the distance to the tunnel centre.

When comparing the relationships in Figure 12-2 with those of Figure 12-4 the later one indicate lower pressures around the prototype tunnel after the drilling of the deposition holes. This is confirmed by studying the boreholes that were not re-monitored in July 1999, see Table 12-2. The changes are, however, minor but consistent except in the low-conductive hole KA3557G where a slight increase is observed.

According to Chapter 9, the water pressure increased in a few borehole sections when the blasting of two niches for the plugs was done in August 2000. Unfortunately most of the packers in the boreholes had been removed so there is no good picture of the pressure distribution around the tunnel after the blasting. The pressure ought to be somewhat higher than shown in Table 12-1.

The boreholes around the Prototype Repository will be instrumented with packers during 2001 and 2002 and the measurements will start as soon as possible after instrumentation.

13 Groundwater salinity and chemical composition

During 1998 and 1999 a number of water, samples were collected from investigation boreholes located in the near vicinity of the prototype repository. In order to provide modellers of the repository with relevant chemistry data the salinity of the groundwater is highlighted in this chapter.

The TBM drilled tunnel where the prototype repository is to be situated was finalized in the early autumn 1994. The drilling of the deposition holes commenced 1999-06-19 (DA3587G01) and continued in stages until the finalisation of the last hole 1999-09-18 (DA3545G01). Most of the sampling results presented in Section 5.3 are from the period before those holes were drilled.

13.1 Sampling procedure

During the drilling campaigns 1 – 3 which occurred in the period of 1997 - 1999 water sampling was made. During the flow logging of each hole, water sampling was carried out if the flow rate exceeded 50 mL/minute in the 1 m-sections or 200 mL/minute in the 3 m-sections. Approximately 2000mL was taken at the of the flow period. The instruction was also that the volume of the out flowing water before the sampling should be at least 3 times the total volume of the test section + pipes up to sampling point.

13.2 Salinity estimations

The salinity has been estimated using two different algorithms. The first equation, Eq. 13-1, uses the electrical conductivity, C, of the sample:

$$S \text{ (mg/l)} = C \text{ (mS/m)} \cdot 4.670 / 0.0741 \quad (13-1)$$

The second equation, Eq. 13-2, uses as many as ten constituents of the water:

$$S \text{ (mg/l)} = [\text{Na}^+] + [\text{Mg}^+] + [\text{Ca}^{2+}] + [\text{K}^+] + [\text{Sr}^{2+}] + [\text{Cl}^-] + 3 \cdot [\text{SO}_4\text{-S}] + [\text{HCO}_3^-] + [\text{Br}^-] + [\text{F}^-] \quad (13-2)$$

All concentrations are given in mg/l in Eq. 13-2.

It can be noted that $[\text{SO}_4^{2-}]$ can be used in Eq. 13-2 instead of $3 \cdot [\text{SO}_4\text{-S}]$. $[\text{SO}_4\text{-S}]$ is the measured concentration of sulphur in the sulphate phase.

In Forsmark et al (2001b) the resulting salinity of the two calculations is presented in detail. Some of the samples were not analyzed regarding especially $[\text{F}^-]$ and $[\text{Sr}^{2+}]$. Those parameters are of minor importance to the salinity and can be disregarded in those cases where they are missing. If other parameters are missing as well the salinity value derived from the electrical conductivity measurements have been used, see Forsmark et al (2001b).

In some holes, several samples were collected. In order to avoid multiple values for the same section, short section samples have been preferred before whole-borehole samples in the statistical analysis shown below. An overview of the spatial distribution is shown in Figures 13-1 and 13-2.

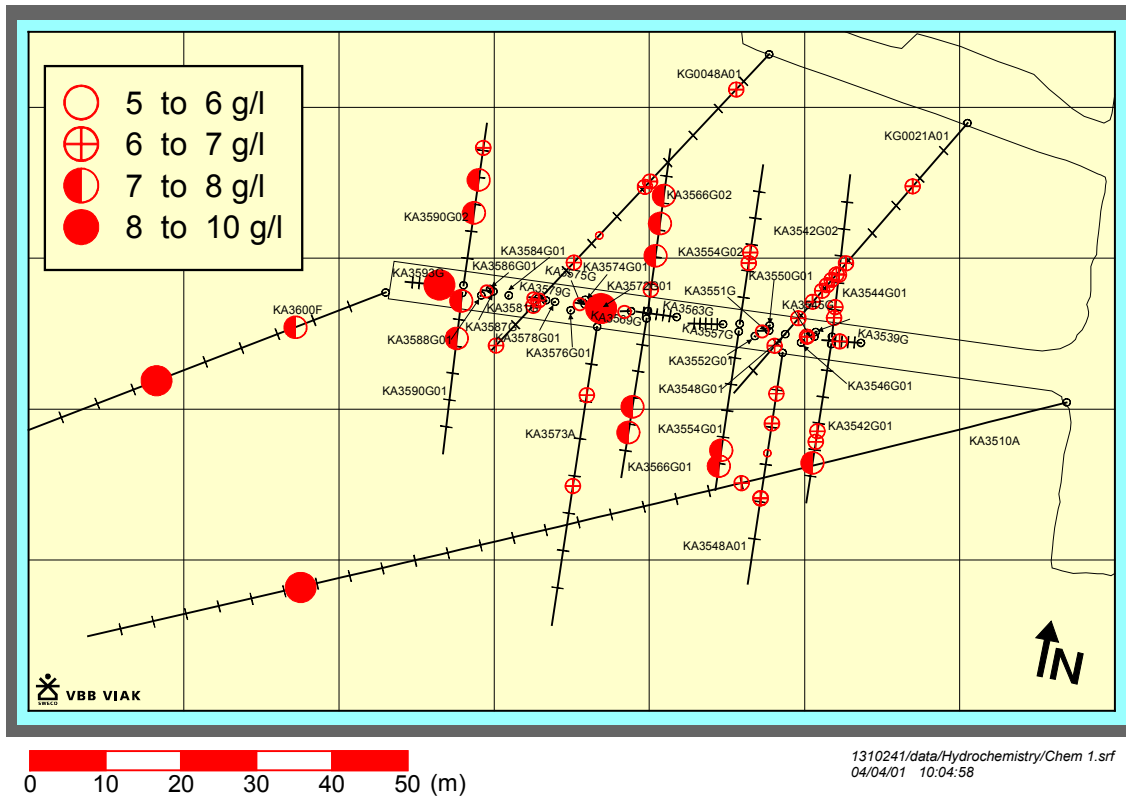


Figure 13-1 Distribution of salinity (g/l) – horizontal view of prototype repository.

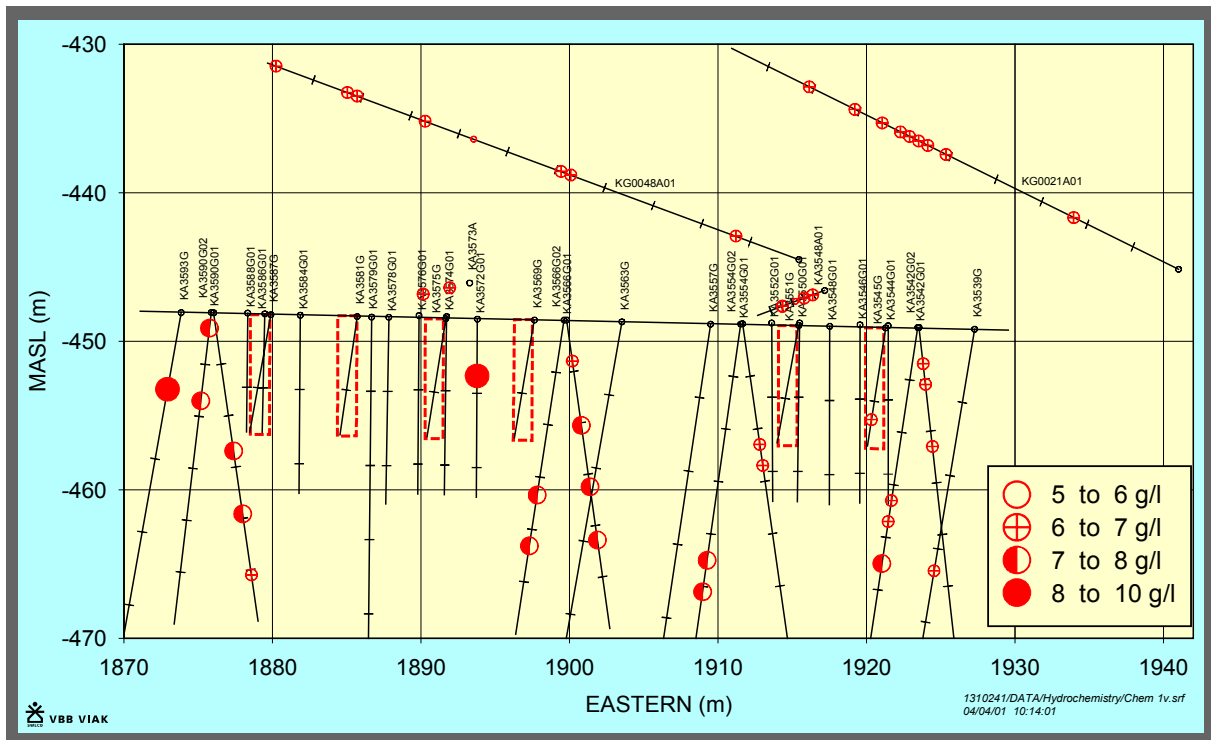


Figure 13-2 Distribution of salinity (g/l) - vertical view of prototype repository.

The salinity tends to be higher in the western part of the repository test area. Four sections indicate a salinity of the highest-ranking class in Figures 13-1 and 13-2 above. One of those values, in KA3572G01, is from a section with low hydraulic conductivity indicating water not transported from a large distance. The other three values, within the highest-ranking class, are from sections with higher hydraulic conductivity, thus indicating possible water transport from larger depth where saline water is occurring.

When comparing boreholes drilled above the repository with those drilled downwards from the repository tunnel, there is an indication of higher values of salinity below than above the tunnel.

The samples analysed has an arithmetic, and a geometrical mean of 6.8 g/l and a standard deviation of 0.69. A normal probability plot is shown in Figure 13-3.

Normal Probability Plot for S

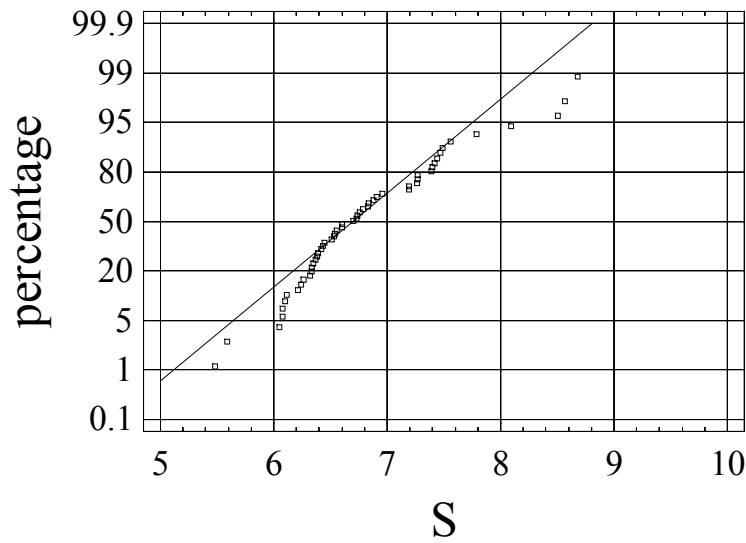


Figure 13-3 Normal probability plot salinity analysis.

In two of the holes, four sections were sampled at five occasions thereby producing a possibility to find possible trends in those areas. In Figure 13-4, the values of those sections are plotted. Four of the samples were collected before the deposition holes were drilled in mid-1999, while the fifth value of all sections represents the salinity after the deposition holes were drilled.

In the diagrams is shown a decrease in the three sections closest to the tunnel system after the deposition holes were drilled while the outermost section show a slight increase. No direct conclusion regarding the effect of drilling the deposition holes on the salinity values can be made.

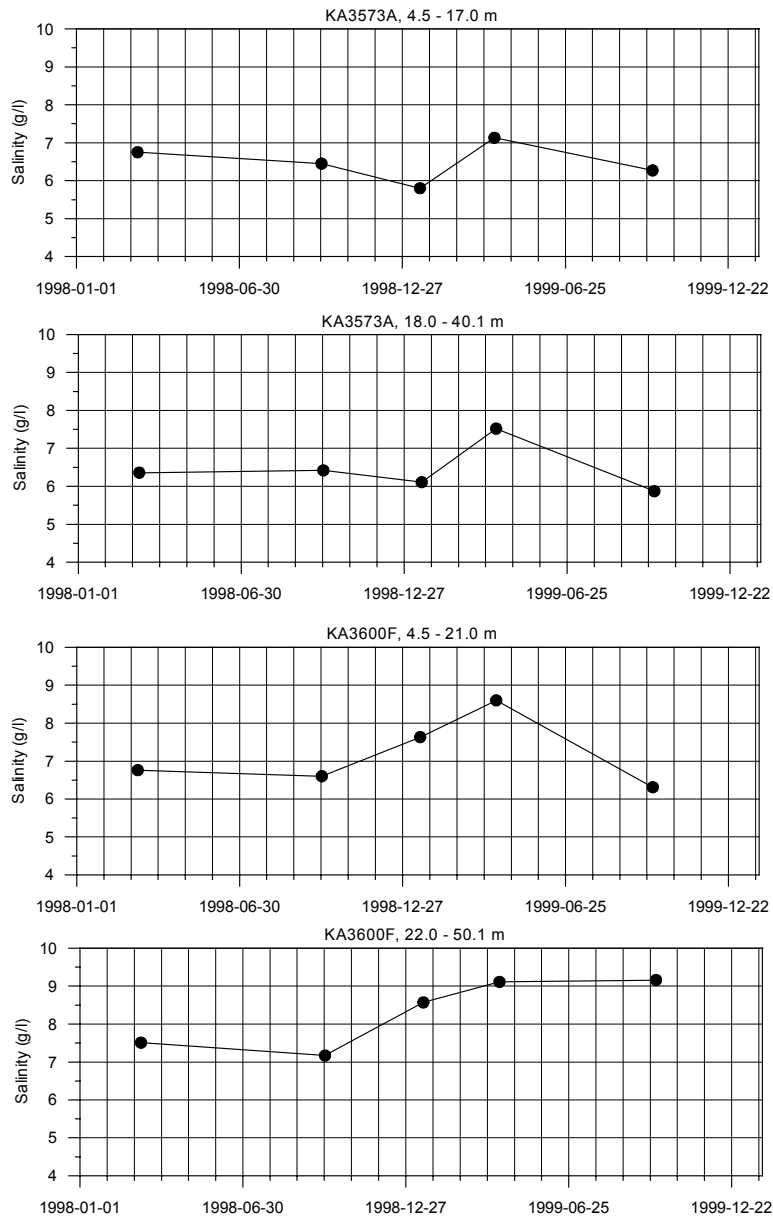


Figure 13-4 Diagrams of salinity distribution over a 2-year period in four hole sections. The six deposition holes were all drilled within the period between the fourth and fifth value above. Deposition holes were drilled from mid-June 1999 to mid-september 1999.

In Table 13-1 the resulting statistical parameters are summarized for the components in equation 13-2 and some other chemical components analyzed from the actual water sample. The detailed analysis results are presented in Forsmark et al (2001b).

Table 13-1 Results of statistical analysis of chemical components.

Chemical Component	Sample size	Mean, mg/L	Median, mg/L	Standard deviation, mg/L	Max value mg/L	Min value mg/L
Na ⁺	49	1721	1680	150	2340	1540
Mg ⁺	49	84.8	87.2	11.6	98.0	24.8
Ca ²⁺	49	655.5	643.0	115.9	974.0	494.0
K ⁺	49	9.5	9.5	0.97	12.0	7.3
Sr ²⁺	49	9.7	9.6	2.3	6.0	15.7
Cl ⁻	53	3936	3880	459	5860	3340
SO ₄ ²⁻	47	315.8	302.0	52.3	617.0	277.0
SO ₄ _S	49	103.2	100.0	17.6	217.0	93.8
HCO ³⁻	48	181.8	190.0	37.2	219.0	26.0
Br ⁻	47	16.9	17.0	3.2	27.2	12.0
F ⁻	30	1.52	1.24	0.91	3.90	0.11
Salinity (g/L)	53	6.82	6.70	0.69	8.68	5.48
Fe ²⁺	42	0.32	0.29	0.18	0.91	0.02
Mn ²⁺	42	0.64	0.58	0.21	1.00	0
Li ⁺	49	0.33	0.32	0.10	0.63	0.16
Si ⁴⁺	49	6.67	6.50	1.16	12.6	5.40
pH (-)	49	7.4	7.4	0.10	7.7	7.2
Cond (mS/m)	53	987	970	116	1360	800

14 CALIBRATION CASES FOR NUMERICAL MODELLING

During interference test campaign 1 six interference tests were made. Of these six tests number 1:3 had some technical failure of the flow section during the test. Test number 1:4 is very short and is excluded for this reason while before test 1:6 water sampling was made in some of the observation bore holes shortly before the test commenced.

During interference test campaign 2 eight interference tests were made. All eight tests were successful. Seven of the eight tests received at least 20 pressure responses in the monitored observation sections in surrounding boreholes. The only test with fewer responses is test 2:13.

Accordingly ten tests are suitable for the task of being a calibration case for a numerical modelling, namely test 1:1, 1:2, 1:5, 2:7, 2:8, 2:9, 2:10, 2:11, 2:12 and 2:14

In order to make estimation if some part of test 1:6 can be used together with test 1:3 a cross plot of the initial pressures, P_0 , was made, see Forsmark and Rhén (1999a). The cross plot show that some observation sections have considerably lower initial pressures during the 1:6 test sequence than during the 1:3 test sequence. Consequently it is clear that the following sections should not be used if using test 1:6 as a calibration case; KA3566G02:3, KA3572G01:2, KA3574G01:2, KA3578G01:1, KA3579G01:2 and KA3579G01:3. For these sections the test 1:3 values of pressure heads should be applied. It is also to be observed that the section KA3590G01:2 of test 1:3 should not be used. Instead, the data of the same section from test 1:6 should be used.

15 Predictions with numerical and analytical models

The characterization was made in steps and it is possible to analyse the increase in knowledge of the properties of the rock mass. During the investigation phase blind predictions were made to test the ability to describe the rock mass conditions. In Hermansson et al (1999) and Stigsson et al (2001) the DFN approach was used to predict fracture densities, water pressure distributions and flow into the deposition holes. A few results are presented in Section 15.1. A simple prediction of the inflow rates to the deposition holes was also made based on analytical equations. The result is presented in Section 15.2. In Svensson (2001) the future pressure and salinity distributions around the Prototype tunnel during the operation phase were modelled with a continuum code and is shortly presented in Section 15.3.

15.1 DFN predictions

A first modelling exercise (DFN model 1) have been performed and presented in Hermansson et al. (1999). This exercise was based on data from boreholes drilled in the TRUE Block Scale project, tunnel fracture mapping of the TBM tunnel and data from holes of the volume. A prediction of inflow and fracture characteristics in the deposition holes and the 2nd drill campaign were made.

The second modelling exercise (DFN model 2) reported in Stigsson et al (2001) started with deriving DFN-parameters from the exploratory drill campaigns 2 and 3. The statistics from the latter drill campaigns were then compared to what was derived by Hermansson et al. (1999).

In Stigsson et al (2001) a DFN groundwater flow model was set up and some of the properties were presented in Sections 3.1 and 11.1.3. Part of the work consists of the prediction of fracture characteristics and flow in the deposition holes of the Prototype Repository in a similar manner as it was made by Hermansson et al. (1999). However in Stigsson et al (2001) the model was based on all available data up to Spring 1999 from drill campaigns 1, 2 and 3 and evaluated deterministic features. After the predictions had been made a comparison between modelled and measured tracemaps and inflow to the deposition holes and also head in packer sections was made. A few results are shown below.

The modelling of the groundwater flow in the Prototype Repository was performed using a Discrete Fracture Network (DFN) approach with the computer modelling codes FracMan and MAFIC.

15.1.1 DFN model 1

The general data used (Not from the TBM tunnel but a rock mass just some 100-200 m from the Prototype tunnel.) was data from boreholes drilled in the TRUE Block Scale project. The tunnel specific information was the tunnel fracture mapping of the TBM tunnel, data from 10 sub vertical, 8m long, pilot boreholes and 3 long sub horizontal core holes drilled from the TBM tunnel. The pilot boreholes were drilled in planned positions for the deposition holes. In 6 of these positions deposition holes were later drilled. Fracture characteristics as orientation and frequency as well as inflow to open borehole were predicted for 10 subvertical, 8-12 m long, boreholes made during drill campaign 2.

Data from True Block Scale and one of the subhorizontal core holes drilled from the TBM tunnel was used for estimation of the orientation and assigning the transmissivities to the fracture network. The mapping of the TBM tunnel was used to estimate the size of the fractures. The rest of the data, core mapping of and hydraulic tests in the other boreholes drilled from the TBM tunnel, was not used to define the DFN model.

The comparison of the fracture parameters are made for the fracture orientation and frequency of the three fracture sub-sets with NW, NE and sub-horizontal orientations. Size (or fracture traces) of the fractures was not predicted in this stage.

Orientation

Used and measured orientations of the three sub-sets in the Prototype repository area are presented in Table 15-1 below. The “All fractures” group of drill campaign might be too exhaustive to be compared with the used statistics since it is constituted by both “sealed” and “natural” fractures. Hermanson et al. (1999) showed that fractures could be sorted in three sets. A new comparison of “Conductive fractures” with “Natural fractures” statistics show only minor differences between the two groups regarding the orientation of the fracture sets. The comparison of the used True Block Scale results for the simulation of drill campaign 2 and field data from drill campaign 2 and 3 shows:

- The main trend of sub-vertical set 1 has a discrepancy of about 17°. The used True Block Scale plunge of this set is in agreement with the field measurements.
- The trend of sub-vertical set 2 shows a difference of about 180° between used and measured trend since fractures are near vertical.
- The sub-horizontal trend of set 3 is almost the same for true block scale data and measured during drill campaign 2. Since the inclination of set 3 is close to horizontal, discrepancies between predicted and measured are small.

In Figure 15-1 is the lower hemisphere projection of the predicted poles of the conductive fractures and of the measured “natural” fractures that intersects the boreholes in drill campaign 2 shown.

Table 15-1. Used and measured for fracture orientation of Drill campaign 2. For more details see Hermanson et al (1999).

SET 1	Used by Hermanson <i>et al.</i> , 1999 <i>Conductive fractures</i>	Drill campaign 2 measurements	
		<i>All fractures</i>	<i>Natural fractures</i>
<i>trend</i>	117.9	129	135.1
<i>plunge</i>	12.9	6.3	23.5
<i>k</i>	5.64	4.84	4.7
<i>%-fractures</i>	12%	26.50%	35.30%
<i>KS-%</i>	0.16;38.5%	0.050;15.7%	0.059;12.4%

SET 2	Hermanson <i>et al.</i> , 1999 <i>Conductive fractures</i>	Drill campaign 2	
		<i>All fractures</i>	<i>Natural fractures</i>
<i>trend</i>	200.4	37	38.3
<i>plunge</i>	2	5.8	13.7
<i>k</i>	15.75	8.35	6.09
<i>%-fractures</i>	46%	35.60%	32.20%
<i>KS-%</i>	0.163;4.6%	0.040;23.4%	0.046;41.4%

SET 3	Hermanson <i>et al.</i> , 1999 <i>Conductive fractures</i>	Drill campaign 2	
		<i>All fractures</i>	<i>Natural fractures</i>
<i>trend</i>	186.5	290.6	280.7
<i>plunge</i>	81.1	84	77
<i>k</i>	13.6	8.33	8.7
<i>%-fractures</i>	42%	37.90%	32.50%
<i>KS-%</i>	0.095;79.7%	0.043;14.4%	0.064;9.3%

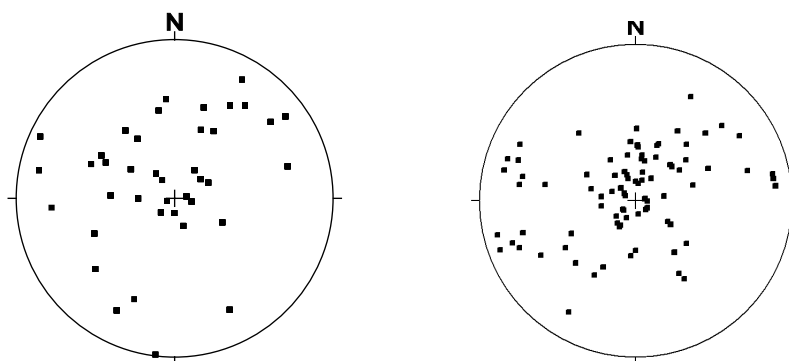


Figure 15-1. Left: Lower hemisphere projection of the predicted poles of the conductive fractures that intersects the boreholes in drill campaign 2. Right: Lower hemisphere projection of the measured poles of the intersecting fractures in the boreholes from drill campaign 2.

Frequency

The predicted statistics of the simulated fracture frequency of drill campaign 2 were based on ten stochastic realisations of the fracture network. Ten sub-vertical exploratory holes were sampled in each realisation.

The conductive fracture frequency was predicted to be on average 0.34 “conductive” fractures per metre. The observed “natural” fracture frequency from drill campaign 2 gave a value of 0.76 “natural” fractures per metre. A “natural” fracture is interpreted to be an open fracture, but it does not have to be waterbearing. Unfortunately the borehole data do not contain information if a “natural” fracture is water bearing or not and Hermanson et al. (1999) only modelled conductive fractures. As shown in Section 11.1.3 the relationship between modelled “natural” and modelled conductive fractures is a factor 2 to 3 in this model. It is most believable that the same ratio could be applied to the data in Hermanson et al. (1999).

Comparison of modelled and measured exploratory holes inflow

Hermanson et al. (1999) used ten stochastic realisations to get statistics for prediction of the inflow to ten exploratory holes in drill campaign 2. The exploratory holes of the TBM tunnel were implemented one at a time to simulate a real situation where each borehole is closed after drilling. The boundary condition of the exploratory holes was set to be atmospheric pressure. The average simulated inflow was 0.07 l/min, c.f. Figure 15-2.

Rhén and Forsmark (1998b) evaluated the measured inflow to the exploratory holes. During the flow tests a packer with a pipe system was put on top of each borehole so that the opening of the borehole was between 1.35 and 1.51 m above the tunnel floor. The average inflow for the ten exploratory holes was 0.013 l/min, c.f. Figure 15-2.

The simulations predict an average inflow that is about 5 times larger than the measured and a maximum inflow that is about 3 times larger than the measured. The minimum inflow is zero for both simulations and measurements, which corresponds to that no conductive fracture intersects the hole. Part of the discrepancies may be explained by the fact that a pressure exceeding atmospheric pressure of ca 1.4 m water was applied during the measurements of the exploratory holes while Hermanson et al. (1999) used atmospheric pressure during simulations. The simulated flow will be smaller if the boundary condition is changed to match the measurements. Another explanation could be that Hermanson et al (1999) used the same transmissivity distribution in all directions that might be more water bearing.

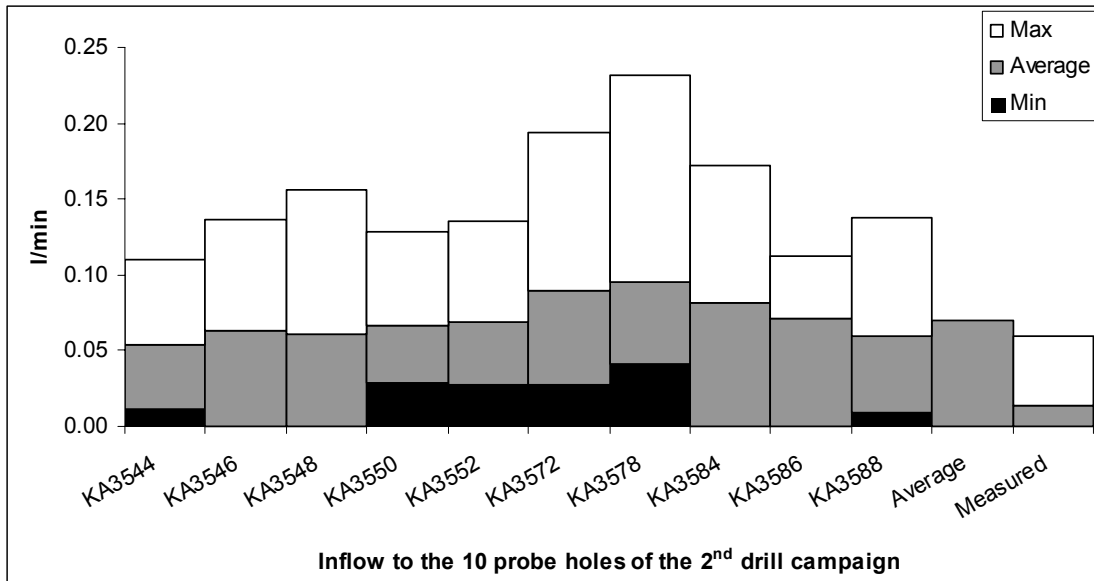


Figure 15-2. Simulated and measured inflow to the ten exploratory holes in drill campaign 2. Unfortunately the simulated and measured inflow tests are made under different circumstances.

15.1.2 DFN model 2. Inner boundaries: tunnels, pilot holes and deposition holes

The tunnels included in the model are shown in Figure 15-3 and Figure 15-4 and comprise segments from the last part of the A-tunnel (i.e. the TBM tunnel), and the G-, I-, and J-tunnels. The tunnels are implemented with a specified head boundary, which corresponds to atmospheric pressure to simulate the effect of open tunnels.

Packed off sections where no measurements are made in the boreholes are implemented in the model but not monitored. The boundary type is a variation of a specified flow boundary. It is called “groupflux” boundary. Groupflux boundaries allow the water to flow from one fracture to another through a packed off section, c.f. Figure 15-5. The inflow to the section is equal to the outflow as mass balance is respected and the head remains constant in the packed off section.

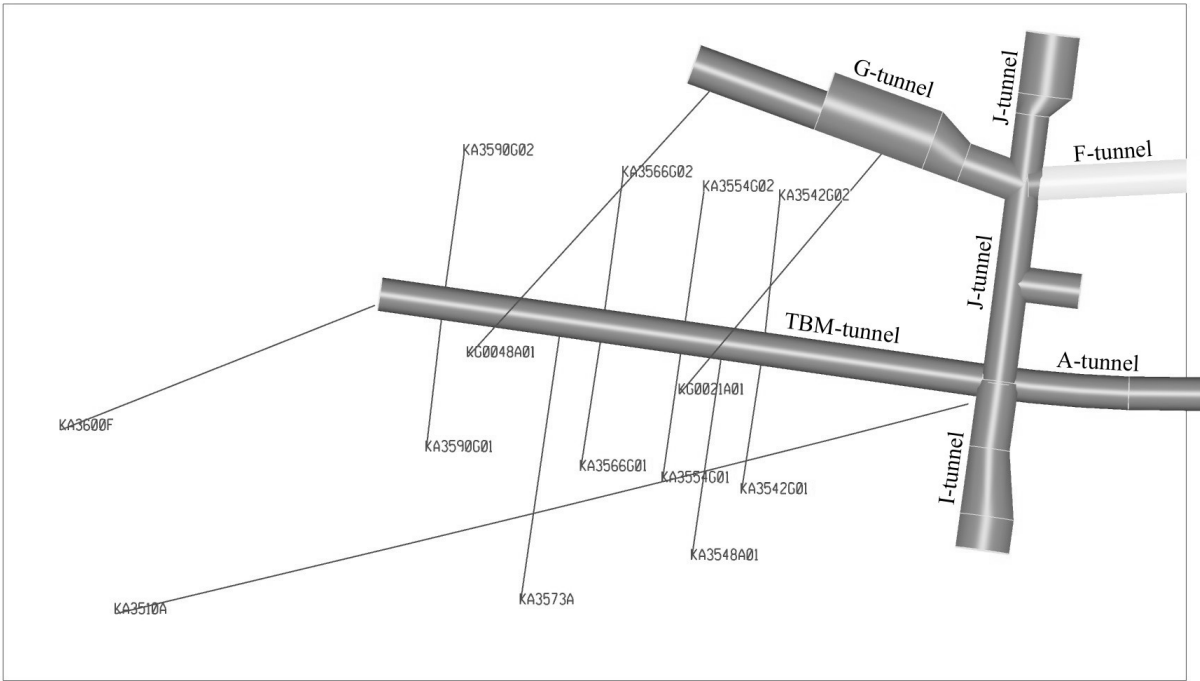


Figure 15-3. Model domain showing sub-horizontal and inclined boreholes together with the included A-, G-, I-, and J-tunnels. The shaded F-tunnel is excluded.

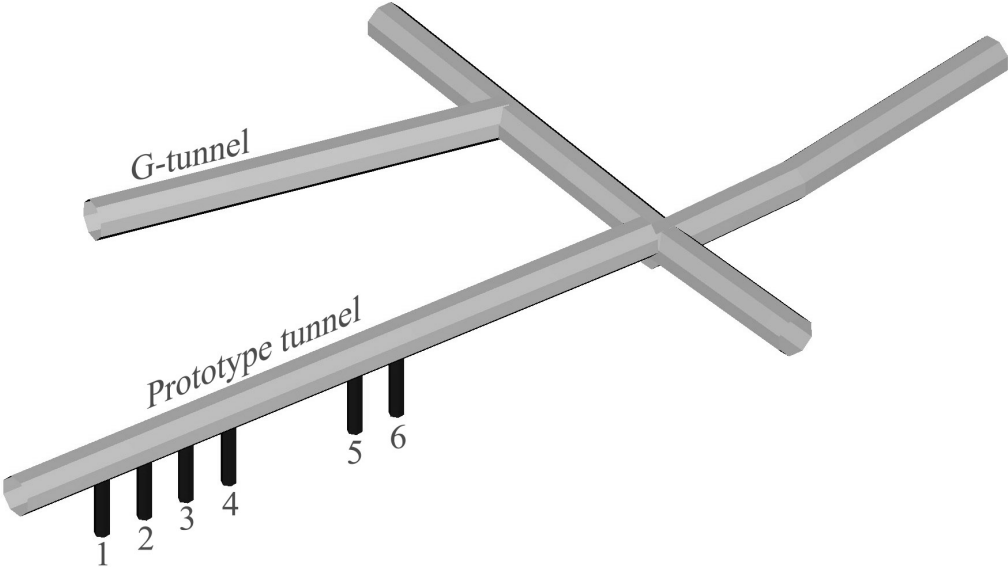


Figure 15-4. The position and numbering of the 6 deposition holes in the Prototype repository tunnel.

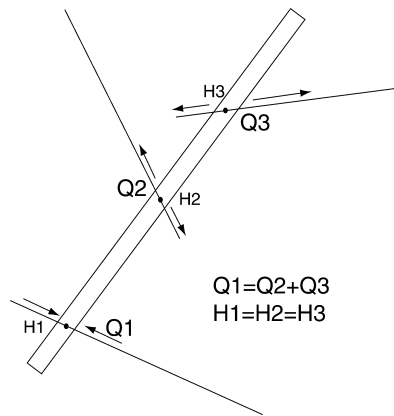


Figure 15-5. Illustration of groupflux boundaries.

15.1.3 DFN model 2. Calibration

The influence of the 8 deterministic features was tested with a minor sensitivity analysis. The conclusions were:

- Large inflows to a deposition hole is not only dependent on a high transmissive fracture intersecting the deposition hole but also needs to be connected to the conductive network of fractures.
- Size variation of the deterministic features has a limited effect on the inflow to the deposition holes. The variation changes the connectivity of the DFN at the vicinity of the deposition holes.
- The effect on the inflow to the deposition holes is limited when the transmissivity of the deterministic fractures is decreased. An increase of the transmissivity will on the other hand have a large effect on the inflow.
- The deterministic hydraulic features close to deposition holes 5 and 6 have great impact in the flow conditions around these deposition holes but also to the other holes.

It was necessary to apply a skin around the tunnel system to reduce the hydraulic conductivity to decrease the modelled flow into the tunnel so it would match the measured inflow.

15.1.4 DFN model 2. Transient simulation

One transient simulation was made for the excavation of the first 4 deposition holes. The storativity (S) assigned was somewhat less than the suggested relation $S = f(\text{Transmissivity})$ in Section 11.4. Transient simulation of the excavation of deposition holes 1 to 4 shows that flow and pressure changes stabilise within a maximum of two days. The modelling of the hydraulic behaviour of the prototype repository with a step-wise steady state approach was therefore considered valid. The simulations also indicated that when a new deposition hole is being drilled the inflow to old deposition holes will decrease. The effect decreases by distance as expected.

15.1.5 DFN model 2. Predictions of fracture traces in the deposition holes

The fracture trace statistics are calculated from 20 stochastic realisations where minimum, maximum, average values and standard deviation has been calculated.

The DFN model can produce fracture trace maps for all, “natural” and conductive fractures in each of the 6 deposition holes, i.e. 18 trace maps for each stochastic realisation. The complete simulation consists of 20 stochastic realisations out of which 360 trace maps can be extracted. Figure 15-6 shows 6 examples of trace maps from realisation 1. Summary statistics from all sampled trace maps are given in Table 15-2 and in Stigsson et al (2001) the detailed predictions are found. The fracture statistics is calculated for the simulated “natural” fractures, which corresponds to open but not necessarily water bearing fractures. A simulated “natural” fracture is a fracture with a transmissivity $> 5 \cdot 10^{-11} \text{ m}^2/\text{s}$, as defined in Section 11.1.3.

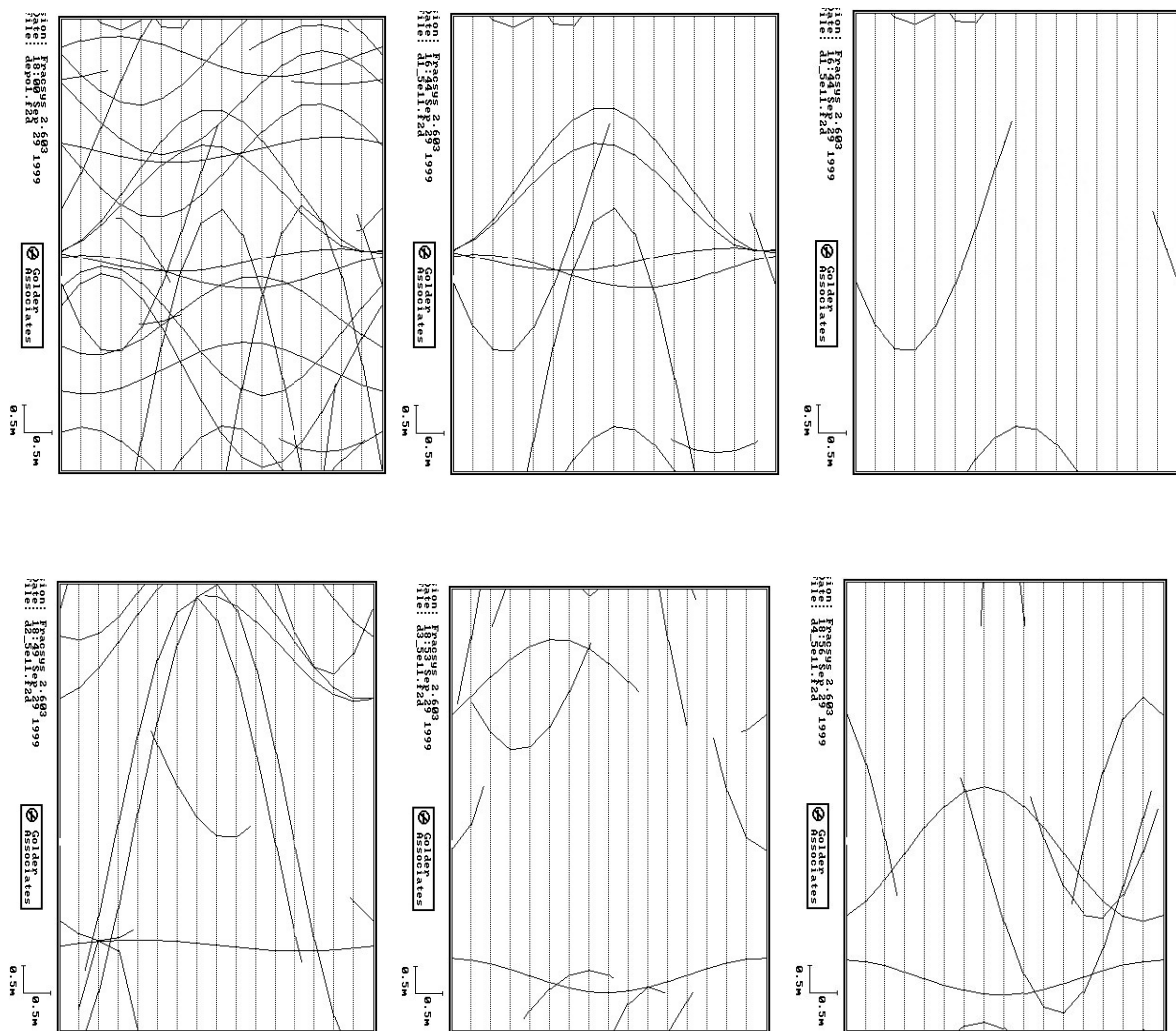


Figure 15-6. Fracture traces on the wall of the deposition holes in realisation 1. Upper row from left: all fractures, “natural” fractures ($T > 5 \cdot 10^{-11} \text{ m}^2/\text{s}$) and conductive fractures ($T > 5 \cdot 10^{-10} \text{ m}^2/\text{s}$) for deposition hole 1. Lower: “natural” fractures in deposition hole 2, 3 and 4.

The number of “natural” fractures for the 6 deposition holes varies between 3 and 15 with an average around 8 “natural” fractures per deposition hole, see Table 15-2 and Figure 15-7.

The average trace length of one fracture is on average 5 m within all deposition holes and the trace lengths vary between 0.01 to 16.9 m, c.f. Table 15-2 and Figure 15-8. As a comparison the circumference in a deposition hole is 5.8 m, which implies that a trace of 16.9 m corresponds to a fracture that is visible along the whole perimeter of the deposition hole at an angle of about 75°.

The density of fracture traces is given by P_{21} and varies between 0.22 and 1.76 m/m^2 with an average around 0.9 m/m^2 , see Table 15-2 and Figure 15-9.

The transmissivity statistics of the fractures that intersects the deposition holes are shown in Table 15-2 and Figure 15-10. The average value is around $5 \cdot 10^{-8} m^2/s$ in all deposition holes. The minimum transmissivity is $5 \cdot 10^{-11} m^2/s$, which is the same value as the truncation for fractures that is assumed to be “natural”. The maximum transmissivity is $6.6 \cdot 10^{-6} m^2/s$, which is half an order of magnitude lower than the upper limit for transmissivity for the northwest striking set. The sub-horizontal fracture set has the largest possibility to intersect the deposition holes and at the same time it has the lowest transmissivity distribution. The steeply dipping northwest striking set has the highest transmissivity distribution and also the lowest possibility of intersecting a deposition hole. This explains how the minimum transmissivity value equals the truncation, but that the highest is half an order of magnitude lower than the upper transmissivity limit.

Table 15-2. Statistics (predictions) of the “natural” fracture traces around the perimeter of deposition holes 1 to 6 based on 20 realisations of the calibrated DFN model. The min and maximum values for trace length and transmissivity is for a single trace in the deposition hole, other values are calculated for a whole hole.

<i>Canister</i>	<i>1</i>	<i>2</i>	<i>3</i>	<i>4</i>	<i>5</i>	<i>6</i>
<i>Average number of traces</i>	7.5	7.7	9.3	8.9	8.85	8.6
<i>Minimum number of traces</i>	3	3	5	4	3	4
<i>Maximum number of traces</i>	11	12	14	15	13	12
<i>Average trace length [m]</i>	4.91	5.31	5.53	4.79	4.85	5.00
<i>Std dev trace length [m]</i>	3.98	3.98	4.03	3.26	2.99	3.47
<i>Minimum trace length [m]</i>	0.09	0.01	0.09	0.08	0.07	0.01
<i>Maximum trace length [m]</i>	16.7	16.9	16.4	16.0	16.3	16.2
<i>Average P_{21} [m/m^2]</i>	0.79	0.88	1.08	0.89	0.93	0.90
<i>Minimum P_{21} [m/m^2]</i>	0.25	0.33	0.51	0.22	0.27	0.41
<i>Maximum P_{21} [m/m^2]</i>	1.48	1.47	1.76	1.66	1.74	1.36
<i>log(Average T) [m^2/s]</i>	-7.48	-7.24	-7.21	-7.09	-7.17	-7.59
<i>log(Std dev T) [m^2/s]</i>	-7.10	-6.85	-6.74	-6.63	-6.77	-7.20
<i>log(Minimum T) [m^2/s]</i>	-10.29	-10.29	-10.29	-10.30	-10.29	-10.30
<i>log(Maximum T) [m^2/s]</i>	-5.99	-5.43	-5.18	-5.18	-5.30	-6.10

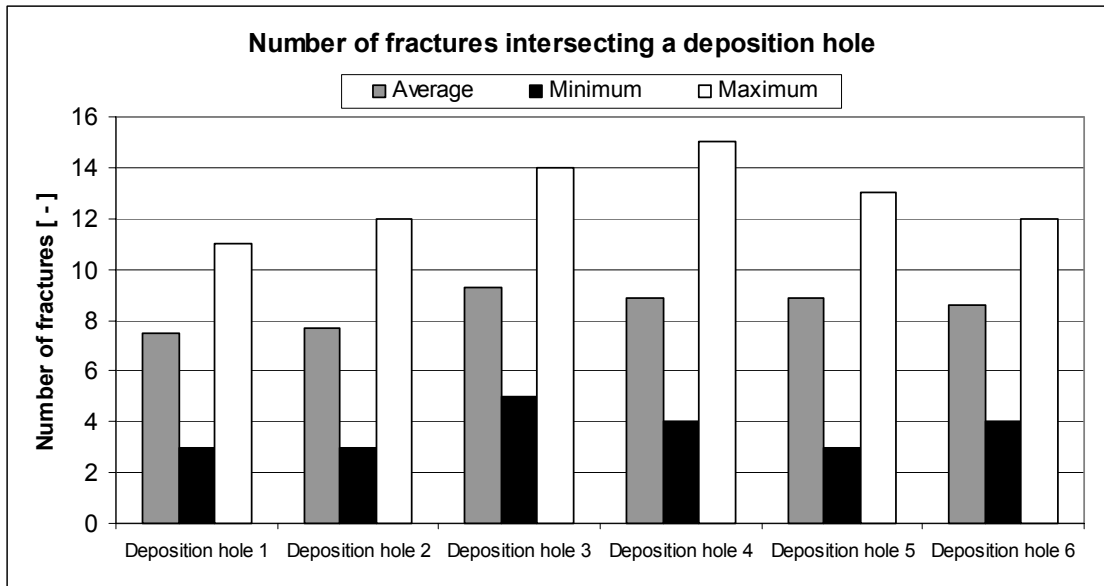


Figure 15-7. Number of “natural” fracture traces per deposition hole. Summary statistics based on 20 realisations of the calibrated DFN model.

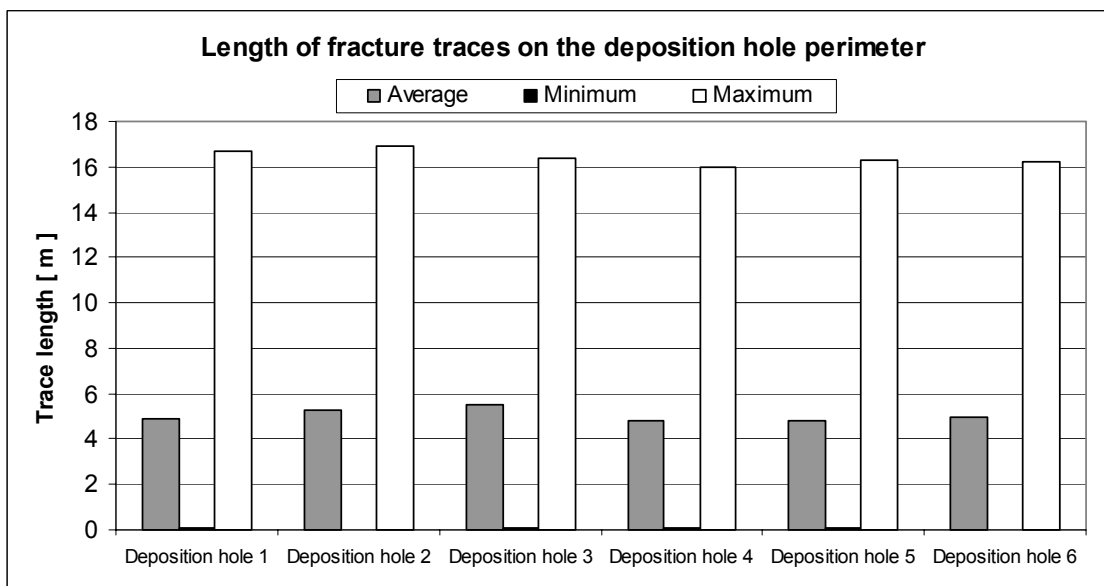


Figure 15-8. Trace length of individual “natural” fractures per deposition hole. Summary statistics based on 20 realisations of the calibrated DFN model.

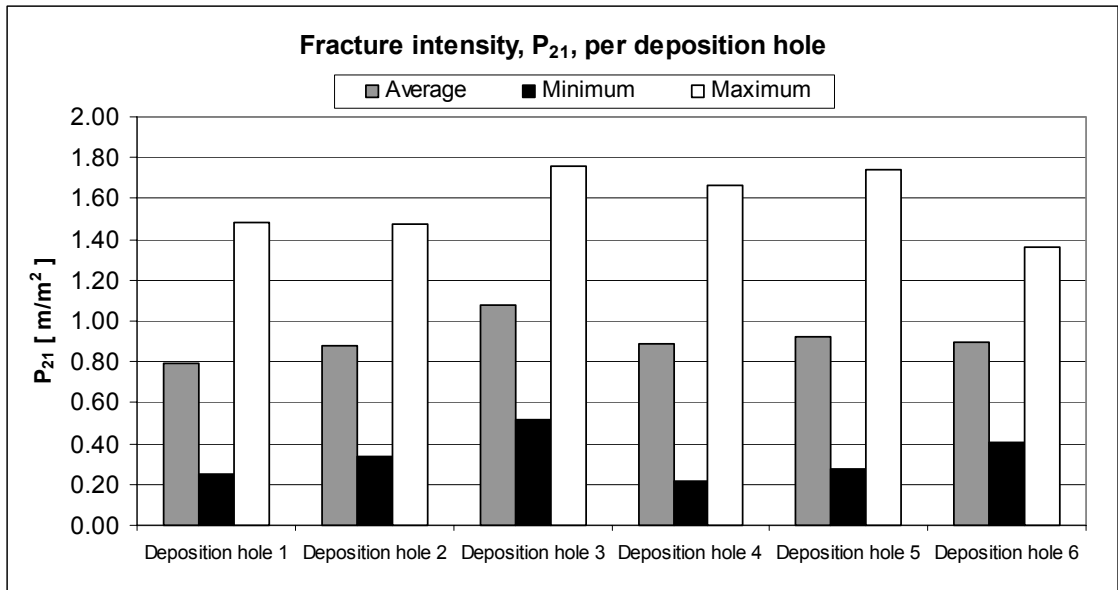


Figure 15-9. Fracture intensity, P_{21} (m/m^2), for “natural” fractures on the deposition hole walls. Summary statistics based on 20 realisations of the calibrated DFN model.

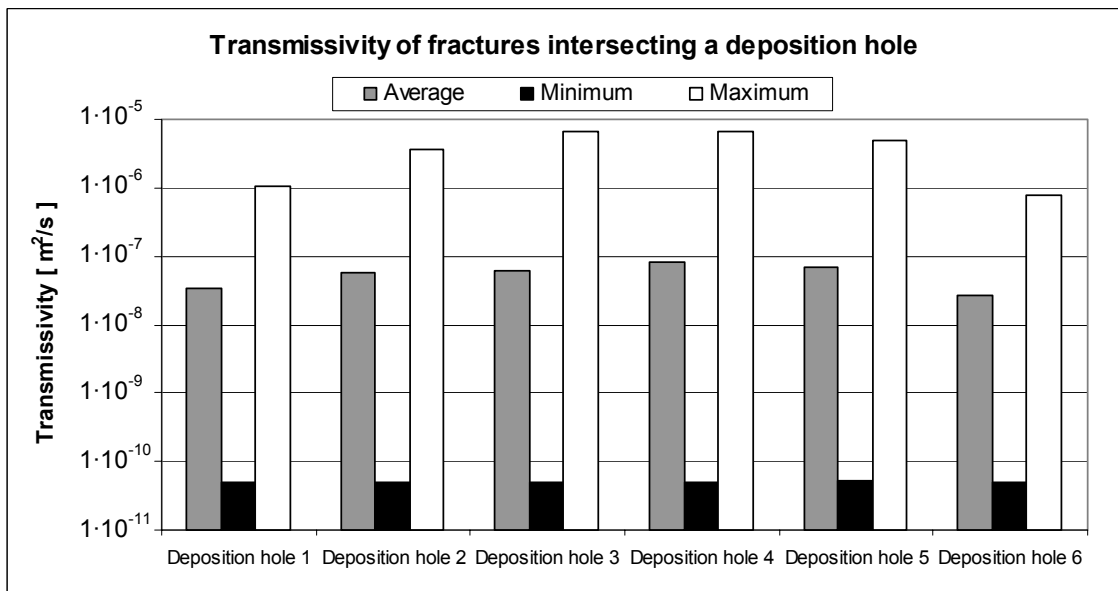


Figure 15-10. Transmissivity of individual conductive fractures intersecting the deposition holes. Summary statistics based on 20 realisations of the calibrated DFN model.

Fracture trace maps are scale dependent, i.e. working in a small scale will result in lots of small fracture traces, while working in a large scale will result in few and long traces. The fracture size distribution in the DFN-model is based on trace maps with a truncation limit of 1 m from the TBM-tunnel. The truncation limit for the trace maps in the deposition holes is, unfortunately, 0.25 m. However the intensity, P_{21} (m fracture trace/ m^2 rock wall), is not dependent on the scale and can be used for comparison.

In Table 15-3 is a brief summary of the statistics from the measured and the modelled trace maps shown. The P_{21} for the modelled deposition holes is a bit small and have a larger dispersion than the measured trace maps. As expected the average trace length for the modelled trace maps are longer than the measured. The reasons for the low modelled P_{21} can be that the orientation statistics of the fractures or the relative fracture density for the 3 sets is not fully understood.

Table 15-3. Comparison of measured and modelled fracture trace length statistics for all fractures.

	P_{21} max	P_{21} min	P_{21} ave	Trace length ave
	[m/m ²]	[m/m ²]	[m/m ²]	[m]
Measured	4.23	2.74	3.38	1.88
Modelled	4.56	0.64	2.77	4.84

One modelled and one measured trace map are shown in Figure 15-11. Trace maps from all 6 deposition holes for 2 realisations are shown in Stigson et al (2001). Apart from that the modelled traces are longer and therefore fewer to maintain the correct P_{21} ratio, the trace maps show a similar picture.

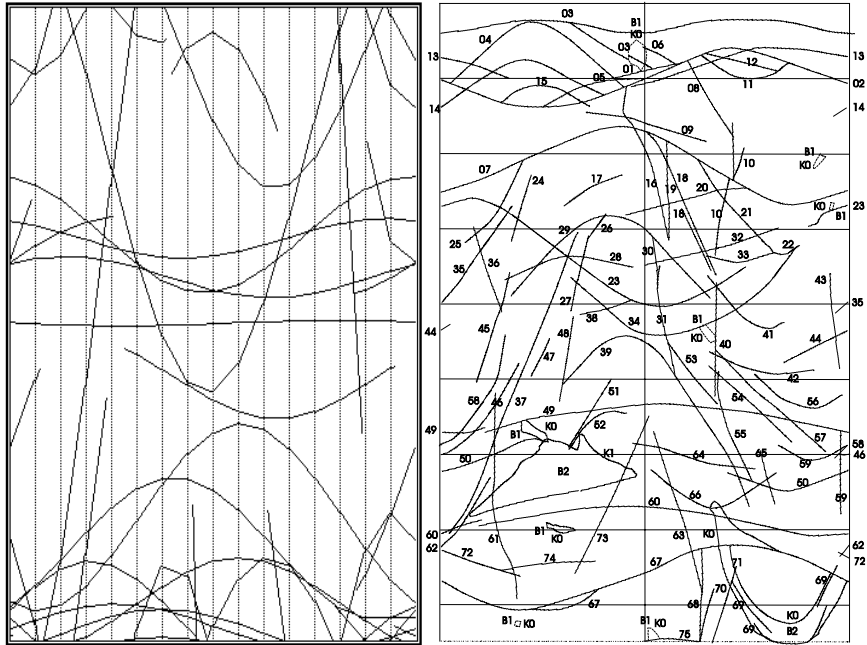


Figure 15-11. Example of modelled (left) and measured (right) trace maps. The modelled traces are fewer but longer compared to the measured.

15.1.6 DFN model 2. Predicted inflow to the deposition holes

In Table 15-4 is modelled average values compared to the measured. The match is poor as can be seen in the table. The inflow is overestimated by two orders of magnitude. The reason is that there is no skin around the deposition holes, which there are around the tunnels in the model or that the measured transmissivity distribution is difficult to model.

Table 15-4. Comparison of measured and calculated inflow to deposition holes.

Boundary	Average	Geomean	Median	Measured
Hole 1	1.141	0.604	0.553	0.0800
Hole 2	1.069	0.563	0.607	0.0016
Hole 3	1.112	0.441	0.943	0.0028
Hole 4	2.966	0.807	0.695	0.0007
Hole 5	3.529	1.253	1.678	0.0027
Hole 6	1.431	0.532	0.934	0.0061
Sum inflow	11.248	4.200	5.410	0.094
Factor	120	45	58	1

15.1.7 DFN model 2. Predicted heads

The pressure was measured continuously during the drilling of the deposition holes and 12 different times during the excavation was identified as useful to show the pressure responses in a more comprehensive way. These data was used to compare with the simulations.

The flow solution in the model is only calculated at 3 different times with assumption of steady state conditions. The 3 times corresponds to the following moments in time; before excavation, after excavation of deposition holes 1 to 4 and after excavation of all 6 deposition holes.

Comparisons can be made between:

- the modelled steady state before excavation and the measurements before drilling, 15 June 1999
- the modelled steady state after excavation of deposition holes 1 to 4 and the measurements after drilling deposition hole 4, 15 July 1999
- the modelled steady state after excavation of deposition holes 1 to 4 and the measurements after re-instrumentation but before drilling deposition hole 5, 26 August 1999
- the modelled steady state after excavation of all 6 deposition holes and the measurements of the undisturbed situation after drilling deposition hole 6, 1 December 1999

In the Prototype tunnel the pressure is measured, while the head is simulated. It is easier to compare heads since they, in the hydrostatic case, are independent of depth. The pressure in every packer section were recalculated to head in accordance to:

$$H = Z + p / (\rho_w \cdot g)$$

Where

H = Fresh water head [m]

Z = Current elevation in [m]

p = Measured pressure [Pa]

ρ_w = density of fresh water [kg/m³]

g = Constant of gravity [m/s²]

The simulated heads are plotted as a function of the measured head, as seen in Figure 15-12. The upper left diagram in shows that the average of the simulated heads are higher than the measured, especially for low values of measured heads which corresponds to the case with no drilled deposition holes. Only a few minimum heads are lower than the measured values.

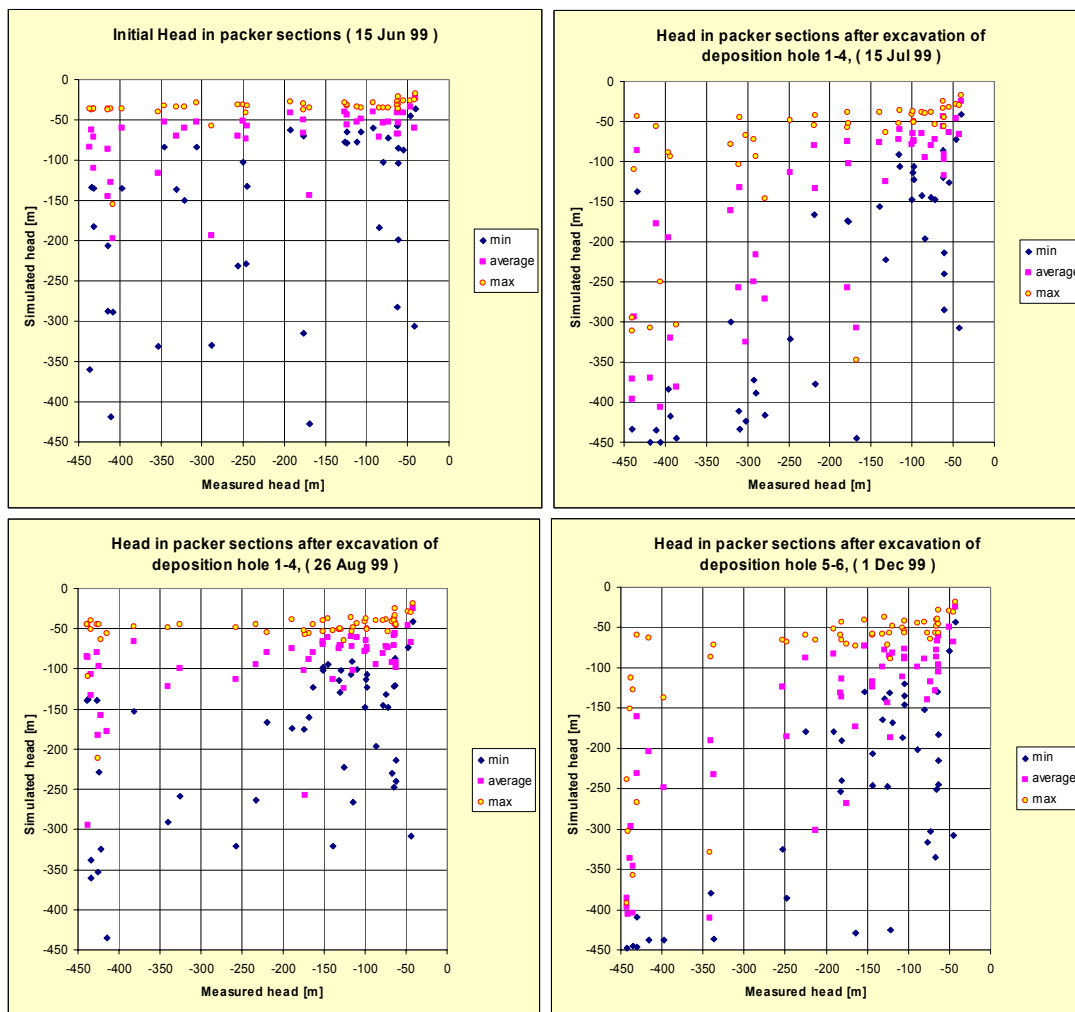


Figure 15-12. Simulated heads versus measured heads.

When the first 4 deposition holes are excavated the cross-plot shows a better correlation to measured values of head, but still the simulated heads are too high for the lowest measured heads as can be seen upper right chart in Figure 15-12.

After the re-instrumentation but before the start of excavating deposition holes 5 and 6 the plot looks worse again, this is explained by the re-instrumentation, i.e. that the instruments in boreholes near deposition hole 1-4 are moved to boreholes near deposition hole 5 and 6.

The cross plot when all deposition holes are excavated and a steady state situation is assumed is shown in the lower right chart in Figure 15-12. The simulated average heads is still too high for the lowest measured values, but is good for the high heads. Since the model is a discrete fracture network model it is naturally that there will be a large difference between the maximum and minimum values due to connections between the fractures. The poor match for the initial state is a result of the skin on the tunnels.

When the head is plotted as a function of distance to the nearest tunnel, i.e. that the match is better when all 6 deposition holes are excavated. The better match is a result of not having a skin around the deposition holes and therefore the skin around the prototype tunnel can be questioned.

A general conclusion is that the pressure responses in the model seem to have less variability compared to the measured values.

15.1.8 DFN model 2. Improvements suggested by the modelling team

The model is sensitive to the applied skin. The skin factor could be better estimated as well as the natural explanation, width and persistence of the skin zone. A better understanding of the EDZ (Excavation Disturbed Zone) and the effect of the injected grout would be helpful. To use measured pressures in the immediate surroundings of the tunnel may improve the estimation of the skin zone effect.

It was difficult to match the measured transmissivity to a lognormal transmissivity distribution. A better understanding of which fractures are playing the dominant role in the conductive network may help to estimate the transmissivity distribution.

More effort to match the different transmissivity data to fracture sets divided not only by their orientation, but also by their geological characteristics, e.g. joints or faults.

A key issue could be to do a new analysis of the fracture orientation using 3 sets that has a low dispersion in orientation and properties, and 1 extra set that reflect the background fracturing with some more or less constant properties. This will probably decrease the connectivity in the fracture network, and as a consequence the inflow will decrease without a skin around the tunnels. The modelled and measured heads will probably show a better match if the skin is removed.

New boundary heads on the outer boundary that reflects the current situation at Äspö will also decrease the driving force for the water flow.

Test different size distributions, e.g. powerlaw, to investigate the effect on the flow and maybe get a better understanding of the hydraulic behaviour.

15.2 Simple prediction of the inflow to the deposition holes

The basis for the estimation was the three drill batches 1, 2 and 3 consisting of pilot and exploratory holes. Drill batch 1 consisted of boreholes drill in the position of the planned deposition holes. They were inclined with a dip direction toward ESE to increase the possibility to intersect the already know transmissive subvertical fracture sets striking NW and N-S. The dip and the length of the boreholes was made in such a way that the borehole would be within the future deposition hole. The second drill batch consisted of vertical boreholes drilled close to the decided positions of the deposition holes or in between them. The third drill batch was made to get a better characterization of the rock volume around the Prototype tunnel. From the tunnel 8 inclined boreholes and one subhorizontal was drilled. Four of the old subvertical holes were extended and 2 new vertical boreholes were drilled. Two boreholes were also drilled from the G-tunnel but they are not included in this study. The predictions below are based on boreholes considered to be close to a made deposition hole and data from the first 8 m of the boreholes was used.

15.2.1 Method

In order to estimate the inflow to the six deposition bore holes two alternative equations (estimating Q_{d1} and Q_{d2}) have been used for each of them. They both assume radial flow, which should be applicable in this situation for an approximate calculation of the inflow. The results of the calculations for Q_{d1} and Q_{d2} for depositions bore hole 1 - 6 are shown in Figures 15-14 to 15-19.

$$Q_{d1} = Q_{TOT} \cdot [P_d \cdot \ln (R_0 / r_w) / (P_0 \cdot \ln (R_0 / r_d))] \quad (15-1)$$

$$Q_{d2} = [P_d \cdot 2 \cdot \Pi \cdot T_{TOT} / \ln (R_0 / r_d)] \quad (15-2)$$

where

Q_{TOT} = measured inflow to exploratory bore hole out from the top of the packer installation

P_0 = undisturbed pressure measured at the top of the packer installation

P_d = Undisturbed pressure in rock volume intended for the deposition bore hole

R_0 = distance from bore hole centre where undisturbed pressure conditions are assumed to prevail

r_w = radius of pilot bore hole

r_d = radius of deposition bore hole

T_{TOT} = evaluated transmissivity of bore holes according to *Chapter 6*

In Figure 15-13 the schematic layout of the estimation of the inflow to the deposition bore hole is shown.

P_0 was selected from the 8 meters pressure build-up test or from the maximum pressure measured during a feature test or from the regression diagram (at $Dt = 10.5$ m), see Chapter 12, in that order. T_{TOT} was selected from an 8-meter pressure build-up test if available or a summation of T , see Chapter 6, for the section 0 - 8 m of each borehole.

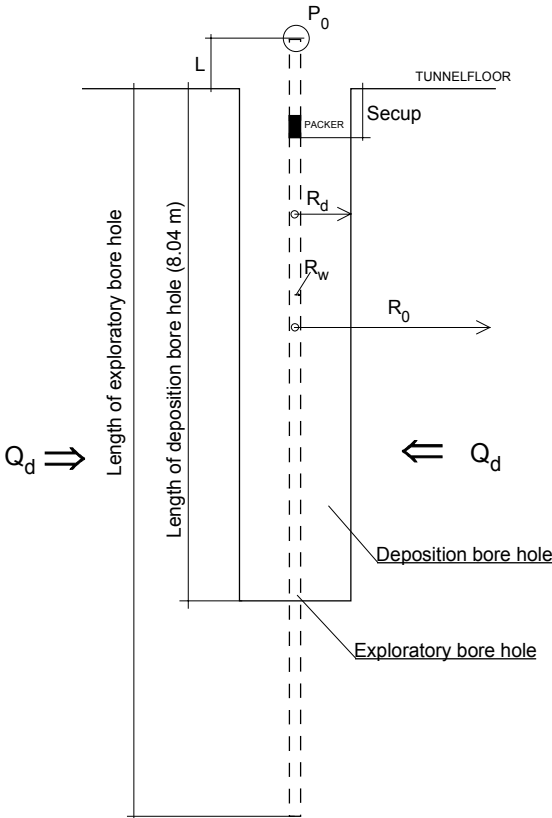


Figure 15-13 Schematic layout of deposition bore hole and exploratory borehole.

Undisturbed maximum pressure in rock volume intended for the deposition bore hole will accordingly be

$$P_d = P_0 + L + 8.04 \text{ m} \quad \text{where}$$

L = distance of pressure transducer above the tunnel floor, see Forsmark and Rhén (1999b)

The pressure difference causing the flow out from the exploratory hole is P_0 and the pressure difference causing the flow into the deposition hole is P_d , as there is atmospheric pressure in the deposition holes after drilling.

15.2.2 Predicted flow rates

The details of the estimation of inleakage to the six separate deposition holes is shown in Tables 7-1 to 7-6 in (Forsmark, Rhén, 1999b).

The predicted mean (arithmetic) flow rate show increases rather much from drill batch 1 to 2 and slightly from drill batch 2 to 3, except for deposition holes 4 and 6 that are almost constant. For deposition boreholes, 1 and 6, the inclined boreholes from drill batch 3 give the extreme values, see Figures 15-15 to 15-18. These values may not be relevant in a case where subvertical pilot boreholes are drilled were deposition holes are planned to be excavated.

As the exploratory borehole radius is very small compared with the radius of the deposition boreholes, it is likely that the deposition holes will intersect one or several features with as high transmissivity as the highest found in the exploratory boreholes. It was therefore considered in the predictions that the maximum calculated flow from a single observation hole might be the most relevant prediction for the inflow to the deposition holes. In Table 15-5, the maximum calculated flow rates (Q_{d1} and Q_{d2}) for each deposition hole is summarised based on data from all drill batches. In Figure 15-14 the predicted mean and max flow rates from each drill batch is shown.

Table 15-5 Maximum and mean values for calculated flow rate (based on drill batch 1-3) and measured flow rate for each deposition bore hole. Measured is according to Table 6-3. Q_{d1} is based on measured flow rate and pressure in pilot bore holes. Q_{d2} is based on evaluated transmissivity and pressure in pilot bore holes.

Deposition bore hole	Mean Q_{d1} (L/min)	Max Q_{d1} (L/min)	Mean Q_{d2} (L/min)	Max Q_{d2} (L/min)	Q_{meas} (L/min)
1	0.0024	1.01	0.012	20.4	0.07935
2	0.0004	0.00448	0.0006	0.0119	0.00190
3	0.0013	0.00448	0.0094	0.0119	0.00295
4	0.0033	0.00513	0.014	0.0305	0.00072
5	0.0072	0.0370	0.025	0.167	0.001575
6	0.041	6.55	0.12	30.5	0.00270
Mean	0.01	1.27	0.03	8.52	0.01

The maximum predicted inflow based on the sub-vertical boreholes is about 0.1 - 0.3 L/min. The highest predicted inflows, which are about 1 - 30 L/min are for deposition holes 1 and 6 and are based on two of the inclined boreholes.

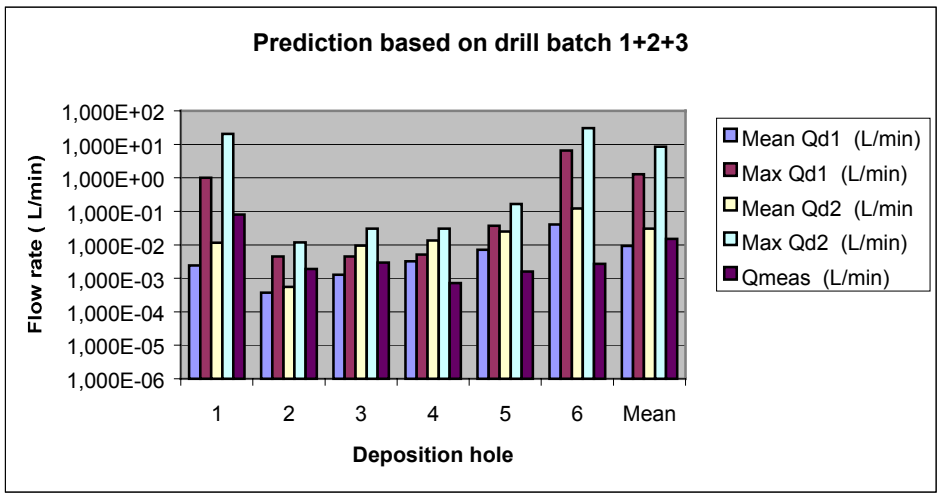
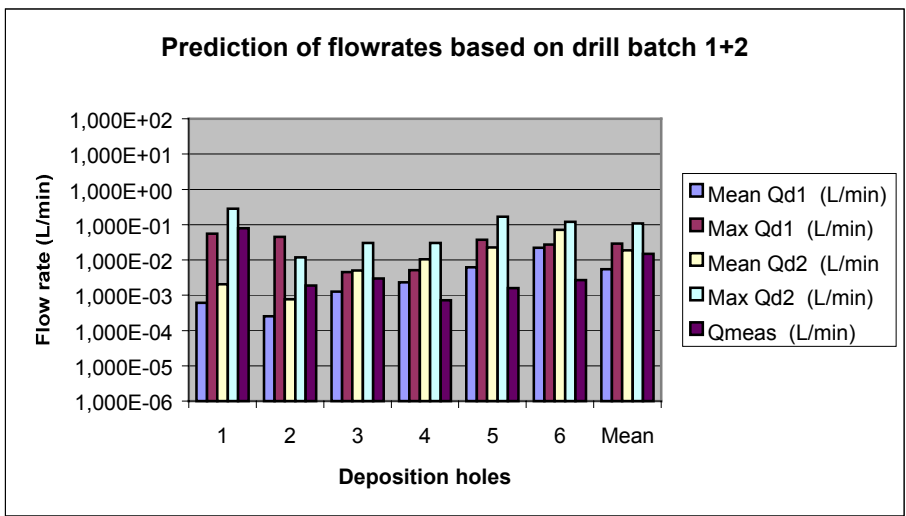
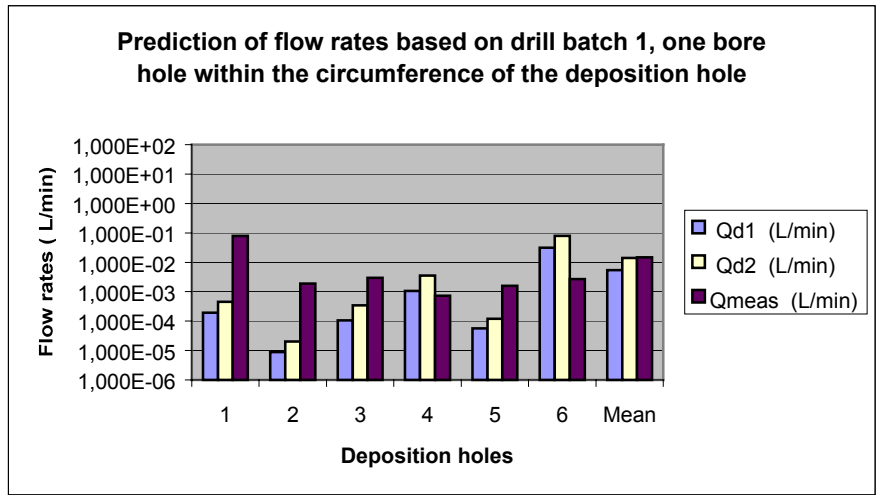


Figure 15-14 Estimated mean flow rates (Qd1 and Qd2) and measure flow rates according to Table 15-5 and Forsmark and Rhen (1999b).

The prediction of the inflow based on the evaluated transmissivity gives higher inflow rates compared to the prediction based on the measured flow rate and pressure in the boreholes. The predictions based on the transmissivity gives on average 3 - 4 times higher flow rates but in single cases 2 - 7 times higher flow rates and in two cases 20 and 50 times higher flow rates and in one case 5 times lower flow rates.

All of the measured rates are below the maximum estimated values, two of them considerably below the maximum value. The mean value of the predicted inflow, especially the flow-pressure based (Q_{d1}), corresponds better to the measured values. Figure 15-14 illustrates this. As can be seen mean Q_{d1} is generally within 10 times to 0.1 of the measured flow rate.

Some of the boreholes drilled in drill batch 2 and 3 are drilled within the circumference of the deposition hole (KA3586G01 and KA3588G01 - Deposition hole 1) or just outside the circumference of the deposition hole (KA3574G01 and KA3576G01 - Deposition hole 3, KA3550G01 and KA3552G01- Deposition hole 5, KA3544G01 and KA3546G01- Deposition hole 6). These boreholes give indications of how useful it may be with several pilot holes drilled within a deposition hole in order to estimate the properties and probable inflow rates. The result is shown in Figure 15-15. As can be seen the predicted flow rate based on Q_{d1} is within 10 times to 0.1 of the measured flow rate

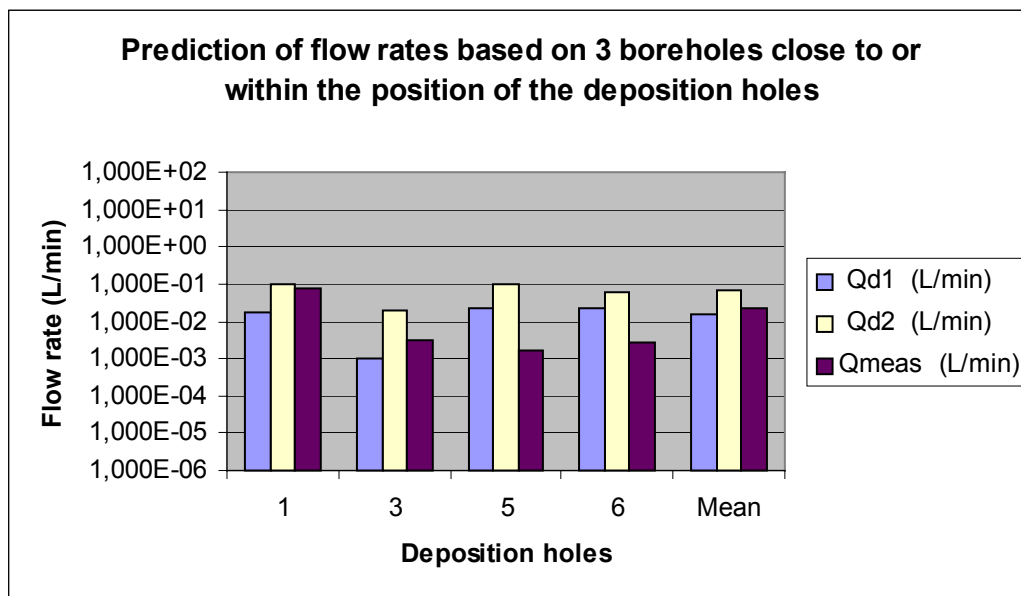


Figure 15-15 Estimated mean flow rates (Q_{d1} and Q_{d2} , based on boreholes drilled close or within the circumference of the deposition holes) and measure flow rates according to Forsmark and Rhen (1999b).

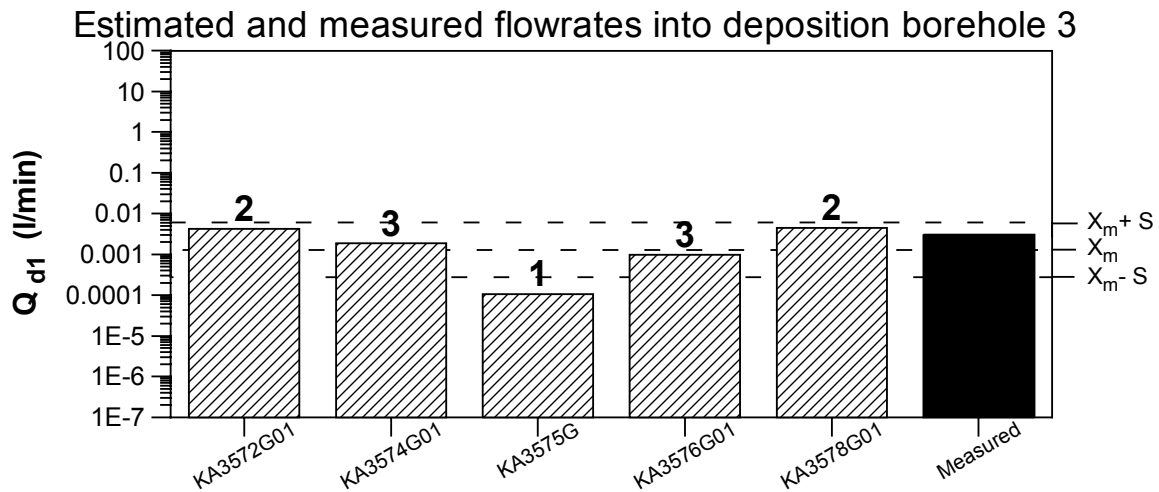
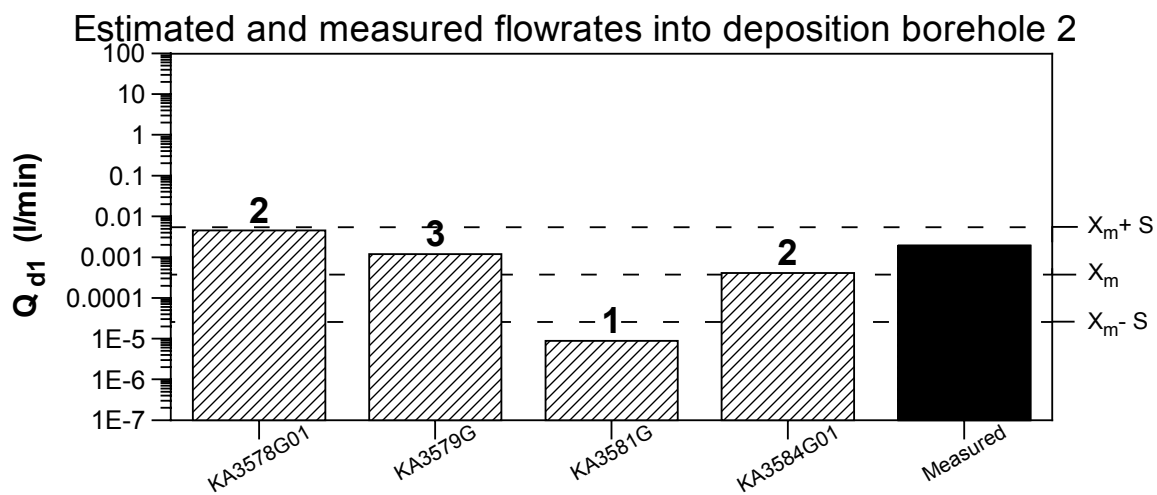
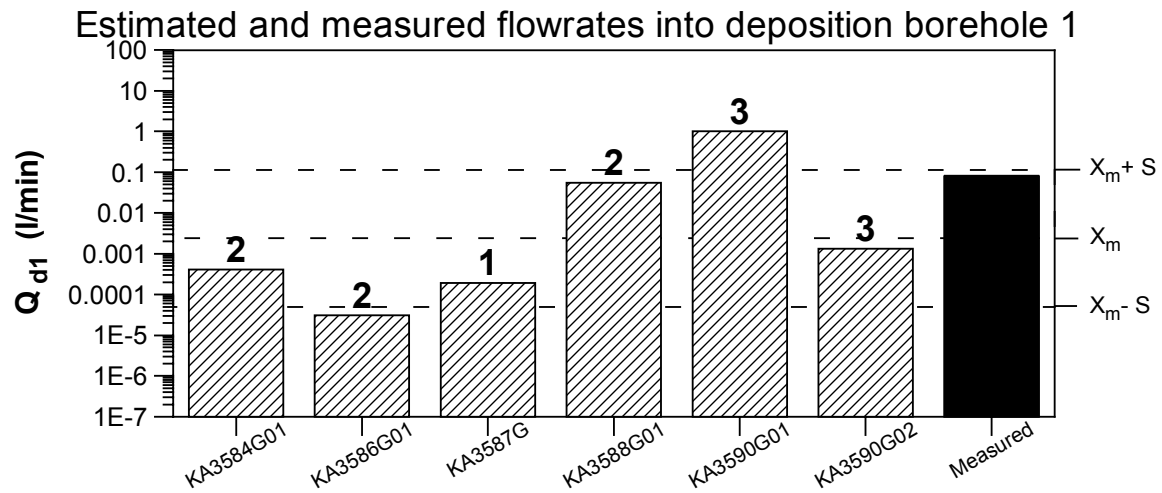


Figure 15-16 Estimated flow rates (Q_{d1}) according to Table 7-1 to 7-3 in (Forsmark, Rhén, 1999b) and measured flow rates according to Table 8-2 in (Forsmark et al, 2001a). X_m = mean at $\text{Log}_{10}(X)$, S = standard deviation of $\text{Log}_{10}(X)$. 1: drill batch 1, 2: drill batch 2 and 3: drill batch 3.

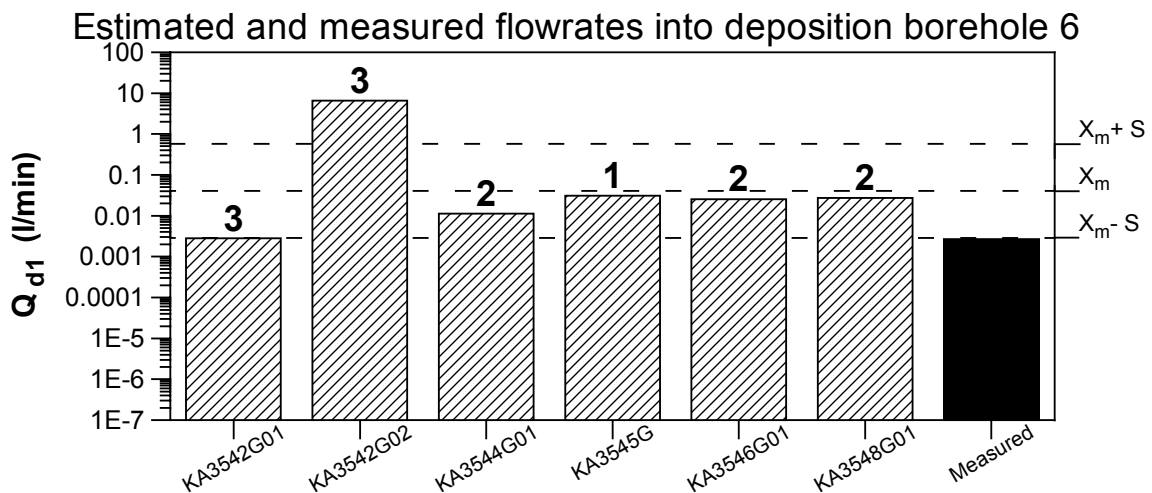
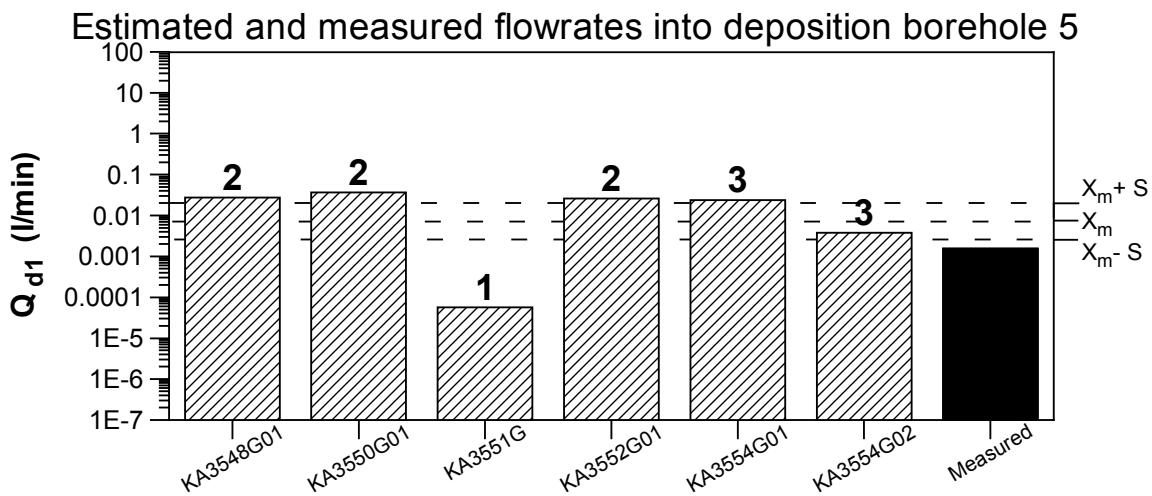
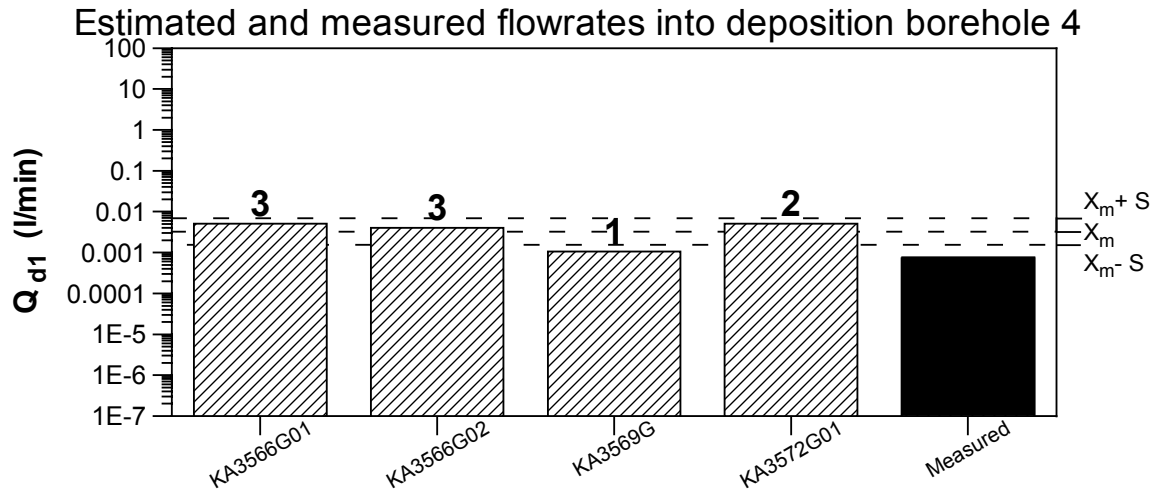


Figure 15-17 Estimated flow rates (Q_{d1}) according to Table 7-4 to 7-6 in (Forsmark, Rhén, 1999b) and measured flow rates according to Table 8-2 in (Forsmark et al, 2001a). X_m = mean at $\text{Log}_{10}(X)$, S = standard deviation of $\text{Log}_{10}(X)$. 1: drill batch 1, 2: drill batch 2 and 3: drill batch 3.

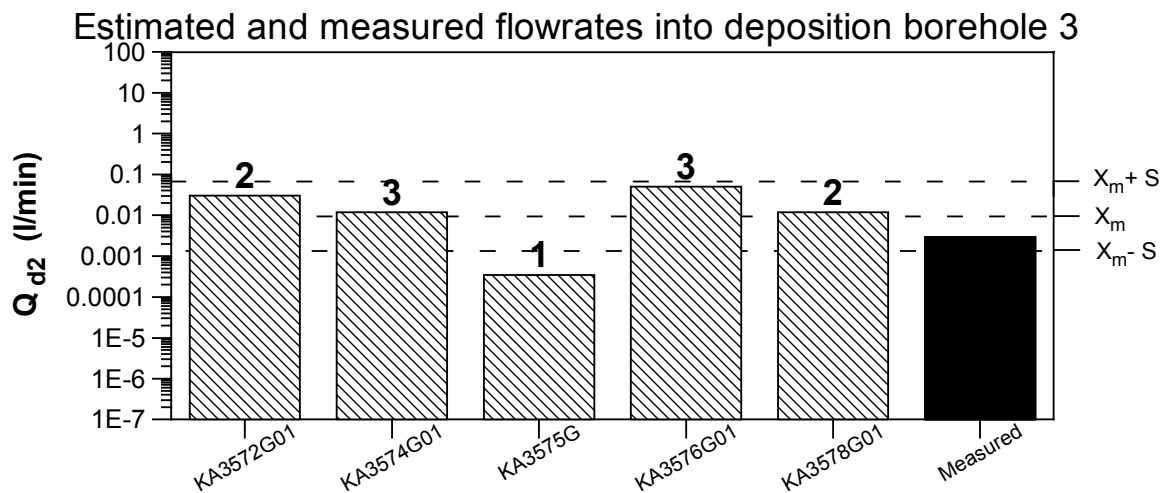
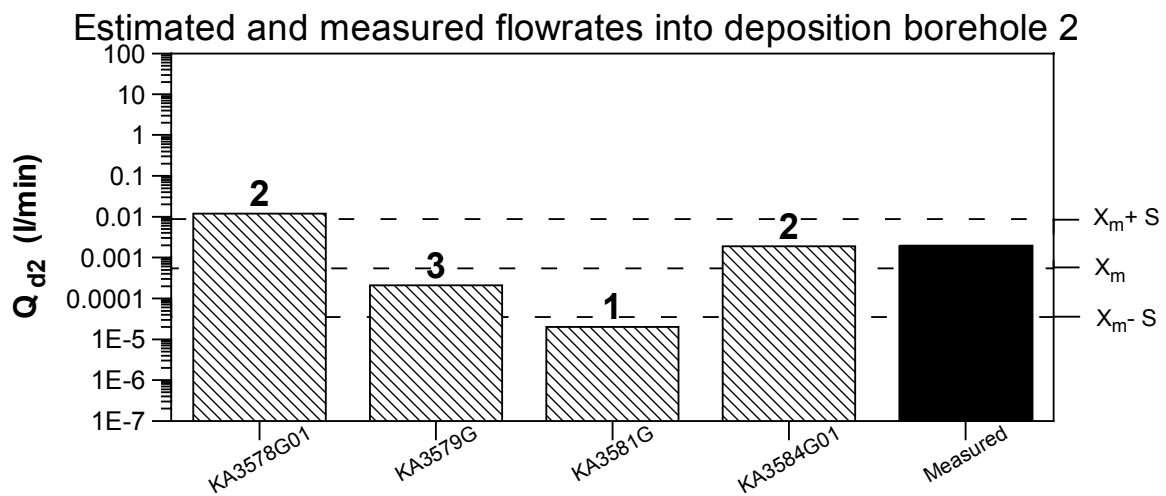
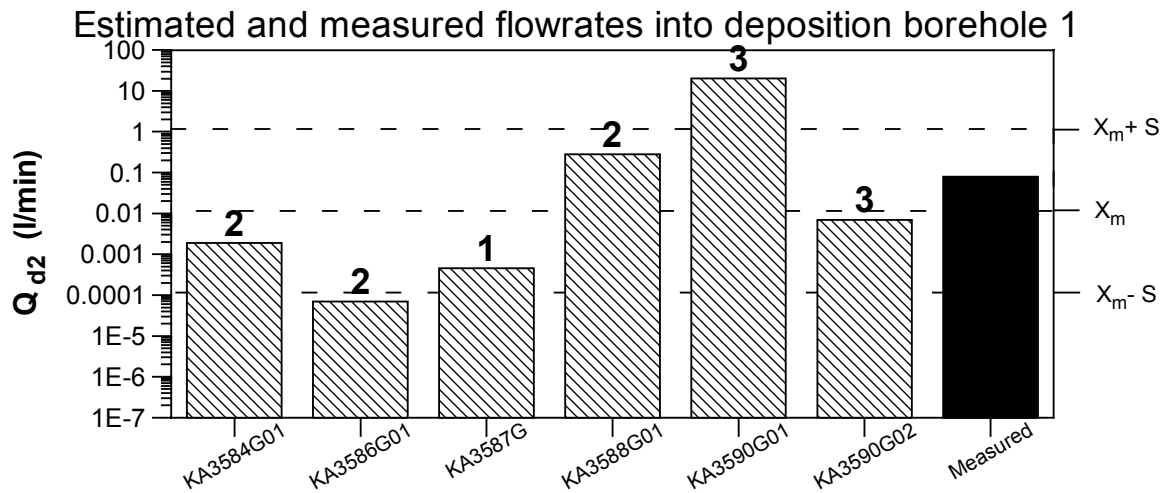


Figure 15-18 Estimated flow rates (Q_{d2}) according to Table 7-1 to 7-3 in (Forsmark, Rhén, 1999b) and measured flow rates according to Table 8-2 in (Forsmark et al, 2001a). X_m = mean at Log10 (X), S = standard deviation of Log10 (X). 1: drill batch 1, 2: drill batch 2 and 3: drill batch 3.

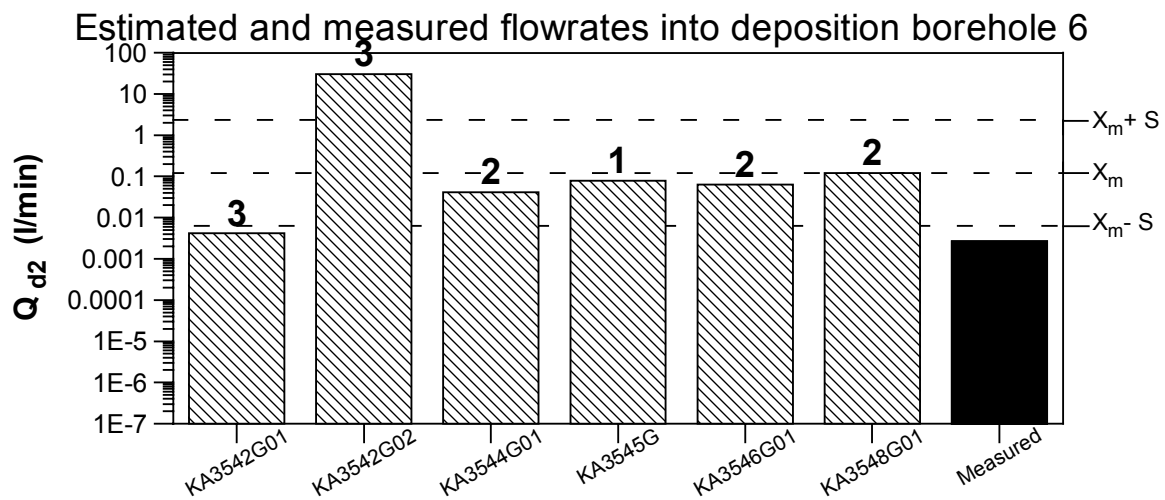
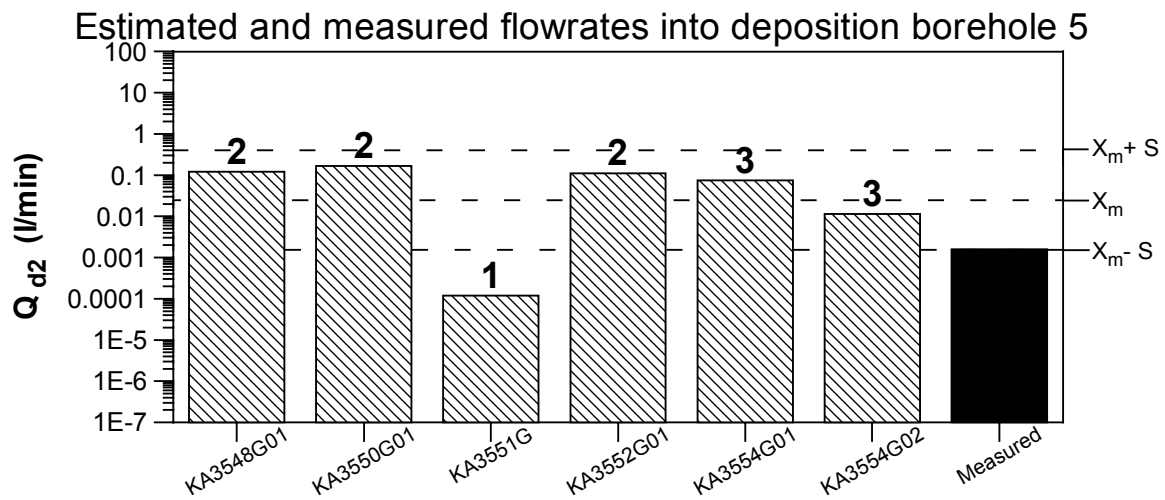
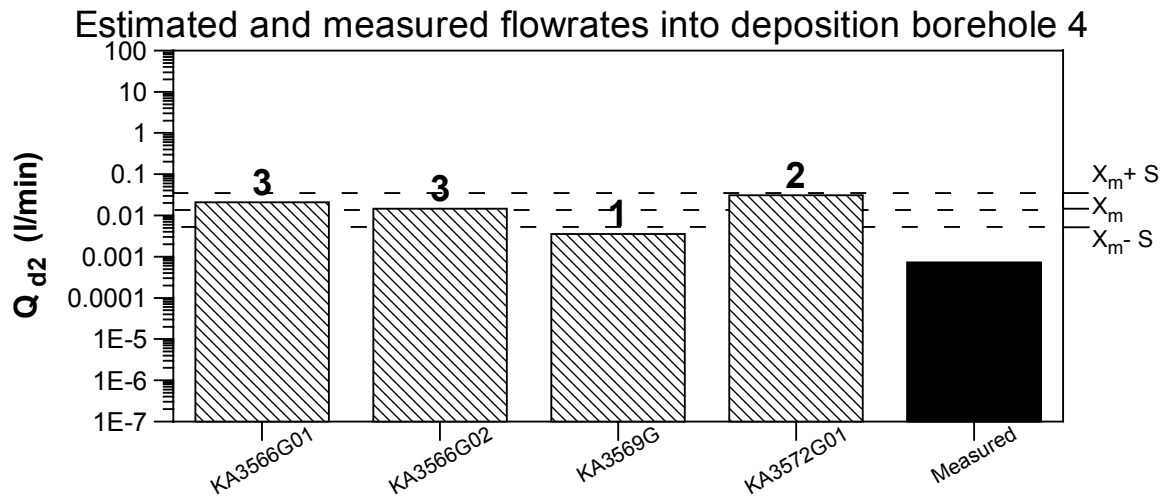


Figure 15-19 Estimated flow rates (Q_{d2}) according to Table 7-4 to 7-6 in (Forsmark, Rhén, 1999b) and measured flow rates according to Table 8-2 in (Forsmark et al, 2001a). X_m = mean at $\text{Log}_{10}(X)$, S = standard deviation of $\text{Log}_{10}(X)$. 1: drill batch 1, 2: drill batch 2 and 3: drill batch 3.

15.2.3 Predicted properties

Table 15-6 shows the summary statistics of the transmissivities for each of the drill batch. In drill campaign 1 the pilot boreholes were drilled within the circumference of the deposition holes. During drill campaign 2 only vertical boreholes were drilled between the planned deposition holes or close to the deposition holes. During drill campaign 3 two bore holes were drilled close to the deposition holes, 8 were inclined and a few others were vertical.

In figures 15-20 and 15-21 the average hydraulic conductivity is shown, based on Table 15-6 and a borehole length of 8m.

The summary statistics for all drill batches (1+2+3) is probably misleading as an estimate for the hydraulic conductivity of the near field of the deposition holes due to that the inclined boreholes are more likely to intersect more of the conductive subvertical fracture set striking NW compared to the deposition holes. The data set for the boreholes closest to the deposition holes (1+2+3(close)) consists each of 3 boreholes and probably gives the best estimate of the average properties of the near field of each deposition hole.

It should be noted that the measured inflow rates to each of the deposition holes according to Table 6-3 is not directly related to the hydraulic conductivity shown in Figures 15-20 and 15-21. The largest inflow is to deposition hole 1 and the smallest to deposition hole 4.

Table 15-6 Transmissivity estimation for each deposition hole position after drill campaign 2 and after campaign 3 respectively. T_A : Arithmetic mean transmissivity. T_G : Geometric mean transmissivity (T), $Std(\log_{10}(T))$: Standard deviation of $\log_{10}(T)$. 1+2+3(close): Only borehole drilled within deposition hole or a few decimetres outside the deposition hole included.

Drill campaign	Parameter	Dep hole 1	Dep hole 2	Dep hole 3	Dep hole 4	Dep hole 5	Dep hole 6
1	T	$2.11 \cdot 10^{-11}$	$8.7 \cdot 10^{-12}$	$1.9 \cdot 10^{-10}$	$4.2 \cdot 10^{-10}$	$8.4 \cdot 10^{-12}$	$2.1 \cdot 10^{-9}$
1 + 2	T_A	$2.1 \cdot 10^{-9}$	$1.7 \cdot 10^{-10}$	$5.7 \cdot 10^{-10}$	$7.6 \cdot 10^{-10}$	$3.6 \cdot 10^{-9}$	$2.4 \cdot 10^{-9}$
1 + 2	T_G	$1.1 \cdot 10^{-10}$	$6.3 \cdot 10^{-11}$	$4.5 \cdot 10^{-10}$	$6.8 \cdot 10^{-10}$	$9.5 \cdot 10^{-10}$	$2.2 \cdot 10^{-9}$
1 + 2	$Std(\log_{10}(T))$	1.29	0.85	0.38	0.3	1.38	0.15
1 + 2 + 3	T_A	$7.1 \cdot 10^{-8}$	$1.3 \cdot 10^{-10}$	$7.9 \cdot 10^{-10}$	$7.0 \cdot 10^{-10}$	$2.9 \cdot 10^{-9}$	$1.1 \cdot 10^{-7}$
1 + 2 + 3	T_G	$5.0 \cdot 10^{-10}$	$3.7 \cdot 10^{-11}$	$5.9 \cdot 10^{-10}$	$6.5 \cdot 10^{-10}$	$9.8 \cdot 10^{-10}$	$3.7 \cdot 10^{-9}$
1 + 2 + 3	$Std(\log_{10}(T))$	1.75	0.83	0.38	0.18	1.1	1.21
1+2+3(close)	T_A	$2.8 \cdot 10^{-9}$	-	$8.1 \cdot 10^{-10}$	-	$3.6 \cdot 10^{-9}$	$2.0 \cdot 10^{-9}$
1+2+3(close)	T_G	$1.3 \cdot 10^{-10}$	-	$5.3 \cdot 10^{-10}$	-	$6.2 \cdot 10^{-10}$	$1.9 \cdot 10^{-9}$
1+2+3(close)	$Std(\log_{10}(T))$	1.57	-	0.49	-	1.62	0.1

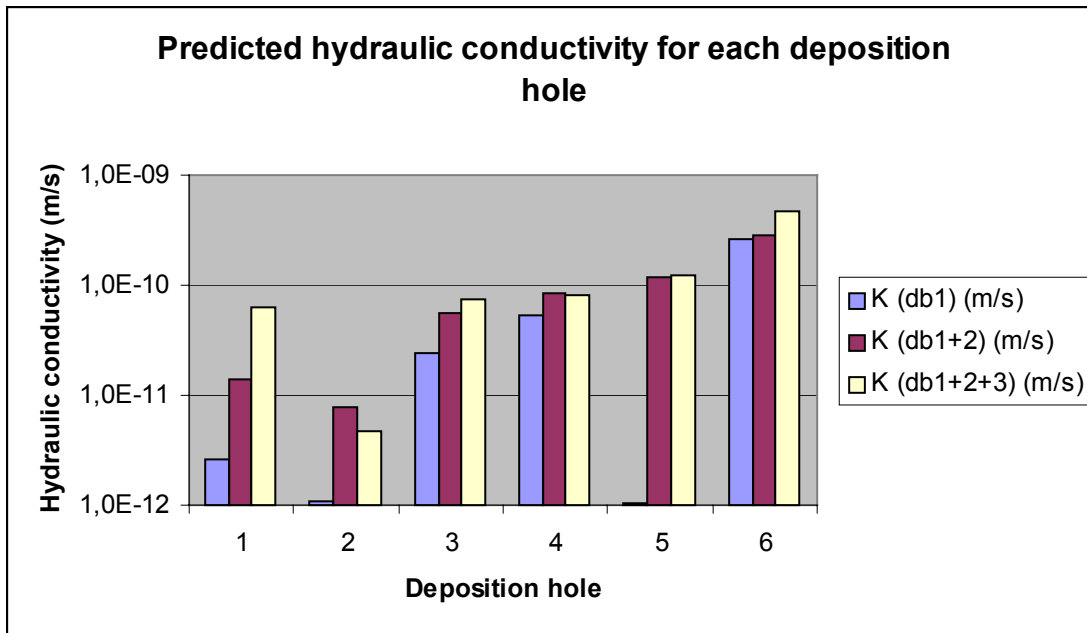


Figure 15-20 Predicted geometric mean hydraulic conductivity for each deposition hole based on boreholes located within a few meters from the deposition hole. (db: drill batch).

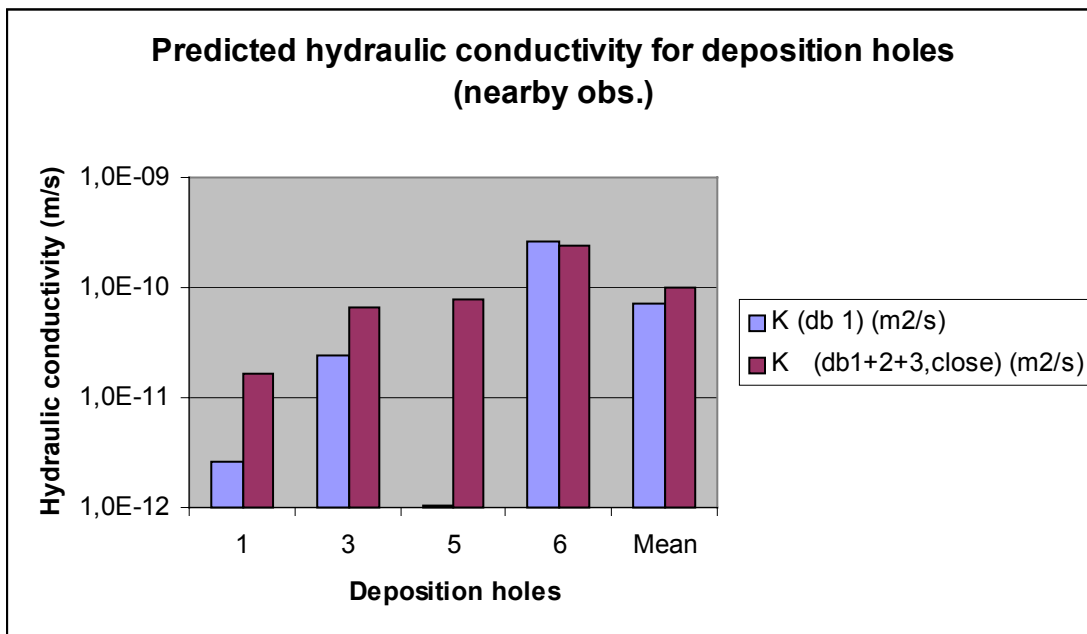


Figure 15-21 Predicted geometric mean hydraulic conductivity for each deposition hole based on boreholes located within the deposition hole (db1) or a few decimetres from the outer radius of the deposition hole. (db: drill batch).

15.3 Continuum model

The main objective of the study presented in Svensson (2001) was to develop and establish an adequate model of the groundwater pressure and salinity distributions around the Prototype Repository. With “adequate model” it was understood that the model should be well balanced with respect to expected use, available data, scientific basis and computational resources. More specifically the project should result in a set of three-dimensional fields of pressure and salinity; fields that are intended to be used in other studies of the Prototype Repository.

The model was based on a fracture network with given transmissivity distribution that was converted to a conductivity field in a continuum model with cell size of 1 m close to the tunnel. Boundary conditions for the laboratory model was generated with larger scale models and variable density flow was included in the modelling.

Model size:

- Laboratory model 800x600x360 m (E to W x N to S x vertical depth)
- Repository model 166x96x76 m

A coupled solution was used for the Laboratory and Repository models.

Two main cases were modelled:

1. Present situation with open deposition holes
2. Tunnel section I and II backfilled. Buffer and canisters in the deposition holes.

The simulations are performed as 2 stationary cases:

1. Atmospheric conditions in all tunnel and deposition holes
2. Water saturated conditions in inner and outer section in the Prototype tunnel.
 - a. Skin for tunnels as in case 1
 - b. Skin for tunnels neglected
 - c. For one realisation of the hydraulic conductivity of the rock mass, max and min values of the hydraulic conductivity of the backfill material are used in both cases 2a and 2b.

Five realisations of the conductivity field were generated. In Figure 15-22 two of realisations is shown and in Figures 15-22 to 15-25 the pressure and salinity field is shown for the same two of the realisations of the fracture network.

The buffer was assumed to have a hydraulic conductivity of 10^{-13} m/s and three cases were considered for the backfill: 10^{-9} , 10^{-10} , 10^{-11} m/s.

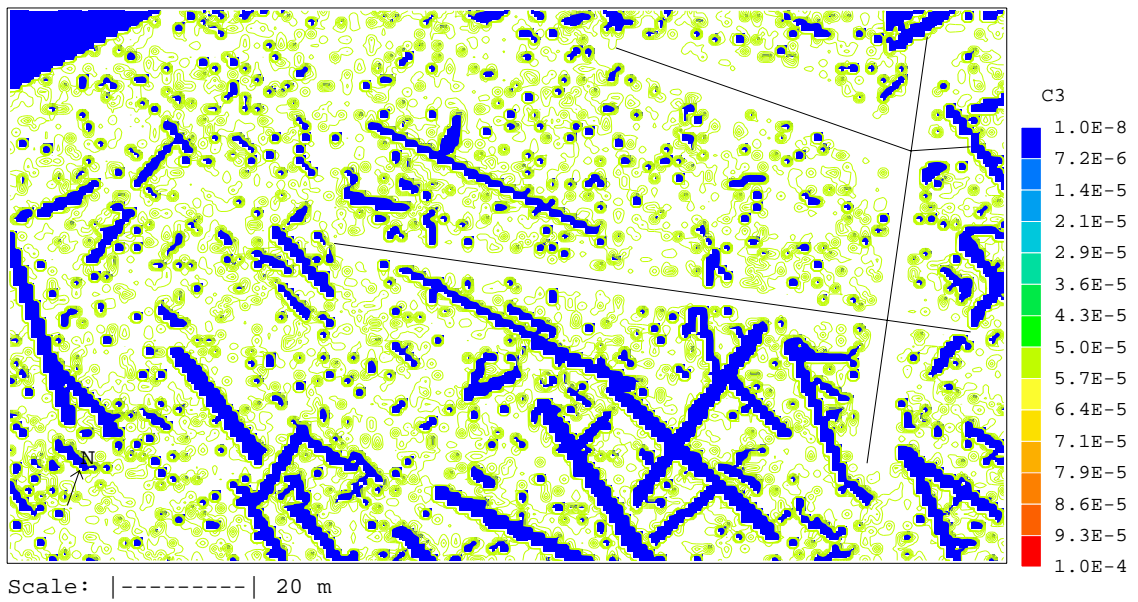
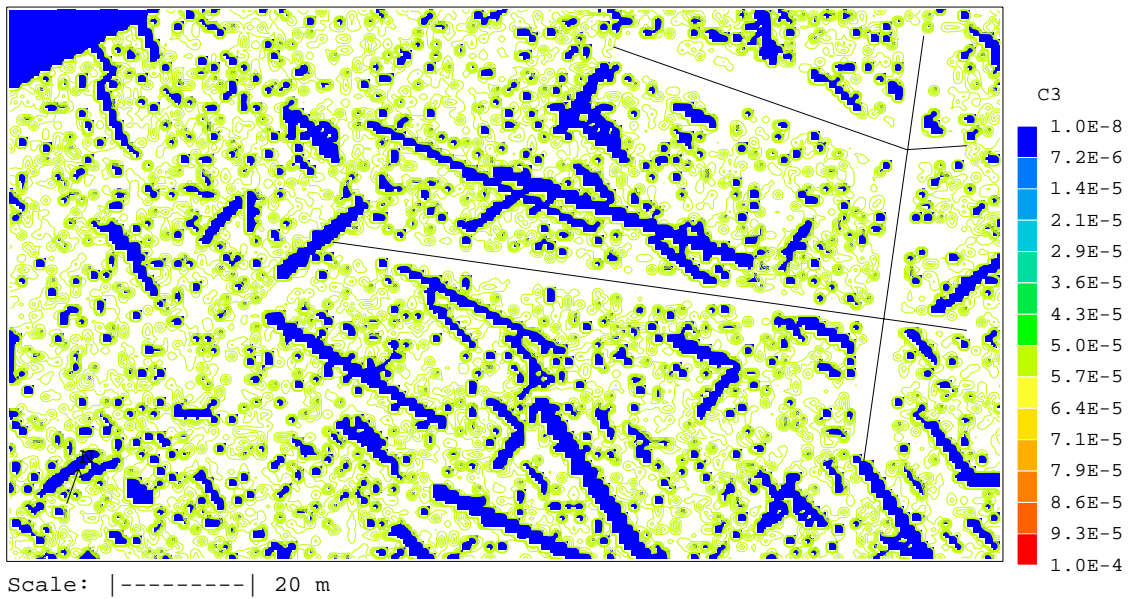


Figure 15-22. Hydraulic conductivity field at a depth of 447 metres below ground level.

Top: Realisation 2

Bottom: Realisation 5

Blue: $K > 1E-8$ m/s

Green: $1E-9 < K < 1E-8$ m/s

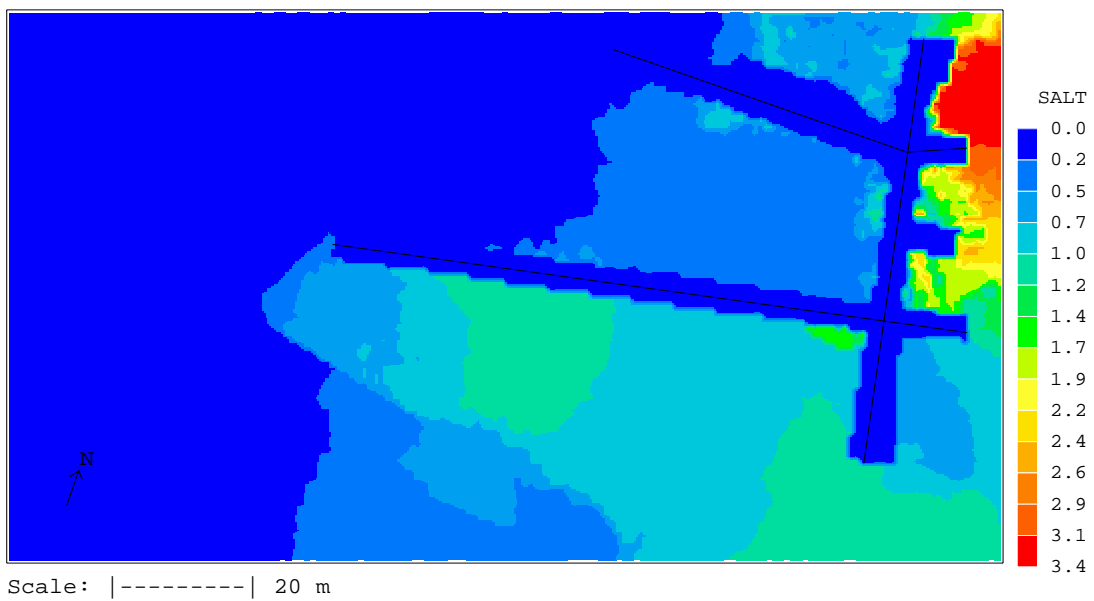
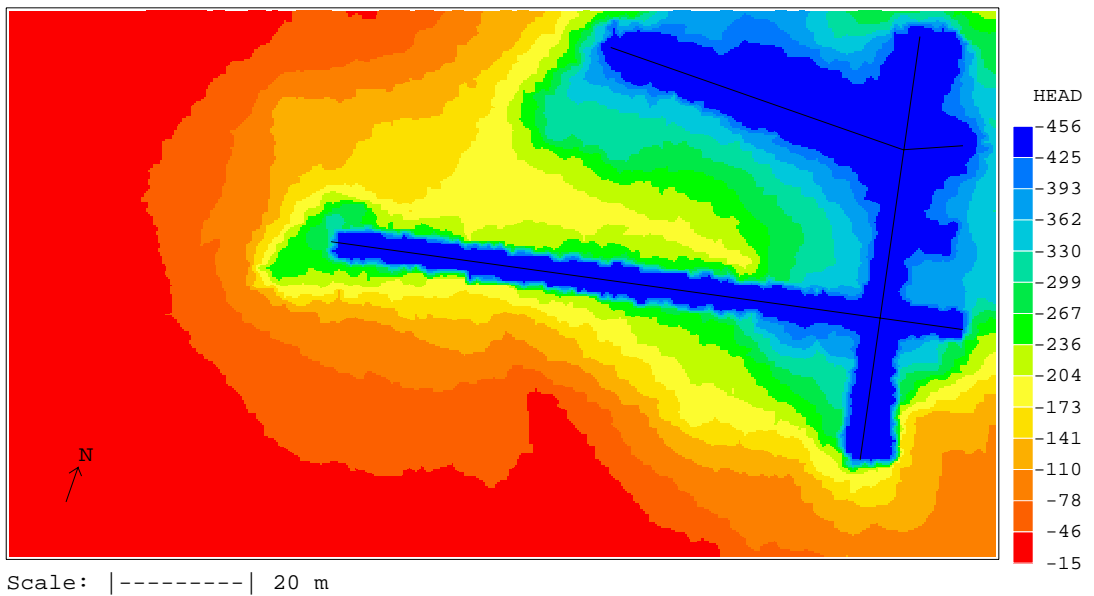


Figure 15-23. Pressure head (in metres) (top) and salinity (in %) distributions at a depth of 447 metres below ground level. Realisation 2.

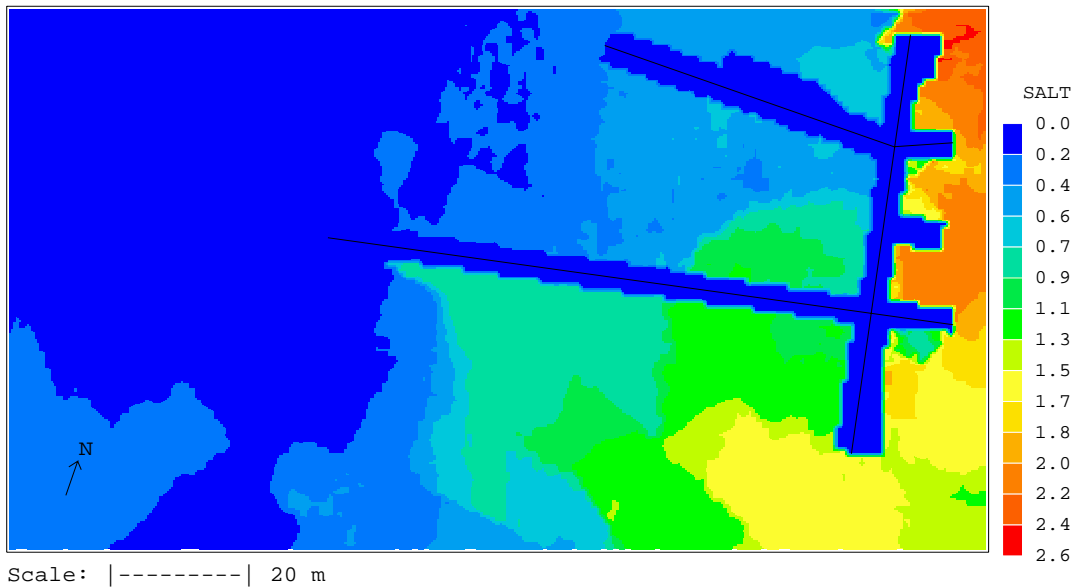
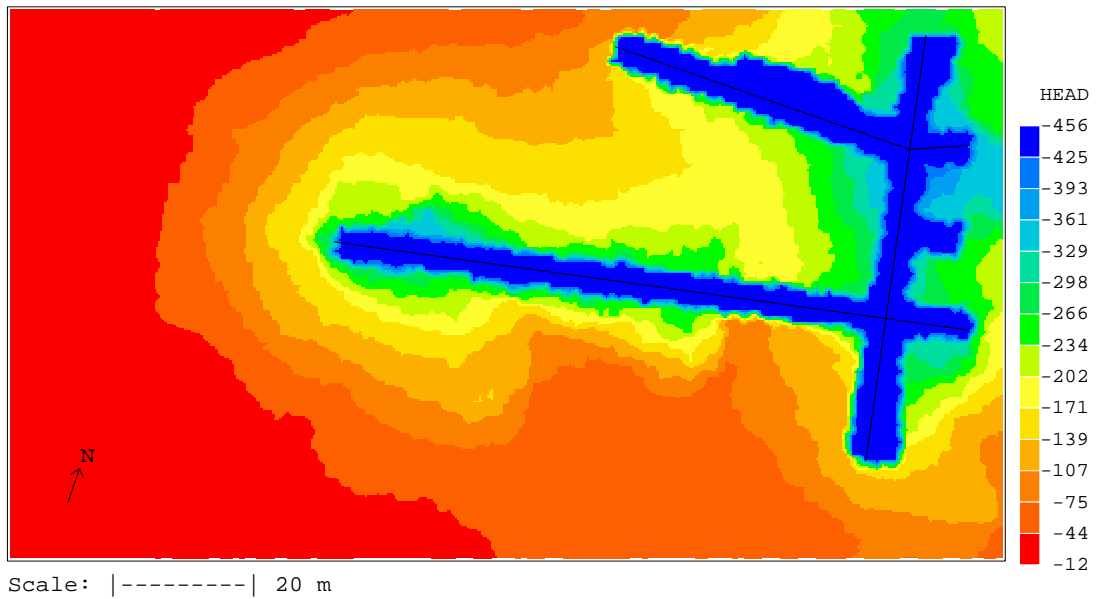


Figure 15-24. Pressure head (in metres) (top) and salinity (in %) distributions at a depth of 447 metres below ground level. Realisation 5.

The realisations with different fracture networks showed rather different pressure fields when the tunnel was open. When the tunnel was closed the differences between the realisations were less compared to the open conditions but was anyhow present.

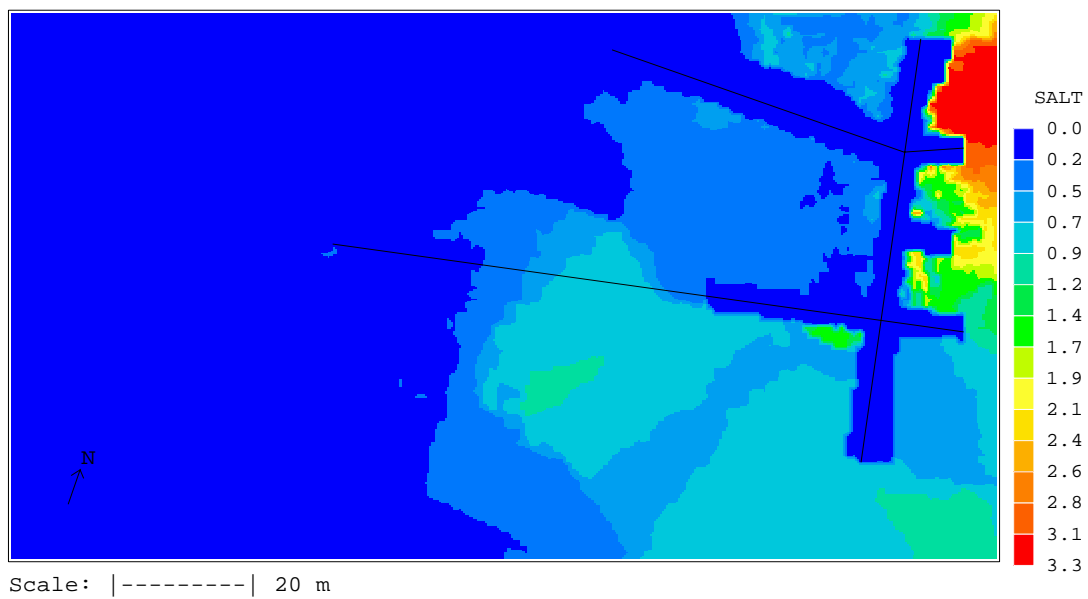
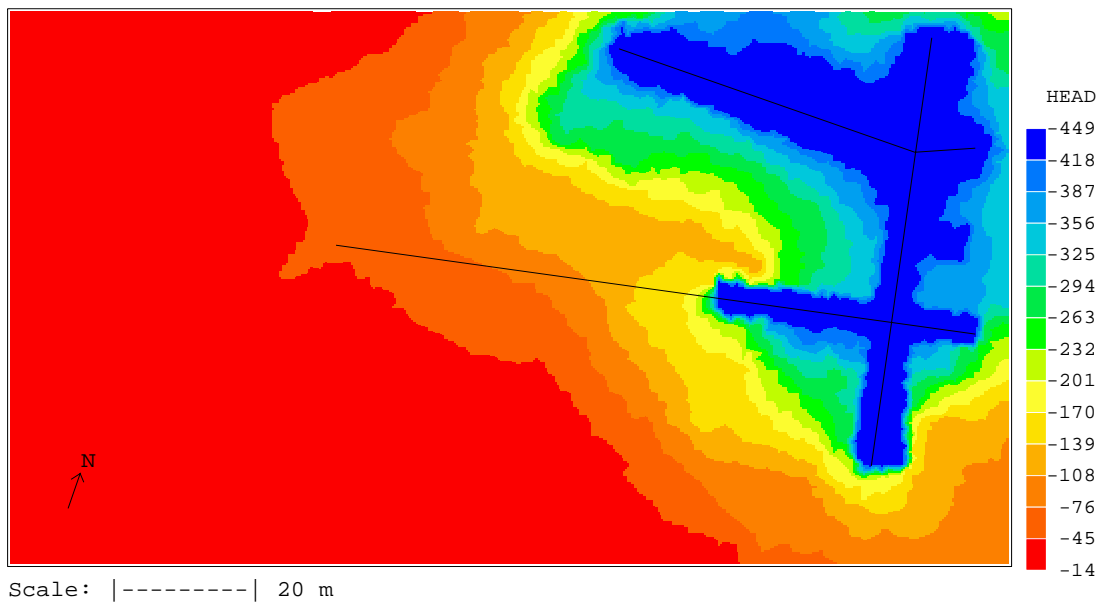


Figure 15-25 Pressure head (in metres) (top) and salinity (in %) distributions at a depth of 447 metres below ground level. Saturated conditions in section I and II. Skin as for open conditions. Hydraulic conductivity for backfill 10^{-10} m/s. Realisation 2.

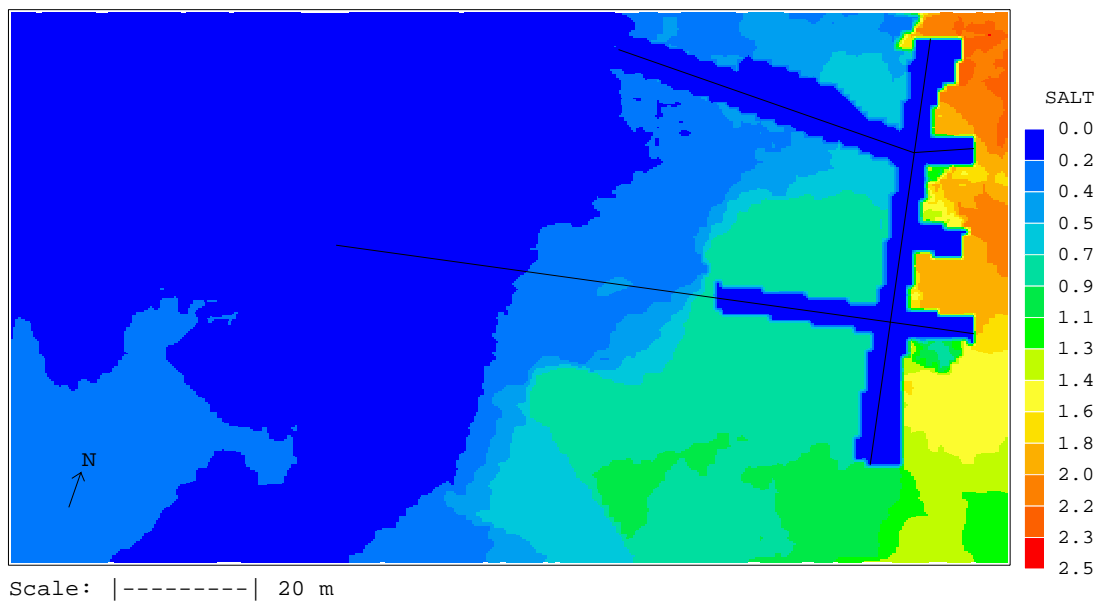
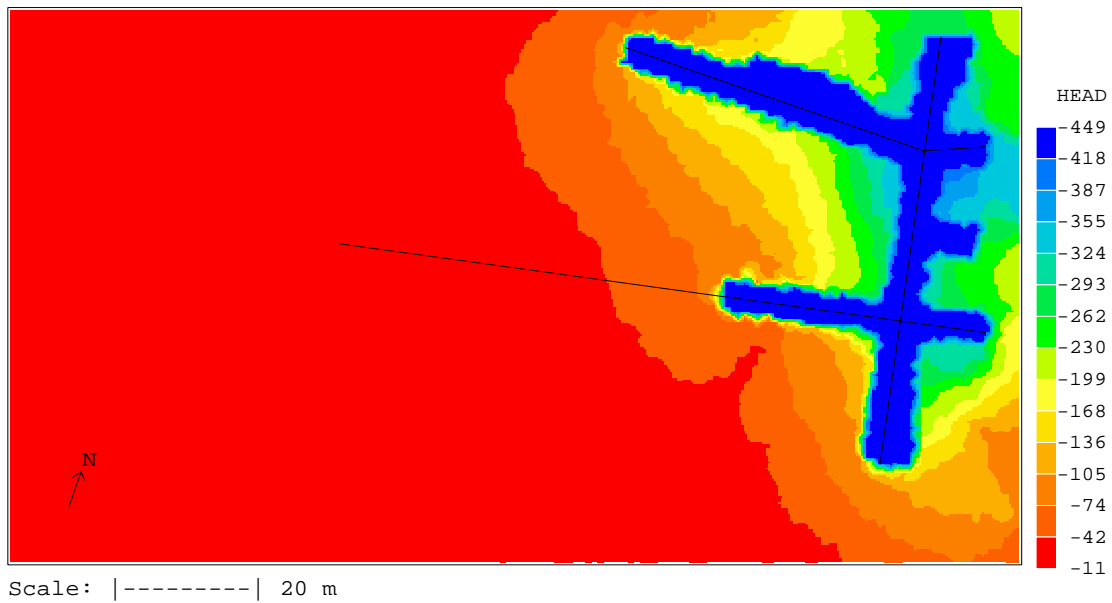


Figure 15-26 Pressure head (in metres) (top) and salinity (in %) distributions at a depth of 447 metres below ground level. Saturated conditions in section I and II. Skin as for open conditions. Hydraulic conductivity for backfill 10^{-10} m/s. Realisation 5.

With the backfill and buffer in the tunnel the cases with no skin (hydraulic resistance around the tunnel) and skin as for open conditions was tested. The hydraulic conductivity of the backfill was also varied with two limiting cases: maximum ($= 10^{-9}$ m/s) conductivity in backfill and no skin (hydraulic resistance around the tunnel) and minimum ($= 10^{-11}$ m/s) conductivity and skin as for open conditions. The result was that the pressure distribution in the rock was very similar between the cases.

15.4 Conclusions

15.4.1 DFN model

The first DFN model was based on a limited data set but succeeded to predict the fracture orientations and fracture frequencies fairly well. The inflow prediction was less good. The predicted inflows were greater than the measured. All available data was not used and possibly the predictions could have improved to some extent if all data had been used.

The second DFN model was based on a large data set but not all now available data. The predictions of fracture frequencies and fracture trace statistics were fairly good but the inflows to the deposition holes were much greater than measured. The predicted pressures were also a bit too high and showed less variability than the measured pressures.

The results indicate that the DFN model can be improved and probably the hydraulic tests can be most useful when testing new modelling ideas. The reason for this is that these test are probably less affected of two phase flow and rock stress conditions that may play a significant role when modelling the inflow to the tunnels and deposition holes. New data that can be useful is the mapping of the deposition holes and a large number of interference tests. Inflow to the deposition holes and the pressure responses during the drilling of the deposition holes is also a data set not used for setting up the present DFN model.

15.4.2 Simple inflow prediction

The simple prediction of the mean inflow rate into the deposition holes, based on measured flow rates and pressures from pilot bore holes drilled within the circumference of the deposition holes and boreholes a few decimetre from the circumference of the deposition holes, were within 10 to 0.1 of the measured flow rate. Predictions based on just the pilot bore holes drilled within the circumference of the deposition holes (one bore hole per deposition hole) were less good but still in several cases within or near the limits mention above. Predictions based on all boreholes showed a rather large variation, mainly depending on results from the inclined boreholes that indicated high transmissivities. In a case with vertical deposition holes and if the most conductive fracture set is subvertical, subvertical boreholes give the most reliable predictions.

16 References

- Alm P, Rhén I, (in prep).** Äspö HRL - Prototype repository. Hydro-mechanical behaviour due to excavation and thermal load (tentative title), SKB, IPR-xx-xx
- Almén K, Zellman O, 1991.** Äspö Hard Rock Laboratory. Field investigation methodology and instruments used in the pre-investigation phase, 1986-1990. SKB TR 91-21.
- Autio J, Maarit Kemppainen M, Olia E, Siitari-Kauppi M, 2001(inprep).** Study of rock damage caused by boring of experimental deposition holes at Äspö Hard Rock Laboratory (tentative title), SKB YYY-xx-xx
- Dershowitz W S, Herda H H, 1992.** Interpretation of fracture spacing and intensity, In Proceedings of the 33rd US symposium on Rock Mechanics, A.A. Balkema, Rotterdam, p.757-766.
- Follin, S. and J. Hermanson ,1996.** A discrete fracture network model of the Äspö TBM Tunnel Rock Mass, SKB AR D-97-001
- Forsmark T, Rhén I, 1999a.** Äspö HRL - Prototype repository. Hydrogeology – Interference test campaign 1 after drill campaign 3, SKB, IPR-00-07
- Forsmark T, Rhén I, 1999b.** HRL - Prototype repository. Hydrogeology - Drill campaign 3A and 3B, SKB, IPR-00-08
- Forsmark T, Rhén I, 2000a.** Äspö HRL - Prototype repository. Hydrogeology – Injection test campaign 1, SKB, IPR-00-20
- Forsmark T, Rhén I, 2000b.** Äspö HRL - Prototype repository. Hydrogeology – Interference test campaign 2 after drill campaign 3, SKB, IPR-00-21
- Forsmark T, Rhén I, Andersson C, 2001a.** Äspö HRL - Prototype repository. Hydrogeology – Deposition- and lead-through boreholes: Inflow measurements, hydraulic responses and hydraulic tests, SKB, IPR-00-33
- Forsmark T, Rhén I, Andersson C, 2001b.** Äspö HRL - Prototype repository. Hydrogeology – Injection test campaign 2, flow measurement of DA3575G01, groundwater salinity, groundwater leakage into G-,I and J-tunnels, SKB, IPR-01-31
- Gentzschein B, 1997a.** Äspö HRL – True Block Scale Experiment. Detailed flowlogging of core boreholes KA2511A, KI0025F and KA3510A using a double packer system, SKB, TN-97-23b
- Gentzschein B, 1997b.** Äspö HRL - Prototype repository. Hydraulic tests in exploratory holes. Drill campaign 1, SKB, IPR-99-27

- Gentzschein B,1998.** Äspö HRL - Prototype repository. Hydraulic tests in exploratory holes. Drill campaign 2, SKB, IPR-99-28
- Gentzschein B,1999a.** Äspö HRL - Prototype repository. Hydraulic tests in exploratory holes. Drill campaign 3a, SKB, IPR-99-29
- Gentzschein B,1999b.** Äspö HRL - Prototype repository. Hydraulic tests in exploratory holes. Drill campaign 3b, SKB, IPR-99-30
- Gentzschein B,1999c.** Äspö HRL - Prototype repository. Hydraulic tests in exploratory holes. Injection tests, SKB, IPR-99-31
- Gentzschein B,1999d.** Äspö HRL - Prototype repository. Hydraulic tests in exploratory holes. Interference tests A after drill campaign 3, SKB, IPR-99-32
- Gentzschein B,1999e.** Äspö HRL - Prototype repository. Hydraulic tests in exploratory holes. Interference tests B after drill campaign 3, SKB, IPR-99-33
- Gentzschein B, 2001.** Äspö HRL - Prototype repository. Hydraulic tests in exploratory holes. Injection tests_II, SKB, IPR-01-21
- Hermanson J, Stigsson M, Pringle A, 1999.** Äspö HRL – Prototype repository DFN Model No. 1, SKB, IPR-99-09
- Klasson H, Persson M, Ljunggren C, 2001 (in press).** Rock stress measurements by overcoring at the Äspö HRL, Prototype repository: borehole KA3579G (revised data) and K-tunnel: borehole KK0045G01, SKB YY- XXXX
- Markström I, Erlström M, 1996.** Äspö Hard Rock Laboratory, Overview of documentation of tunnel, niches and core boreholes, SKB PR HRL-96-19
- Nyberg G, Jönsson S, Ekman L, 1997.** Äspö HRL - Hydro Monitoring Program. Report for 1996. SKB PR HRL 97-17.
- Nyberg G, Jönsson S, Ekman L, 1998.** Äspö HRL - Hydro Monitoring Program. Report for 1997. SKB PR HRL 98-19.
- Nyberg G, Jönsson S, Onkenhout J, 1999.** Äspö HRL - Hydro Monitoring Program. Report for 1998. SKB PR-99-20
- Nyberg G, Jönsson S, 2000.** Äspö HRL - Hydro Monitoring Program. Report for 1999. SKB IPR-00-17
- Persson G, Broman O, 2000.** Äspö Hard Rock Laboratory, Prototype Repository, Project plan, FIKW-CT-2000-00055, SKB, IPR-00-31
- Patel S, Dahlström L-O, Stenberg L, 1997.** Äspö HRL, Characterisation of the rock mass in the Prototype Repository at Äspö HRL, Stage 1, SKB HRL-97-24

Patel S, Dahlström L-O, 2001(inprep). Äspö HRL, Geology - Summary report of investigations before the operation phase (tentative title), SKB IPR-xx-xx

Rhén I (ed), Gustafson G, Stanfors R, Wikberg P, 1997. Äspö HRL - Geoscientific evaluation 1997/5. Models based on site characterization 1986-1995. SKB TR 97-06.

Rhén I, Forsmark T, 1998a. Äspö HRL - Prototype repository. Hydrogeology - Drill campaign 1, SKB, PR HRL 98-12.

Rhén I, Forsmark T, 1998b. Äspö HRL - Prototype repository. Hydrogeology - Drill campaign 2, SKB, PR HRL 98-22.

Rhén I, Forsmark T, Torin L, Puigdomenech I, 2001(in prep). Äspö HRL - Prototype repository. Hydrogeological, Hydro chemical and temperature measurements in boreholes during the operation phase of the Prototype Repository. Tunnel section I, SKB, IPR-01-32

Rouhianen P, 1998. Äspö HRL, Flow measurements in boreholes KA3510A and KA2598A at the Äspö Hard Rock Laboratory, SKB TD-99-14

Stigsson M, Outters N, Hermansson J, 2001. Äspö HRL – Prototype repository Hydraulic DFN Model No. 2, SKB, IPR-01-039

Svensson, U. (1997). A site scale analysis of groundwater flow and salinity distribution in the Äspö area. SKB TR 97-17.

Svensson U, 2001. Groundwater Flow, Pressure and Salinity around the Prototype Repository, Continuum model No 1, SKB, IPR-01-040

Svemar C, Pusch R, 2000. Äspö Hard Rock Laboratory, Prototype Repository, Project description, FIKW-CT-2000-00055, SKB, IPR-00-30

Terzaghi R D, 1965. Sources of error in joint surveys. Geotechnique, 15, pp. 287-304.

APPENDIX 1

Summary of hydrogeology in WellCad sheets

Explanations to the columns in the WellCad sheets.

Rock: Mapped rock type.

Fract freq: Fracture frequency.

Nat Min: Fractures mapped as Natural fractures (open fractures).

BIPS fract: Fractures in the borehole observed with BIPS. The diagram shows the result of the analysis of studying BIPS images of the borehole walls. BIPS (Borehole Image Processing System) is a borehole-TV system. The purpose is to indicate where potential water-bearing fractures may be located in the hole. From the image an approximate mean width is estimated. If the fracture is judged open, but less than 1 mm wide the width has been set to 1 mm. It should be observed that the width interpreted from the images can not be used as a hydraulic effective aperture.

Flow drilling: Observed inflow during drilling of the borehole.

Diff Flow: Measured differential flow with the Posiva Flowlogg (only in KA3510A)

Flow testing: Measured inflow when logging the borehole with double-packer system with test section length of 1 or 3m.

UCM Flow: Flow rate measured with the UCM tool.

Temperature: Temperature measured with the UCM tool.

Resistivity: Resistivity measured with the UCM tool.

Hydr Cond (K): The bars show estimates of hydraulic conductivity K_{sec} of sections in each borehole based on flow logging, using a double-packer system, done in the borehole after the completion of drilling.

The entire borehole was tested during a pressure build-up test and if radial flow occurred the evaluation of the transmissivity (T_{tot}) was made using a radial flow model (Jacob semi-logarithmic evaluation). In some of the holes radial flow could not be identified and a relationship for transforming the specific capacity to a transmissivity value presented in Rhén et al. (1997) was used.

The flow rate Q_{sec} of the section were used to scale the evaluated whole borehole transmissivity T_{tot} to get a section transmissivity T_{sec} using the equation below:

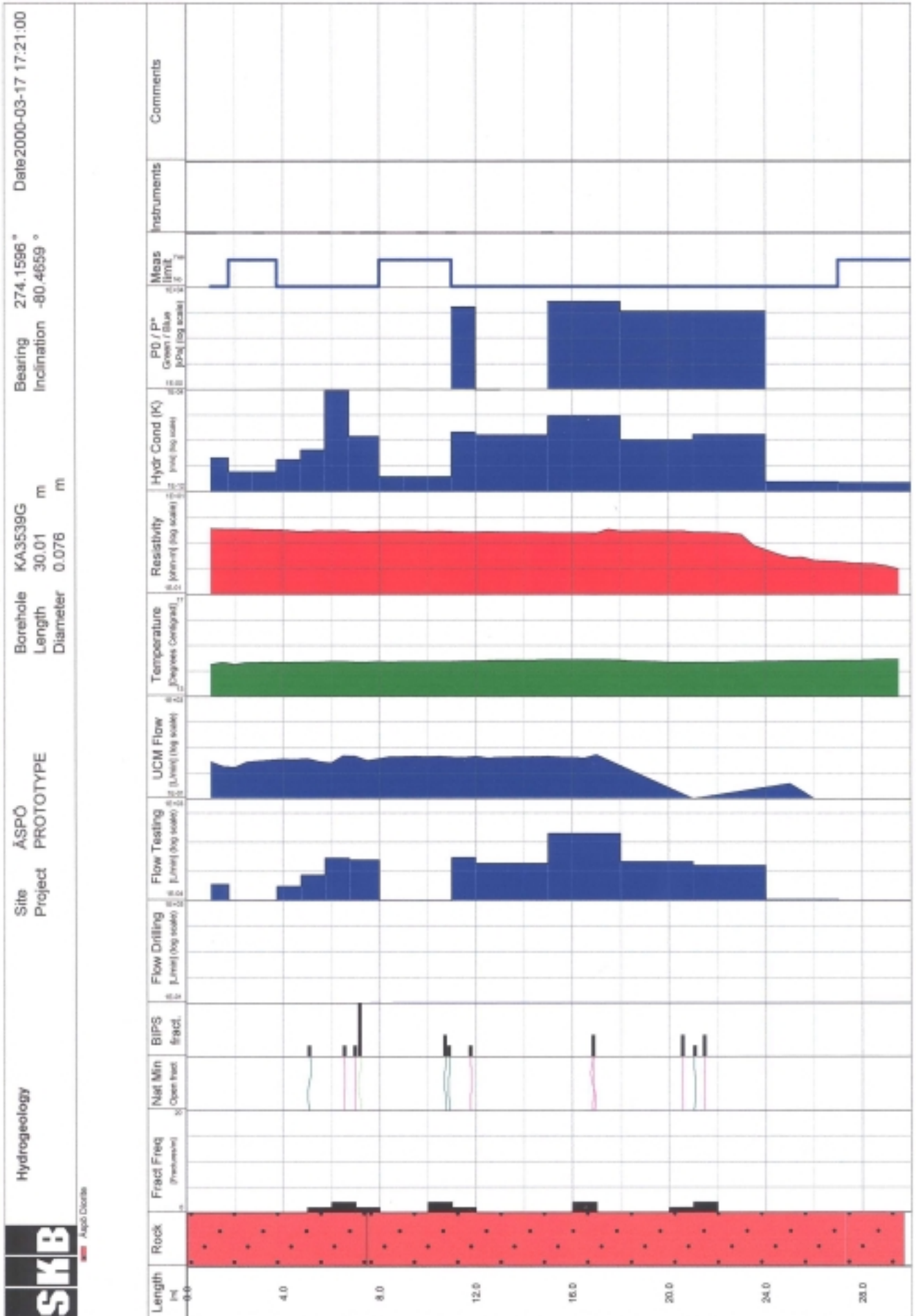
$$T_{sec} = [Q_{sec} \cdot T_{tot}] / Q_{sectot}$$

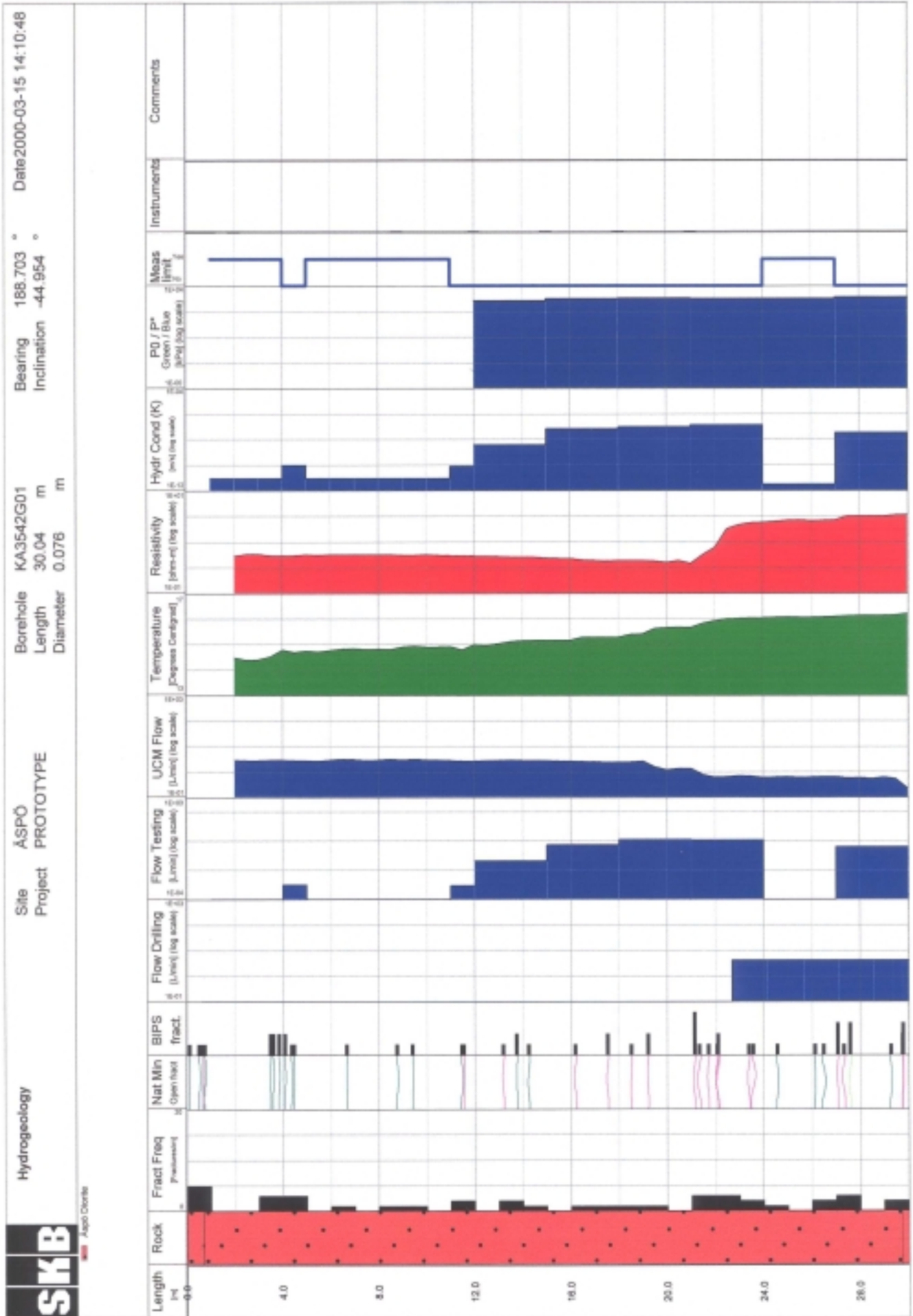
Q_{sectot} is the flow rate of the whole borehole

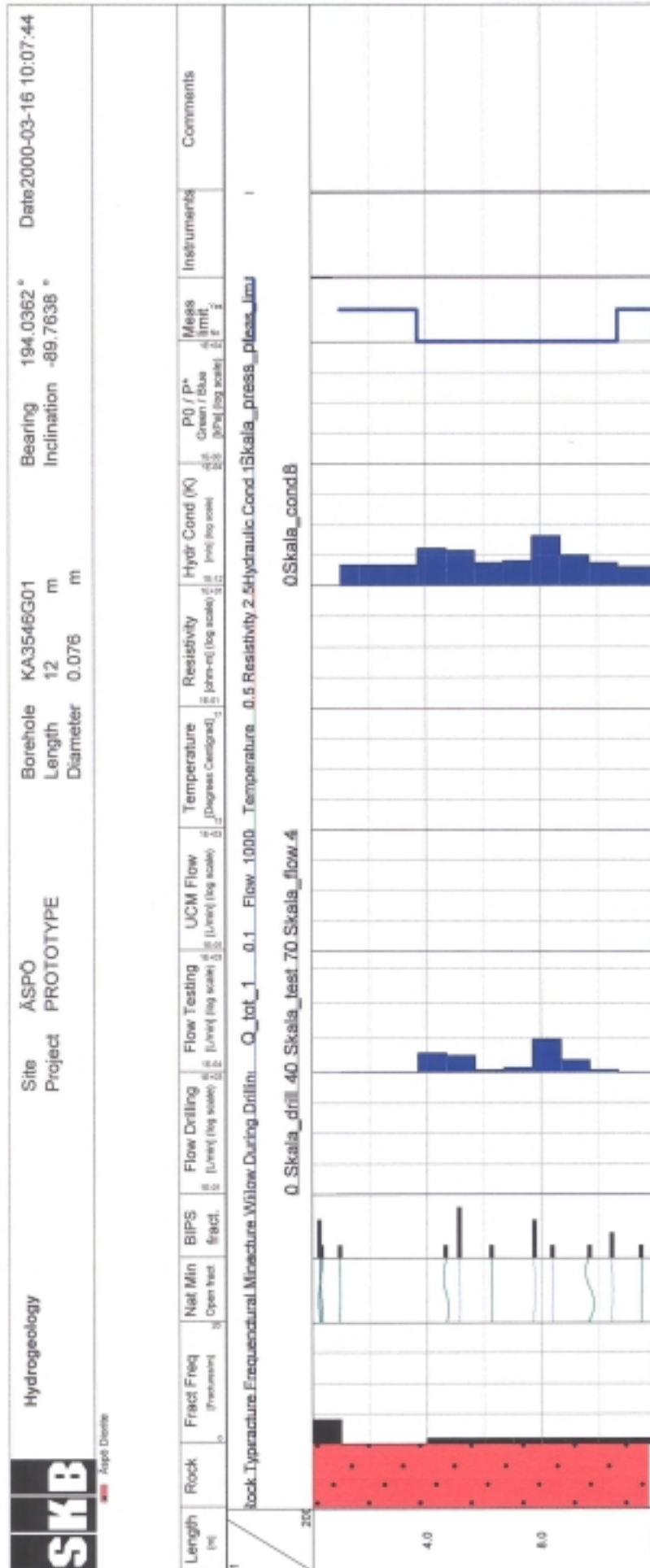
The transmissivity value was then divided by the section length to get the estimate of K_{sec} .

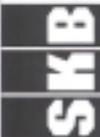
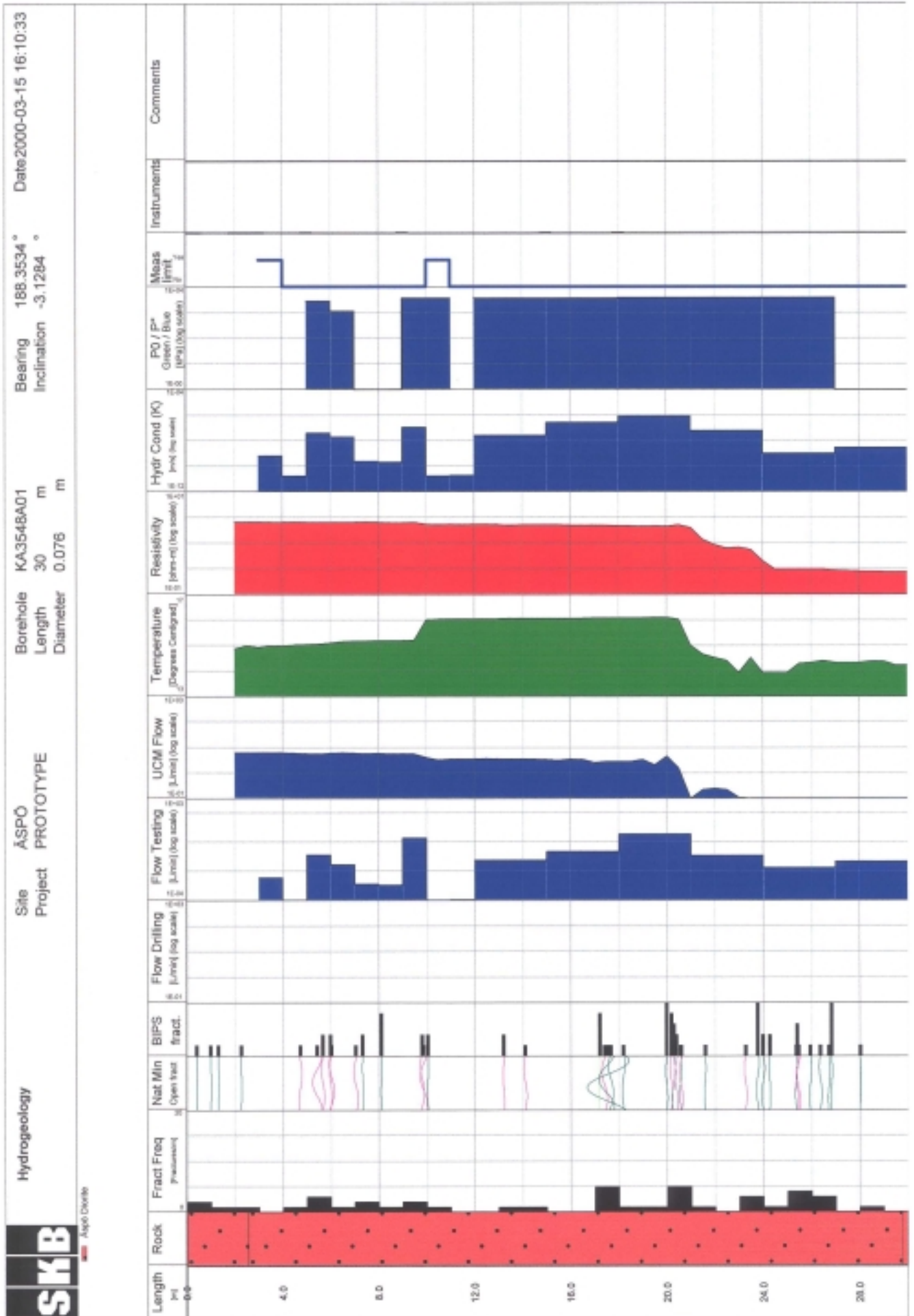
P0/P*: Undisturbed pressure based on measurement undisturbed pressure (P0) or estimated from the pressure build-up period (P*). Data from the flow logging with the double packer system.

Meas limit: Indicates when the flow rate is below the estimated measurement limit during the flow logging with the double packer system.

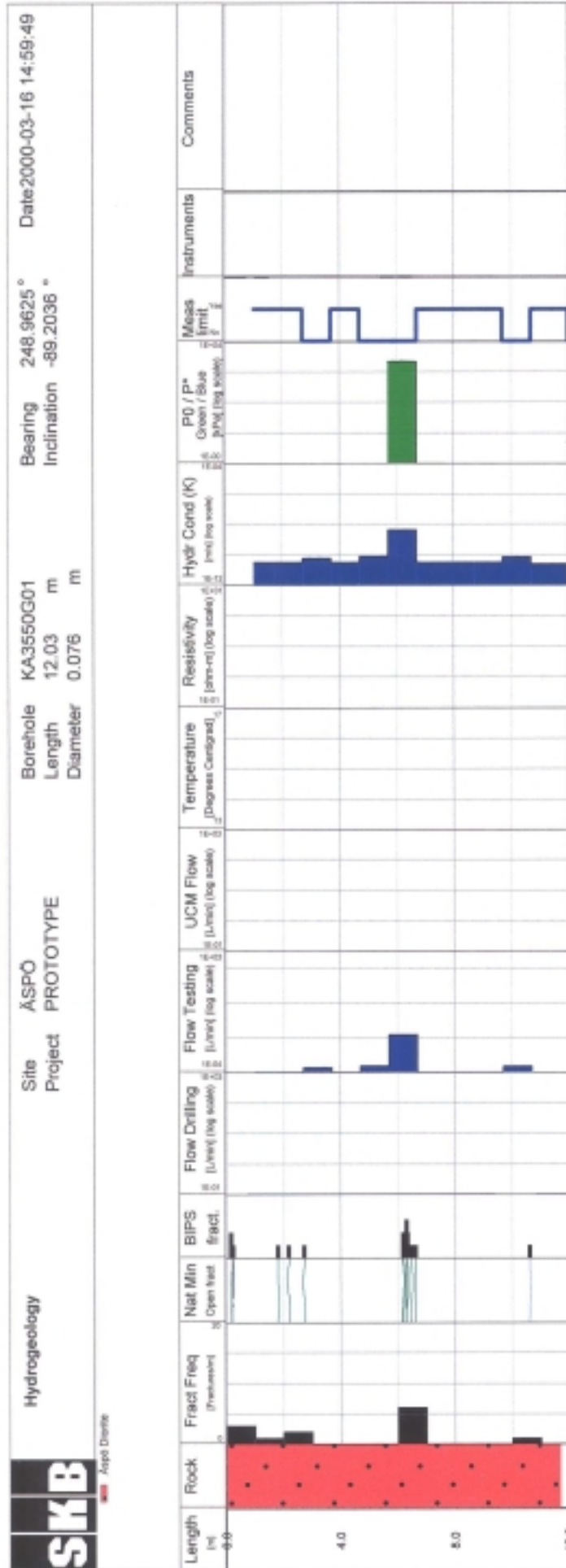


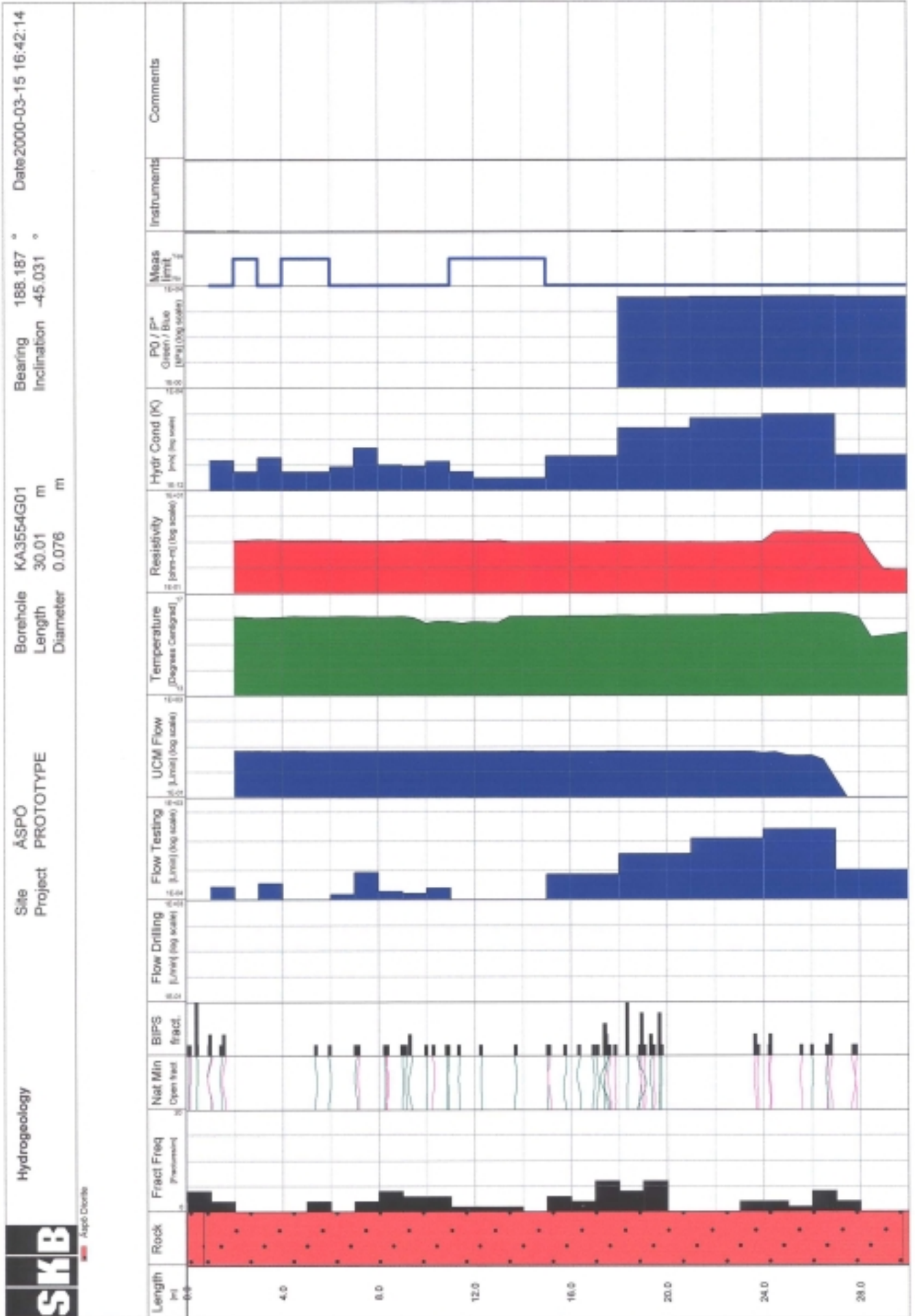


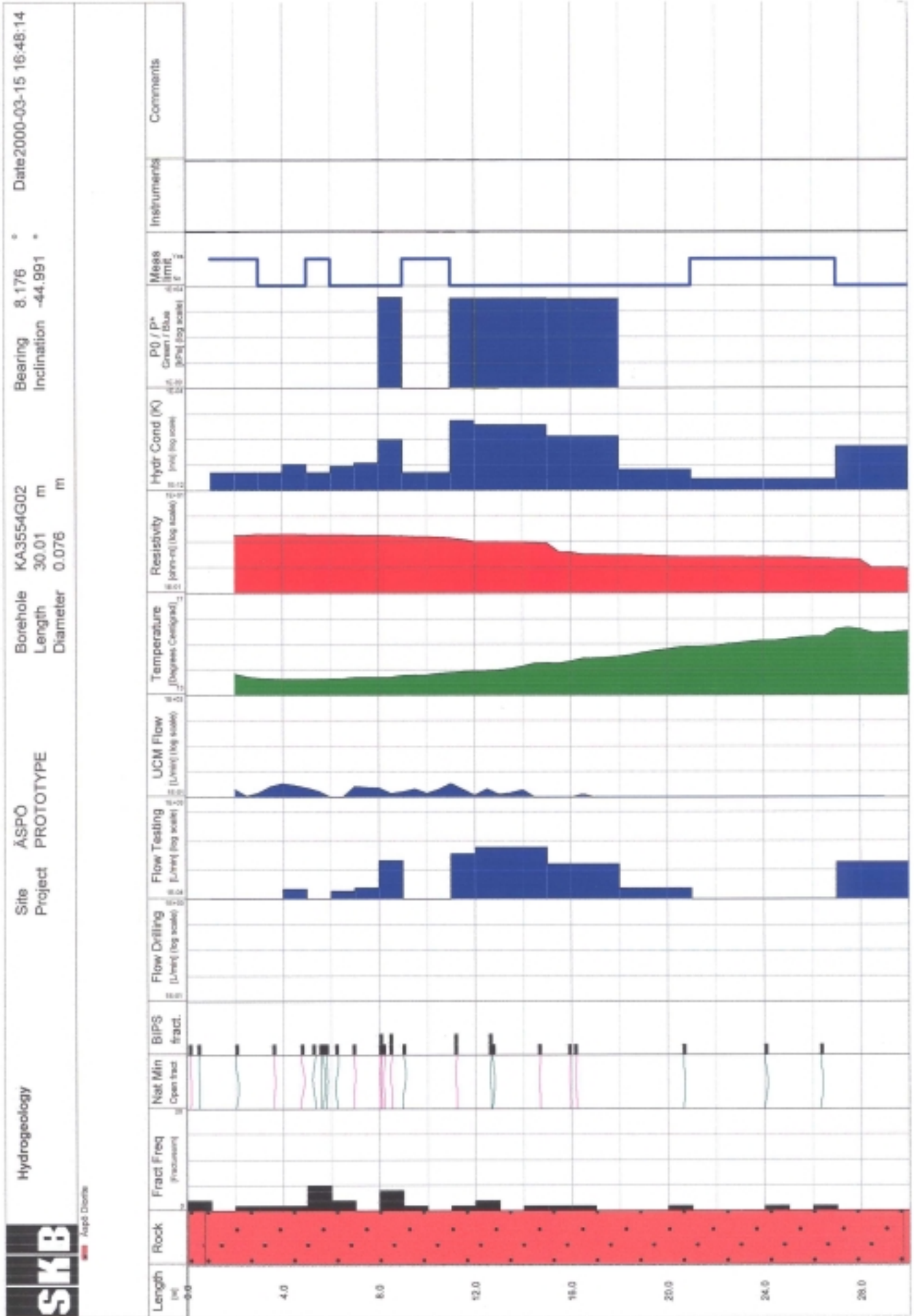


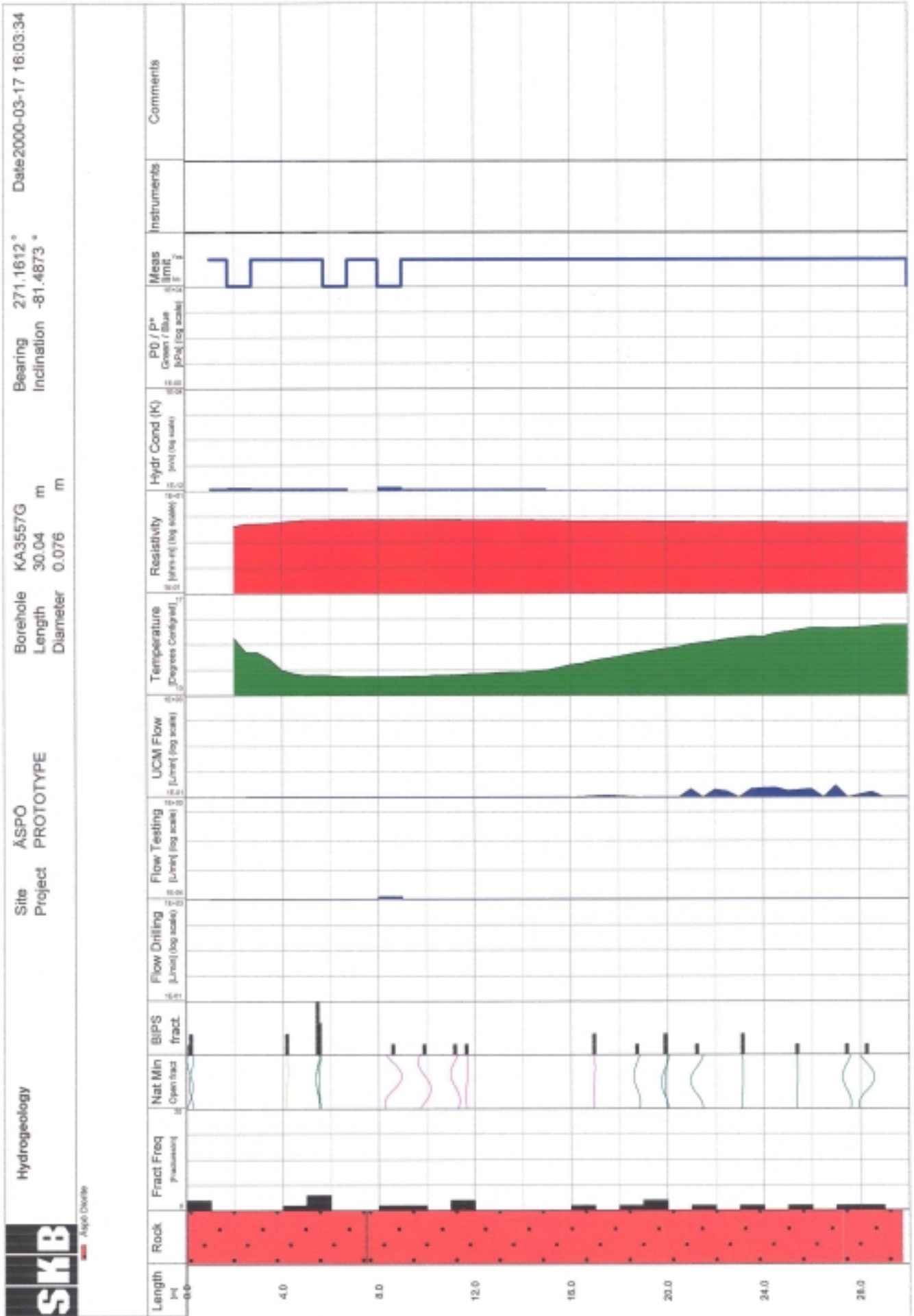


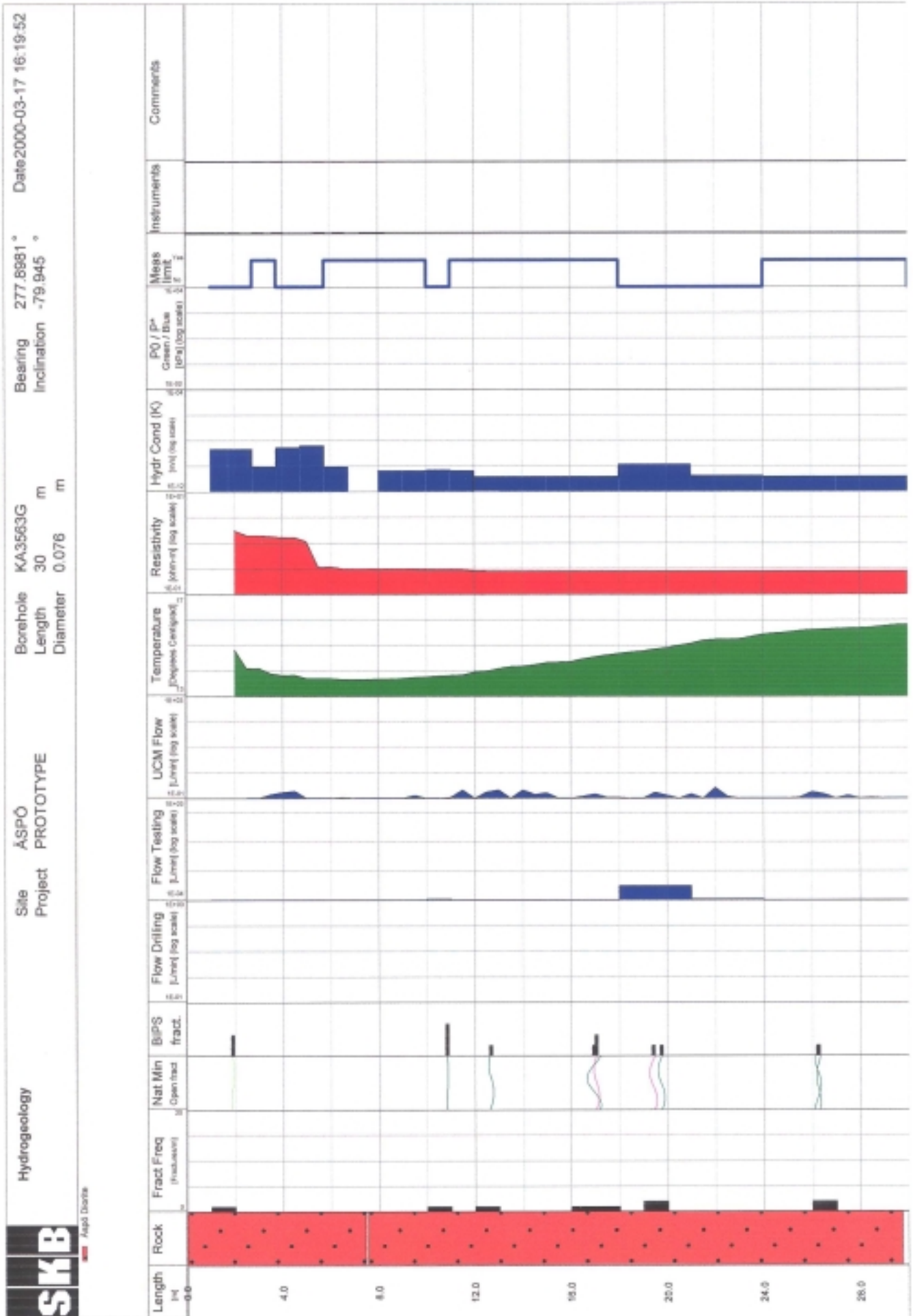
Aspo Climate

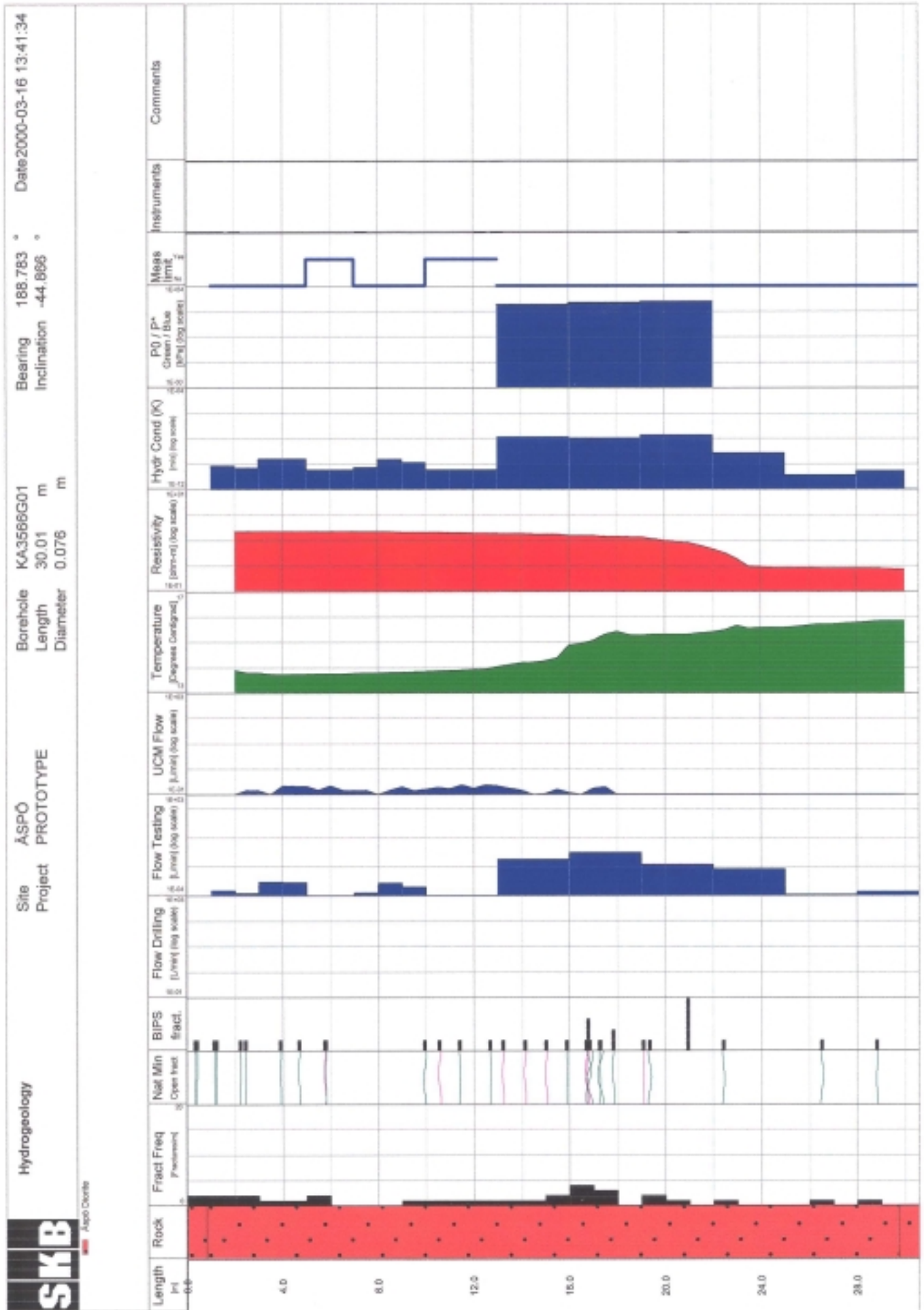


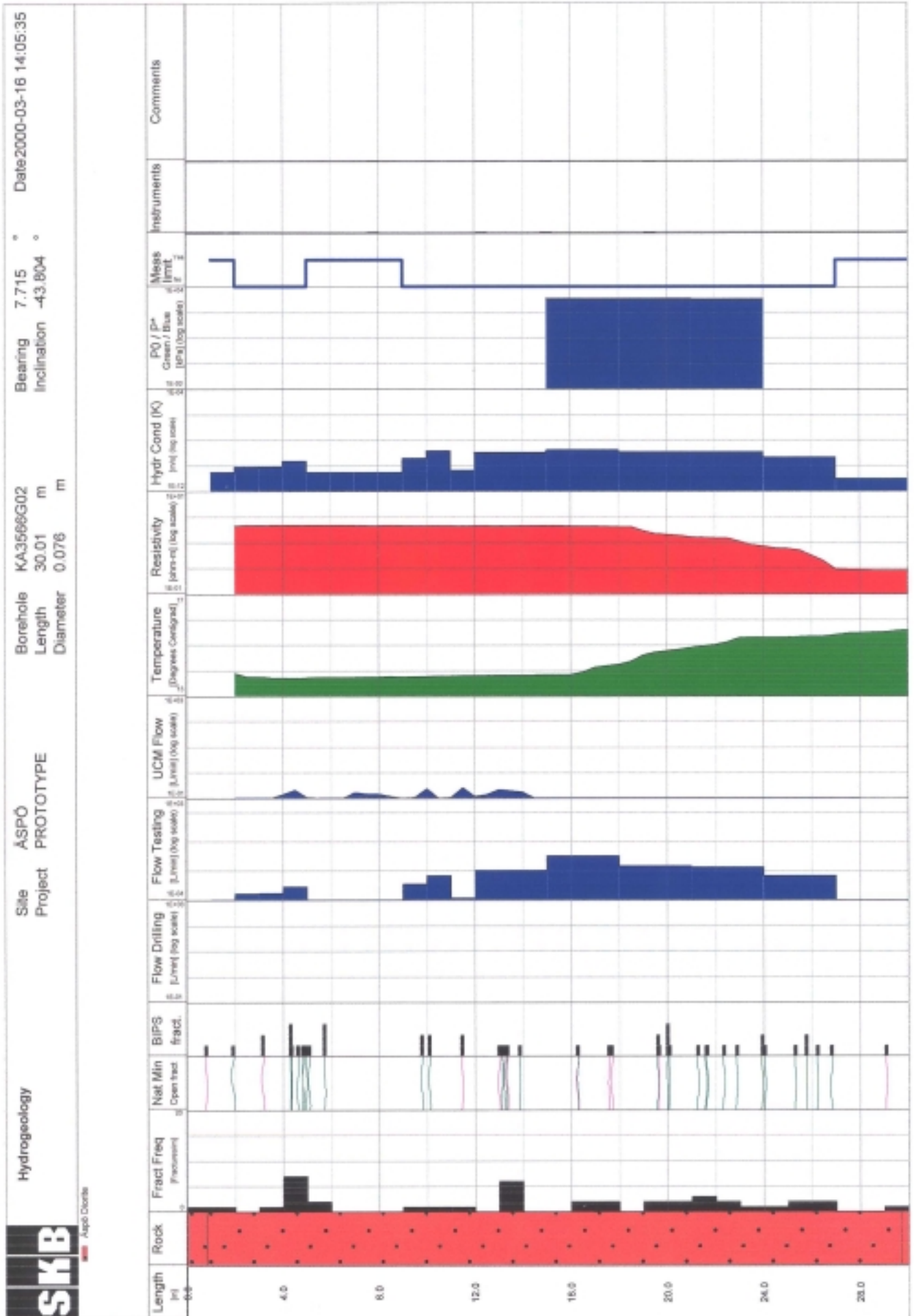




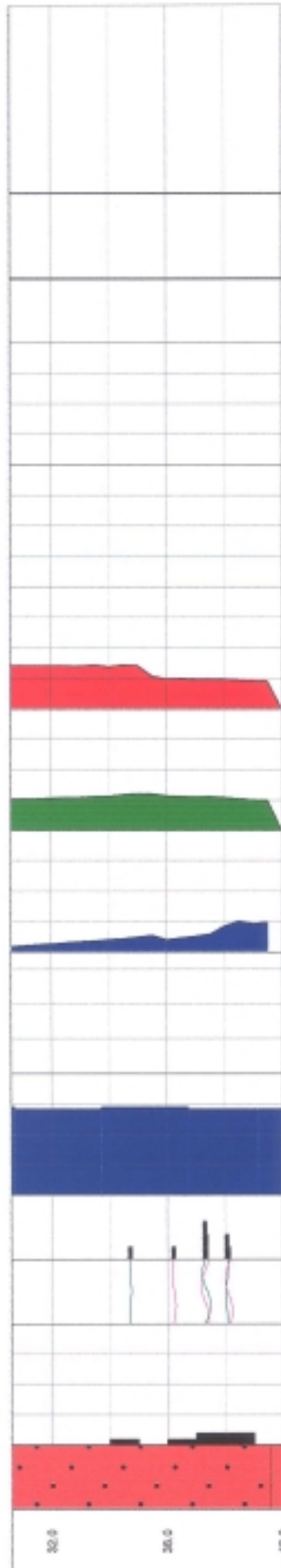


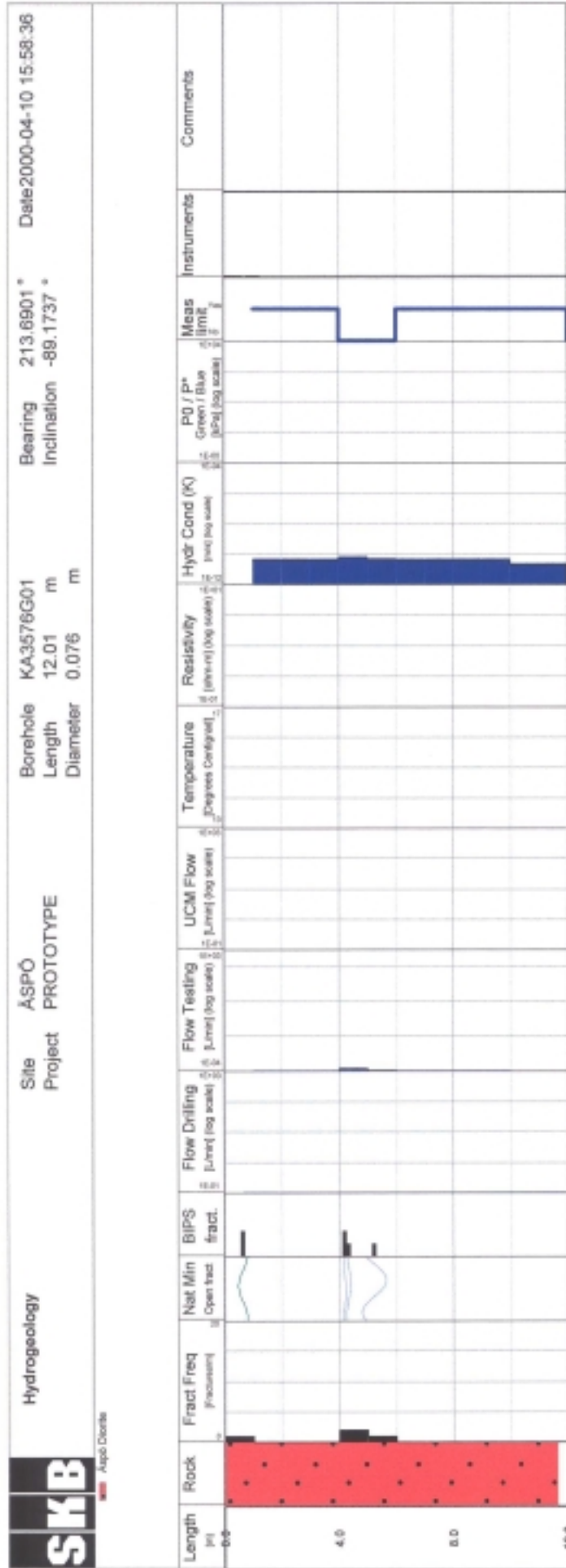


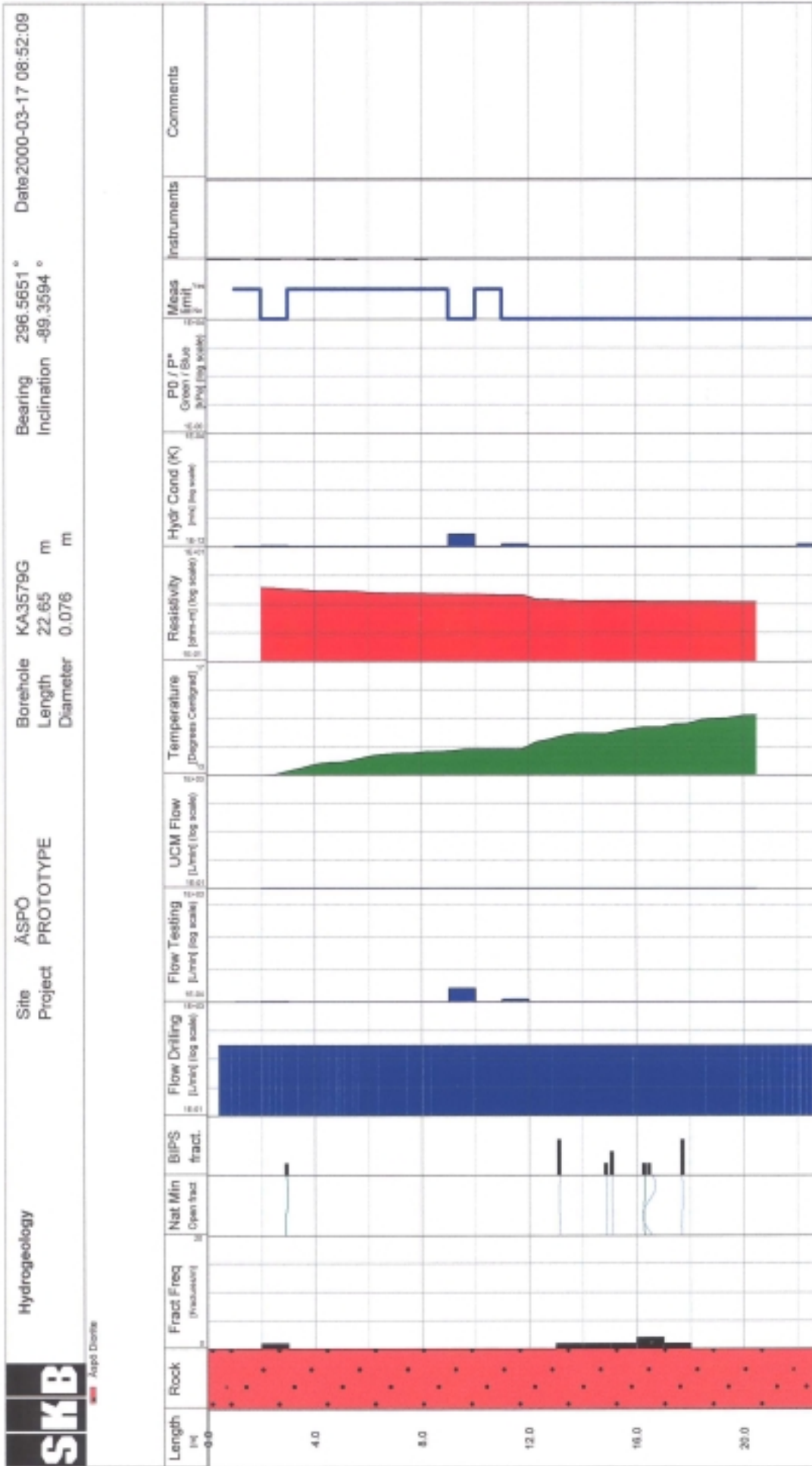


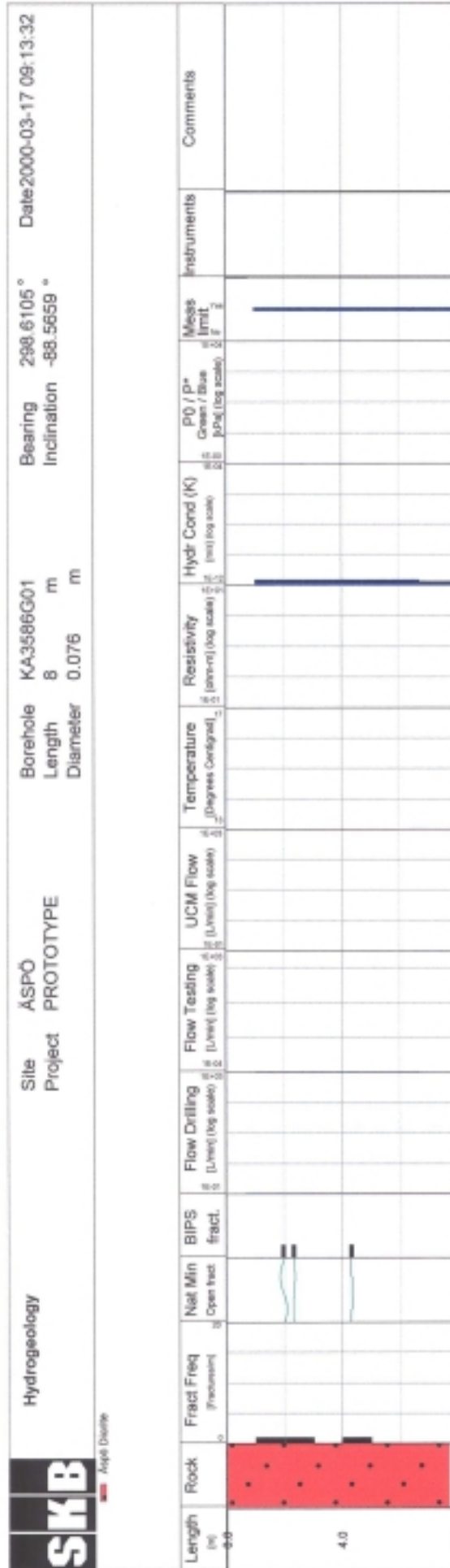


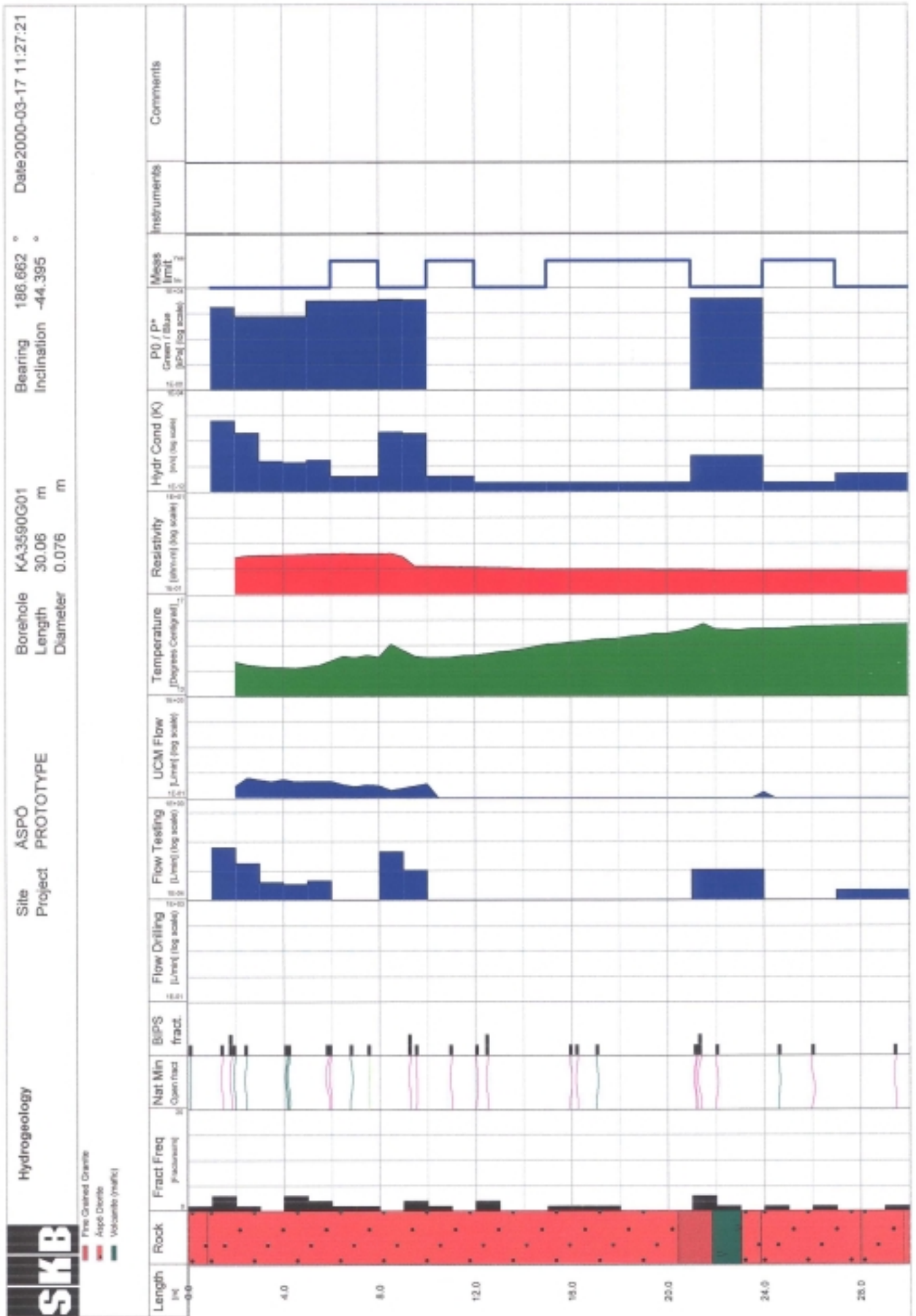
KA3573A, cont

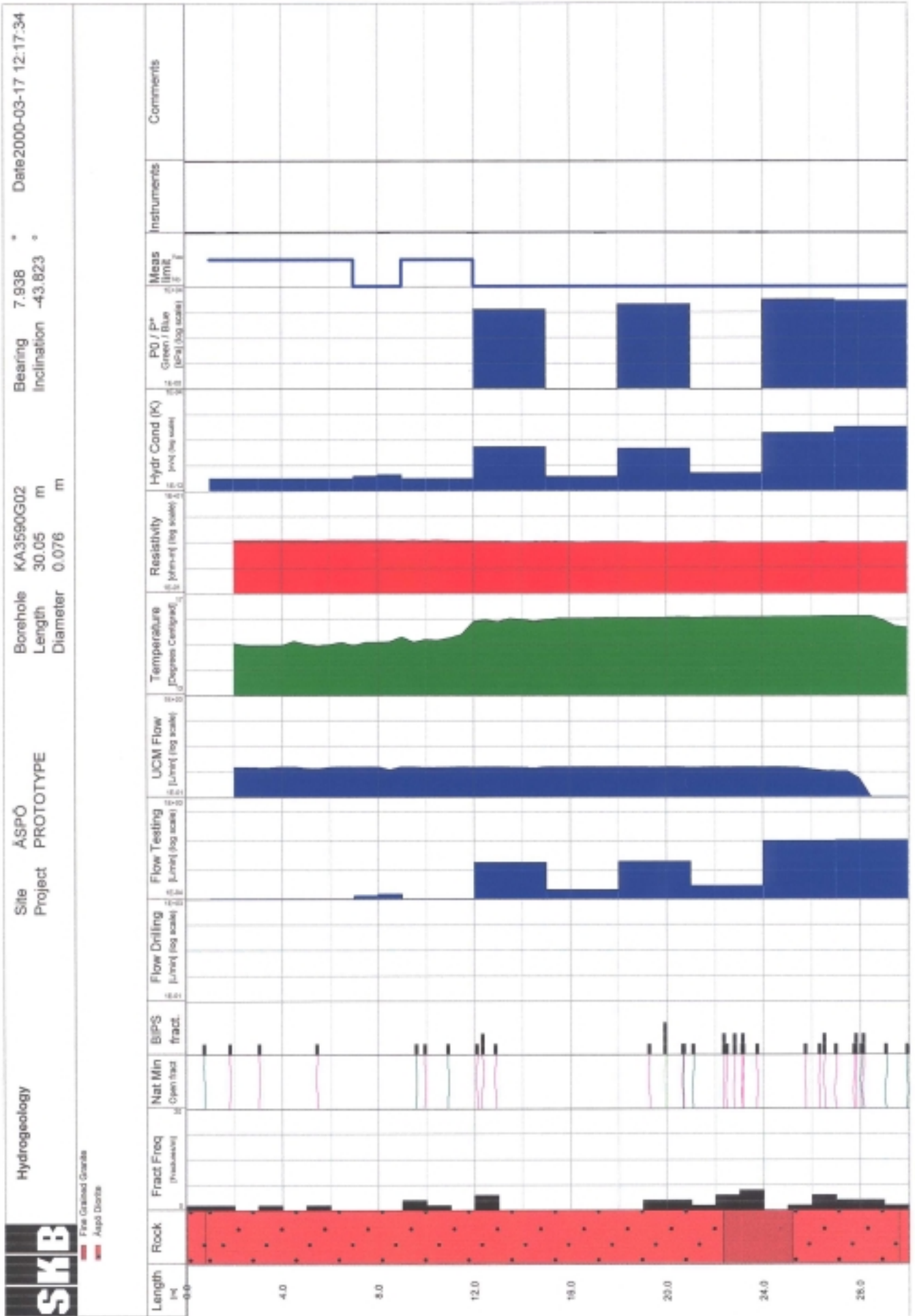


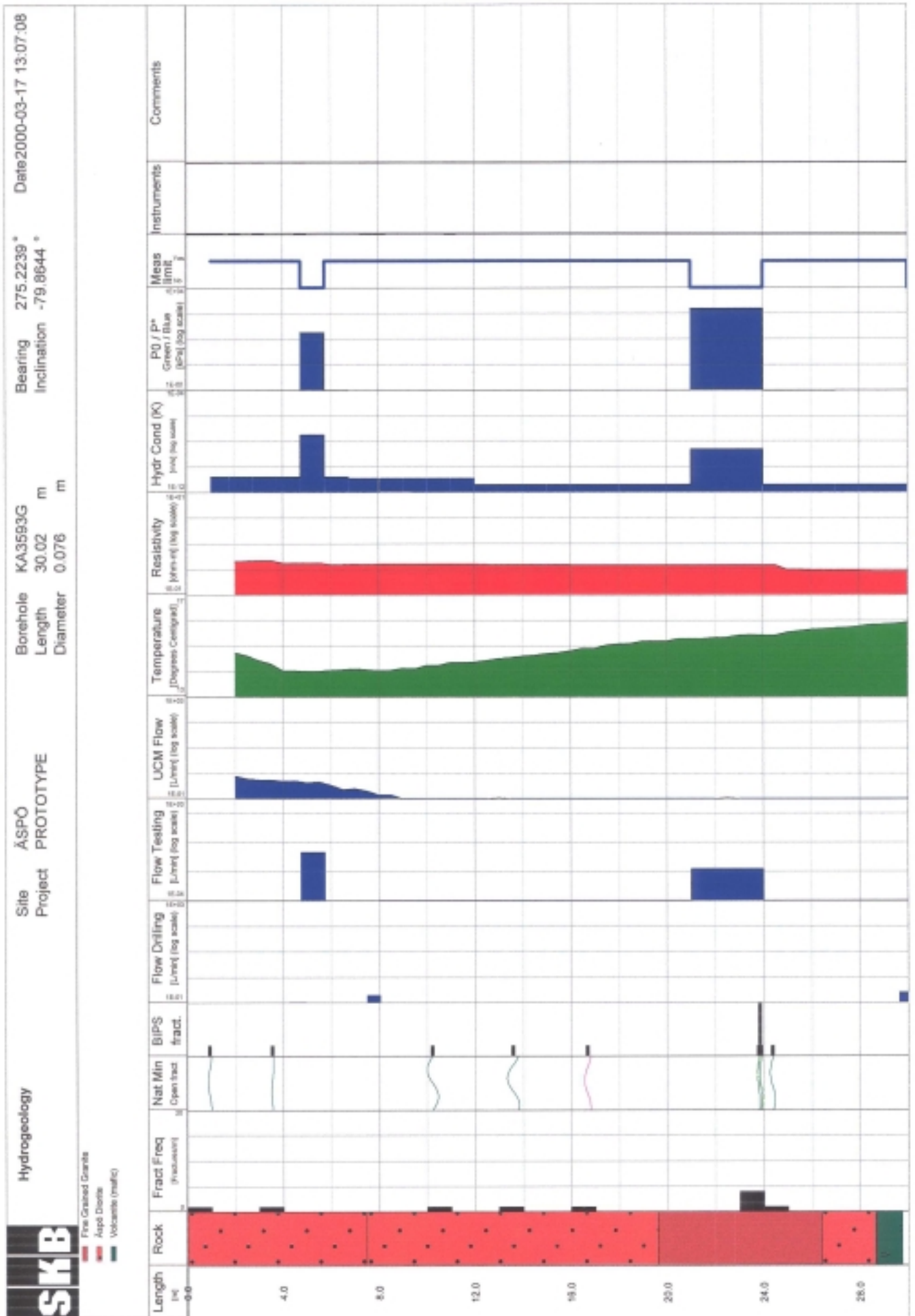




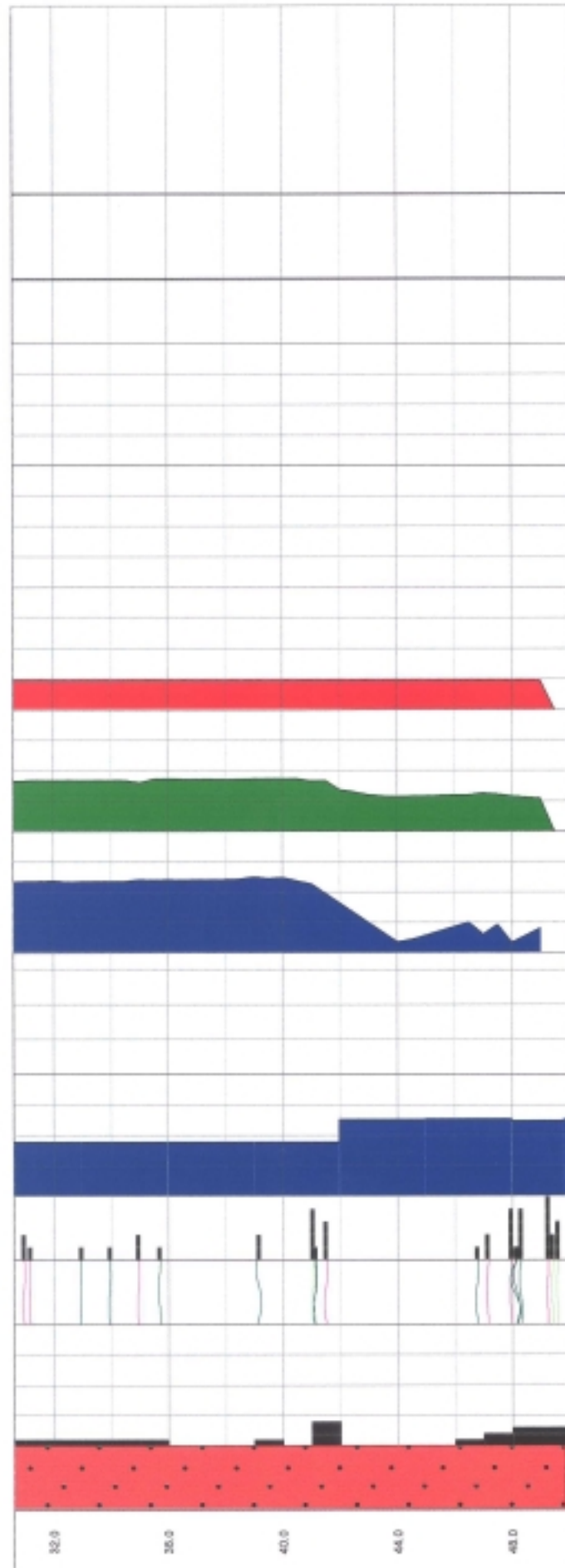


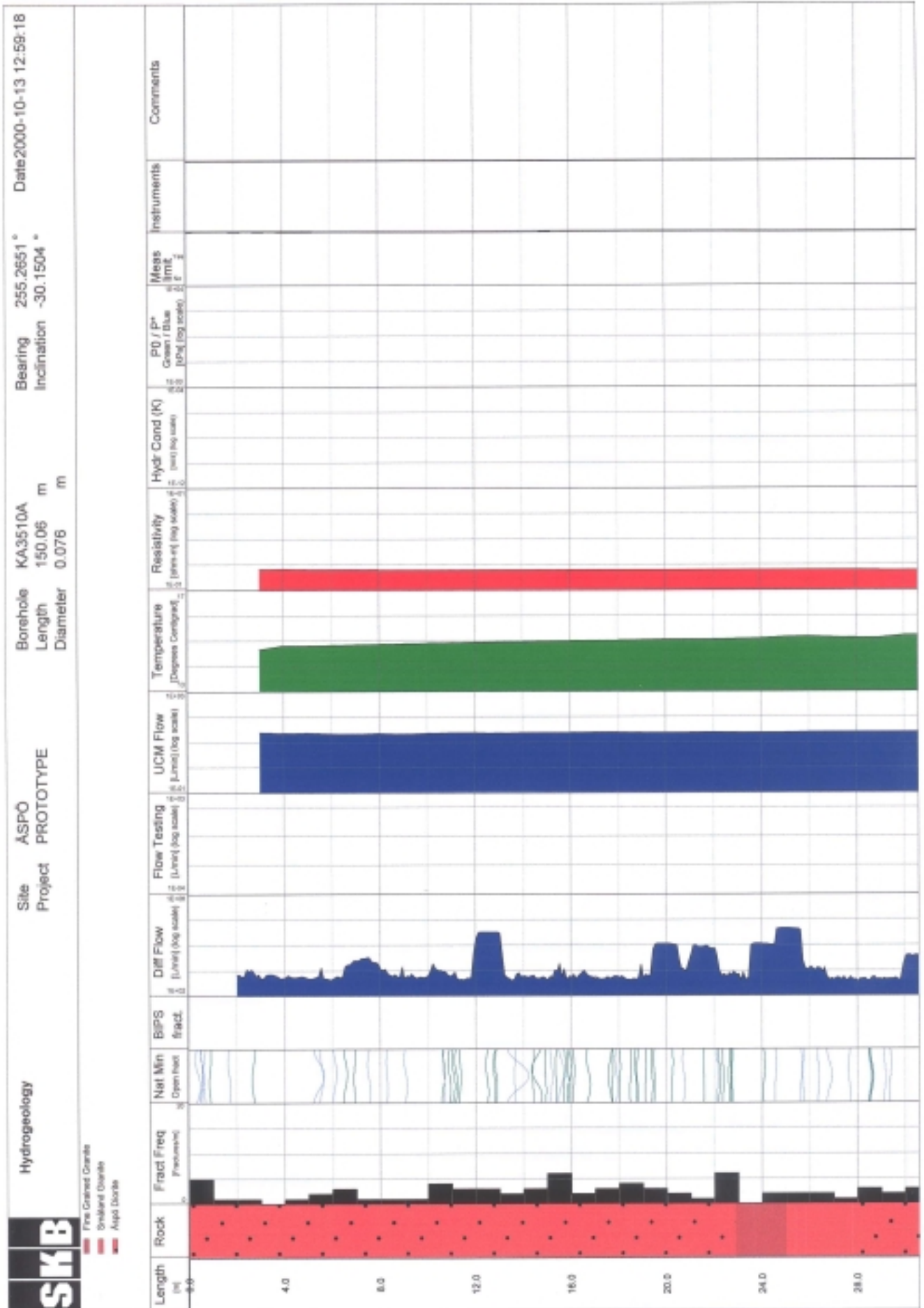




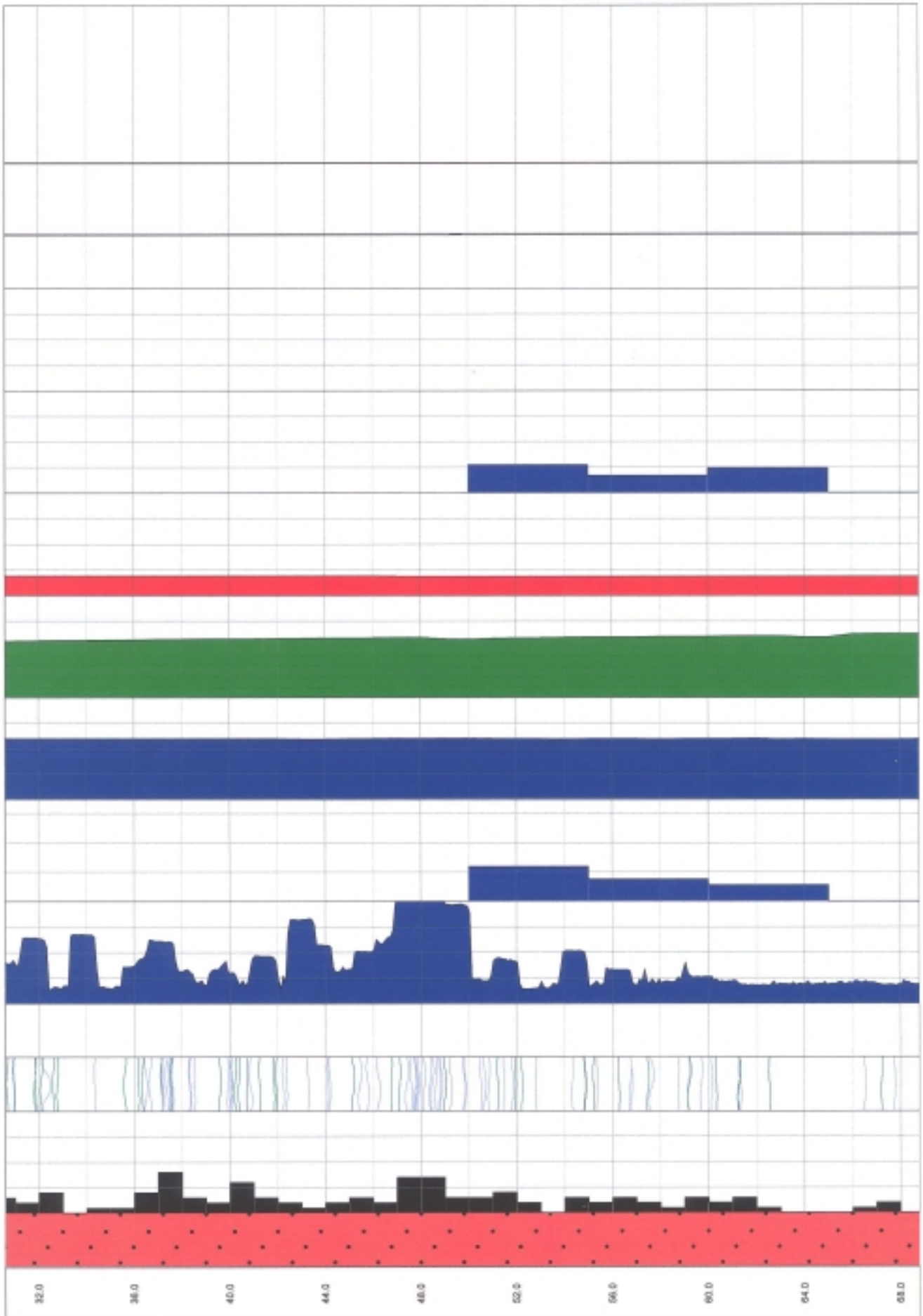


KA3600F, cont.

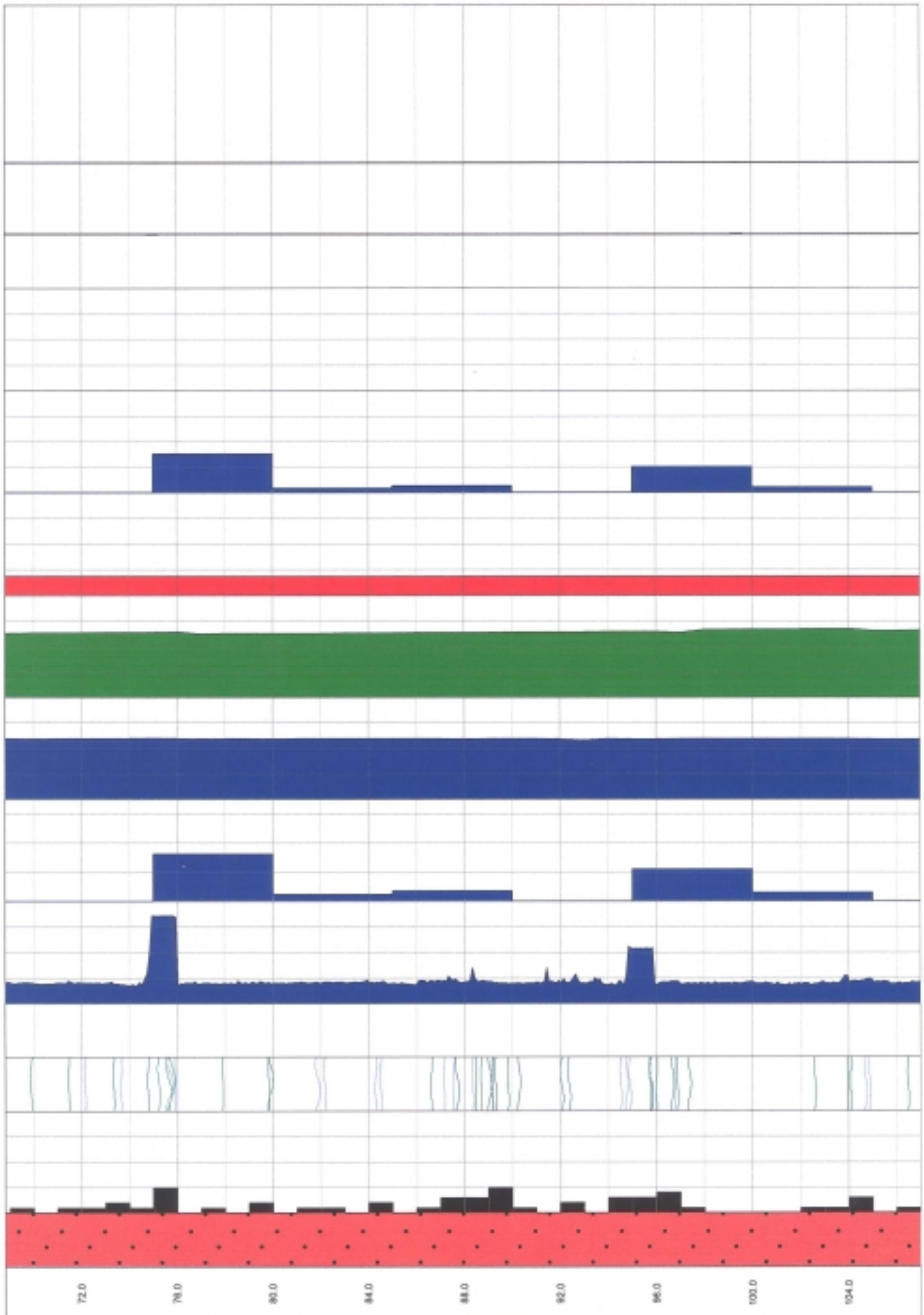




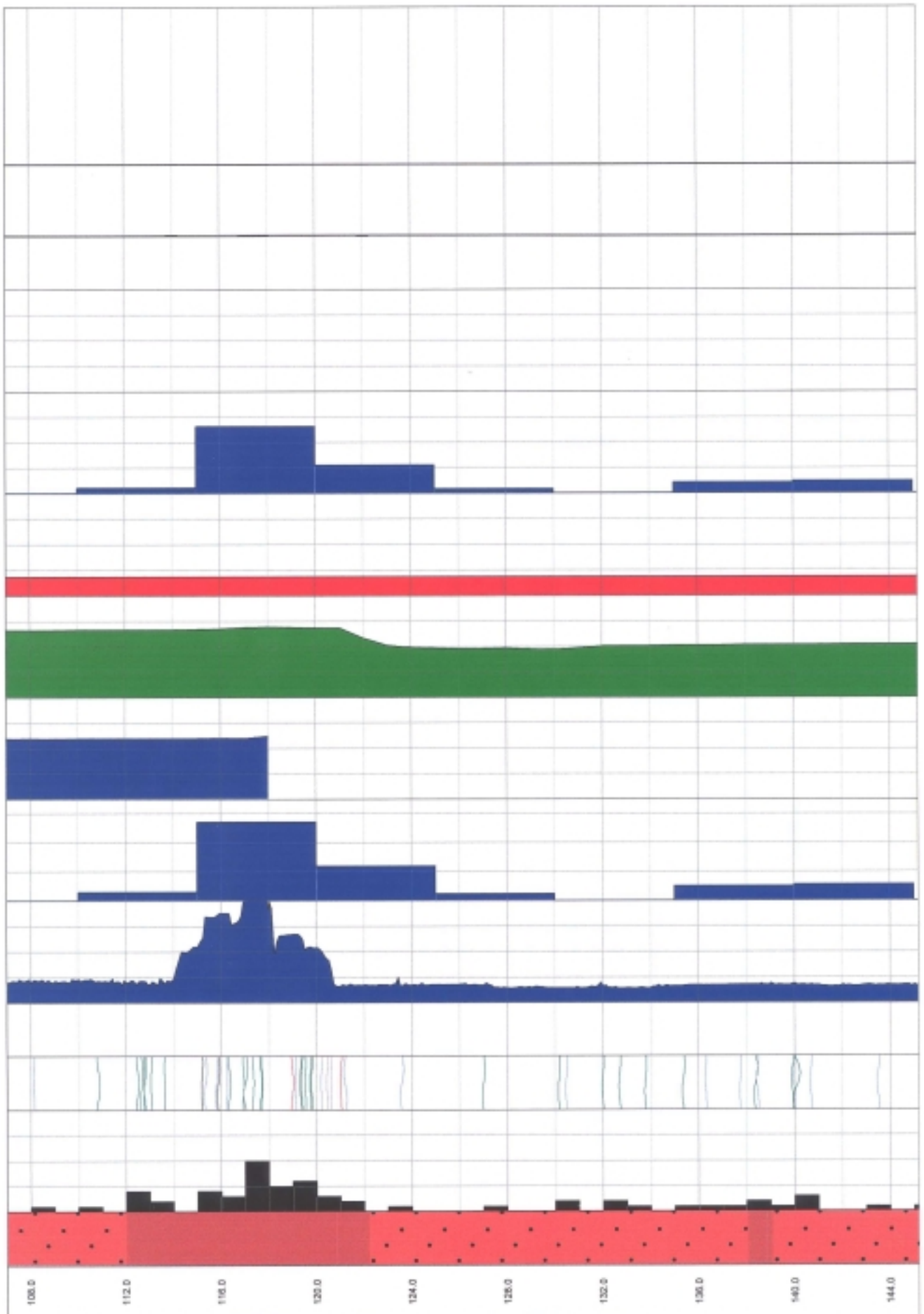
KA3510A, cont. 1



KA3510A, cont. 2



KA3510A, cont. 3



KA3510A, cont. 4



KG0021A01, cont.

